

Design, Syntheses and Biological Activities of Paclitaxel Analogs

Jielu Zhao

Dissertation submitted to the faculty of the Virginia Polytechnic Institute and State University in partial fulfillment of the requirements for the degree of

Doctor of Philosophy
In
Chemistry

David G. I. Kingston, Committee Chair
Paul R. Carlier
Harry C. Dorn
Felicia A. Etzkorn
Richard D. Gandour

January 31, 2011
Blacksburg, Virginia

Keywords: paclitaxel, simplified paclitaxel, T-taxol, tubulin, microtubules, bioactive conformation, thiolated paclitaxel, gold nanoparticles, conformationally constrained paclitaxel

Design, Syntheses and Biological Activities Paclitaxel Analogs

Jielu Zhao

ABSTRACT

The conformation of paclitaxel in the bound state on the protein has been proposed to be the T-taxol conformation, and paclitaxel analogs constrained to the T-taxol conformation proved to be significantly more active than paclitaxel in both cytotoxicity and tubulin polymerization assays, thus validating the T-taxol conformation as the tubulin-binding conformation. In this work, eight compounds containing an aza-tricyclic moiety as a mimic of the baccatin core of paclitaxel have been designed and synthesized as water-soluble simplified paclitaxel analogs, among which **3.50-3.52** and **3.55** were conformationally constrained analogs designed to bind to the paclitaxel binding site of tubulin, based on their similarity to the T-taxol conformation. The open-chain analogs **3.41-3.43** and **3.57** and the bridged analogs **3.50-3.52** and **3.55** were evaluated for their antiproliferative activities against the A2780 cell lines. Analogs **3.50-3.52** and **3.55** which were designed to adopt the T-taxol conformation showed similar antiproliferative activities compared to their open-chain counterparts. They were all much less active than paclitaxel. In the second project, a series of paclitaxel analogs with various thio-containing linkers at C-2' and C-7 positions were designed and synthesized in our lab. These analogs were attached to the surfaces of gold nanoparticles by CytImmune Sciences for the development of multifunctional tumor-targeting agents. The native analogs and the gold bound analogs were evaluated for their antiproliferative activities against the A2780 cell

line. All the compounds tested showed comparable or better activities than paclitaxel. Stability studies were performed for selected analogs in hydrolysis buffer, which showed that the analogs released paclitaxel in buffer over time. In the third project, the synthesis of a conformationally constrained paclitaxel analog which was designed to mimic the REDOR-taxol conformation was attempted. Two synthetic routes were tried and significant progress was made toward the synthesis of the conformationally constrained analog. However, both of the current synthetic routes failed to produce the key intermediate that would serve as the precursor for a ring-closing metathesis reaction to furnish the macrocyclic ring.

ACKNOWLEDGEMENTS

This dissertation would not have been possible without the guidance and the help of people who in one way or another contributed and extended their valuable assistance in the completion of my study.

First and foremost, my utmost gratitude to my advisor Dr. David G. I. Kingston, University Distinguished Professor of Virginia Polytechnic Institute and State University whose sincerity, encouragement, guidance and help I will never forget. Dr. Kingston has been my inspiration as I hurdle all the obstacles in the completion my research work.

My committee members, Dr. Paul Carlier, Dr. Harry Dorn, Dr. Felicia Etzkorn and Dr. Richard Gandour always gave encouragement, patience and valuable insights in the fulfillment of my study.

Dr. Qiaohong Chen for her instruction and advice in organic synthesis; Ms. Peggy Brodie for performing the bioassays; Dr. Liva Harinantenaina for his help in structure elucidation; all former and current group members, Drs. Yanpeng Hou, Brian Murphy, Chao Yang, and Jun Qi, Mr. Ende Pan, Mr. Yumin Dai, Ms. Yixi Liu, Mr. Alex Xu, and Mrs. Melody Windsor for their help and moral support.

The departmental analytical service staff Dr. Hugo Azurmendi, Dr. Mehdi Ashraf-Khorassani, Mr. William Bebout, Mr. Tom Glass, Mr. Geno Iannaccone, and Dr. Carla Slebodnick for their kind assistance.

Last but not the least, my supportive family, especially my wife, Liaoliao Li, for their continuous encouragement and support.

TABLE OF CONTENT

	Page
LIST OF FIGURES	viii
LIST OF SCHEMES	ix
LIST OF TABLES	xi
LIST OF ABBREVIATIONS	xii
I. Introduction to paclitaxel	1
1.1 History of paclitaxel	1
1.2 Synthetic studies	2
1.3 Docetaxel and cabazitaxel	4
1.4 Medicinal chemistry and structure-activity relationships	5
1.5 Mechanism of action of paclitaxel	8
References	10
II. The bioactive conformation of paclitaxel	20
2.1 Determination of the bioactive conformation of paclitaxel	20
2.2. Synthetic efforts to make conformationally restricted analogs of paclitaxel	24
2.2.1 Validation of the T-taxol model	25
2.2.2 Other attempts to make constrained analogs for conformational studies	27
References	33

III. Design and synthesis of simplified paclitaxel analogs based on T-taxol bioactive conformation	39
3.1 Simplified paclitaxel analogs	39
3.2 Design and synthesis of simplified analogs based on the T-taxol bioactive conformation	41
3.2.1 Introduction	41
3.2.2 Design of a new generation of simplified paclitaxel analogs	43
3.2.3 Synthesis of new generation simplified paclitaxel analogs	45
3.2.4 Biological evaluation of the simplified paclitaxel analogs	55
3.2.5 Computer modeling	57
3.2.6 Conclusions	58
3.3 Experimental section	58
References	101
IV. Synthesis of thiolated paclitaxel analogs for reaction with gold nanoparticles as drug delivery agents	107
4.1 Targeted delivery of paclitaxel to tumor	107
4.1.1 Paclitaxel prodrugs designed to target tumor tissue	107
4.1.2 Macromolecular prodrugs of paclitaxel	113
4.1.3 paclitaxel-nanoparticle conjugates	119
4.2 Synthesis of new thiolated paclitaxel analogs for reaction with gold nanoparticles as drug delivery agents	121

4.2.1 Synthesis of analog 4.26	123
4.2.2 Synthesis of analog 4.27	124
4.2.3 Synthesis of analogs 4.28 and 4.29	124
4.2.4 Synthesis of analog 4.30	126
4.2.5 Manufacture of a gold-nanoparticle-based multifunctional anticancer drug delivery system	127
4.2.6 Biological evaluation of the native analogs and gold-bound analogs	128
4.2.7 Stability studies of the analogs	129
4.3 Conclusions	133
4.4 Experimental section	134
References	148
V. Approaches to the synthesis of a conformationally constrained paclitaxel analog	153
5.1 Introduction	153
5.2 Synthesis of 5.1	156
5.3 Conclusions	160
5.4 Experimental section	160
References	170
APPENDIX (NMR spectra of compounds)	172

LIST OF FIGURES

Figure 1.1 The structure-activity relationships of paclitaxel	5
Figure 2.1 ^{13}C - ^{19}F intramolecular distances indicated by REDOR-NMR	22
Figure 2.2 Illustration of the T-taxol model	23
Figure 3.1 General structure of second generation T-taxol mimics	43
Figure 3.2 Low energy conformations of compounds 3.10 , 3.11 and 3.8 in the paclitaxel tubulin binding site.	45
Figure 3.3 3-D structures of 3.32 and 3.33 by X-ray crystallography	52
Figure 3.4 3-D structure of 3.42 optimized with PM3 method in Spartan	53
Figure 3.5 Intramolecular distances between ring A and ring B	57
Figure 4.1 <i>In vivo</i> efficacy of gold-bound analogs Au- 4.26 and Au- 4.28	129
Figure 4.2 Hydrolytic conversion of 4.27 to paclitaxel	130
Figure 4.3 Kinetics of the hydrolysis of 4.27 in buffer	131
Figure 4.4 Comparison of the hydrolytic profiles of gold-bound analogs and native analogs in hydrolysis buffer	132
Figure 4.5 Delivery of paclitaxel to tumor by the gold nanoparticle-based drug delivery system	132
Figure 5.1 Comparison of the C-13 side chains of T-taxol and REDOR-taxol by looking down the C2'-C1' bonds	154
Figure 5.2 Optimized 3-D structure of analog 5.1	155

LIST OF SCHEMES

Scheme 3.1 Retrosynthesis of simplified paclitaxel analogs	45
Scheme 3.2 Synthesis and ring closure of 3.13	46
Scheme 3.3 Synthesis of 3.14	47
Scheme 3.4 Synthesis of 3.17	48
Scheme 3.5 Cyclization of 3.17	49
Scheme 3.6 Retrosynthesis of aza-tricyclic core	49
Scheme 3.7 Synthesis of 3.18	50
Scheme 3.8 Synthesis of 3.19	50
Scheme 3.9 Synthesis of alcohols 3.32-3.34	51
Scheme 3.10 Synthesis of open-chain analogs 3.41-3.43	53
Scheme 3.11 Synthesis of open-chain and bridged paclitaxel analogs	54
Scheme 4.1 Gold nanoparticle-based multifunctional anticancer drug delivery system	121
Scheme 4.2 Synthesis of 4.26	123
Scheme 4.3 Synthesis of 4.27	124
Scheme 4.4 Synthesis of 4.28	125
Scheme 4.5 Synthesis of 4.29	126
Scheme 4.6 Synthesis of 4.30	127
Scheme 4.7 Conversion of 4.27 to paclitaxel	129
Scheme 5.1 Retrosynthesis of analog 5.1	156
Scheme 5.2 Coupling of 5.5 and 5.6	157
Scheme 5.3 Modified retrosynthesis of 5.3	158

Scheme 5.4 Synthesis of 5.4	158
Scheme 5.5 Synthesis of 5.9	159
Scheme 5.6 Coupling of 5.4 with 5.9	159

LIST OF TABLES

Table 3.1 Antiproliferative activities of paclitaxel and the simplified paclitaxel analogs 56

Table 4.1 Antiproliferative activities of paclitaxel and analogs against A2780 cell line 128

LIST OF ABBREVIATIONS

10-DAB	10-deacetylbaccatin III
A2780	a human ovarian cancer cell line
ADEPT	antibody-directed enzyme prodrug therapy
Boc	<i>N-tert</i> -butoxycarbonyl
CD44	a hyaluronic acid receptor
DCC	<i>N,N'</i> -dicyclohexylcarbodiimide
DHA	docosahexaenoic acid
DIAD	diisopropyl azodicarboxylate
DMAP	4-dimethylaminopyridine
DMF	dimethylformamide
DMSO	dimethyl sulfoxide
EPR	enhanced permeability and retention
ER	estrogen receptor
ESI	Electrospray Ionization
FDA	Food and Drug Administration
FR	folate receptor
GPC	Gel Permeation Chromatography
HPLC	High-performance Liquid Chromatography
HRMS	High Resolution Mass Spectrometry

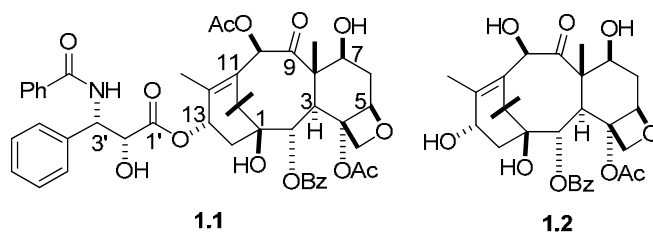
IC ₅₀	half maximal inhibitory concentration
KB	a human epidermoid carcinoma
LiHMDS	lithium bis(trimethylsilyl)amide
MDR	multidrug resistance
MMFF	Merck Molecular Force Field
MMGBSA	Molecular Mechanics Generalized Born Surface Area
MOM	methoxymethyl ether
MTD	maximum tolerated dose
NAMFIS	Analysis of Molecular Flexibility in Solution
NCI	National Cancer Institute
NMR	Nuclear Magnetic Resonance
NP	nanoparticle
PAMPAM	polyamidoamine
PBS	Phosphate buffered saline
PC3	a human prostate cancer cell line
PEG	polyethylene glycol
PM3	parameterized model number 3
PMP	<i>p</i> -methoxyphenyl
PVA	polyvinyl alcohol
REDOR	Rotational Echo Double Resonance

RHAMM	hyaluronan-mediated motility receptor
SAR	Structure-Activity Relationship
TBAH	tetrabutylammonium hydrogen sulfate
TBDPS	<i>tert</i> -butyldiphenylsilyl
TBS	<i>tert</i> -butyldimethylsilyl
TES	triethylchlorosilane
TFA	trifluoroacetic acid
THF	tetrahydrofuran
TLC	Thin Layer Chromatography
TMS	trimethylsilyl
TNF α	Tumor Necrosis Factor Alpha

Chapter 1. Introduction to Paclitaxel

1.1 History of Paclitaxel

The naturally occurring diterpene alkaloid, paclitaxel (Taxol[®]) (**1.1**), is considered to be one of the most important drugs for the treatment of cancers. The chemical and biological studies of paclitaxel started from the early 1960's when an extract of the stem and bark of *Taxus brevifolia* Nutt. was found to be cytotoxic to KB (human epidermoid carcinoma) cells. Further study of this active extract led to the isolation of the active natural product taxol (now known as paclitaxel), whose structure was first published by Wall and Wani in 1971.¹



Despite the promising initial activities paclitaxel showed both *in vitro* and *in vivo* against various cancers, the early development of paclitaxel into a clinically useful anticancer drug was impeded by several obstacles. It was found to be highly insoluble in water, which made drug formulation a big problem. In addition, it presented a big supply problem due to the low isolated yield (0.02% w/w) from the bark of a rare and slow-growing tree.² However, the National Cancer Institute (NCI) persisted in the preclinical development. NCI introduced some new *in vivo* bioassays, and paclitaxel proved to be strongly active against a B16 melanoma in the early 1970's.³ Moreover, the solubility

problem was successfully solved by a formulation in ethanol and Cremophor EL. These kept paclitaxel alive during its long development into an excellent drug.

In 1979, it was reported⁴ that paclitaxel had a completely new mechanism of action, in which it intervenes in the equilibrium between tubulin and microtubules during cell division by promoting the assembly of α - and β -tubulin into microtubules.⁵ The mechanism will be explained in detail below. The discovery of this mechanism of action also provoked great research interest in the scientific community.

Paclitaxel went into Phase I clinical trials in 1983, and into Phase II trials in 1985, in which it proved to be clinically active against ovarian cancer⁶ and breast cancer.⁷ The Food and Drug Administration (FDA) approved paclitaxel for the treatment of ovarian cancer in 1992 and for breast cancer in 1994. Currently paclitaxel is used (either as a single agent or in combination with other drugs such as cisplatin) as an anticancer drug in the treatment of a variety of solid tumours.⁸

Despite its excellent anticancer activity, paclitaxel is not flawless. Several drawbacks, including poor water solubility and side effects, limit its clinical usefulness. The side effects include hair loss, decrease in white blood cells (which may cause susceptibility to infections), nausea, vomiting, diarrhea, an acute pulmonary reaction, and numbness of the fingers and toes.⁹⁻¹¹ Although the use of Cremophor EL eased the solubility problem of paclitaxel, the agent itself causes serious allergic reactions in some cases.¹¹

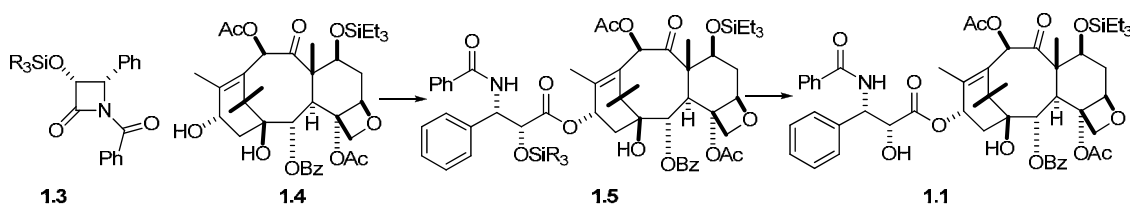
1.2 Synthetic Studies

After the emergence of paclitaxel as a promising anticancer agent, it attracted great attention from synthetic chemists around the world because of its unusual structure

containing a complex tetracyclic core, multiple side chains and stereochemistries. Meanwhile its preclinical and clinical studies were hindered by the limited supply from its natural source of *T. brevifolia* bark. Synthetic studies became quite meaningful in the sense that they might provide a solution to the supply crisis. Quite fruitfully, six independent total syntheses were reported from 1994 to 2000. These include the Holton synthesis,^{12,13} the Nicolaou synthesis,¹⁴ the Danishefsky synthesis,¹⁵ the Wender synthesis,^{16,17} the Kuwajima synthesis,¹⁸ and the Mukaiyama synthesis.¹⁹ However, none of the above syntheses of paclitaxel turned out to be commercially useful for its production due to low overall yields and thus high economic cost. Nevertheless these synthetic studies provided much useful information for the development of new chemistry.

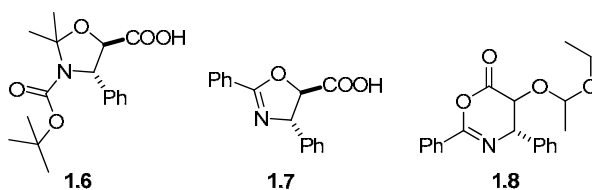
The supply issue was addressed more successfully by semisynthetic methods. Most semisyntheses of paclitaxel and its analogs start with 10-deacetylbaccatin III (10-DAB, **1.2**), which can be obtained in a higher yield than paclitaxel from the leaves of the European yew, *Taxus baccata*. In addition, what makes it more favorable is that the European yew grows more rapidly and the leaves can be harvested without killing the plant. 10-DAB can be selectively protected at the more reactive sites at C7 and C10 and acylated at C13 by coupling it with a suitable side chain precursor.²⁰ Different strategies have been used for the coupling of baccatin III with side chain precursors. The most successful method from a commercial point of view is the one that is based on β -lactam chemistry, which was developed by Holton²¹ and Ojima.²² This strategy was later adopted by Bristol-Myers Squibb for their commercial production of paclitaxel. An example of this method is shown in Scheme 1.1. Coupling of the protected β -lactam with

protected baccatin III yields the protected paclitaxel derivative **1.5**, which can be deprotected to give paclitaxel.



Scheme 1.1

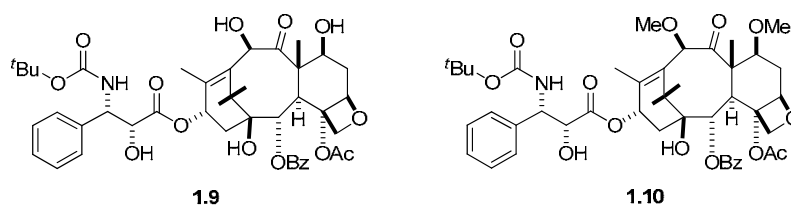
Many other semisynthetic strategies from baccatin III to paclitaxel have been established, most of which also involve cyclic intermediates as these minimize the steric constraints in acylating the hindered C13 hydroxyl group of baccatin III. These intermediates include oxazolidines (**1.6**),²³ oxazolines (**1.7**)²⁴ and oxazinones (**1.8**).²⁵



1.3 Docetaxel and Cabazitaxel

Docetaxel (taxotere[®]) (**1.9**) is a semisynthetic product from 10-DAB discovered by the Potier group in 1986²⁶ and found to be more active than paclitaxel in some assays. Docetaxel entered phase I clinical trials in 1990²⁷ and was approved for the treatment of advanced breast cancer in 1996 and for non-small cell lung cancer in 1999.²⁸

Cabazitaxel (Jevtana[®]) (**1.10**) is another semisynthetic derivative of paclitaxel developed by Sanofi-Aventis. It was recently approved by FDA for the treatment of hormone-refractory prostate cancer.²⁹



1.4 Medicinal Chemistry and Structure-Activity Relationships

With the success of paclitaxel as a powerful anticancer drug, its medicinal chemistry has been extensively studied. Virtually every position of the molecule has been modified and numerous analogs have been prepared.³⁰⁻³² None of these analogs has yet proved to be clinically useful except the above mentioned compounds docetaxel (**1.9**) and cabazitaxel (**1.10**). The SAR of paclitaxel can be summarized by Figure 1.1.³¹

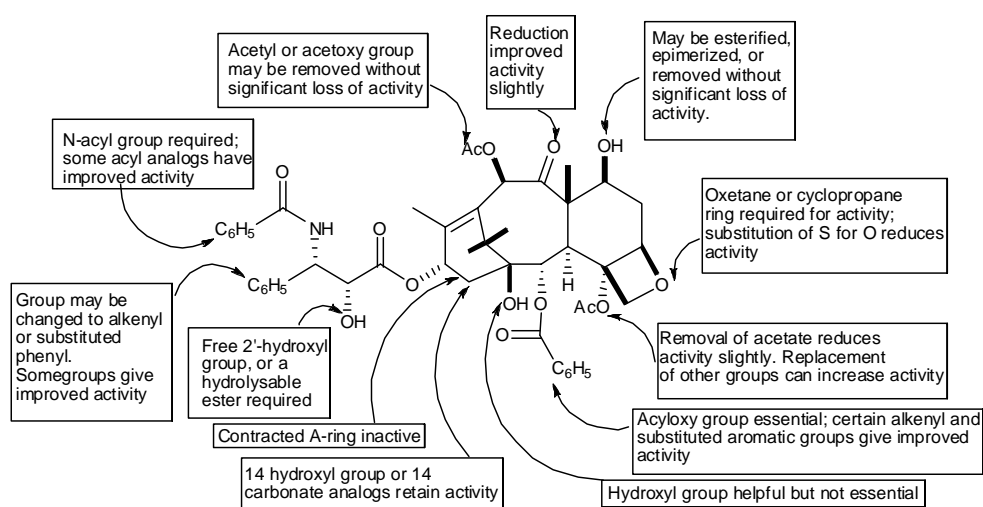


Figure 1.1 The Structure-Activity Relationships of Paclitaxel³¹

The unique tetracyclic core of paclitaxel was proved to be important to maintain the optimum conformation and drug-protein interaction. However, it was found that not all

functional groups in the main body of paclitaxel contribute to the bioactivity significantly. In general, it is believed that the northern hemisphere is not as crucial and can tolerate structural modifications better than the southern hemisphere.

It was reported that hydroxylation of the C6 position reduced the bioactivity by 30 fold.³³ Acylation and dehydroxylation of the C7 position did not change the activity significantly.³⁴⁻³⁸ However, oxidation of the C7 hydroxy group to a ketone significantly decreased the activity of paclitaxel because it facilitated the opening of the oxetane ring at the C4-C5 position.³⁹ The carbonyl group at the C9 position can be reduced to a hydroxyl group without loss of bioactivity.⁴⁰ Deacetylation at the C10 position preserved the activity of paclitaxel.⁴¹ The formation of a C7-C8-C19 cyclopropane ring did not dramatically affect the binding of paclitaxel to the microtubule binding site.^{41,42}

In comparison with the northern hemisphere, the southern hemisphere is far more essential for paclitaxel to maintain its activity. This region is believed to play a more important role in maintaining the optimum conformation of paclitaxel, and the modifications in the southern hemisphere affect the bioactivity of paclitaxel. Dehydroxylation at the C1 position decreased the activity slightly, indicating that the C1 hydroxy group is helpful but not essential.⁴³ The C2 benzyloxy group was proved to be crucial for the bioactive conformation, and aromatic substitutions affect the activity of paclitaxel dramatically.⁴⁴ Interestingly, analogs with the *meta* position substituted by certain functional groups or with the benzyloxy group replaced by certain alkenyl groups gave improved bioactivities.⁴⁵ Both the stereochemistries at the C2 and C13 positions were proved to be essential for the activity of paclitaxel.^{46,47} The removal of the acetate group at the C4 position decreases the activity significantly, but replacement by

the methyl carbonate group improves the activity.⁴⁸⁻⁵³ The oxetane ring at the C4-C5 position is required and the opening of the four-membered ring decreases the bioactivity significantly.⁵⁴ Paclitaxel analogs with oxygen replaced by sulfur⁵⁵ or nitrogen⁵⁶ gave poor activity, but the paclitaxel analog with the oxetane ring replaced with a cyclopropane ring was still active.⁵⁷ Hydroxylation at the C14 position does not affect the activity of paclitaxel.^{58,59}

The side chain at the C13 position of paclitaxel is crucial for the maintenance of its bioactive conformation and tubulin-binding activity. Its removal leads to dramatic reduction or total loss of the activity, and major modifications on the side chain affect the activity significantly in either positive or negative ways. An important example is docetaxel, which has a side chain with the *N*-benzoyl group of paclitaxel replaced by an *N*-Boc group at the C3' position, and shows better tubulin-binding activity and cytotoxicity than paclitaxel, indicating that well-manipulated modifications on the side chain can improve the activity of paclitaxel.

The stereochemistries at the C2' and C3' positions have been investigated and analogs with the naturally occurring stereochemistry always had better bioactivity than others with different stereochemistries.³⁴ The free C2' hydroxyl group or a hydrolysable ester is required for the activity of paclitaxel.^{34,60,61} The insertion of a methylene group between the C1' and C2' positions reduces the activity dramatically.⁶² The phenyl group at the C3' position can be replaced by large alkyl groups, alkenyl groups or substituted phenyl groups without losing the activity.⁶³ In some cases the replacement even improves the activity, but replacement with small alkyl groups such as the methyl group results in a significant loss of activity.³⁴ The *N*-acyl group at the C3' position is crucial for good

bioactivity, but modifications are still allowed and some of the acyl analogs have improved activity.³⁴

1.5 Mechanism of Action of Paclitaxel

Paclitaxel promotes the polymerization of tubulin into microtubules and stabilizes them, leading to cell death by apoptosis. In the cell cycle the mitotic spindle, composed of microtubules and some proteins, must be created for the chromosomes to separate, and after that it must be destroyed. Therefore, many anticancer chemotherapeutic drugs are designed to interfere with this subcellular target.⁶⁴ This discovery spurred great interest among researchers, and spurred efforts to overcome the problems associated with paclitaxel.

Microtubules are long, hollow cylinders with an outer diameter of 25 nm, and an inner diameter of about 15 nm. They are formed by polymerization of α - and β -tubulin dimers, which are structurally similar but distinct proteins with molecular weight about 50,000, and there is about 35-40% homology between them. In the presence of guanosine 5'-triphosphate (GTP) and magnesium ions, α -tubulin and β -tubulin form a dimer with a dissociation constant of about 10^{-6} mol/L. Each α -tubulin and β -tubulin molecule associates with one GTP molecule. The dimers then start to form a nucleation center for further polymerization to form protofilaments. Continuous growth occurs both along and perpendicular to the axis of the initial protofilaments in a slightly staggered manner, and the edge filaments meet together to form a microtubule with a left-handed helix.⁶⁵ A normal microtubule is formed by 13 protofilaments.⁶⁶ In a cell, the formation and decomposition of microtubules are at equilibrium, with constant loss and gain of tubulin

subunits at both ends. The formation and decomposition of microtubules are totally reversible processes during a normal cell cycle.^{67,68}

Microtubule-targeted chemotherapeutic anticancer drugs act by interfering with the exchange of tubulin subunits between the microtubules and the free tubulin in the mitotic spindle. There are two types of drugs defined by this mechanism.^{69, 70} One class of cytotoxic agents, which includes colchicine, vinblastine and vincristine, prevents the polymerization of microtubules. These compounds bind to tubulin and prevent microtubule polymerization, resulting in the rapid disappearance of the mitotic spindle and leading many abnormally dividing cells to die.⁷¹ In contrast, members of the other class of cytotoxic agents, including paclitaxel, the epothilones, and discodermolide, promote the polymerization of microtubules.⁷² Microtubule polymerization-promoting agents shift the tubulin-microtubule equilibrium towards the formation of microtubules by decreasing both the critical concentration of tubulin for polymerization and the induction time for polymerization.

In the presence of paclitaxel, the microtubules formed are quite different from those formed under normal conditions. Compared with normal microtubules, they are thinner with a mean diameter of 22 nm rather than 24 nm, and they are composed of 12 protofilaments, instead of 13. The binding site of paclitaxel is found to be on the β -tubulin subunit.^{72,73}

The determination of the taxol binding conformation on tubulin is important to understand the molecular mechanism of this binding and to achieve a logical understanding of the design of better anticancer analogues. This will be discussed in the next chapter.

References:

1. Wani, M. C.; Taylor, H. L.; Wall, M. E.; Coggon, P.; McPhail, A. T. Plant Antitumor Agents. VI. The Isolation and Structure of Taxol, a Novel Antileukemic and Antitumor Agent from *Taxus brevifolia*. *J. Am. Chem. Soc.* **1971**, *93*, 2325-2327.
2. Baloglu, E.; Miller, M. L.; Cavanagh, E. E.; Marien, T. P.; Roller, E. E.; Chari, R. V. J. A Facile One-Pot Synthesis of 7-Triethylsilylbaccatin III. *Synlett* **2005**, *5*, 0817-0818.
3. Fuchs, D. A.; Johnson, R. K. Cytologic Evidence That Taxol, an Antineoplastic Agent From *Taxus brevifolia*, Acts as a Mitotic Spindle Poison. *Cancer Treat. Rep.* **1978**, *62*, 1219-1222.
4. Schiff, P. B.; Fant, J.; Horwitz, S. B. Promotion of Microtubule Assembly *in vitro* by Taxol. *Nature* **1979**, *277*, 665-667.
5. Wilson, L.; Jordan, M. A. Microtubule Dynamics: Taking Aim at a Moving Target. *Chem. Biol.* **1995**, *2*, 569-573.
6. McGuire, W. P.; Rowinsky, E. K.; Rosenshein, N. B.; Grumbine, F. C.; Ettinger, D. S.; Armstrong, D. K.; Donehower, R. C. Taxol: A Unique Antineoplastic Agent with Significant Activity in Advanced Ovarian Epithelial Neoplasms. *Ann. Intern. Med.* **1989**, *111*, 273-279.
7. Holmes, F. A.; Walters, R. S.; Theriault, R. L.; Forman, A. D.; Newton, L. K.; Raber, M. N.; Buzdar, A. U.; Frye, D. K.; Hortobagyi, G. N. Phase II Trial of Taxol, an Active Drug in the Treatment of Metastatic Breast Cancer. *J. Nat. Cancer Inst.* **1991**, *83*, 1797-1805.

8. Wood, A. J. J.; Rowinsky, E. K.; Donehower, R. C. Paclitaxel (Taxol). *N. Engl. J. Med.* **1995**, *332*, 1004-1014.
9. Grem, J. L.; Tutsch, K. D.; Simon, K. J.; Alberti, D. B.; Willson, J. K. V.; Tormey, D. C.; Swaminathan, S.; Trump, D. L. Phase I Study of Taxol Administered as a Short IV Infusion Daily for 5 Days. *Cancer Treat. Rep.* **1987**, *71*, 1179-1184.
10. Donehower, R. C.; Rowinsky, E. K.; Grochow, L. B.; Longnecker, S. M.; Ettinger, D. S. Phase I Trial of Taxol in Patients with Advanced Cancer. *Cancer Treat. Rep.* **1987**, *71*, 1171-1177.
11. Rowinsky, E. K.; Burke, P. J.; Karp, J. E.; Tucker, R. W.; Ettinger, D. S.; Donehower, R. C. Phase I and Pharmacodynamic Study of Taxol in Refractory Acute Leukemias *Cancer Res.* **1989** *49*, 4640-4647
12. Holton, R. A.; Somoza, C.; Kim, H.-B.; Liang, F.; Biediger, R. J.; Boatman, P. D.; Shindo, M.; Smith, C. C.; Kim, S.; Nadizadeh, H.; Suzuki, Y.; Tao, C.; Vu, P.; Tang, S.; Zhang, P.; Murthi, K. K.; Gentile, L. N.; Liu, J. H. First Total Synthesis of Taxol. 1. Functionalization of the B Ring. *J. Am. Chem. Soc.* **1994**, *116*, 1597-1598.
13. Holton, R. A.; Kim, H.-B.; Somoza, C.; Liang, F.; Biediger, R. J.; Boatman, P. D.; Shindo, M.; Smith, C. C.; Kim, S.; Nadizadeh, H.; Suzuki, Y.; Tao, C.; Vu, P.; Tang, S.; Zhang, P.; Murthi, K. K.; Gentile, L. N.; Liu, J. H. First Total Synthesis of Taxol. 2. Completion of the C and D Rings. *J. Am. Chem. Soc.* **1994**, *116*, 1599-1600.
14. Nicolaou, K. C.; Yang, Z.; Liu, J. J.; Ueno, H.; Nantermet, P. G.; Guy, R. K.; Claiborne, C. F.; Renaud, J.; Couladouros, E. A.; Paulvannan, K.; Sorensen, E. J. Total Synthesis of Taxol. *Nature* **1994**, *367*, 630-634.

15. Danishefsky, S. J.; Masters, J. J.; Young, W. B.; Link, J. T.; Snyder, L. B.; Magee, T. V.; Jung, D. K.; Isaacs, R. C. A.; Bornmann, W. G.; Alaimo, C. A.; Coburn, C. A.; Di Grandi, M. J. Total Synthesis of Baccatin III and Taxol. *J. Am. Chem. Soc.* **1996**, *118*, 2843-2859.
16. Wender, P. A.; Marquess, D. G.; McGrane, L. P.; Taylor, R. E. First Total Synthesis of Taxol. 1. Functionalization of the B Ring and First Total Synthesis of Taxol. 2. Completion of the C and D Rings. Total Synthesis of Taxol. *Chemtracts: Org. Chem.* **1994**, *7*, 160-171.
17. Wender, P. A.; Glass, T. E. The Pinene Approach to Taxanes 2: Development of a Versatile C₉,C₁₀ Linker. *Synlett Lett.* **1995**, 516-518.
18. Kusama, H.; Hara, R.; Kawahara, S.; Nishimori, T.; Kashima, H.; Nakamura, N.; Morihira, K.; Kuwajima, I. Enantioselective Total Synthesis of (-)-Taxol. *J. Am. Chem. Soc.* **2000**, *122*, 3811-3820.
19. Mukaiyama, T.; Shiina, I.; Iwadare, H.; Saitoh, M.; Nishimura, T.; Ohkawa, N.; Sakoh, H.; Nishimura, K.; Tani, Y.-I.; Hasegawa, M.; Yamada, K.; Saitoh, K. Asymmetric Total Synthesis of Taxol. *Chem. Eur. J.* **1999**, *5*, 121-161.
20. Wuts, P. G. M. Semisynthesis of Taxol. *Curr. Opin. Drug Discovery Dev.* **1998**, *1*, 329-337.
21. Holton, R. A.; Biediger, R. J.; Boatman, P. D., Semisynthesis of Taxol and Taxotere. In *Taxol: Science and Applications*, Suffness, M., Ed. CRC Press, Inc.: Boca Raton, FL, 1995; pp 97-121.
22. Ojima, I.; Habus, I.; Zhao, M.; Zucco, M.; Park, Y. H.; Sun, C. M.; Brigaud, T. New and Efficient Approaches to the Semisynthesis of Taxol and its C-13 Side

- Chain Analogs by Means of β -Lactam Synthon Method. *Tetrahedron* **1992**, *48*, 6985-7012.
23. Commercon, A.; Bezard, D.; Bernard, F.; Bourzat, J. D. Improved Protection and Esterification of a Precursor of the Taxotere and Taxol Side Chains. *Tetrahedron Lett.* **1992**, *33*, 5185-5188.
24. Kingston, D. G. I.; Chaudhary, A. G.; Gunatilaka, A. A. L.; Middleton, M. L. Synthesis of Taxol from Baccatin III via an Oxazoline Intermediate. *Tetrahedron Lett.* **1994**, *35*, 4483-4484.
25. Swindell, C. S.; Krauss, N. E.; Horwitz, S. B.; Ringel, I. Biologically Active Taxol Analogues with Deleted A-Ring Side Chain Substituents and Variable C-2' Configurations. *J. Med. Chem.* **1991**, *34*, 1176-1184.
26. Gueritte-Voegelein, F.; Senilh, V.; David, B.; Guenard, D.; Potier, P. Chemical Studies of 10-Deacetyl Baccatin III. Hemisynthesis of Taxol Derivatives. *Tetrahedron* **1986**, *42*, 4451-4460
27. Bissery, M.-C.; Nohynek, G.; Sanderink, G.-J.; Lavelle, F. Docetaxel (Taxotere): a Review of Preclinical and Clinical Experience. Part I: Preclinical Experience. *Anti-Cancer Drugs* **1995**, *6*, 339-355.
28. Gueritte, F. General and Recent Aspects of the Chemistry and Structure-Activity Relationships of Taxoids. *Curr. Pharm. Des.* **2001**, *7*, 1229-1249.
29. Galsky, M. D.; Dritselis, A.; Kirkpatrick, P.; Oh, W. K. Cabazitaxel. *Nat. Rev. Drug Discov.* **2010**, *9*, 677-678.

30. Kingston, D. G. I.; Jagtap, P. G.; Yuan, H.; Samala, L., The Chemistry of Taxol and Related Taxoids. In *Progress in the Chemistry of Organic Natural Products*, Herz, W.; Falk, H.; Kirby, G. W., Eds. Springer: Wien, 2002; Vol. 84, pp 53-225.
31. Kingston, D. G. I., Taxol and Its Analogs. In *Anticancer Agents from Natural Products*, Gordon M. Cragg, D. G. I. K., David J. Newman, Ed. Taylor and Francis: Boca Raton, Florida, 2005; pp 89-122.
32. Fu, Y.; Li, S.; Zu, Y.; Yang, G.; Yang, Z.; Luo, M.; Jiang, S.; Wink, M.; Efferth, T. Medicinal Chemistry of Paclitaxel and its Analogues. *Curr. Med. Chem.* **2009**, *16*, 3966-3985.
33. Harris, J. W.; Katki, A.; Anderson, L. W.; Chmurny, G. N.; Paukstelis, J. V.; Collins, J. M. Isolation, Structural Determination, and Biological Activity of 6a-Hydroxytaxol, the Principal Human Metabolite of Taxol. *J. Med. Chem.* **1994**, *37*, 706-709.
34. Gueritte-Voegelein, F.; Guenard, D.; Lavelle, F.; Le Goff, M.-T.; Mangatal, L.; Potier, P. Relationships between the Structure of Taxol Analogues and Their Antimitotic Activity. *J. Med. Chem.* **1991**, *34*, 992-998.
35. Lataste, H.; Senilh, V.; Wright, M.; Guenard, D.; Potier, P. Relationships between the Structures of Taxol and Baccatine III Derivatives and Their *in vitro* Action on the Disassembly of Mammalian Brain and Physarum Amoebal Microtubules. *Proc. Natl. Acad. Sci. U.S.A.* **1984**, *81*, 4090-4094.
36. Mathew, A. E.; Mejillano, M. R.; Nath, J. P.; Himes, R. H.; Stella, V. J. Synthesis and Evaluation of Some Water-Soluble Prodrugs and Derivatives of Taxol with Antitumor Activity. *J. Med. Chem.* **1992**, *35*, 145-151.

37. Kingston, D. G. I.; Samaranayake, G.; Ivey, C. A. The chemistry of taxol, a clinically useful anticancer agent. *J. Nat. Prod.* **1990**, *53*, 1-12.
38. Chaudhary, A. G.; Rimoldi, J. M.; Kingston, D. G. I. Modified Taxols. 10. Preparation of 7-Deoxytaxol, a Highly Bioactive Taxol Derivative, and Interconversions of Taxol and 7-*epi*-Taxol. *J. Org. Chem.* **1993**, *58*, 3798-3799.
39. Magri, N. F.; Kingston, D. G. I. Modified Taxols. 2. Oxidation Products of Taxol. *J. Org. Chem.* **1986**, *51*, 797-802.
40. Klein, L. L. Synthesis of 9-Dihydrotaxol: A Novel Bioactive Taxane. *Tetrahedron Lett.* **1993**, *34*, 2047-2050.
41. Chen, S.-H.; Huang, S.; Wei, J.; Farina, V. Serendipitous Synthesis of a Cyclopropane-Containing Taxol Analog via Anchimeric Participation of an Unactivated Angular Methyl Group. *J. Org. Chem.* **1993**, *58*, 4520-4521.
42. Margraff, R.; Bezdard, D.; Bourzat, J. D.; Commercon, A. Synthesis of 19-Hydroxy Docetaxel from a Novel Baccatin. *Bioorg. Med. Chem. Lett.* **1994**, *4*, 233-236.
43. Kingston, D. G. I.; Chordia, M. D.; Jagtap, P. G. Synthesis and Biological Evaluation of 1-Deoxytaxol Analogues. *J. Org. Chem.* **1999**, *64*, 1814-1822.
44. Chen, S.-H.; Wei, J.-M.; Farina, V. Taxol Structure-Activity Relationships: Synthesis and Biological Evaluation of 2-Deoxytaxol. *Tetrahedron Lett.* **1993**, *34*, 3205-3206.
45. Chaudhary, A. G.; Gharpure, M. M.; Rimoldi, J. M.; Chordia, M. D.; Gunatilaka, A. A. L.; Kingston, D. G. I.; Grover, S.; Lin, C. M.; Hamel, E. Unexpectedly Facile Hydrolysis of the 2-Benzoate Group of Taxol and Synthesis of Analogs with Increased Activities. *J. Am. Chem. Soc.* **1994**, *116*, 4097-4098.

46. Chordia, M. D.; Kingston, D. G. I. Synthesis and Biological Evaluation of 2-*epi*-Paclitaxel. *J. Org. Chem.* **1996**, *61*, 799-801.
47. Hoemann, M. Z.; Vander Velde, D.; Aube, J.; Georg, G. I.; Jayasinghe, L. R. Synthesis of 13-*epi*-Taxol via a Transannular Delivery of a Borohydride Reagent. *J. Org. Chem.* **1995**, *60*, 2918-2921.
48. Datta, A.; Jayasinghe, L. R.; Georg, G. I. 4-Deacetyltaxol and 10-Acetyl-4-deacetyltaxotere: Synthesis and Biological Evaluation *J. Med. Chem.* **1994**, *37*, 4258-4260.
49. Neidigh, K. A.; Gharpure, M. M.; Rimoldi, J. M.; Kingston, D. G. I.; Jiang, Y. Q.; Hamel, E. Synthesis and Biological Evaluation of 4-Deacetylpaclitaxel. *Tetrahedron Lett.* **1994**, *35*, 6839-6842.
50. Chen, S.-H.; Kadow, J. F.; Farina, V.; Fairchild, C. R.; Johnston, K. A. First Syntheses of Novel Paclitaxel(Taxol) Analogs Modified at the C4-Position. *J. Org. Chem.* **1994**, *59*, 6156-6158.
51. Georg, G. I.; Ali, S. M.; Boge, T. C.; Datta, A.; Falborg, L.; Himes, R. H. Selective C-2 and C-4 Deacylation and Acylation of Taxol: The First Synthesis of a C-4 Substituted Taxol Analogue. *Tetrahedron Lett.* **1994**, *35*, 8931-8934.
52. Chen, S.-H.; Fairchild, C.; Long, B. H. Synthesis and Biological Evaluation of Novel C-4 Aziridine Bearing Paclitaxel (Taxol) Analogs. *J. Med. Chem* **1995**, *38*, 2263-2267.
53. Chen, S.-H.; Wei, J.-M.; Long, B. H.; Fairchild, C. A.; Carboni, J.; Mamber, S. W.; Rose, W. C.; Johnston, K.; Casazza, A. M.; Kadow, J. F.; Farina, V.; Vyas, D.;

- Doyle, T. W. Novel C-4 Paclitaxel (Taxol) Analogs: Potent Antitumor Agents. *Bioorg. Med. Chem. Lett.* **1995**, *5*, 2741-2746.
54. Samaranayake, G.; Magri, N. F.; Jitrangsri, C.; Kingston, D. G. I. Modified Taxols. 5. Reaction of Taxol with Electrophilic Reagents, and Preparation of a Rearranged Taxol Derivative with Tubulin Assembly Activity. *J. Org. Chem.* **1991**, *56*, 5114-5119.
55. Gunatilaka, A. A. L.; Ramdayal, F. D.; Sarragiotto, M. H.; Kingston, D. G. I.; Sackett, D. L.; Hamel, E. Synthesis and Biological Evaluation of Novel Paclitaxel (Taxol) D-Ring Modified Analogues. *J. Org. Chem.* **1999**, *64*, 2694-2703.
56. Marder-Karsenti, R.; Dubois, J.; Bricard, L.; Guenard, D.; Gueritte-Voegelein, F. Synthesis and Biological Evaluation of D-Ring-Modified Taxanes: 5(20)-Azadocetaxel Analogs. *J. Org. Chem.* **1997**, *62*, 6631-6637.
57. Dubois, J.; Thoret, S.; Gueritte, F.; Guenard, D. Synthesis of 5(20)deoxydocetaxel, a New Active Docetaxel Analogue. *Tetrahedron Lett.* **2000**, *41*, 3331-3334.
58. Chen, S.-H.; Huang, S.; Kant, J.; Fairchild, C.; Wei, J.; Farina, V. Synthesis of 7-Deoxy- and 7,10-Dideoxytaxol via Radical Intermediates. *J. Org. Chem.* **1993**, *58*, 5028-5029.
59. Samaranayake, G.; Magri, N. F.; Jitrangsri, C.; Kingston, D. G. I. Modified Taxols. 5. Reaction of Taxol with Electrophilic Reagents and Preparation of a Rearranged Taxol Derivative with Tubulin Assembly Activity. *J. Org. Chem.* **1991**, *56*, 5114-5119.
60. Kant, J.; Huang, S.; Wong, H.; Fairchild, C.; Vyas, D.; V., F. Studies toward Structure-Activity Relationships of Taxol: Synthesis and Cytotoxicity of Taxol

Analogues with C-2' Modified Phenylisoserine Side Chains. *Bioorg. Med. Chem. Lett.* **1993**, *3*, 2471-2474.

61. Magri, N. F.; Kingston, D. G. I. Modified Taxols. 4. Synthesis and Biological Activity of Taxols Modified in the Side Chain. *J. Nat. Prod.* **1988**, *51*, 298-306.
62. Jayasinghe, L. R.; Datta, A.; Ali, S. M.; Zygmunt, J.; Vander Velde, D. G.; Georg, G. I. Structure-Activity Studies of Antitumor Taxanes: Synthesis of Novel C-13 Side Chain Homologated Taxol and Taxotere Analogs. *J. Med. Chem.* **1994**, *37*, 2981-2984.
63. Kingston, D. G. I., History and Chemistry. In *Paclitaxel in Cancer Treatment*, McGuire, W. P.; Rowinsky, E. K., Eds. Marcel Dekker, Inc.: New York, Basel, Hong Kong, 1995; Vol. 8, pp 1-33.
64. Geney, R.; Sun, L.; Pera, P.; Bernacki, R. J.; Xia, S.; Horwitz, S. B.; Simmerling, C. L.; Ojima, I. Use of the Tubulin Bound Paclitaxel Conformation for Structure-Based Rational Drug Design. *Chem. Biol.* **2005**, *12*, 339-348.
65. Purich, D. L.; Kristofferson, D. Microtubule Assembly: A Review of Progress, Principles, and Perspectives. *Adv. Protein Chem.* **1984**, *36*, 133-211
66. Olmsted, J. B. Non-motor Microtubule-associated Proteins. *Curr. Opin. Cell Biol.* **1991**, *3*, 52-58.
67. Andreu, J. M.; Bordas, J.; Diaz, J. F.; Garcia de Ancos, J.; Gil, R.; Medran, F. J.; Nogales, E.; Pantos, E.; Towns-Andrews, E. Low Resolution Structure of Microtubules in Solution. Synchrotron X-ray Scattering and Electron Microscopy of Taxol-Induced Microtubules Assembled from Purified Tubulin in Comparison with Glycerol and MAP-Induced Microtubules. *J. Mol. Biol.* **1992**, *226*, 169-184.

68. Haimo, L. T. Dynein Decoration of Microtubules - Determination of Polarity. *Methods Cell Bio.* **1982**, *24*, 189-206.
69. DeBrabander, M. Microtubule Dynamics during the Cell Cycle: The Effects of Taxol and Nocodazole on the Microtubule System of Pt K2 Cells at Different Stages of the Mitotic Cycle. *Int. Rev. Cytol.* **1986**, *101*, 215-274.
70. Inouse, S. Cell Division and the Mitotic Spindle. *J. Cell. Biol.* **1981**, *91*, 131-147.
71. Salmon, E. D.; McKeel, M.; Hays, T. Rapid Rate of Tubulin Dissociation from Microtubules in the Mitotic Spindle *in vivo* Measured by Blocking Polymerization with Colchicine. *J. Cell. Biol.* **1984**, *99*, 1066-1075.
72. Rao, S.; Horwitz, S. B.; Ringel, I. Direct Photoaffinity Labeling of Tubulin with Taxol. *J. Natl. Cancer Inst.* **1992**, *84*, 785-788.
73. Schibler, M. J.; Huang, B. The *col^R4* and *col^R15* β -Tubulin Mutations in *Chlamydomonas reinhardtii* Confer Altered Sensitivities to Microtubule Inhibitors and Herbicides by Enhancing Microtubule Stability. *J. Cell Biol.* **1991**, *113*, 605-614.

Chapter 2. The Bioactive Conformation of Paclitaxel

2.1 Determination of the Bioactive Conformation of Paclitaxel

The determination of the binding mode and binding conformation of paclitaxel on tubulin is essential to fundamentally understand the molecular mechanism of this binding and to achieve rational design of new antimitotic agents. However it was not until the beginning of this century that this goal was achieved. The difficulty was partly due to the structural complexity of the paclitaxel molecule with four flexible side chains, which could generate numerous conformations, as well as the lack of a structure of the binding site with atomic resolution.

Paclitaxel was discovered as a promoter of tubulin polymerization in 1979.¹ Early photoaffinity labeling studies showed that paclitaxel bound to β -tubulin.²⁻³ In one photoaffinity labeling study,² 3'-*N*-(*p*-azidobenzoyl)paclitaxel photolabeled the N-terminal 31 amino acids of β -tubulin, while in another study³ 2-debenzoyl-2-(*m*-azidobenzoyl)paclitaxel photolabeled amino acids 217-231 of β -tubulin, which defined a second element of the binding site.

An important discovery was made in 1998, when an atomic model of the α,β -tubulin dimer with a resolution of 3.7Å was obtained by electron crystallography of zinc induced tubulin sheets stabilized by paclitaxel,⁴ and this was later refined to 3.5 Å.⁵ The X-ray crystallographic structure of docetaxel was docked into the electron density map of the tubulin. In this map, the electron density of the rigid taxane ring was found, but unfortunately that of the flexible side chains was not clear due to the low resolution. Nonetheless, the location of the drug was consistent with the photoaffinity labeling

studies stated above. This discovery became a milestone in understanding the binding conformation of paclitaxel, in that it allowed studies integrating computer models of the experimentally obtained electron crystallographic data with those of proposed paclitaxel conformations.

Solution NMR spectroscopy was the most commonly applied spectroscopic method in early studies of the conformational assignment of paclitaxel in its uncomplexed state. Such studies in nonpolar⁶⁻⁹ and polar solvents^{8,10-11} yielded two proposed models, namely the “Nonpolar” and “Polar” models, respectively. The former was characterized by hydrophobic interactions between the benzoyl group on C2 and the C-3' benzamido phenyl. However, in polar solvents, hydrophobic collapse occurs between the C-3' phenyl group and the C-2 benzoyl phenyl.¹² Both the nonpolar and polar conformations had then been proposed to be the bioactive forms.

In spite of these numerous early NMR studies, it was pointed out by Snyder¹³ that the common fundamental proposition underlying all these studies was that the molecule only adopts one single or largely dominant conformation in solution, and this structure leads to the experimental NMR data. This interpretation is incomplete, since with the existence of several easily rotatable single bonds the molecule is unlikely to adopt only one conformation in solution at ambient temperature. In a reexamination of the paclitaxel conformation in chloroform with the NMR Analysis of Molecular Flexibility in Solution (NAMFIS) methodology by Snyder and his coworkers, several distinct conformers were identified with populations from 1% to 35%. Among them was the so-called “T-taxol” conformation, which is a minor conformer (less than 3% in population).¹³

The conformation of uncomplexed paclitaxel in the solid state was studied by X-ray crystallography.¹⁴⁻¹⁵ The first crystallographic structure of a paclitaxel analogue, docetaxel, was published by Guéritte-Voegelein¹⁴ in 1990 before most of the NMR studies were carried out. This solid-state conformation of docetaxel was later¹⁶⁻¹⁷ found to resemble the nonpolar conformation of paclitaxel deduced by NMR studies. In a similar study of paclitaxel in 1995, two different conformations were obtained in a single crystal unit cell.¹⁵ One of them was consistent with the “polar” conformation in solution, while the other was a new conformer that had not been identified by previous studies. All these conformations, together with those derived from NMR studies, provided a large number of 3-dimensional paclitaxel structures for molecular modeling studies^{11,18} of the docking of paclitaxel into the β -tubulin binding site.

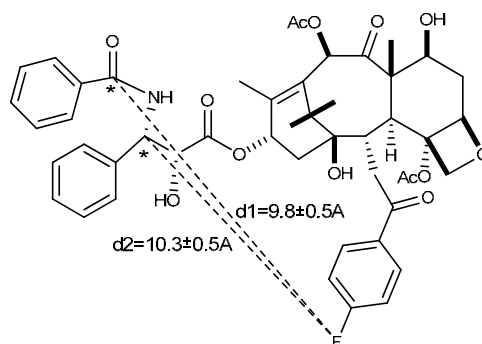


Figure 2.1 ^{13}C - ^{19}F Intramolecular distances indicated by REDOR-NMR¹⁹

Solid state rotational echo double resonance NMR (REDOR-NMR) and fluorescence spectroscopy are techniques capable of providing information on the paclitaxel orientation and conformation in the bound state. In one study¹⁹ a combination of these two approaches yielded data in support of a hydrophobically collapsed conformation. It is noticeable that REDOR studies on an isotopically-labeled tubulin-bound paclitaxel

allowed the determination of the distances between ^{19}F at the para-position of the C-2 benzoyl group and ^{13}C atoms at the 3'-amide carbonyl and the C-3' methine carbons. The measured values were $9.8 \pm 0.5 \text{ \AA}$ and $10.3 \pm 0.5 \text{ \AA}$, respectively, which are consistent with both the polar conformation and the T-taxol conformation (Figure 2.1).

In 2001, the Snyder group proposed that the T-taxol conformation was the tubulin-bound conformation based on computational studies.¹¹ This model is characterized by equidistance between the C-2 benzoyl phenyl and both of the phenyl rings emanating from C-3' (Figure 2.2). In this study a large number of paclitaxel conformers were docked individually into the experimental density map of the paclitaxel site on β -tubulin. Among these paclitaxel conformers, 26 were derived from the former X-ray crystallographic²⁰⁻²¹ and NMR studies^{6-8,10,13,22-24} and the others were computer-generated. The T-taxol conformation gave the best fit to the experimental density. The intramolecular distances between both phenyls emanating from C-3' and the C-2 benzoyl phenyl obtained in this study were similar to those obtained in the previous REDOR-NMR study on labeled tubulin-bound paclitaxel.¹⁹

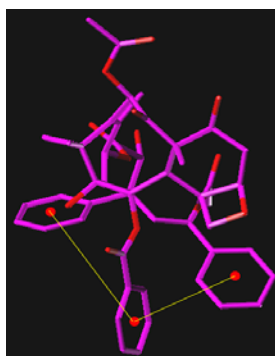


Figure 2.2 Illustration of the T-taxol model

Recently, the Ojima group proposed a REDOR-taxol model¹⁸ based on the results of the REDOR NMR studies¹⁹ mentioned above. They had previously shown that the C-7-benzodihydrocinnamoyl (C-7BzDC) derivative of paclitaxel formed a complex with tubulin, and that irradiation of this complex only labeled the Arg²⁸² residue.²⁵ Using this information, 16 conformers derived from a Monte Carlo conformational search of 2-(*p*-fluorobenzoyl)-paclitaxel were docked into tubulin. The internuclear distances acquired from these data were then compared to the experimental distances given by the previous REDOR study.¹⁹ The structure with the least deviation was considered to be the preferred binding model and was named “REDOR-taxol”. It was pointed out that this conformation differs from the T-taxol model in the orientation of the 2'-hydroxyl group. In REDOR-taxol, the 2'-hydroxyl group is H-bonded to His²²⁷, while in T-taxol similar bonding occurs with Arg³⁵⁹.¹⁸ The synthetic substantiation of this proposition will be detailed in the following chemistry section.

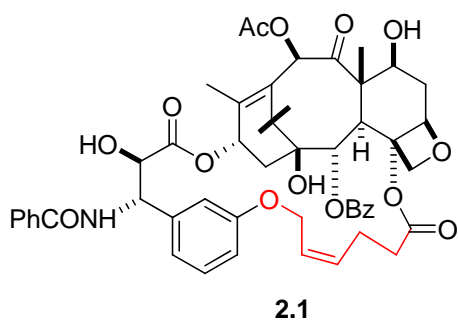
2.2 Synthetic Efforts to Make Conformationally Restricted Analogues of Paclitaxel

An understanding of the bioactive tubulin-binding conformation of paclitaxel in principle would allow molecular design and synthesis of analogues designed to constrain paclitaxel to these conformations. Subsequent evaluation of the bioactivity of the analogues could in turn provide validation of the model being tested and information for better understanding of the tubulin-bound conformation and for designing better tubulin-binding agents.

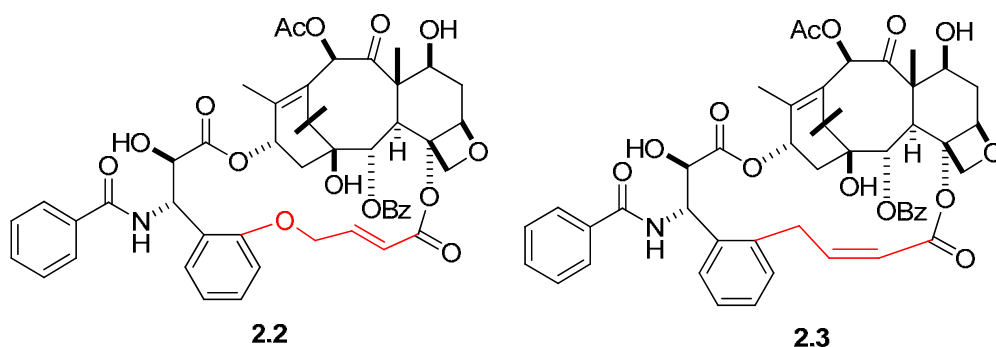
2.2.1 Validation of the T-taxol Model

After the proposal of the T-taxol model its validity was debated for two reasons: the relatively low resolution of the tubulin structure used for docking and the fact that the tubulin structure was of zinc-induced sheets rather than native microtubules. The obvious difference in the arrangement of protofilaments in the two types of tubulin aroused concerns that the binding conformation derived from the zinc-stabilized sheets may be different from the binding conformation in native microtubules.²⁶ To provide experimental evidence that T-taxol stabilizes genuine microtubules, our group has successfully constructed analogues constrained to the T-conformation.²⁷⁻²⁸ In these studies the T-conformation was achieved synthetically by bridging between the 4-OAc methyl and the C-3'-phenyl groups. This tethering strategy was developed by the analysis of the 3-D topographic diagram of proposed T-taxol model which displayed that the above two moieties are actually close to each other.²⁸ This indicates that tethering the two centers to a proper distance should mimic the parent T-conformation.

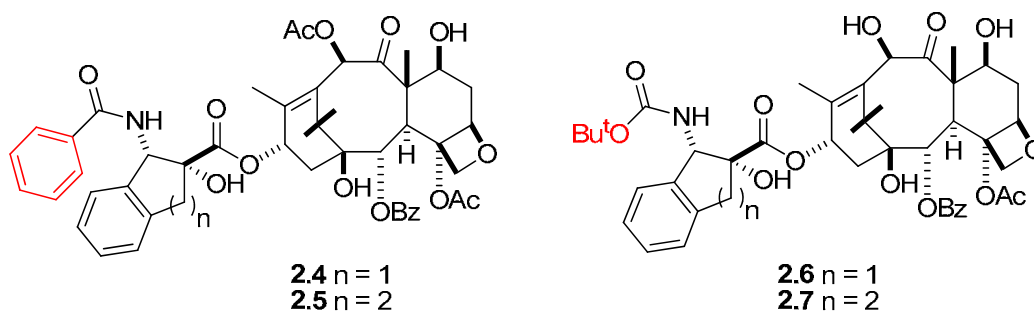
Compound **2.1** was the first analogue based on this strategy. It used a 5-atom tether between the methyl and phenyl centers.²⁷ NMR/NAMFIS analysis in solution demonstrated that the compound exists in the T conformation with a population very similar to paclitaxel itself (5%). It was then concluded that the compound should be able to achieve the conformation as a low energy form. Nonetheless, the compound proved to be 8–10 fold less active than paclitaxel in both tubulin assembly and cytotoxicity assays. A substrate-protein steric interaction between the tubulin's His-227 in the binding pocket and the lower part of the tether accounted for the absence of activity.¹¹



To overcome this problem, compounds **2.2** and **2.3** were designed and synthesized.²⁸ In these compounds the tethers contained fewer atoms and were attached to the *ortho* instead of *meta* position of the 3'-phenyl, thus forcing the bridge inside the concave baccatin core. Because of these changes, NMR/NAMFIS analysis confirmed that the molecules retained the T-shape, with a population of over 80% T-taxol in solution. As predicted, compound **2.2** was 2-fold more active in the tubulin polymerization assay and equally potent against PC3 and A2780 cell lines, and compound **2.3** was 20 times more potent than paclitaxel in the A2780 cell line. These results prove that a compound constrained to the T-taxol conformation can bind to genuine microtubules, and thus that the T-taxol structure is an excellent model of the binding conformation of paclitaxel.

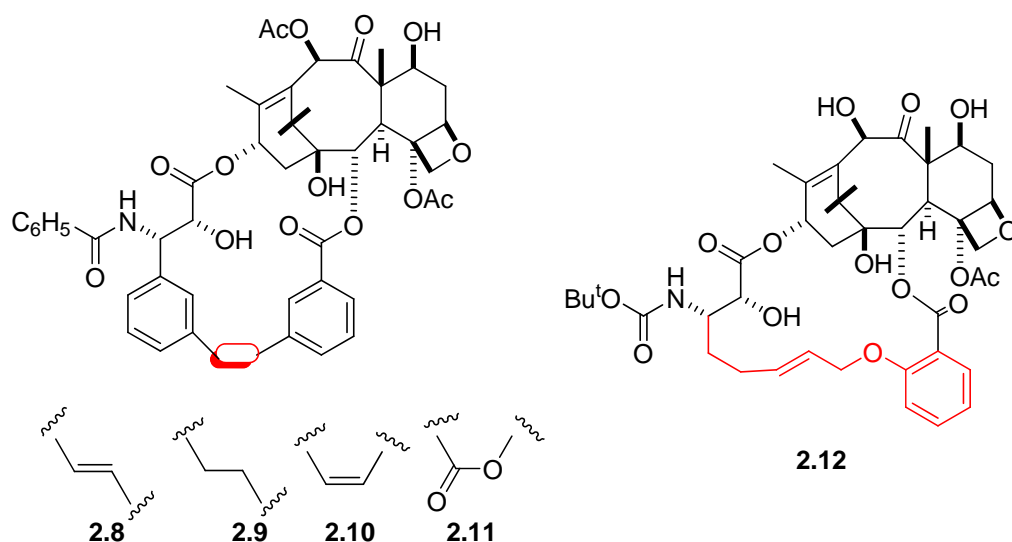


In another study by Snyder,²⁹ analogues **2.4-2.7** with conformationally constrained C-13 side chains were synthesized. The NAMFIS analysis of compound **2.4** resulted in the detection of seven conformations, among which all three types of conformation were found: “polar”, “nonpolar” and T-conformation. The latter was populated at 47%. While compounds **2.4** and **2.6** displayed tubulin binding and cytotoxicity values comparable to those of paclitaxel, the six-membered ring compounds **2.5** and **2.7** were 30-42 and 239-333 less active in tubulin binding and cytotoxicity, respectively. This sharp contrast could again be explained by the previously mentioned ligand-tubulin interaction.

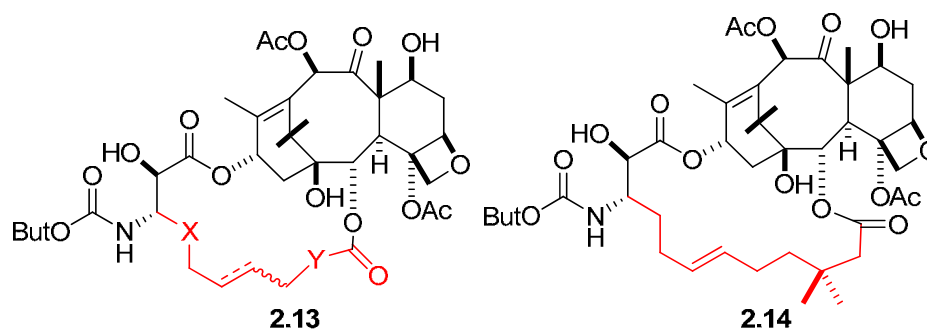


2.2.2 Other Attempts to Make Constrained Analogues for Conformational Studies

One of the earliest bridged paclitaxel analogues to mimic the “hydrophobic collapse” conformation was prepared by the Georg group,³⁰ who identified this conformation¹⁰ in solution. Short tethers were bridged between the C-2 benzoyl phenyl and C-3’ phenyl to yield compound **2.8-2.11**. Unfortunately, none of these compounds showed desirable activity in a tubulin assembly assay. It was thus concluded that the bound conformation of paclitaxel is not the “hydrophobic collapse” conformation.

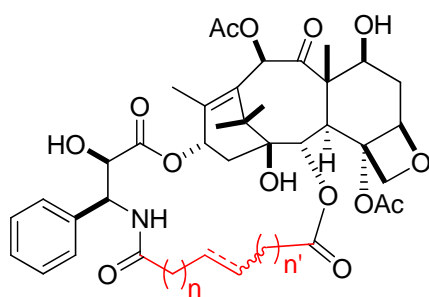


In a study aimed to build a paclitaxel-epothilone hybrid, Ojima and coworkers obtained the tethered compound **2.12**, which was found unexpectedly to adopt predominantly the hydrophobically collapsed conformation in DMSO- d_6 /D $_2$ O, based on NMR analysis. This compound exhibited submicromolar level cytotoxicity against a human breast cancer cell line and 37% of the activity of paclitaxel in the tubulin polymerization assay.³¹ In a subsequent paper,³² the same group reported the preparation of a series of macrocyclic taxoids tethered between C-3' and C-2 with variable length and composition (illustrated by **2.13**). Three of these compounds, including **2.14**, demonstrated submicromolar cytotoxicity against a human breast cancer cell line, but were not as cytotoxic as paclitaxel.

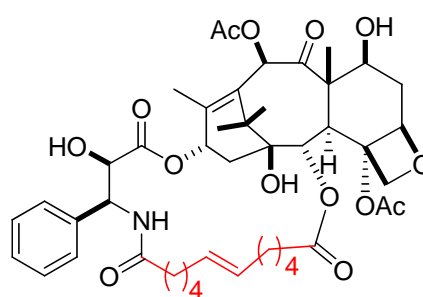


Constrained analogs were also achieved mimicking the “nonpolar” conformation which was also formerly regarded as the tubulin bound structure. This included a first effort³³ to mimic the tubulin-bound docetaxel conformation based on Nogales’s study³³⁻³⁴ in which the analogue was used as a surrogate for paclitaxel. Implanting linkers between the C-2 and C-3’ positions of the taxoid skeleton generated a group of N-linked macrocyclic taxoids (illustrated by **2.15**). In the subsequent cytotoxicity evaluation, some analogues showed submicromolar level activity. It is worth mentioning that the compounds containing linkers with *Z* double bonds were more active than those containing linkers with *E* double bonds. In a continuing study³⁴ by the same group a series of similar N-linked macrocyclic taxoids were prepared by intramolecular Heck coupling reactions. This series was reported to be more cytotoxic than the previous one. Also interestingly, *exo* compounds (illustrated by **2.16**) tended to be more active than *endo* ones (illustrated by **2.17**). No conformational analysis was reported in these two studies.

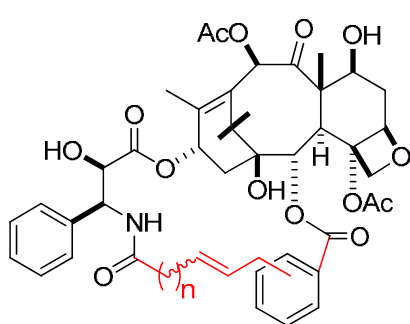
In a related study,³⁶ macrocyclic analogues bearing only carbon tethers (shown by **2.20**) were built because of a suspicion that sulfur may be deleterious to tubulin binding. Eleven cyclic compounds were subjected to evaluation of microtubule disassembly. Among them compound **2.21** was only 7-fold less active than paclitaxel in inhibiting microtubule disassembly. All the other compounds were either 30-100 fold less active than paclitaxel or inactive. In a cytotoxicity assay against the KB cell line, all compounds were found at least 1000 fold less potency than paclitaxel. The conformations of these taxoids in solution were investigated by NMR and molecular modeling studies, which indicated that compound **2.21** adopted a conformation between “nonpolar” and T-shaped. Other analogues were shown to take conformations not recognized by tubulin.



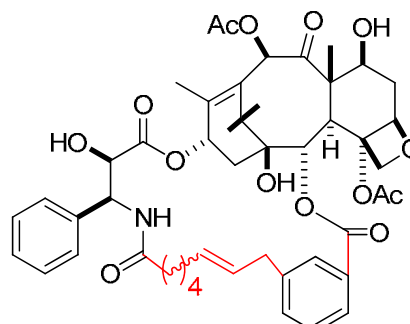
2.20



2.21

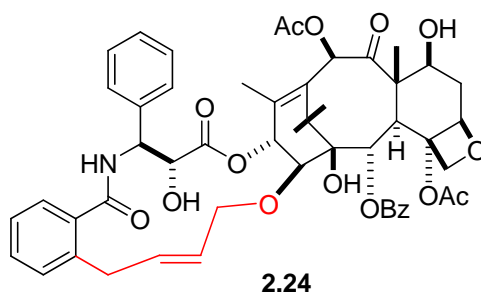


2.22



2.23

A more recent endeavor to establish bridged analogues resembling tubulin-bound docetaxel was published by Dubois and his collaborators in 2004.³⁷ The macrocyclic taxoids represented by **2.22** with varied ring sizes were constructed by inserting tethers between N-3' and the *ortho*, *meta* or *para* positions of the C-2 benzoate. Five compounds in this series were evaluated for inhibition of cold-induced microtubule disassembly and for cytotoxicity against the KB cell line. All compounds except one exhibited submicromolar IC₅₀ values against the tumor cell line. While *Z*- and *E*-**2.23** proved to be as active as paclitaxel in microtubule assembly, analogues bearing linkers to the *para* positions were totally inactive. This difference of activity is consistent with the results obtained from modeling studies, which showed selective interaction between tubulin and *meta*-substituted compounds. The possible presence of a π -stacking interaction observed between the His229-imidazolyl and C-2 benzoyl may account for the enhancement of bioactivity of these compounds compared with those obtained in the two previous studies.³⁵⁻³⁶ Computational studies suggested the molecules mainly adopt the T-conformation in solution, and a modeling study verified the T-shape as the better docking conformation. Nevertheless, the corresponding acyclic compound proved to be as active as the cyclic compound **2.23**. It was pointed out later that the 22-membered ring in this compound is too flexible to be restricted to a specific conformation.¹²



The previously discussed study¹⁸ identifying the REDOR-taxol structure by the Ojima group was accompanied by the synthesis of the corresponding constrained analogue **2.24**. This was designed to mimic the REDOR-taxol conformation. This compound proved to be comparable to paclitaxel in inducing microtubule polymerization and was only 3 times less cytotoxic than paclitaxel against LCC6-WT. Conformational studies gave C-13 side chain dihedral angle distributions which were more similar to those of the REDOR-taxol than those of T-taxol.

References

1. Schiff, P. B.; Fant, J.; Horwitz, S. B. Promotion of Microtubule Assembly *in Vitro* by Taxol. *Nature* **1979**, *277*, 665-667.
2. Rao, S.; Krauss, N. E.; Heerding, J. M.; Swindell, C. S.; Ringel, I.; Orr, G. A.; Horwitz, S. B. 3'-(*p*-Azidobenzamido)taxol Photolabels the N-Terminal 31 Amino Acids of β -Tubulin. *J. Biol. Chem.* **1994**, *269*, 3132-3134.
3. Rao, S.; Orr, G. A.; Chaudhary, A. G.; Kingston, D. G. I.; Horwitz, S. B. Characterization of the Taxol Binding Site on the Microtubule. *J. Biol. Chem.* **1995**, *270*, 20235-20238.
4. Nogales, E.; Wolf, S. G.; Downing, K. H. Structure of the $\alpha\beta$ Tubulin Dimer by Electron Crystallography. *Nature* **1998**, *39*, 199-203.
5. Lowe, J.; Li, H.; Downing, K. H.; Nogales, E. Refined Structure of $\alpha\beta$ -Tubulin at 3.5 Å Resolution. *J. Mol. Biol.* **2001**, *313*, 1045-1057.
6. Dubois, J.; Guenard, D.; Gueritte-Voeglein, F.; Guedira, N.; Potier, P.; Gillet, B.; Betoil, J.-C. Conformation of Taxotere and Analogues Determined by NMR

- Spectroscopy and Molecular Modeling Studies. *Tetrahedron* **1993**, *49*, 6533-6544.
7. Ojima, I.; Kuduk, S. D.; Chakravarty, S.; Ourevitch, M.; Begue, J.-P. A Novel Approach to the Study of Solution Structures and Dynamic Behavior of Paclitaxel and Docetaxel Using Fluorine-Containing Analogs as Probes. *J. Am. Chem. Soc.* **1997**, *119*, 5519-5527.
 8. Williams, H. J.; Scott, A. I.; Dieden, R. A.; Swindell, C. S.; Chirlian, L. E.; Francl, M. M.; Heerding, J. M.; Krauss, N. E. NMR and Molecular Modeling Study of the Conformations of Taxol and of its Side Chain Methylene Ester in Aqueous and Non-Aqueous Solution. *Tetrahedron* **1993**, *49*, 6545-6560.
 9. Milanesio, M.; Ugliengo, P.; Viterbo, D. *ab Initio* Conformational Study of the Phenylisoserine Side Chain of Paclitaxel. *J. Med. Chem.* **1999**, *42*, 291-299.
 10. Vander Velde, D. G.; Georg, G. I.; Grunewald, G. L.; Gunn, C. W.; Mitscher, L. A. "Hydrophobic Collapse" of Taxol and Taxotere Solution Conformations in Mixtures of Water and Organic Solvent. *J. Am. Chem. Soc.* **1993**, *115*, 11650-11651.
 11. Snyder, J. P.; Nettles, J. H.; Cornett, B.; Downing, K. H.; Nogales, E. The Binding Conformation of Taxol in Beta Tubulin: A Model Based on the Electron Crystallographic Density. *Proc. Natl. Acad. Sci. USA* **2001**, *98*, 5312-5316.
 12. Kingston, D. G. I.; Bane, S.; Snyder, J. P. The Taxol Pharmacophore and the T-Taxol Bridging Principle. *Cell Cycle* **2005**, *4*, 279-289.
 13. Snyder, J. P.; Nevins, N.; Cicero, D. O.; Jansen, J. The Conformations of Taxol in Chloroform. *J. Am. Chem. Soc.* **2000**, *122*, 724-725.

14. Gueritte-Voegelein, F.; Guenard, D.; Mangatal, L.; Potier, P.; Guilhem, J.; Cesario, M.; Pascard, C. Structure of a Synthetic Taxol Precursor: N-*tert*-Butoxycarbonyl-10-deacetyl-N-debenzoyletaxol. *Acta Cryst.* **1990**, *C46*, 781-784.
15. Mastropaolo, D.; Camerman, A.; Luo, Y.; Brayer, G. D.; Camerman, N. Crystal and Molecular Structure of Paclitaxel (Taxol). *Proc. Natl. Acad. Sci.* **1995**, *92*, 6920-6924.
16. Beutler, J. A.; Chmurny, G. N.; Brobst, S.; Look, S. A.; M., W. K. NMR and Molecular Modeling of the Conformation of Taxol. *J. Nat. Prod.* **1992**, *55*, 414-423.
17. Chmurny, G. N.; B.D., H.; Brobst, S.; Look, S. S.; K.M., W.; J.A., B. ¹H- and ¹³C-NMR assignments for Taxol, 7-*epi*-Taxol, and Cephalonannine. *J. Nat. Prod.* **1992**, *55*, 414-423.
18. Geney, R.; Sun, L.; Pera, P.; Bernacki, R. J.; Xia, S.; Horwitz, S. B.; Simmerling, C. L.; Ojima, I. Use of the Tubulin Bound Paclitaxel Conformation for Structure-Based Rational Drug Design. *Chem. Biol.* **2005**, *12*, 339-348.
19. Li, Y.; Poliks, B.; Cegelski, L.; Poliks, M.; Cryczynski, Z.; Piszczek, G.; Jagtap, P., G.; Studelska, D. R.; Kingston, D. G. I.; Schaefer, J.; Bane, S. Conformation of Microtubule-Bound Paclitaxel Determined by Fluorescence Spectroscopy and REDOR NMR. *Biochemistry* **2000**, *39*, 281-291.
20. Gao, Q.; Wei, J.-M.; Chen, S.-H. Crystal Structure of 2-Debenzoyl,2-Acetoxy Paclitaxel (Taxol): Conformation of the Paclitaxel Side-Chain. *Pharm. Res.* **1995**, *12*, 337-341.

21. Gao, Q.; Chen, S.-H. An Unprecedented Side Chain Conformation of Paclitaxel (Taxol): Crystal Structure of 7-Mesylopaclitaxel. *Tetrahedron Lett.* **1996**, *37*, 3425-3428.
22. Cachau, R. E.; Gussio, R.; Beutler, J. A.; Chmurny, G. N.; Hilton, B. D.; Muschik, G. M.; Erickson, J. W. Solution Structure of Taxol Determined Using a Novel Feedback-Scaling Procedure for Noe-Restrained Molecular Dynamics. *Supercomputer Applications and High Performance Computing* **1994**, *8*, 24-34.
23. Paloma, L. G.; Guy, R. K.; Wrasidlo, W.; Nicolaou, K. C. Conformation of a Water-Soluble Derivative of Taxol in Water by 2D-NMR Spectroscopy. *Chem. Biol.* **1994**, *1*, 107-112.
24. Jimenez-Barbero, J.; Souto, A. A.; Abal, M.; Barasoain, I.; Evangelio, J. A.; Acuna, A. U.; andreu, J. M.; Amat-Guerri, F. Effect of 2'-OH Acetylation on the Bioactivity and Conformation of 7-O-[N-(4'-Fluoresceincarboxyl)-L-alanyl]taxol. A NMR-fluorescence Microscopy Study. *Bioorg. Med. Chem.* **1998**, *6*, 1857-1863.
25. Rao, S.; He, L.; Chakravarty, S.; Ojima, I.; Orr, G. A.; Horwitz, S. B. Characterization of the Taxol Binding Site on the Microtubule. *J. Biol. Chem.* **1999**, *274*, 37990-37994.
26. Ivery, M. T.; Le, T. Modeling the Interaction of Paclitaxel With β -Tubulin. *Oncol. Res.* **2003**, *14*, 1-19.
27. Metaferia, B. B.; Hoch, J.; Glass, T. E.; Bane, S. L.; Chatterjee, S. K.; Snyder, J. P.; Lakdawala, A.; Cornett, B.; Kingston, D. G. I. Synthesis and Biological

- Evaluation of Novel Macrocyclic Paclitaxel Analogues. *Org. Lett.* **2001**, *3*, 2461-2464.
28. Ganesh, T.; Guza, R. C.; Bane, S.; Ravindra, R.; Shanker, N.; Lakdawala, A. S.; Snyder, J. P.; Kingston, D. G. I. The Bioactive Taxol Conformation of β -Tubulin: Experimental Evidence from Highly Active Constrained Analogs. *Proc. Natl. Acad. Sci. USA* **2004**, *101*, 10006-10011.
29. Barboni, L.; Lambertucci, C.; Appendino, G.; Vander Velde, D. G.; Himes, R. H.; Bombardelli, E.; Wang, M.; Snyder, J. P. Synthesis and NMR-Driven Conformational Analysis of Taxol Analogues Conformationally Constrained on the C13 Side Chain. *J. Med. Chem.* **2001**, *44*, 1576-1587.
30. Boge, T. C.; Wu, Z.-J.; Himes, R. H.; Vander Velde, D. G.; Georg, G. I. Conformationally Restricted Paclitaxel Analogues: Macrocyclic Mimics of the "Hydrophobic Collapse" Conformation. *Bioorg. Med. Chem. Lett.* **1999**, *9*, 3047-3052.
31. Chakravarty, S.; Lin, S.; Inoue, T.; Horwitz, S. B.; Kuduk, S. D.; Danishefsky, S. J.; Ojima, I. In *A Common Pharmacophore for Cytotoxic Microtubule-Stabilizing Agents: Interpretation of SAR Studies*, 217th ACS National Meeting, Anaheim, CA (Mar. 21-25), Anaheim, CA (Mar. 21-25), 1999.
32. Ojima, I.; Lin, S.; Inoue, T.; Miller, M. L.; Borella, C. P.; Geng, X.; Walsh, J. J. Macrocycle Formation by Ring-Closing Metathesis. Application to the Syntheses of Novel Macrocyclic Taxoids. *J. Am. Chem. Soc.* **2000**, *122*, 5343-5353.

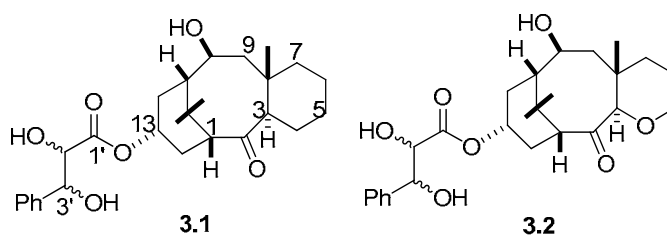
33. Ojima, I.; Geng, X.; Lin, S.; Pera, P.; Bernacki, R. J. Design, Synthesis and Biological Activity of Novel C2-C3' N-Linked Macrocyclic Taxoids. *Bioorg. Med. Chem. Lett.* **2002**, *12*, 349-352.
34. Geng, X.; Miller, M. L.; Lin, S.; Ojima, I. Synthesis of Novel C2-C3'N-Linked Macrocyclic Taxoids by Means of Highly Regioselective Heck Macrocyclization. *Org. Lett.* **2003**, *5*, 3733-3736.
35. Querolle, O.; Dubois, J.; Thoret, S.; Dupont, C.; Gueritte, F.; Guenard, D. Synthesis of Novel 2-O,3'-N-Linked Macrocyclic Taxoids with Variable Ring Size. *Eur. J. Org. Chem.* **2003**, 542-550.
36. Querolle, O.; Dubois, J.; Thoret, S.; Roussi, F.; Montiel-Smith, S.; Gueritte, F.; Guenard, D. Synthesis of Novel Macrocyclic Docetaxel Analogues. Influence of Their Macrocyclic Ring Size on Tubulin Activity. *J. Med. Chem.* **2003**, *46*, 3623-3630.
37. Querolle, O.; Dubois, J.; Thoret, S.; Roussi, F.; Guéritte, F.; Guénard, D. Synthesis of C2-C3'N-Linked Macrocyclic Taxoids. Novel Docetaxel Analogues with High Tubulin Activity. *J. Med. Chem.* **2004**, *47*, 5937-5944.

Chapter 3. Design and Synthesis of Simplified Paclitaxel Analogs Based on T-taxol Bioactive Conformation

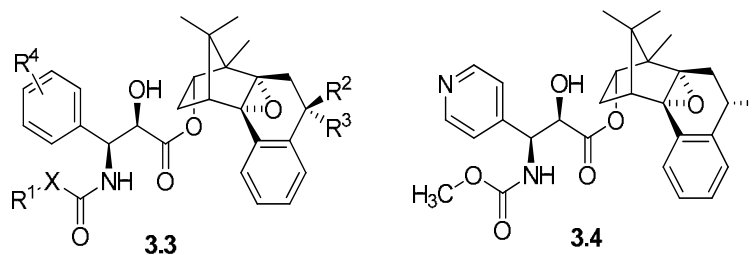
3.1 Simplified Paclitaxel Analogues

The complexity of the paclitaxel molecule (**1.1**) has made its synthesis very difficult. As discussed in Chapter 1, a number of total syntheses of paclitaxel have been accomplished in the laboratory,¹⁻⁸ but none of these are applicable commercially. Therefore it would be very desirable if structurally simplified analogues with retained or improved activity could be designed. Progress in the understanding of the SAR and tubulin-binding conformation of paclitaxel has spurred continuous attempts in this area. A major strategy is to replace the taxane polycyclic core with mimics with simple structures and to assemble the paclitaxel pharmacophore by putting side chains onto the core.

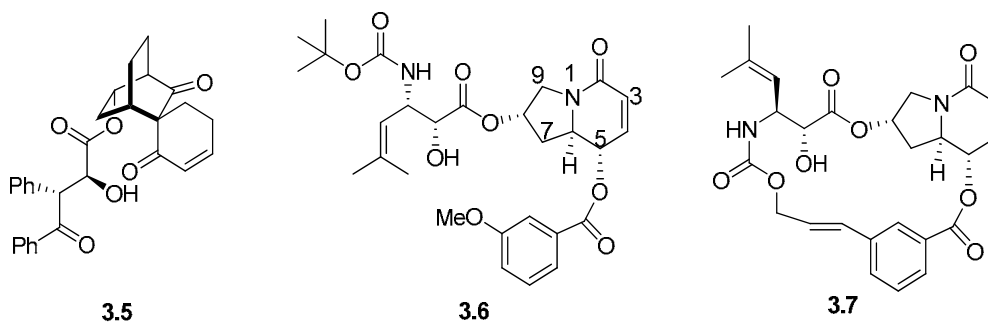
Two early studies in 1991⁹ and 1994¹⁰ produced two taxoids (**3.1**, **3.2**) with preservation of the taxane core but with fewer substituents. The C-13 side chain was retained based on the knowledge that this unit, and especially the C-2' hydroxyl, is essential to bioactivity.¹¹⁻¹² These simplified analogues were reported to show reduced activity in inhibition of tubulin depolymerization, but no detailed data were presented.



A series of even more simplified paclitaxel analogs (**3.3**) was designed by Klar and his coworkers in 1998.¹³ Based on the SAR of paclitaxel showing that the C-13 side chain, an ester group at C-2 and the oxetane moiety at C-4/C-5 are essential to activity, and that the northern region has only a minor influence on activity, the polycyclic core of paclitaxel was replaced by the borneol skeleton in this strategy. SAR studies of this type of analogue were addressed based on the outcomes of microtubule assays. The optimized structure **3.4** was reported to be superior to paclitaxel in terms of tubulin depolymerization. Nevertheless it was at least 100-fold less cytotoxic than paclitaxel against all the cell lines tested.



In a more recent effort,¹⁴ the baccatin core of paclitaxel was mimicked by a spirobicyclo [2,2,2] octane derivative based on computer modeling. The designed compound **3.5** was synthesized in 6 steps from a simple starting material. Compound **3.5** was subjected to a microtubule polymerization assay with no obvious microtubule stabilization shown. It was thus proposed that the absence of activity was due to the lack of counterparts of the paclitaxel C-2 benzoate and oxetane/4-OAc in this structure.



None of the above studies related either their structure design or analysis of activity to any proposed binding conformation, which unavoidably reduced the possibility of finding active analogs. The first conformationally restricted simplified analog was designed in a recent study.¹⁵ Indolizidinone with hydroxyls at C-5 and C-8 was utilized to model the baccatin core and moieties mimicking the paclitaxel C-2 and C-13 side chains were subsequently attached to the two hydroxyl groups to yield **3.6**. To constrain the side chain conformation, macrocyclic compound **3.7** with a 19-membered ring was prepared. Unfortunately, both of the compounds proved to be inactive in promoting microtubule assembly. However, they displayed micromolar cytotoxicity against several human tumor cell lines.

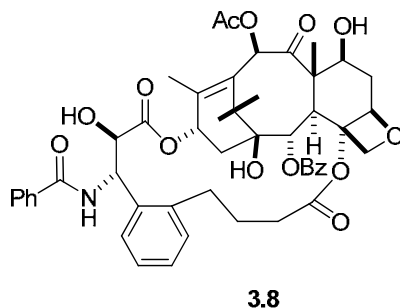
3.2 Design and Synthesis of Simplified Analogs Based on the T-taxol Bioactive

Conformation

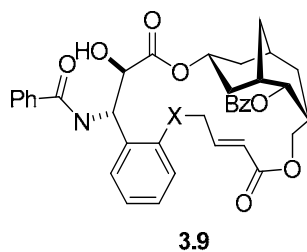
3.2.1 Introduction

As discussed in Chapter 2, the validity of the T-taxol model has been established experimentally by the determination of intramolecular distances in tubulin-bound paclitaxel by REDOR NMR experiments¹⁶⁻¹⁷ and by the synthesis of constrained paclitaxel analogs such as compound **3.8**. This compound adopts the T-Taxol

conformation and is significantly more active than paclitaxel in both cytotoxicity and tubulin polymerization assays.¹⁸ Analog **3.8**, in its 3-D representation, thus defines the required conformation for the effective binding of paclitaxel analogs to tubulin.



Based on the T-taxol conformation, the Kingston group has designed and synthesized the simplified paclitaxel analog **3.9**, where a bicyclo [3,3,1] nonane moiety was used as a structurally simpler surrogate of the baccatin core.



The logic behind this design was that the northern hemisphere of the paclitaxel structure is less crucial to its bioactivity based on its SAR (Figure 1.1), and that a structure with the T-taxol pharmacophore could be achieved by installation of the paclitaxel side chains on a simple bicyclic skeleton and subsequent constraining of the conformation by a suitable bridge. A conformational study indicated that these molecules

approximate the bioactive T-conformation with minor deviations due to the replacement of the baccatin core with a nonane core.¹⁹

Compound **3.9** and its analogs exhibited moderate cytotoxicity and tubulin assembly inhibitory activity. However, they were found to be highly insoluble in water, which made their biological evaluation very difficult. It is possible that their reduced activity was due to their insolubility in the aqueous testing environment.¹⁹

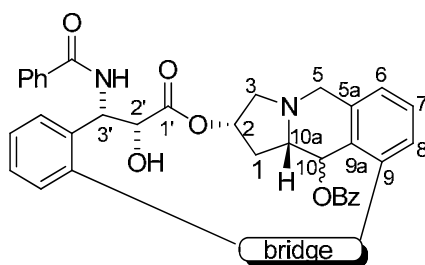


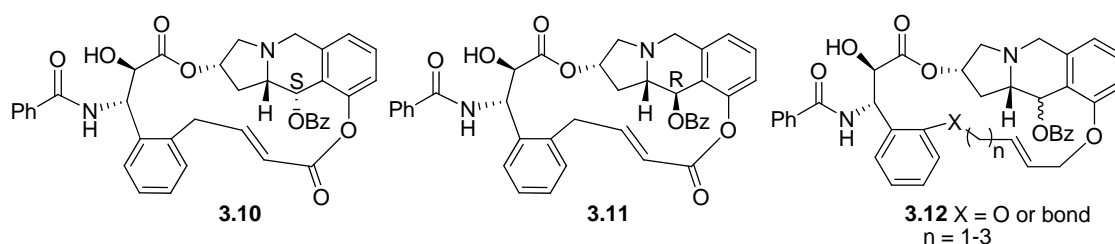
Figure 3.1 General structure of second generation T-taxol mimics

3.2.2 Design of a New Generation of Simplified Paclitaxel Analogs

In an approach to developing a new generation of water-soluble simplified paclitaxel analogs, an aza-tricyclic moiety (Figure 3.1) was designed to mimic the baccatin core of paclitaxel. The basic tertiary nitrogen was anticipated to increase water-solubility, and the aza-tricyclic moiety was functionalized with three hydroxyl groups to attach the key side chains. The final construct can be constrained to the T-taxol conformation by the selection of an appropriate length for the bridge linking the side chain and the tricyclic core. This new core bears three stereogenic centers which can lead to eight possible stereoisomers, but the availability of various hydroxyprolines as starting materials allows for control of two of these three centers.

A preliminary computer modeling study was performed by Professor Jim Snyder at Emory University to determine which of the eight possible isomers served as the best replacement of the baccatin structure. A conformational search was carried out for each of the eight isomers using the MMFF force field, and each of the eight global minima was fitted with the side chains and various bridges. Each such structure was then optimized and docked into the paclitaxel binding site on tubulin. Each docking returned a variety of conformations (i.e. binding modes). Those that best mimicked the shape and extension of **3.9** were selected and treated with an independent MMGBSA energy evaluation. Figure 3.2 shows the two lowest binding structures (**3.10** and **3.11**) together with the active analog **3.9** in a 3-D representation of the tubulin binding site. Compounds **3.10** and **3.11** are derived from two different stereoisomers of the aza-tricyclic moiety, with *S* and *R* configurations at C-10, respectively.

Encouraged by these results we elected to prepare analogs arising from both stereoisomers and with different bridge lengths for comparison. For easier synthetic manipulation, the bridge structure was modified to that of **3.12**, containing an ether linkage rather than the ester linkage of compounds **3.10** and **3.11**.



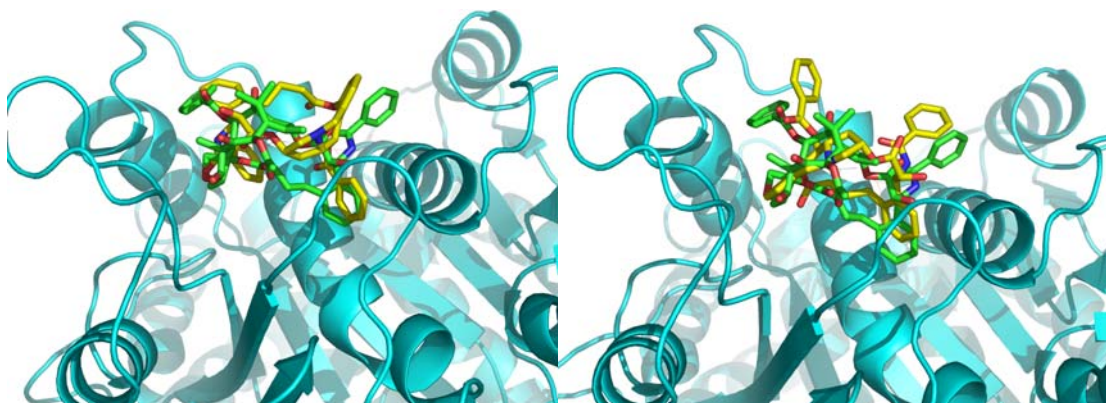
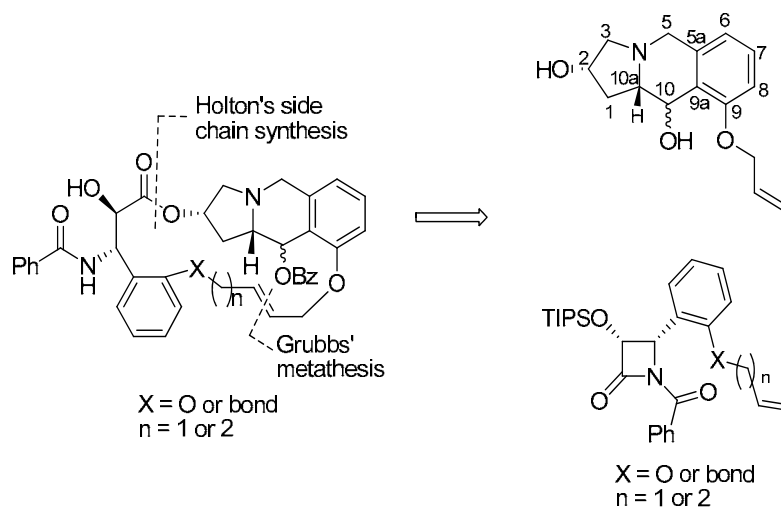


Figure 3.2 Left: low energy conformations of compounds **3.10** (in green) and **3.8** (in yellow) in the paclitaxel tubulin binding site. Right: low energy conformations of compounds **3.11** (in green) and **3.8** (in yellow) in the paclitaxel tubulin binding site. The models were prepared by Jim Snyder at Emory University.

3.2.3 Synthesis of New Generation Simplified Paclitaxel Analogs

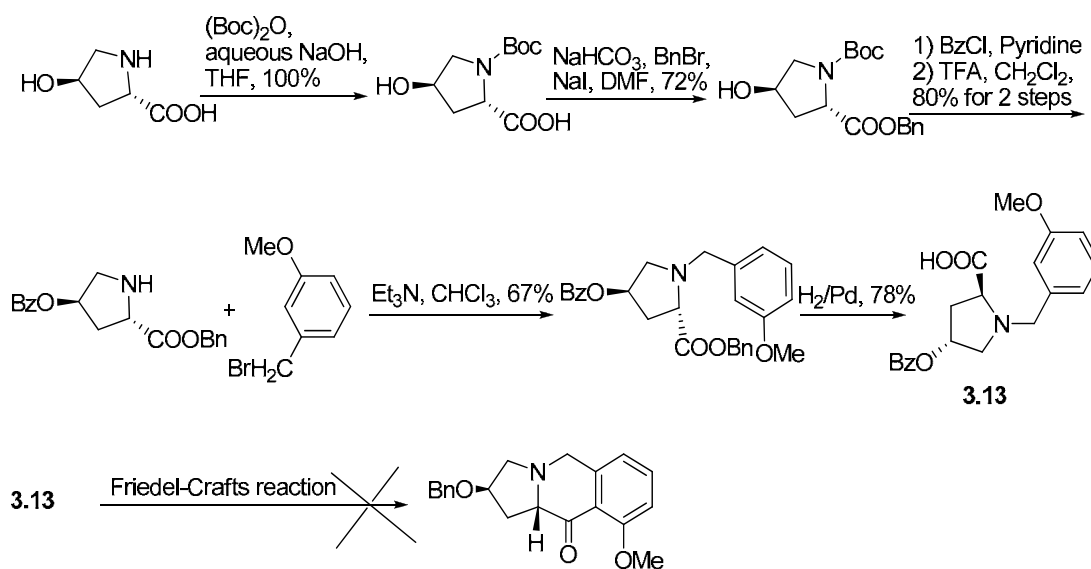
The retrosynthetic analysis of compounds of general structure **3.12** is shown in Scheme 3.1. The target molecules can be constructed from the aza-tricyclic moiety and the β -lactams followed by Grubbs' metatheses to furnish the bridges (Scheme 3.1).



Scheme 3.1 Retrosynthesis of simplified paclitaxel analogs

It was noticed that an easy way to install the multiple stereocenters in the aza-tricyclic core is to incorporate the enantiomerically pure 4-hydroxyproline into the target structure since all four stereoisomers of 4-hydroxyproline are commercially available.

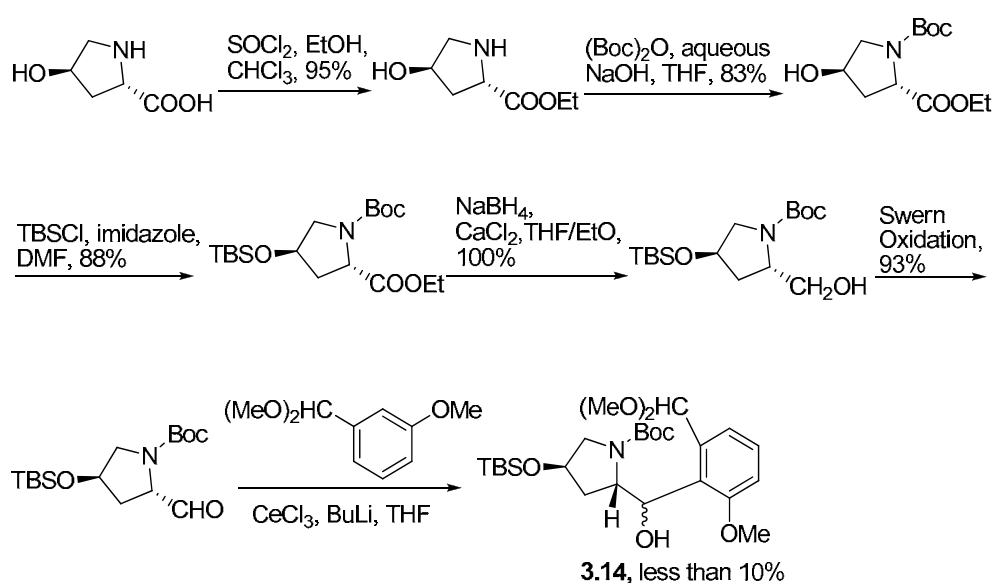
However, our first three synthetic routes toward the synthesis of the tricyclic core were not successful. The first synthetic attempt started from the efficient conversion of (2*S*,4*R*)-4-hydroxyproline into the key precursor **3.13** in 6 straightforward steps. The ring closure of **3.13** under several different Friedel-Crafts conditions,²⁰⁻²¹ however, could not deliver the desired tricyclic system (Scheme 3.2). In both cases a complex mixture resulted and the desired product was not detected.



Scheme 3.2 Synthesis and ring closure of **3.13**

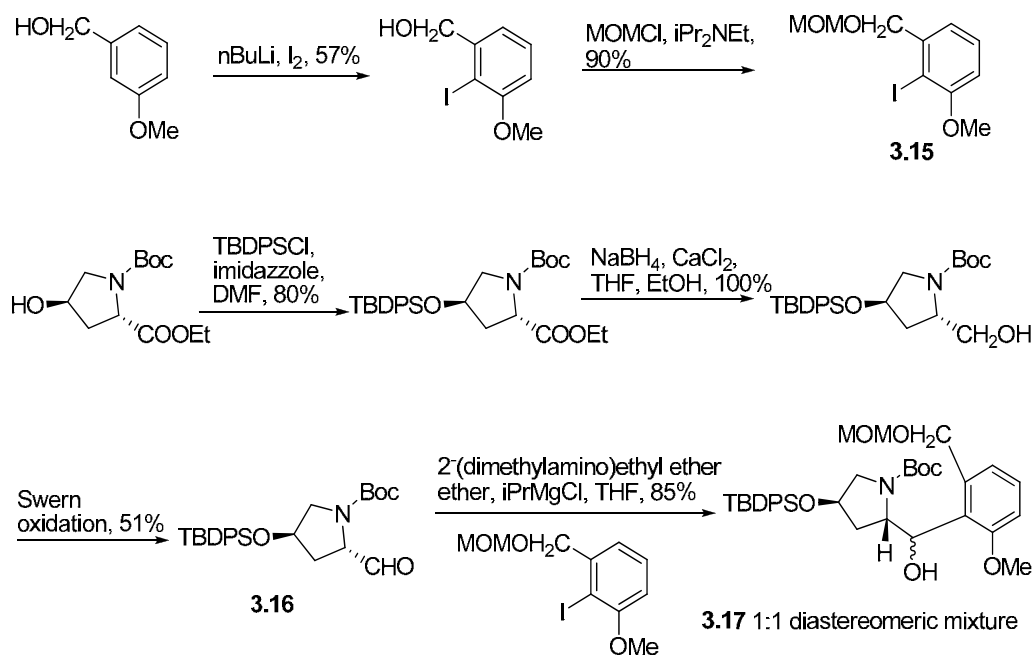
In the second attempt, the key intermediate **3.14** was designed to undergo intramolecular reductive amination upon deprotection of the aldehyde and the amine to

furnish the tricyclic ring system. After appropriate manipulations on the 4-hydroxyproline and its subsequent coupling with 3-methoxybenzaldehyde dimethyl acetal mediated by CeCl_3 ,²² the diastereomeric mixture of isomers **3.14** was successfully obtained. However, the yield was extremely low, and attempts at optimizing it failed to improve the yield. This approach was then abandoned.



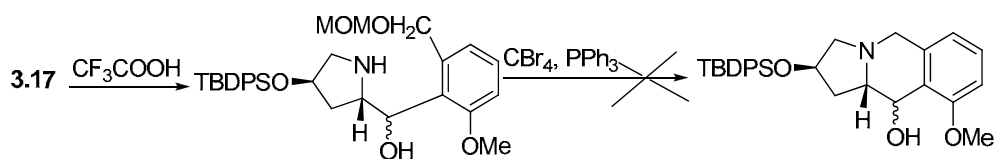
Scheme 3.3 Synthesis of **3.14**

In a third approach, the synthetic route was modified as shown in Scheme 3.4 for the synthesis of the new cyclization precursor **3.17**. The modified 4-hydroxyproline derivative **3.16** was successfully coupled with the Grignard intermediate resulting from compound **3.15**, and **3.17** was obtained in 85% yield as a pair of diastereomers in 1:1 ratio.



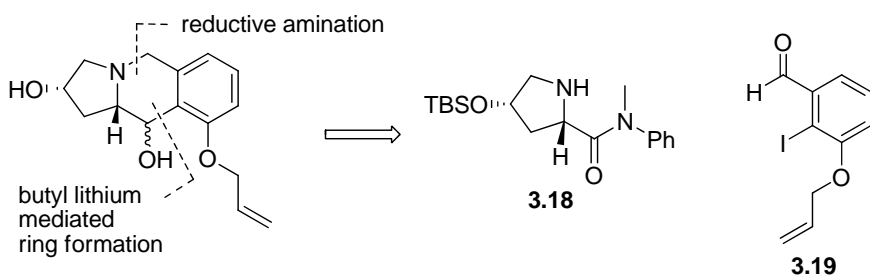
Scheme 3.4 Synthesis of **3.17**

Compound **3.17** was proposed to undergo an intramolecular S_N2 reaction to deliver the cyclized product upon liberation of the hydroxyl and the amine groups and subsequent conversion of the benzyl alcohol into benzyl bromide (Scheme 3.5). However, several problems were encountered during this sequence. Firstly, although the more acid-resistant *tert*-butyldiphenylsilyl group was used to protect the hydroxyl group at C4 of the proline unit, the selective deprotection of the N-boc and the O-MOM groups was far from clean and complex mixtures of globally deprotected and partially deprotected products were obtained under different conditions. Secondly, compound **3.17** was unstable under the deprotection conditions, presumably due to the fact that the newly generated hydroxyl group is benzylic. These problems made the seemingly easily reactions difficult to handle and the desired ring formation was not observed.



Scheme 3.5 Cyclization of **3.17**

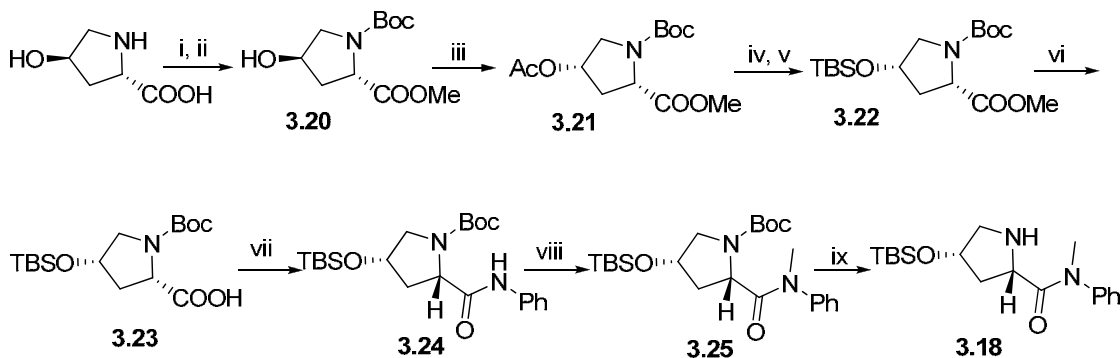
After the previous failure, a new synthetic route was proposed for the synthesis of the tricyclic core where the (2*S*,4*S*)-hydroxyproline derivative **3.18** is coupled with aldehyde **3.19** via reductive amination and the subsequent ring closure mediated by *n*-BuLi to afford the ring system (Scheme 3.6).



Scheme 3.6 Retrosynthesis of aza-tricyclic core

The *cis*-4-hydroxyproline derivative **3.18** was synthesized from commercially available *trans*-4-hydroxy-L-proline in 9 straightforward steps with high yields (Scheme 3.7). The amino acid was protected as its carbamate and methyl ester **3.20**,²³⁻²⁴ followed by a Mitsunobu reaction, which successfully inverted the stereochemistry at C-4.²⁵ The resulting ester **3.21** was hydrolyzed and reprotected as its TBS ether **3.22** with an overall yield of 63% in 5 steps. Compound **3.22** was hydrolyzed to acid **3.23**, which was converted into amide **3.25** in two steps. The Boc protecting group was selectively

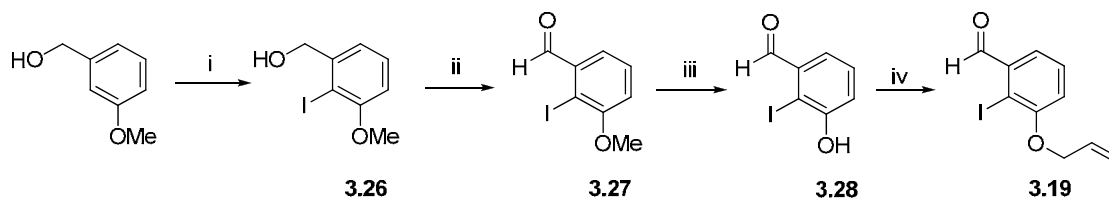
removed in 95% yield with ZnBr_2 to produce **3.18**. The overall yield was 42% from *trans*-4-hydroxy-L-proline.



a) i) aqueous NaOH, Di-*tert*-butyl dicarbonate, THF/H₂O, overnight. ii) Cs₂CO₃, MeI, DMF, overnight. iii) AcOH, PPh₃, DIAD, THF, overnight. iv) K₂CO₃, MeOH, 1 h. v) TBSCl, imidazole, DMF, 16h, 63% for 5 steps. vi) aqueous LiOH, MeOH, 45 °C, 6 h, 95%. vii) TEA, ClCOOCH₃, 0 °C, THF, 1h; aniline, THF, 1h, 79%. viii) NaH, MeI, DMF, 93%. ix) ZnBr₂, CH₂Cl₂, 95%.

Scheme 3.7 Synthesis of intermediate **3.18**^a

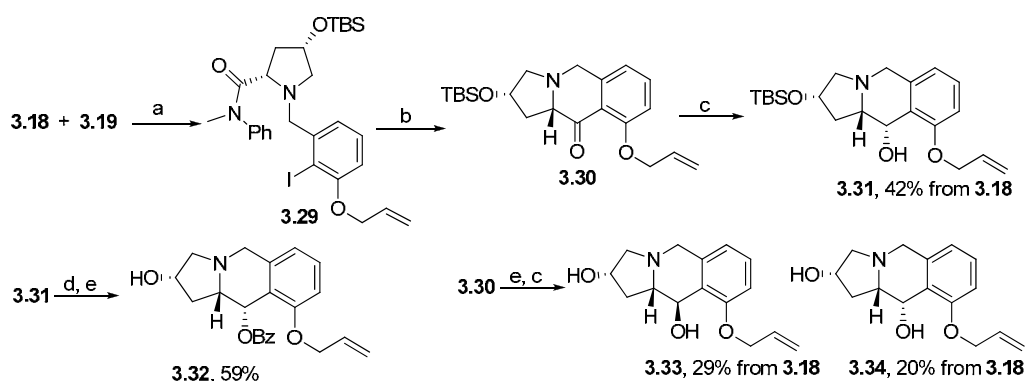
Aldehyde **3.19** was synthesized from 3-methoxybenzyl alcohol in four steps (Scheme 3.8). Commercially available 3-methoxybenzyl alcohol was treated with *n*-butyllithium and iodine to afford compound **3.26**,²⁶ which was oxidized with Jones' reagent. The resulting aldehyde **3.27** was treated with boron tribromide to cleave the methyl ether and then reacted with allyl bromide in the presence of base to generate compound **3.19**.



^a i) *n*-BuLi, I₂, hexane/ether, -78 °C, 57%. ii) Jones reagent, acetone/water. iii) BBr₃, CH₂Cl₂, 41% for 2 steps. iv) Allyl bromide, K₂CO₃, DMF, 96%.

Scheme 3.8 Synthesis of compound **3.19**^a

Reductive amination of compounds **3.18** and **3.19** with sodium triacetoxyborohydride went smoothly, generating compound **3.29** (Scheme 3.9). Cyclization of **3.29** mediated with *n*-BuLi afforded the key aza-tricyclic intermediate **3.30**. This compound was found to be unstable on a silica gel column, and so it was reduced directly with sodium borohydride to afford **3.31** as the only stereoisomer in an overall yield of 42% for three steps. The stereoselectivity seen in this reaction was conceivably due, in part at least, to the bulky TBS protecting group. The absolute stereochemistry of **3.31** was determined by X-ray crystallography of compound **3.32** (Figure 3.3), which was prepared by acylation of the newly generated hydroxyl group followed by deprotection of the silyl ether of compound **3.31**. If it is true that the stereoselectivity was due to the bulky silyl ether, removal of the substituent would lead to some change in the stereochemistry of the products. As expected, reduction of **3.30** after deprotection of the large protecting group produced the epimeric diol **3.33** as the major product, together with lesser amounts of diol **3.34** (**3.33** : **3.34** = 3 : 2). The absolute stereochemistry of the former was also determined by X-ray crystallography (Figure 3.3).



^a a) NaBH(OAc)₃, ClCH₂CH₂Cl. b) BuLi, THF, -78 °C. c) NaBH₄, MeOH. d) LiHMDS, PhCOCl, THF. e) HF.pyridine, THF

Scheme 3.9 Synthesis of alcohols **3.32-3.34**^a

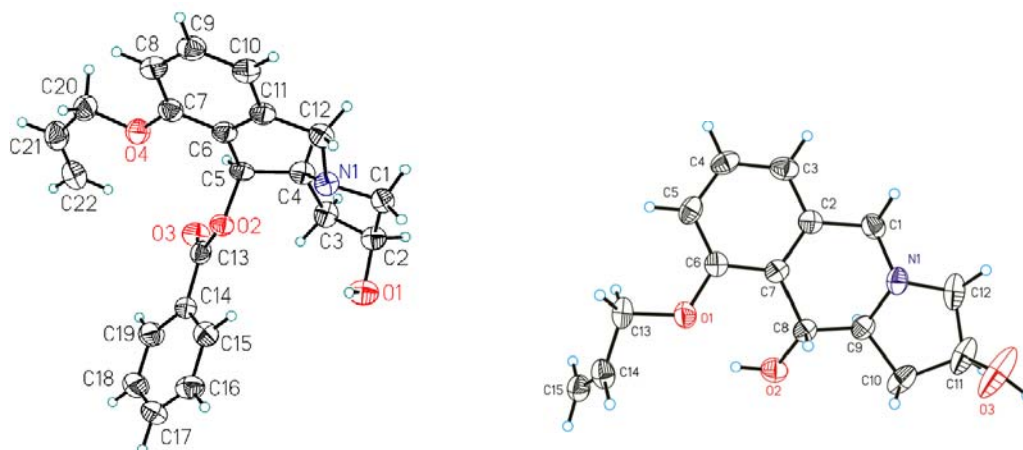
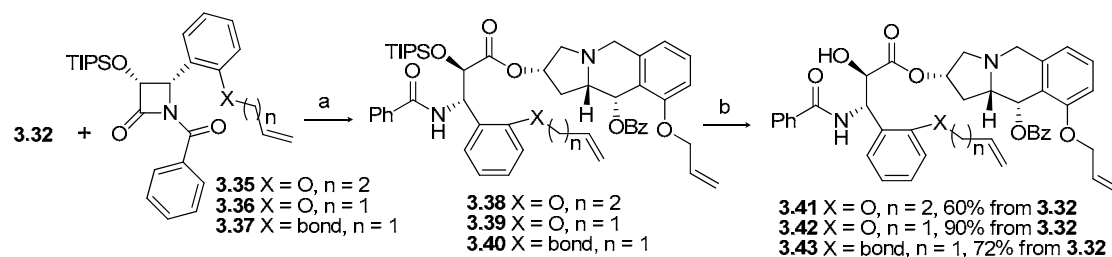


Figure 3.3 Left: 3-D drawing of **3.32** generated by X-ray crystallography. Right: 3-D structure of **3.33** generated by X-ray crystallography. X-ray crystallography was carried out by Dr. Carla Slebodnick at Virginia Tech.

The known β -lactams **3.35-3.37** were prepared following the literature procedures.²⁷ Pretreatment of alcohol **3.32** with sodium hydride followed by addition of the β -lactams yielded compounds **3.38-3.40** in good yields. Deprotection of the silyl ethers with HF produced the open-chain analogs **3.41-3.43** (Scheme 3.10). The subsequent ring-closing metatheses of these alkenes with Grubbs' 2nd generation catalyst failed to bring about the desired bridged products, even though several different catalysts and conditions were evaluated. Examination of the 3-D structure of compound **3.42** (Figure 3.4) suggested that the benzoyl group could be responsible for the low reactivity. Thus, an alternate synthesis was thus developed that allowed introduction of the benzoyl group after alkene metathesis.



Reagents and Conditions: a) NaH, THF, 0 °C, 76-92%; b) HF.Py, THF, 0 °C-RT,

Scheme 3.10 Synthesis of open chain analogs **3.41-3.43**

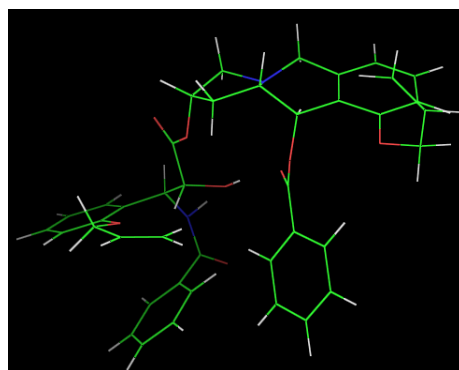
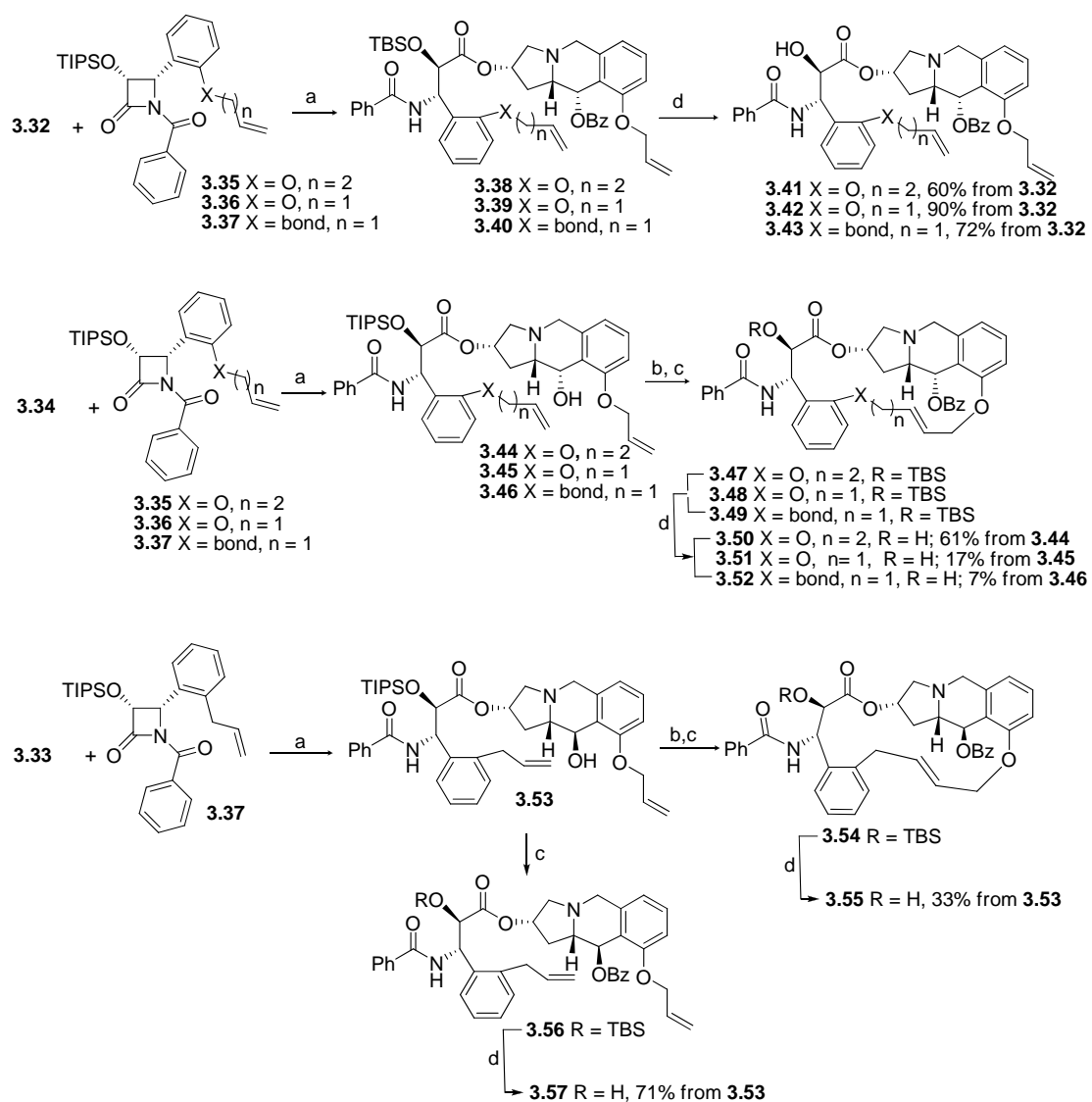


Figure 3.4 3-D structure of **3.42** optimized with PM3 method in Spartan

Alkenes **3.44-3.46** were prepared by coupling alcohol **3.34** with β -lactams **3.35-3.37**, respectively, and **3.53** was synthesized from alcohol **3.33** and β -lactam **3.37** in good yield (Scheme 3.11). Fortunately, the ring closing metathesis of alkene **3.44** gave the desired bridged product, but only in trace amounts. Since it has been reported that some nitrogen containing compounds, especially amines, are poor substrates for Grubbs' ruthenium catalysts,²⁸ we surmised that the low yield was due to the presence of the tertiary amine in **3.44**. To overcome this problem, compound **3.44** was protonated with 10-camphorsulfonic acid before the addition of the Grubbs' catalyst, and the yield of the metathesis reaction was found to be greatly improved. The resulting macrocyclic

compound was benzoylated and deprotected to afford the target analog **3.50** with an overall yield of 61% in 3 steps from **3.44**. Compound **3.51** with a shorter bridge was prepared from alkene **3.45** by similar procedures, although the overall yield was much lower.



^a a) NaH, THF, 0 °C, 76-92%; b) 10-camphorsulfonic acid, CH₂Cl₂, 40 °C; Grubbs' 2nd generation catalyst, CH₂Cl₂, 40 °C; c) LiHMDS, benzoyl chloride, -78 °C, THF; d) HF.Py, THF, 0 °C-RT

Scheme 3.11 Synthesis of open-chain and bridged paclitaxel analogs^a

In the case of compound **3.46**, the metathesis reaction to generate a 5-atom bridge proved to be the most difficult one in the series, and analog **3.52** was prepared from **3.46** with only 7% overall yield. Interestingly, the C-2 epimeric alkene **3.53** reacted smoothly under the same ring closing metathesis conditions. Compound **3.55** with a 5-atom bridge was obtained with a 33% overall yield from compound **3.53**. The different reactivities of **3.46** and **3.53** were probably due to the opposite orientation of the free hydroxyl groups. The corresponding open-chain analog **3.57** was synthesized in two steps from **3.53**.

3.2.4 Biological Evaluation of the Simplified Paclitaxel Analogs

The open-chain analogs **3.41-3.43**, **3.57** and bridged analogs **3.50-3.52**, **3.55** were evaluated for their antiproliferative activities against the A2780 cell line. The results are summarized in Table 1. The simplified analogs showed moderate to good antiproliferative activities. The bridged analogs **3.50-3.52** exhibited similar activities to their open-chain counterparts **3.41-3.43** respectively. Compound **3.55** was over 4-times more active than the corresponding open-chain analog **3.57**. All the analogs were much less active than paclitaxel.

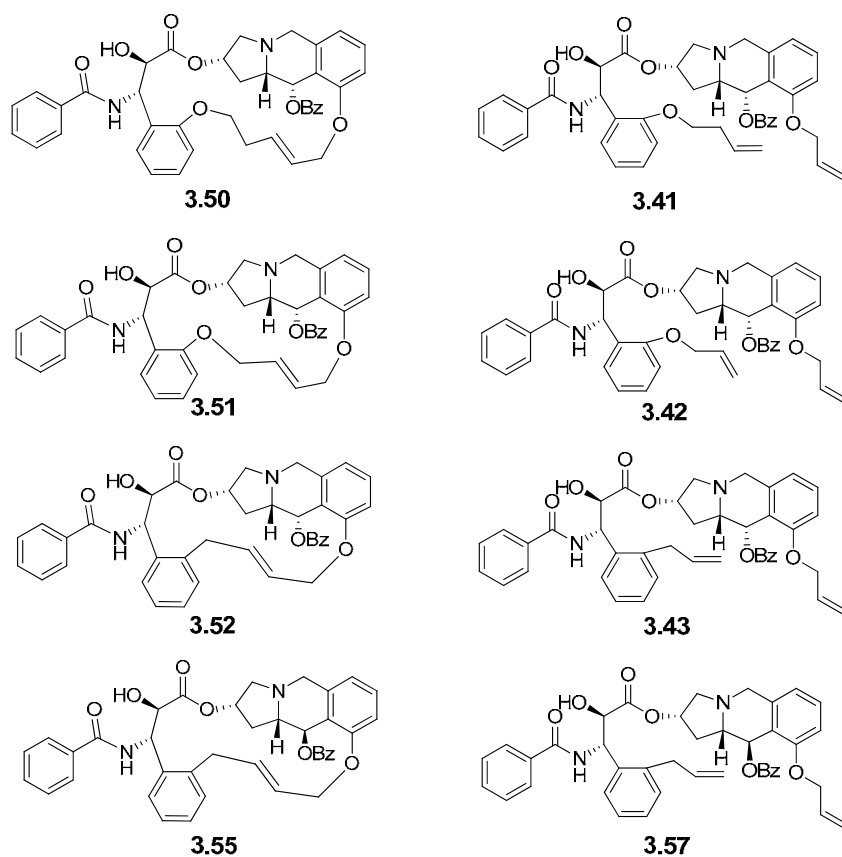


Table 3.1 Antiproliferative activities (IC_{50} , μM)^a of paclitaxel and the simplified paclitaxel analogs

Compound#	3.50	3.41	3.51	3.42	3.52	3.43	3.55	3.57	paclitaxel
A2780 ^b	4.5±0.7	5.8±0.5	4.1±0.4	8.3±0.7	4.0±1.5	4.7±0.6	5.1±0.7	23.8±5.2	0.015±0.001

^a The concentration at which the compound inhibits 50% of the cell growth. ^b human ovarian cancer cell line.

The analogs were also evaluated by Dr. Susan Bane at the State University of New York at Binghamton for antiproliferative activities against the PC3 human prostate cancer cell line as well as tubulin assembly inhibitory activities, but the low aqueous solubilities of the compounds prevented her from determining accurate IC_{50} values.

3.2.5 Computer Modeling

A recent computer modeling study performed by Dr. Snyder at Emory University suggested the weak activities of the simplified analogs can, in part, be attributed to the complex conformational profile of the macrocyclic rings relative to paclitaxel and its bridged analogs such as **3.8**.

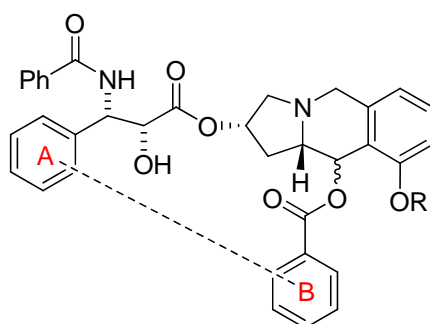


Figure 3.5 Intramolecular distances between ring A and ring B

It was shown in this study that the MMGBSA energies of the open-chain series and the bridged series analogs are not significantly different. In addition, the distances between phenyl rings A and B in all the analogs were measured. These distances were compared to the distance between the two corresponding phenyl rings in paclitaxel, which help to prevent the M-loop of β -tubulin from closing (Figure 3.5). The distance measured for paclitaxel is 13.1 Angstroms. The distances measured for the analogs ranged from 13.0 to 14.5 Angstroms, which are quite close the values for paclitaxel, except that for analog **3.57** the number is only 11.0 Angstroms. This could be one of the reasons that **3.57** was much less active than the others.

As discussed in Section 3.2.2, the ester groups in the bridges of the designed analogs were replaced with ether groups for easier synthetic manipulations. The modeling study

showed that the replacement of the lactone containing bridge with an ether containing bridge significantly increased the MMGBSA energy. For example, **3.11** and **3.55** presented similar conformations when docked into the receptor. However, the MMGBSA energy calculated for compound **3.11** was -92.22 kcal/mol, while the energy calculated for analog **3.55** was $+122.79$ kcal/mol. The lack of biological activities of the synthesized analogs is possibly related to this difference in energy. This point can be better justified if analogs that contain lactone bridges can be synthesized and if they show enhanced activity compared with the current analogs.

3.2.6 Conclusions

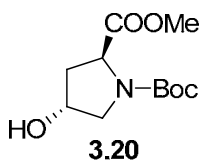
The simplified paclitaxel analogs **3.41-3.43**, **3.50-3.52**, **3.55** and **3.57** containing an aza-tricyclic moiety were designed and synthesized. The bridged analogs **3.50-3.52** and **3.55**, which were designed to adopt the T-taxol conformation, did not show significantly improved activities compared to their open-chain counterparts. All the analogs were much less active than paclitaxel.

3.3 Experimental Section

General experimental methods The following standard conditions apply unless otherwise stated. All reactions were performed under Ar or N₂ in oven-dried glassware using dry solvents and standard syringe techniques. Tetrahydrofuran (THF) was distilled from the sodium benzophenone ketyl radical ion. CH₂Cl₂ was distilled from CaH₂. All reagents were of commercial quality and used as received. After workup, partitioned organic layers were washed with water and brine and dried over Na₂SO₄. Reaction

progress was monitored using Al-backed thin layer chromatography (TLC) plates pre-coated with silica UV254. Purification of products by column chromatography was conducted using a column filled with silica gel 60 (220-240 mesh) using eluting solvent systems as indicated. Purification by preparative thin layer chromatography (PTLC) was performed using glass-backed plates pre-coated with silica UV254. HPLC was conducted on Shimadzu SCL-10AVP system using a column purchased from Phenomenex (Luna 5 μ C18 (2) 25 \times 4.6 mm). ^1H and ^{13}C NMR spectra were recorded on a 400 MHz (400 MHz for ^1H and 100 MHz for ^{13}C) spectrometer or a 500 MHz (500 MHz for ^1H and 126 MHz for ^{13}C) spectrometer in CDCl_3 unless otherwise stated. All chemical shifts (δ) were referenced to the solvent peaks of CDCl_3 (7.26 ppm for ^1H , 77.0 ppm for ^{13}C). Optical rotation was measured on a polarimeter operating at the sodium D-line.

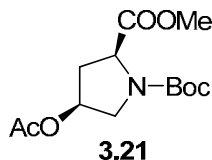
(2*S*,4*R*)-*N*-Boc-4-hydroxy-proline methyl ester (3.20)



A solution of *trans*-4-hydroxy-*L*-proline (5.24 g, 40 mmol) in THF (50 mL) and water (25 mL) was treated with aqueous NaOH (10%, 17 mL) and di-*tert*-butyl dicarbonate (13.1 g, 60 mmol, 1.5 equiv). The mixture was stirred overnight at rt. THF was evaporated under reduced pressure. The aqueous solution was adjusted to pH 2 with 10% aqueous NaHSO_4 solution and extracted with EtOAc (3 \times 50 mL). The combined organic phase was washed, dried and concentrated to yield the crude product, which was

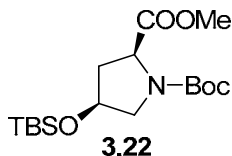
used in the next step without further purification. To a solution of the above mentioned crude product in DMF (180 mL) at rt was added Cs₂CO₃ (18.5 g, 56.8 mmol). After the mixture was stirred for 15 min, MeI (4.05 mL, 59.4 mmol) was added dropwise. The resulting mixture was then stirred overnight and filtered through a short column packed with Celite[®]. The filtrate was concentrated under reduced pressure and the residue was partitioned between saturated aqueous NaHCO₃ (50 mL) and EtOAc (50 mL). The aqueous phase was further extracted with EtOAc (2×50 mL). The combined organic layers were washed, dried and concentrated. Column chromatography (1:1 EtOAc:hexanes) afforded compound **3.20** as a yellowish oil (9.5g, 97% for two steps). [α]_D²³ -69.4 (*c* 1.3, MeOH); ¹H NMR (400 MHz) δ 4.48 (s, 1H), 4.44 (t, *J* = 7.7 Hz, 0.4H), 4.38 (t, *J* = 8.0 Hz, 0.6H), 3.72 (d, *J* = 4.7 Hz, 3H), 3.61 (dt, *J* = 15.6, 7.8 Hz, 1H), 3.55 (d, *J* = 11.7 Hz, 0.6H), 3.44 (d, *J* = 11.3 Hz, 0.4H), 2.28 (m, 1.6H), 2.16 (s, 0.4H), 2.11 – 2.00 (m, 1H), 1.75 (s, 0.6H), 1.42 (m, 9H); ¹³C NMR (126 MHz) δ 173.73, 173.51, 154.61, 154.05, 80.47, 80.38, 77.36, 77.31, 77.11, 76.85, 70.31, 69.57, 57.98, 57.55, 54.84, 54.78, 52.35, 52.14, 39.21, 38.56, 28.46, 28.33, 0.07; HRMS (ESI) calcd for C₁₁H₂₀NO₅ *m/z* 246.1341 ([M + H]⁺), found *m/z* 246.1333.

(2S,4S)-N-Boc-4-acetoxy-proline methyl ester (3.21).



To a solution of **3.20** (9.5 g, 38.7 mmol), triphenyl phosphine (21 g, 80 mmol, 2.1 equiv) and acetic acid (4.6 mL, 80 mmol, 2.1 equiv) in THF was added diisopropyl azodicarboxylate (DIAD) dropwise (15.8 mL, 80 mmol, 2.1 equiv) at 0 °C. The resulting mixture was warmed up to rt and stirred overnight. The solvent was evaporated under reduced pressure and the residue was purified by column chromatography (1:2 EtOAc:hexanes) to yield **3.21** as a colorless oil (9.7 g, 87%). $[\alpha]_D^{23}$ -18.4 (*c* 1.1, MeOH); ^1H NMR (500 MHz) δ 5.23 – 5.17 (m, 1H), 4.48 (d, *J* = 9.0 Hz, 0.5H), 4.36 (d, *J* = 9.2 Hz, 0.5H), 3.75 – 3.66 (m, 4H), 3.57 (d, *J* = 12.4 Hz, 0.5H), 3.49 (d, *J* = 12.4 Hz, 0.5H), 2.43 (m, 1H), 2.31 – 2.20 (m, 1H), 1.98 (s, 3H), 1.41 (m, 9H); ^{13}C NMR (126 MHz) δ 172.63, 172.28, 170.50, 170.33, 154.18, 80.40, 72.94, 71.79, 62.63, 57.81, 57.43, 52.32, 52.16, 51.82, 36.37, 35.43, 28.44, 28.33; HRMS (ESI) calcd for $\text{C}_{13}\text{H}_{21}\text{NNaO}_6$ *m/z* 310.1267.1341 ($[\text{M} + \text{Na}]^+$), found *m/z* 310.1263.

(2*S*,4*S*)-*N*-Boc-4-(*tert*-butyldimethylsilyloxy)proline methyl ester (3.22)

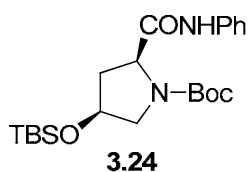


To a solution of **3.21** (9.7 g, 33.8 mmol) in methanol (250 mL) was added K_2CO_3 (5.5 g, 36 mmol, 1.07 equiv). The mixture was stirred for 1 hour at rt and filtered. The solvent was evaporated in vacuo and the residue purified by column chromatography (1:1 EtOAc:hexanes) to yield (2*S*,4*S*)-*N*-Boc-4-hydroxy-proline methyl ester as a colorless oil (6.5g, 78%). $[\alpha]_D^{23}$ -64.1 (*c* 0.5, MeOH); 1H NMR (500 MHz) δ 4.29 – 4.24 (m, 7H), 3.75 (s, 1H), 3.77 (s, 2H), 3.66 (d, *J* = 12.0 Hz, 0.5H), 3.59 (d, *J* = 12.0 Hz, 0.5H), 3.51 (m, 1.5 H), 3.29 (d, *J* = 9.5 Hz, 0.5H), 2.40 – 2.17 (m, 1H), 2.11 – 2.03 (m, 1H), 1.44 (s, 2.5H), 1.39 (s, 6.5H); ^{13}C NMR (126 MHz) δ 175.80, 175.50, 154.55, 153.77, 80.52, 71.36, 70.32, 60.48, 57.95, 57.76, 56.02, 55.43, 52.87, 52.58, 38.62, 37.79, 28.43, 28.32, 22.02, 21.12, 14.26; HRMS (ESI) calcd for $C_{11}H_{20}NO_5$ *m/z* 246.1341 ($[M + H]^+$), found *m/z* 246.1325.

The product obtained above (6.5 g, 26.5 mmol), *tert*-butyldimethylsilyl chloride (9.6 g, 63.6 mmol, 2.4 equiv) and imidazole (9.0 g, 132.5 mmol, 5 equiv) were stirred in DMF (50 mL) overnight at rt. The reaction mixture was diluted with EtOAc (100 mL), washed with water (10 mL \times 2) and brine (10 mL \times 2), dried with anhydrous Na_2SO_4 and concentrated in vacuo. Purification by column chromatography (1:4 EtOAc:hexanes) yielded **3.22** as a colorless oil (8.8g, 93%). $[\alpha]_D^{23}$ -35.0 (*c* 0.7, MeOH); 1H NMR (500 MHz) δ 4.43 - 4.21 (m, 2H), 3.67 (s, 3H), 3.60 (dd, *J* = 11.1, 5.4 Hz, 0.63 H), 3.54 (dd, *J*

= 11.1, 5.4 Hz, 1H), 3.30 (dd, $J = 11.1, 3.6$ Hz, 0.63 H), 3.25 (dd, $J = 11.1, 3.2$ Hz, 1H), 2.33 – 2.16 (m, 1H), 2.09 – 2.02 (m, 1H), 1.44 (s, 3H), 1.39 (s, 6H), 0.83 (s, 3H), 0.82 (s, 6H), 0.04 – -0.02 (m, 6H); ^{13}C NMR (126 MHz) δ 172.95, 172.51, 154.44, 153.93, 79.96, 70.73, 69.80, 57.84, 57.44, 54.82, 54.25, 52.10, 51.96, 39.63, 38.81, 28.50, 28.38, 25.68, 25.66, 17.96, -4.88, -4.98; HRMS (ESI) calcd for $\text{C}_{17}\text{H}_{34}\text{NO}_5\text{Si}$ m/z 360.2206 ($[\text{M} + \text{H}]^+$), found m/z 360.2199.

(2*S*,4*S*)-*tert*-butyl 4-(*tert*-butyldimethylsilyloxy)-2-(phenylcarbamoyl)pyrrolidine-1-carboxylate (3.24)

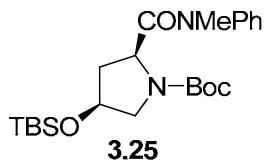


To a solution of **3.22** (8.8g, 24.5 mmol) in methanol (45 mL) was added aqueous lithium hydroxide (2.5 M, 15 mL). The mixture was stirred for 6 hours at 45 °C. The solution was adjusted to pH 3 with 3M HCl solution and extracted with EtOAc (30 mL \times 3). The organic solution was dried and concentrated at reduced pressure. Column chromatography (5% MeOH in CH_2Cl_2) afforded the carboxylic acid as a colorless oil (5.8 g, 77%).

To a stirred solution of the acid (5.8 g, 16.8 mmol) and triethylamine (2.6 mL, 18.5 mmol) in THF (60 mL) at 0 °C was added methyl chloroformate (1.4 mL, 18.5 mmol, 1.1 equiv) dropwise. After stirring for 1 hour at 0 °C, aniline (1.7 mL, 18.5 mmol, 1.1 equiv) was added. The resulting mixture was stirred for 1 hour at 0 °C, 16 hours at rt and then 3 hours under reflux. The reaction was cooled to rt and diluted with EtOAc (100 mL). The

organic solution was washed, dried and concentrated to produce the crude product, which was purified by column chromatography (1:6 EtOAc:hexanes) to yield compound **3.24** as a colorless oil (5.5 g, 78%). $[\alpha]_D^{23}$ -32.8 (*c* 0.7, MeOH); $^1\text{H NMR}$ (500 MHz) δ 7.50 (d, $J = 7.9$ Hz, 2H), 7.29 (t, $J = 7.6$ Hz, 2H), 7.07 (t, $J = 6.9$ Hz, 1H), 4.38 (m, 2H), 3.70 – 3.26 (br, s, 2H), 2.27 (br, s, 2H), 1.42 (br, s, 9H), 0.76 (br, s, 9H); $^{13}\text{C NMR}$ (126 MHz) δ 170.99, 155.15, 128.96, 124.07, 119.52, 81.24, 70.70, 61.41, 56.39, 39.65, 28.40, 25.67, 18.10, -4.85; HRMS (ESI) calcd for $\text{C}_{22}\text{H}_{37}\text{N}_2\text{O}_4\text{Si}$ m/z 421.2523 ($[\text{M} + \text{H}]^+$), found m/z 421.2516.

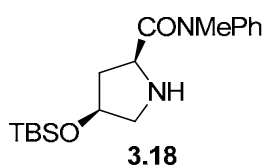
(2*S*,4*S*)-tert-butyl 4-(tert-butyldimethylsilyloxy)-2-(*N*-methyl-*N*-phenylcarbamoyl)-pyrrolidine-1-carboxylate (3.25).



To a solution of **3.24** (5.4 g, 12.8 mmol) in DMF (75 mL) was added NaH (3.1 g, 60%, dispersed in mineral oil, 77.5 mmol, 6.6 equiv) at 0 °C and the resulting mixture was stirred at the same temperature for 1 hour, followed by the slow addition of MeI (4.8 mL, 76.6 mmol, 6 equiv). The reaction was stirred for another 15 min at 0 °C and quenched by adding cold water. The aqueous phase was extracted with EtOAc (50 mL \times 3) and the combined organic phase was washed, dried and concentrated. The crude product was purified with column chromatography (1:4 EtOAc:hexanes) to afford the **3.25** as a crystalline solid (5.2 g, 93%). $[\alpha]_D^{23}$ -22.1 (*c* 1.0, MeOH); $^1\text{H NMR}$ (500 MHz)

δ 7.52 – 7.28 (m, 5H), 7.21 (d, J = 8.5 Hz, 1H), 4.22 – 3.99 (m, 2H), 3.78 – 3.58 (m, 1H), 3.26 (s, 3H), 3.23 – 3.16 (m, 1H), 2.06 – 1.91 (m, 1H), 1.89 – 1.69 (m, 1H); ^{13}C NMR (126 MHz) δ 171.88, 154.16, 153.59, 143.50, 143.19, 129.86, 129.76, 128.62, 128.17, 127.99, 127.85, 127.75, 125.72, 124.81, 79.89, 79.51, 69.55, 68.91, 55.66, 55.30, 53.38, 52.81, 39.52, 38.52, 37.88, 37.82, 28.59, 28.54, 25.69, 17.91, 17.89, -4.82, -4.83, -4.86, -4.95; HRMS (ESI) calcd for $\text{C}_{23}\text{H}_{39}\text{N}_2\text{O}_4\text{Si}$ m/z 435.2679 ($[\text{M} + \text{H}]^+$), found m/z 435.2714.

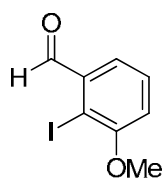
(2*S*,4*S*)-4-(*tert*-butyldimethylsilyloxy)-*N*-methyl-*N*-phenylpyrrolidine-2-carboxamide (3.18)



To a cold solution (0 °C) of **3.25** (0.94 g, 2.2 mmol) in CH_2Cl_2 (100 mL) was added ZnBr_2 (2.43 g, 10.8 mmol, 4.9 equiv) and the resulting suspension was warmed up to rt and stirred overnight. The reaction was quenched by adding saturated aqueous NaHCO_3 (20 mL). The aqueous phase was extracted with CH_2Cl_2 (40 mL \times 3) and the combined organic phase was dried and concentrated. The crude product was purified by column chromatography (50% EtOAc in hexanes, then 10% methanol in CH_2Cl_2) to yield compound **3.18** as a colorless oil (0.69 g, 93%). $[\alpha]_D^{23}$ -46.4 (c 0.5, CHCl_3); ^1H NMR (500 MHz) δ 7.40 (t, J = 7.5 Hz, 2H), 7.33 (t, J = 7.5 Hz, 1H), 7.18 (d, J = 7.5 Hz, 2H), 4.14 (br, 1H), 3.48 (t, J = 8.1 Hz, 1H), 3.27 (s, 3H), 2.92 (d, J = 11.6 Hz, 1H), 2.74 (s, 2H), 2.58 (dd, J = 11.6, 4.3 Hz, 1H), 1.78 – 1.67 (m, 1H), 1.59 – 1.46 (m, 1H), 0.84 (s,

9H), -0.02 (s, 6H); ^{13}C NMR (126 MHz) δ 173.40, 129.80, 128.08, 127.89, 73.39, 58.25, 56.39, 41.37, 37.85, 25.84, 18.02, -4.70, -4.72; HRMS (ESI) calcd for $\text{C}_{18}\text{H}_{31}\text{N}_2\text{O}_2\text{Si}$ m/z 335.2155 ($[\text{M} + \text{H}]^+$), found m/z 335.2193.

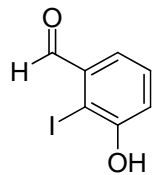
2-Iodo-3-methoxybenzaldehyde (3.27)



3.27

To a stirred solution of (2-iodo-3-methoxyphenyl)methanol²⁶ (1.05 g, 4.0 mmol) in acetone (16 mL) at 0 °C was added Jones' reagent (1.5 mL) dropwise. The resulting yellow solution was stirred at 0 °C for 10 min. Saturated aqueous NaHCO_3 (10 mL) was added to quench the reaction. The mixture was extracted with ether (20 mL \times 3) and the resulting organic solution was dried and concentrated to afford the crude **3.27** as a yellow solid (0.9 g). This was used in the next step without further purification. ^1H NMR (500 MHz) δ 10.18 (s, 1H), 7.49 (d, $J = 7.7$ Hz, 1H), 7.38 (t, $J = 7.8$ Hz, 1H), 7.04 (d, $J = 8.0$ Hz, 1H), 3.94 (s, 3H); ^{13}C NMR (126 MHz) δ 196.61, 158.37, 136.81, 129.58, 122.38, 116.11, 94.01, 56.93.

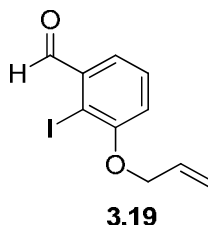
3-Hydroxy-2-iodobenzaldehyde (3.28)



3.28

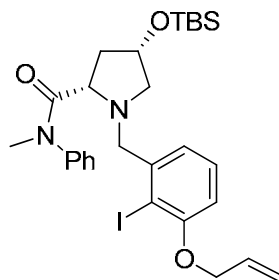
To a cooled solution (0 °C) of **3.27** (0.86 g, 3.3 mmol) in CH₂Cl₂ (30 mL) was added a 1 M solution of BBr₃ in CH₂Cl₂ (8.2 mL, 8.2 mmol, 2.5 equiv) dropwise. The resulting solution was brought to rt and stirred for 4 h. The reaction was stopped by adding cold water (10 mL). The aqueous phase was extracted with CH₂Cl₂ (20 mL × 3) and the combined organic phase was washed, dried and concentrated. The crude product was purified by column chromatography (1:4 EtOAc:hexanes) to give compound **3.28** as a crystalline solid (0.40 g, 49%). ¹H NMR (500 MHz) δ 10.03 (s, 1H), 7.45 (dd, *J* = 7.5, 1.6 Hz, 1H), 7.35 (t, *J* = 7.7 Hz, 1H), 7.26 (dd, *J* = 8.1, 1.5 Hz, 1H); ¹³C NMR (126 MHz) δ 194.69, 155.56, 135.79, 130.01, 124.13, 120.83, 100.00.

3-(Allyloxy)-2-iodobenzaldehyde (3.19)



A solution of **3.28** (0.38 g, 1.5 mmol) in DMF (10 mL) was treated with K_2CO_3 (0.63 g, 4.5 mmol, 3 equiv) and allylbromide (0.15 mL, 1.7 mmol, 1.1 equiv). The resulting suspension was stirred for 6 hours at rt. Water (5 mL) and ether (15 mL) were added to the reaction mixture and the aqueous phase was extracted with ether (15 mL \times 2). The combined ether layers was dried and concentrated. The residue was purified by column chromatography (1:9 EtOAc:hexanes) to afford compound **3.19** as a colorless oil (0.42 g, 96%). 1H NMR (400 MHz) δ 10.20 (s, 1H), 7.50 (d, $J = 8.6$ Hz, 1H), 7.36 (t, $J = 7.9$ Hz, 1H), 7.03 (d, $J = 8.1$ Hz, 1H), 6.16 – 6.00 (m, 1H), 5.56 (d, $J = 17.2$ Hz, 1H), 5.36 (d, $J = 10.6$ Hz, 1H), 4.65 (s, 2H); ^{13}C NMR (126 MHz) δ 196.66, 157.39, 136.88, 132.13, 129.47, 122.58, 118.21, 117.65, 94.67, 70.32.

(2*S*,4*S*)-1-(3-(Allyloxy)-2-iodobenzyl)-4-(*tert*-butyldimethylsilyloxy)-*N*-methyl-*N*-phenylpyrrolidine-2-carboxamide (3.29**)**

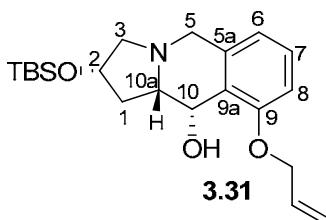


3.29

A mixture of **3.19** (0.60 g, 2.1 mmol) and **3.18** (0.70 g, 2.1 mmol, 1 equiv) in 1,2-dichloroethane (15 mL) was treated with NaBH(OAc)₃ (0.62 g, 2.9 mmol, 1.4 equiv). The resulting solution was stirred at rt overnight followed by the addition of saturated aqueous NaHCO₃ (5 mL). The aqueous phase was extracted with CH₂Cl₂ (15 mL × 2) and the combined organic phase was dried and concentrated in vacuo. The residue was purified by column chromatography (11% isopropanol in hexanes) to afford **3.29** as a colorless oil (1.1 g, 87%). $[\alpha]_D^{23}$ -49.4 (*c* 0.5, MeOH); ¹H NMR (400 MHz) δ 7.34 (m, 3H), 7.21 (t, *J* = 7.8 Hz, 1H), 7.13 (d, *J* = 6.8 Hz, 1H), 7.01 (d, *J* = 7.2 Hz, 1H), 6.71 (d, *J* = 8.5 Hz, 1H), 6.17 – 6.02 (m, 1H), 5.57 (ddd, *J* = 17.2, 3.2, 1.4 Hz, 1H), 5.33 (ddd, *J* = 10.4 Hz, 4.1, 1.5 Hz, 1H), 4.62 (dt, *J* = 4.7, 1.6 Hz, 1H), 4.32 – 4.18 (m, 1H), 3.88 (d, *J* = 14.5 Hz, 1H), 3.73 (d, *J* = 14.8 Hz, 1H), 3.45 (t, *J* = 7.1 Hz, 1H), 3.27 (s, 3H), 3.17 (dd, *J* = 9.0, 6.0 Hz, 1H), 2.73 – 2.65 (m, 1H), 2.18 – 2.08 (m, 1H), 2.00 – 1.89 (m, 1H), 0.87 (s, 9H), 0.01 (s, 6H); ¹³C NMR (126 MHz) δ 173.26, 156.98, 143.57, 132.84, 129.77, 129.34, 128.81, 127.83, 127.57, 123.07, 121.14, 118.19, 117.73, 117.59, 111.64, 111.00,

92.64, 70.63, 70.02, 69.78, 61.31, 60.93, 60.28, 40.06, 37.79, 25.91, 18.12, 1.10, 0.08, -4.66, -4.67, -4.69, -4.70; HRMS (ESI) calcd for C₂₈H₄₀IN₂O₃Si *m/z* 607.1853 ([M + H]⁺), found *m/z* 607.1883.

(2*S*,10*S*,10*aS*)-9-Allyloxy-10-hydroxy-2-(*tert*-butyldimethylsilyloxy)-1,2,3,5,10,10*a*-hexahydropyrrolo[1,2-*b*]isoquinoline (3.31)

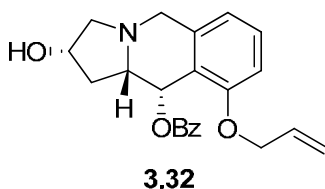


A solution of **3.29** (150 mg, 0.25 mmol) in THF (10 mL) was cooled to -78 °C and a 2.5 M solution of *n*-BuLi in hexanes (0.1 mL, 0.25 mmol) was added over 10 min. The resulting yellow solution was stirred for 3 hours at -78 °C and quenched by adding saturated aqueous NaHCO₃ (5 mL). The aqueous phase was extracted with EtOAc (10 mL × 2) and the combined organic phase was dried and concentrated to afford the crude ketone. This was used in the next step without further purification.

The crude ketone from the previous step was dissolved in MeOH (5 mL) and the resulting solution was treated with NaBH₄ (38 mg, 1 mmol). After stirring for 1 hour at rt, saturated aqueous NaHCO₃ (5 mL) was added carefully to quench the unreacted hydride. To the resulting solution was added ether (20 mL). The aqueous phase was extracted with ether (20 mL × 2) and the combined organic phase was washed, dried and concentrated. The residue was purified by preparative thin layer chromatography (PTLC)

(1:3 EtOAc:hexanes) to yield **3.31** as a colorless oil (53 mg, 57% for two steps). $[\alpha]_D^{23} +13.7$ (*c* 1.0, MeOH); $^1\text{H NMR}$ (500 MHz) δ 7.16 (t, *J* = 7.9 Hz, 1H), 6.73 (d, *J* = 8.2 Hz, 1H), 6.67 (d, *J* = 7.7 Hz, 1H), 6.08 (ddt, *J* = 17.2, 10.4, 5.1 Hz, 1H), 5.43 (dq, *J* = 17.3, 1.6 Hz, 1H), 5.26 (dq, *J* = 10.5, 1.4 Hz, 1H), 4.86 (dd, *J* = 9.7, 1.7 Hz, 1H), 4.66 (ddt, *J* = 12.9, 5.0, 1.6 Hz, 1H), 4.55 (ddt, *J* = 13.0, 5.3, 1.5 Hz, 1H), 4.45 – 4.38 (m, 1H), 4.10 (d, *J* = 14.9 Hz, 1H), 3.32 (d, *J* = 14.8 Hz, 1H), 3.16 (d, *J* = 9.7 Hz, 1H), 2.62 (d, *J* = 9.9 Hz, 1H), 2.48 – 2.40 (m, 2H), 2.26 – 2.15 (m, 2H), 0.88 (s, 9H), 0.07 (s, 3H), 0.07 (s, 3H); $^{13}\text{C NMR}$ (126 MHz) δ 157.14, 136.70, 133.48, 128.40, 127.18, 118.89, 117.44, 109.68, 70.55, 69.06, 64.84, 64.00, 61.87, 55.62, 36.49, 26.02, 18.26, -4.52, -4.70; HRMS (ESI) calcd for $\text{C}_{21}\text{H}_{34}\text{NO}_3\text{Si}$ *m/z* 376.2364 ($[\text{M} + \text{H}]^+$), found *m/z* 376.2308.

(2*S*,10*S*,10*aS*)-9-Allyloxy-10-benzoyloxy-2-hydroxy-1,2,3,5,10,10*a*-hexahydropyrrolo[1,2-*b*]isoquinoline (3.32**)**

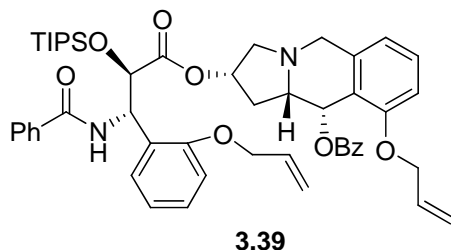


To a cooled (0 °C) solution of **3.31** (55 mg, 0.15 mmol) in THF (6 mL) was added slowly a 1.0 M solution of LiHMDS in THF (0.22 mL, 0.22 mmol, 1.5 equiv) and the resulting solution was stirred for 10 min at 0 °C. Benzoyl chloride (0.034 mL, 0.30 mmol, 2 equiv) was added to the mixture in one portion and the reaction was stirred for 4 hours at the same temperature. Saturated aqueous NaHCO_3 (5 mL) was added. Usual

A solution of **3.29** (470 mg, 0.77 mmol) in THF (15 mL) was cooled to -78 °C and a 2.5 M solution of *n*-BuLi in hexanes (0.34 mL, 0.85 mmol) was added over 10 min. The resulting yellow solution was stirred for 3 hours at -78 °C and quenched by adding saturated aqueous NaHCO₃ (8 mL). The aqueous phase was extracted with EtOAc (20 mL × 2). The combined organic layers were dried and concentrated to afford the crude ketone. A solution of this ketone in THF (8 mL) was cooled to 0 °C and treated with HF (0.3 mL, 70% in pyridine). The reaction mixture was warmed up to rt and stirred overnight. Saturated aqueous NaHCO₃ (15 mL) was added carefully to quench the unreacted HF and the resulting solution was extracted with EtOAc (20 mL × 3). The combined organic solution was washed, dried and concentrated to afford the crude product containing the deprotected ketone as an orange oil. To a stirred solution of this crude product in methanol (5 mL) was added NaBH₄ (117 mg, 3.1 mmol) in portions. After stirring for 1 hour at rt saturated aqueous NaHCO₃ (15 mL) was added slowly and the resulting solution was extracted with diethyl ether (20 mL × 3). The combined ether layers were dried and concentrated. The resulting crude product was purified by a short silica gel column and eluted first with hexanes : EtOAc = 1 : 2 (50 mL) and then CH₂Cl₂ : MeOH = 9 : 1 (50 mL). The second eluate was concentrated to give a diastereomeric mixture of **3.33** and **3.34**. The mixture was further separated by a short column packed with reversed phase silica gel C-18 (40% methanol in water) to afford **3.33** (59 mg, 29% for 3 steps) and **3.34** (40 mg, 20% for 3 steps) as white crystalline solids. **3.33**: [α]²³_D +100.3 (*c* 0.3, CHCl₃); ¹H NMR (500 MHz) δ 7.15 (t, *J* = 7.9 Hz, 1H), 6.75 (d, *J* = 8.2 Hz, 1H), 6.72 (d, *J* = 7.7 Hz, 1H), 6.06 (qd, *J* = 10.6, 5.3 Hz, 1H), 5.41 (d, *J* = 17.3 Hz,

1H), 5.32 (d, $J = 10.5$ Hz, 1H), 4.90 (d, $J = 8.7$ Hz, 1H), 4.61 (d, $J = 5.1$ Hz, 2H), 4.36 (t, $J = 4.7$ Hz, 1H), 4.20 (s, 1H), 3.97 (d, $J = 14.4$ Hz, 1H), 3.39 (d, $J = 14.4$ Hz, 1H), 3.13 (d, $J = 10.0$ Hz, 1H), 2.79 (dt, $J = 14.9, 7.6$ Hz, 1H), 2.41 (dd, $J = 10.0, 4.9$ Hz, 1H), 2.30 (q, $J = 8.3$ Hz, 1H), 1.76 (dd, $J = 13.5, 8.5$ Hz, 1H); ^{13}C NMR (126 MHz) δ 157.18, 137.07, 132.59, 128.13, 126.73, 119.56, 118.64, 110.00, 72.45, 70.35, 69.20, 65.85, 63.89, 55.54, 41.60; HRMS (ESI) calcd for $\text{C}_{15}\text{H}_{20}\text{NO}_3$ m/z 262.1443 ($[\text{M} + \text{H}]^+$), found m/z 262.1423. **3.34**: $[\alpha]_{\text{D}}^{23} +63.8$ (c 0.6, CHCl_3); ^1H NMR (500 MHz) δ 7.18 (t, $J = 7.9$ Hz, 1H), 6.75 (d, $J = 8.1$ Hz, 1H), 6.55 (d, $J = 7.7$ Hz, 1H), 6.09 (ddt, $J = 17.2, 10.2, 5.1$ Hz, 1H), 5.46 (dd, $J = 17.3, 1.5$ Hz, 1H), 5.29 (dd, $J = 10.6, 1.4$ Hz, 1H), 4.82 (s, 1H), 4.64 (dd, $J = 12.9, 4.8$ Hz, 1H), 4.56 (dd, $J = 12.9, 5.3$ Hz, 1H), 4.28 (t, $J = 6.5$ Hz, 1H), 3.37 (d, $J = 14.9$ Hz, 1H), 3.06 (d, $J = 14.8$ Hz, 1H), 2.95 (d, $J = 10.1$ Hz, 1H), 2.37 – 2.22 (m, 3H), 2.22 – 2.16 (m, 1H); ^{13}C NMR (126 MHz) δ 157.25, 136.35, 133.26, 128.49, 126.34, 119.24, 117.57, 109.53, 77.36, 77.11, 76.86, 69.93, 68.98, 65.12, 64.18, 61.80, 54.84, 36.04; HRMS (ESI) calcd for $\text{C}_{15}\text{H}_{20}\text{NO}_3$ m/z 262.1443 ($[\text{M} + \text{H}]^+$), found m/z 262.1424.

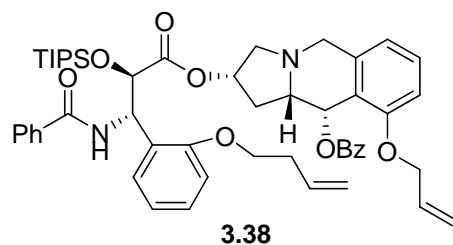
**(2*S*,10*S*,10*aS*)-9-Allyloxy-10-benzoyloxy-1,2,3,5,10,10*a*-hexahydropyrrolo[1,2-
b]isoquinolin-2-yl (2'*S*,3'*R*)-3'-benzoylamino-2'-triisopropylsilyloxy-3'-(2-
(allyloxy)phenyl)-propanoate (3.39)**



To a stirred suspension of NaH (100 mg, 60 %, dispersed in mineral oil, 2.5 mmol, 25 equiv) in THF (1 mL) at 0 °C was added a solution of **3.32** (36.5 mg, 0.1 mmol, 1 equiv) in THF (1 mL) and the resulting mixture was stirred for 10 min at 0 °C. To this mixture was added a solution of **3.36**²² (75 mg, 0.16 mmol, 1.6 equiv) in THF (1 mL). The reaction was allowed to warm up gradually to rt overnight and quenched by careful addition of excess aqueous NaHCO₃. The aqueous phase was extracted with EtOAc (10 mL × 3) and the combined organic phase was dried and concentrated. Purification by PTLC (hexanes:EtOAc = 2:1) yielded compound **3.39** as a colorless oil (82 mg, 97 %). [α]_D²³ -16.6 (*c* 1.0, MeOH); ¹H NMR (500 MHz) δ 8.06 (dd, *J* = 8.3, 1.3 Hz, 2H), 7.88 – 7.83 (m, 2H), 7.50 (t, *J* = 7.4 Hz, 1H), 7.39 – 7.33 (m, 3H), 7.32 – 7.21 (m, 4H), 7.17 – 7.12 (m, 1H), 7.09 (d, *J* = 7.8 Hz, 1H), 6.82 (t, *J* = 7.5 Hz, 1H), 6.74 – 6.67 (m, 2H), 6.64 (d, *J* = 7.8 Hz, 1H), 6.49 (d, *J* = 3.2 Hz, 1H), 5.88 – 5.68 (m, 3H), 5.37 (dd, *J* = 17.3, 1.5 Hz, 1H), 5.25 – 5.20 (m, 1H), 5.18 (ddd, *J* = 17.3, 3.1, 1.6 Hz, 1H), 5.09 – 5.03 (m, 2H), 4.87 (d, *J* = 2.7 Hz, 1H), 4.41 (qd, *J* = 12.7, 5.2 Hz, 2H), 4.32 (dt, *J* = 4.7, 1.3 Hz, 2H),

3.87 (d, $J = 15.0$ Hz, 1H), 3.23 – 3.14 (m, 2H), 2.62 – 2.48 (m, 2H), 2.45 – 2.36 (m, 1H), 1.95 – 1.86 (m, 1H), 0.93 – 0.82 (m, 3H), 0.80 – 0.69 (m, 18H); ^{13}C NMR (125 MHz) δ 172.55, 166.61, 166.38, 157.56, 155.71, 137.64, 134.58, 132.71, 132.70, 131.39, 130.67, 130.08, 129.43, 128.82, 128.55, 128.26, 127.98, 127.24, 121.54, 120.64, 118.81, 117.38, 111.65, 109.41, 77.29, 73.54, 72.96, 68.90, 68.59, 64.89, 63.59, 61.31, 55.19, 53.80, 32.44, 17.71, 17.67, 12.16; HRMS (ESI) calcd for $\text{C}_{50}\text{H}_{61}\text{N}_2\text{O}_8\text{Si}$ m/z 845.4197 ($[\text{M} + \text{H}]^+$), found m/z 845.4203.

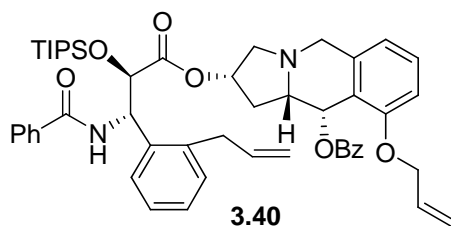
(2*S*,10*S*,10*aS*)-9-Allyloxy-10-benzoyloxy-1,2,3,5,10,10*a*-hexahydropyrrolo[1,2-*b*]isoquinolin-2-yl (2'*S*,3'*R*)-3'-benzoylamino-2'-triisopropylsilyloxy-3'-(2-(but-3-enyloxy)phenyl)-propanoate (3.38)



To a stirred suspension of NaH (79 mg, 60 %, dispersed in mineral oil, 2.0 mmol, 27 equiv) in THF (2.5 mL) at 0 °C was added slowly a solution of **3.32** (27 mg, 0.074 mmol) in THF (2.5 mL) and the resulting mixture was stirred for 10 min at 0 °C. To this mixture was added a solution of **3.35**²² (61 mg, 0.12 mmol, 1.7 equiv) in THF (2.5 mL). The reaction was allowed to warm up gradually to rt overnight and quenched by careful addition of excess aqueous NaHCO_3 . The aqueous phase was extracted with EtOAc (10 mL \times 3) and the combined organic phase was dried and concentrated. Purification by

PTLC (hexanes:EtOAc = 2:1) yielded compound **3.38** as a colorless oil (44 mg, 72 %). $[\alpha]_D^{23}$ -27.4 (*c* 0.5, MeOH); $^1\text{H NMR}$ (500 MHz) δ 8.05 (d, J = 7.8 Hz, 2H), 7.86 (d, J = 7.7 Hz, 2H), 7.50 (t, J = 7.4 Hz, 1H), 7.43 – 7.13 (m, 8H), 7.08 (d, J = 7.4 Hz, 1H), 6.80 (t, J = 7.5 Hz, 1H), 6.71 (t, J = 7.6 Hz, 2H), 6.62 (d, J = 7.7 Hz, 1H), 6.49 (d, J = 3.0 Hz, 1H), 5.86 – 5.67 (m, 3H), 5.29 – 4.94 (m, 5H), 4.88 (d, J = 2.6 Hz, 1H), 4.41 (ddd, J = 27.5, 12.6, 5.0 Hz, 2H), 3.85 (ddd, J = 23.5, 17.9, 12.2 Hz, 3H), 3.22 – 3.11 (m, 2H), 2.63 – 2.46 (m, 2H), 2.45 – 2.27 (m, 2H), 1.96 – 1.86 (m, 1H), 1.01 – 0.60 (m, 21H); $^{13}\text{C NMR}$ (125 MHz) δ 172.53, 166.73, 166.37, 157.54, 156.00, 137.69, 134.62, 134.58, 132.70, 131.38, 130.68, 130.06, 129.41, 128.85, 128.52, 128.25, 127.91, 127.30, 126.39, 121.56, 120.42, 118.81, 117.37, 117.35, 111.07, 109.38, 73.59, 72.89, 68.89, 67.17, 64.88, 63.55, 61.27, 55.13, 53.92, 33.52, 32.43, 17.71, 17.66, 12.16; HRMS (ESI) calcd for $\text{C}_{51}\text{H}_{63}\text{N}_2\text{O}_8\text{Si}$ m/z 859.4354 ($[\text{M} + \text{H}]^+$), found m/z 859.4358.

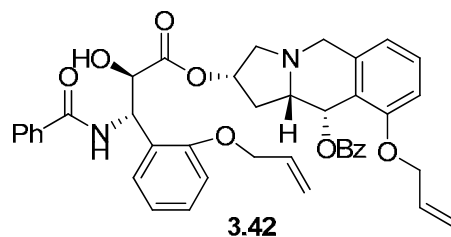
(2*S*,10*S*,10*aS*)-9-Allyloxy-10-benzoyloxy-1,2,3,5,10,10*a*-hexahydropyrrolo[1,2-*b*]isoquinolin-2-yl (2'*S*,3'*R*)-3'-benzoylamino-2'-triisopropylsilyloxy-3'-(2-allylphenyl)-propanoate (3.40)



To a stirred suspension of NaH (41 mg, 60 %, dispersed in mineral oil, 1.0 mmol, 25 equiv) in THF (1.5 mL) at 0 °C was added slowly a solution of **3.32** (15 mg, 0.041 mmol)

in THF (1.5 mL) and the resulting mixture was stirred for 10 min at 0 °C. To this mixture was added a solution of **3.37**²² (28.5 mg, 0.062 mmol, 1.5 equiv) in THF (1.5 mL). The reaction was allowed to warm up gradually to rt overnight and quenched by careful addition of excess aqueous NaHCO₃. The aqueous phase was extracted with EtOAc (10 mL × 3) and the combined organic phase was dried and concentrated. Purification by PTLC (hexanes:EtOAc = 2:1) yielded compound **3.40** as a colorless oil (28 mg, 83 %). [α]_D²³ -24.8 (*c* 0.8, CHCl₃); ¹H NMR (500 MHz) δ 8.04 (d, *J* = 7.5 Hz, 2H), 7.84 (d, *J* = 7.4 Hz, 2H), 7.51 (t, *J* = 7.4 Hz, 1H), 7.36 (m, 3H), 7.28 (m, 3H), 7.25 – 7.22 (m, 1H), 7.20 – 7.10 (m, 2H), 7.10 – 7.02 (m, 2H), 6.73 (d, *J* = 8.2 Hz, 1H), 6.64 (d, *J* = 7.7 Hz, 1H), 6.52 (d, *J* = 3.0 Hz, 1H), 5.82 – 5.71 (m, 2H), 5.62 (t, *J* = 8.1 Hz, 1H), 5.32 – 5.25 (m, 2H), 5.18 (d, *J* = 17.3 Hz, 1H), 5.06 (d, *J* = 9.8 Hz, 1H), 4.54 (s, 1H), 4.42 (qd, *J* = 12.7, 5.2 Hz, 2H), 3.90 (d, *J* = 15.0 Hz, 1H), 3.40 (dd, *J* = 15.9, 5.6 Hz, 1H), 3.30 – 3.11 (m, 3H), 2.65 – 2.44 (m, 3H), 2.10 – 1.96 (m, 1H), 0.83 – 0.63 (m, 21H); ¹³C NMR (126 MHz) δ 172.37, 166.60, 166.45, 137.55, 137.02, 136.97, 136.28, 136.26, 132.75, 132.69, 131.50, 131.49, 130.56, 130.30, 130.07, 129.45, 128.58, 128.24, 127.83, 127.24, 126.89, 126.22, 121.48, 118.81, 117.40, 116.49, 109.45, 74.65, 73.48, 68.91, 64.81, 63.77, 61.52, 55.14, 53.63, 36.53, 32.50, 29.78, 17.70, 17.66, 12.20; HRMS (ESI) calcd for C₅₀H₆₁N₂O₇Si *m/z* 829.4248 ([M + H]⁺), found *m/z* 829.4196.

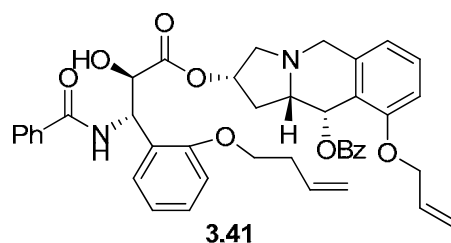
**(2*S*,10*S*,10*aS*)-9-Allyloxy-10-benzoyloxy-1,2,3,5,10,10*a*-hexahydropyrrolo[1,2-
b]isoquinolin-2-yl (2'*S*,3'*R*)-3'-benzoylamino-2'-hydroxy-3'-(2-(allyloxy)phenyl)-
propanoate (3.42)**



A solution of compound **3.39** (18 mg, 0.038 mmol) in THF (5 mL) was cooled to 0 °C with an ice bath and treated with HF pyridine (0.15 mL, 70%). The ice bath was removed and the reaction was continued overnight. Saturated aqueous NaHCO₃ (10 mL) was added slowly and the resulting solution was extracted with EtOAc (20 mL × 3). The EtOAc solution was washed, dried and concentrated. The crude product was purified by PTLC (50 % EtOAc in hexanes) to yield compound **3.42** (11.5 mg, 84 %) as a white solid. $[\alpha]_D^{23}$ -47.8 (*c* 0.5, MeOH); ¹H NMR (400 MHz) δ 8.08 (d, *J* = 7.8 Hz, 2H), 7.73 (d, *J* = 7.8 Hz, 2H), 7.52 (t, *J* = 7.4 Hz, 1H), 7.49 – 7.32 (m, 6H), 7.25 – 7.16 (m, 2H), 7.08 (d, *J* = 7.4 Hz, 1H), 6.84 (t, *J* = 7.5 Hz, 1H), 6.73 (d, *J* = 7.8 Hz, 1H), 6.70 (d, *J* = 8.2 Hz, 1H), 6.52 (d, *J* = 8.3 Hz, 1H), 6.43 (d, *J* = 2.9 Hz, 1H), 5.85 – 5.67 (m, 2H), 5.52 (dd, *J* = 9.0, 6.8 Hz, 1H), 5.28 (m, 2H), 5.20 – 5.12 (m, 2H), 5.05 (d, *J* = 10.4 Hz, 2H), 4.52 (br, s, 1H), 4.38 (ddd, *J* = 35.2, 12.6, 5.1 Hz, 2H), 4.19 – 4.08 (m, 2H), 3.99 (dd, *J* = 12.6, 4.8 Hz, 1H), 3.33 (d, *J* = 11.5 Hz, 1H), 3.26 (d, *J* = 15.1 Hz, 1H), 2.56 – 2.40 (m, 2H), 2.23 – 2.10 (m, 1H); ¹³C NMR (126 MHz) δ 173.07, 167.39, 166.28, 157.54, 156.19, 137.37, 134.30, 132.84, 132.65, 132.52, 131.60, 130.63, 130.20, 129.68, 129.54,

129.31, 128.53, 128.30, 127.14, 125.22, 121.40, 121.19, 118.78, 118.18, 117.39, 112.06, 109.49, 73.87, 73.20, 68.89, 68.64, 64.81, 63.79, 61.22, 55.78, 55.32, 32.38; HRMS (ESI) calcd for C₄₁H₄₁N₂O₈ *m/z* 689.2863 ([M + H]⁺), found *m/z* 689.2858.

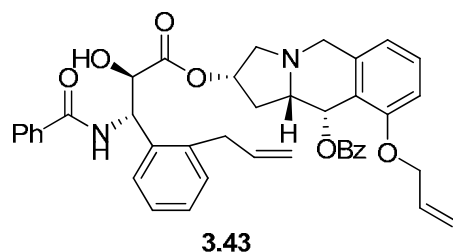
(2*S*,10*S*,10*aS*)-9-Allyloxy-10-benzoyloxy-1,2,3,5,10,10*a*-hexahydropyrrolo[1,2-*b*]isoquinolin-2-yl (2'*S*,3'*R*)-3'-benzoylamino-2'-hydroxy-3'-(2-(but-3-enyloxy)phenyl)-propanoate (3.41)



A solution of compound **3.38** (8 mg, 0.009 mmol) in THF (3 mL) was cooled to 0 °C with an ice bath and treated with HF (0.1 mL, 70% in pyridine). The ice bath was removed and the reaction was continued overnight. Saturated aqueous NaHCO₃ (10 mL) was added slowly and the resulting solution was extracted with EtOAc (20 mL × 3). The EtOAc solution was washed, dried and concentrated. The crude product was purified by PTLC (1:1 EtOAc:hexanes) to yield compound **3.41** (5.5 mg, 85 %) as an amorphous solid. $[\alpha]_D^{23}$ -31.8 (*c* 0.5, MeOH); ¹H NMR (500 MHz) δ 8.10 – 8.05 (m, 2H), 7.75 – 7.67 (m, 2H), 7.54 – 7.48 (m, 1H), 7.48 – 7.42 (m, 1H), 7.41 – 7.33 (m, 5H), 7.24 – 7.14 (m, 2H), 7.07 (dd, *J* = 7.6, 1.6 Hz, 1H), 6.84 – 6.79 (m, 1H), 6.72 (d, *J* = 7.8 Hz, 1H), 6.70 (d, *J* = 8.3 Hz, 1H), 6.52 (d, *J* = 8.2 Hz, 1H), 6.42 (d, *J* = 3.0 Hz, 1H), 5.82 – 5.60 (m, 2H), 5.47 (dd, *J* = 9.1, 6.9 Hz, 1H), 5.15 (dd, *J* = 17.3, 1.5 Hz, 1H), 5.07 – 4.96 (m,

3H), 4.90 (dd, $J = 10.2, 1.2$ Hz, 1H), 4.50 (m, 1H), 4.44 – 4.29 (m, 2H), 4.11 (m, 2H), 3.72 (ddd, $J = 9.0, 7.4, 5.8$ Hz, 1H), 3.52 – 3.32 (m, 2H), 3.29 (d, $J = 11.5$ Hz, 1H), 3.24 (d, $J = 14.9$ Hz, 1H), 2.53 – 2.38 (m, 2H), 2.32 – 2.18 (m, 2H), 2.17 – 2.05 (m, 1H); ^{13}C NMR (126 MHz) δ 173.08, 167.91, 166.23, 157.53, 156.58, 137.39, 134.47, 134.35, 132.85, 132.64, 131.59, 130.62, 130.18, 129.80, 129.54, 129.46, 128.48, 128.31, 127.29, 124.94, 121.37, 121.04, 118.79, 117.88, 117.39, 111.62, 109.48, 74.03, 73.01, 68.87, 66.77, 64.80, 63.78, 61.21, 56.39, 55.34, 33.68, 32.36, 29.78; HRMS (ESI) calcd for $\text{C}_{42}\text{H}_{43}\text{N}_2\text{O}_8$ m/z 703.3014 ($[\text{M} + \text{H}]^+$), found m/z 703.3027.

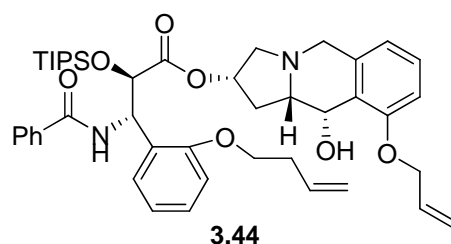
(2*S*,10*S*,10*aS*)-9-Allyloxy-10-benzoyloxy-1,2,3,5,10,10*a*-hexahydropyrrolo[1,2-*b*]isoquinolin-2-yl (2'*S*,3'*R*)-3'-benzoylamino-2'-hydroxy-3'-(2-allylphenyl)-propanoate (3.43)



A solution of compound **3.40** (5 mg, 0.006 mmol) in THF (3 mL) was cooled to 0 °C with an ice bath and treated with HF (0.1 mL, 70% in pyridine). The ice bath was removed and the reaction was continued overnight. Saturated aqueous NaHCO_3 (10 mL) was added slowly and the resulting solution was extracted with EtOAc (10 mL \times 3). The EtOAc solution was washed, dried and concentrated. The crude product was purified by

PTLC (1:1 EtOAc:hexanes) to yield compound **3.43** (3.5 mg, 87 %) as a colorless oil. $[\alpha]_D^{23} -16.0$ (c 0.3, CHCl_3); $^1\text{H NMR}$ (500 MHz) δ 8.00 (d, $J = 7.9$ Hz, 2H), 7.71 (d, $J = 7.8$ Hz, 2H), 7.47 – 7.42 (m, 1H), 7.39 (m, 2H), 7.34 (m, 2H), 7.31 – 7.22 (m, 3H), 7.18 (t, $J = 7.4$ Hz, 1H), 7.12 – 7.05 (m, 2H), 6.76 – 6.68 (m, 3H), 6.54 (d, $J = 2.8$ Hz, 1H), 5.83 – 5.64 (m, 3H), 5.27 (t, $J = 8.6$ Hz, 1H), 5.18 (d, $J = 17.3$ Hz, 1H), 5.06 (d, $J = 10.6$ Hz, 1H), 4.85 – 4.77 (m, 2H), 4.48 – 4.32 (m, 3H), 4.15 (d, $J = 14.9$ Hz, 1H), 3.43 (d, $J = 11.6$ Hz, 1H), 3.31 (d, $J = 14.8$ Hz, 1H), 3.26 (m, 2H), 2.68 – 2.47 (m, 3H), 1.95 (m, 1H). $^{13}\text{C NMR}$ (126 MHz) δ 173.09, 166.84, 166.49, 157.60, 138.03, 137.36, 137.08, 136.47, 134.14, 132.77, 132.69, 131.68, 130.47, 130.43, 130.02, 129.54, 128.61, 128.18, 128.16, 127.16, 126.89, 126.76, 121.55, 118.78, 117.45, 116.33, 109.54, 77.35, 77.09, 76.84, 74.78, 72.90, 68.93, 64.70, 63.94, 61.01, 55.28, 51.55, 36.91, 29.78; HRMS (ESI) calcd for $\text{C}_{41}\text{H}_{41}\text{N}_2\text{O}_7$ m/z 673.2914 ($[\text{M} + \text{H}]^+$), found m/z 673.2878.

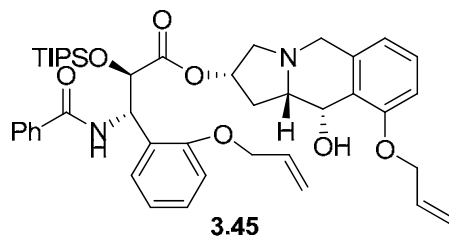
(2*S*,10*S*,10*aS*)-9-Allyloxy-10-hydroxy-1,2,3,5,10,10*a*-hexahydropyrrolo[1,2-*b*]isoquinolin-2-yl (2'*S*,3'*R*)-3'-benzoylamino-2'-triisopropylsilyloxy-3'-(2-(but-3-enyloxy)phenyl)-propanoate (3.44**)**



A solution of **3.34** (12 mg, 0.046 mmol, 1 equiv) in THF (1.5 mL) was added into a stirred cold (0 °C) suspension of NaH (52.3 mg, 60 %, dispersed in mineral oil, 1.3

mmol, 28 equiv) in THF (1.5 mL) at and the resulting mixture was stirred for 10 min at 0 °C. To this mixture was added a solution of **3.35** (22.7 mg, 0.046 mmol, 1.0 equiv) in THF (1.5 mL) and the reaction was allowed to continue for 20 min at 0 °C. Aqueous NaHCO₃ (5 mL) was added and the aqueous phase was extracted with EtOAc (10 mL × 3) and the combined organic phase was dried and concentrated. Purification by PTLC (hexanes:EtOAc = 3:1) yielded compound **3.44** as a colorless oil (26 mg, 75 %). $[\alpha]_D^{23}$ -15.2 (*c* 1.5, CHCl₃); ¹H NMR (500 MHz) δ 7.89 – 7.83 (m, 2H), 7.44 – 7.28 (m, 4H), 7.23 – 7.14 (m, 3H), 6.88 – 6.81 (m, 2H), 6.74 (d, *J* = 8.2 Hz, 1H), 6.62 (d, *J* = 7.7 Hz, 1H), 6.14 – 5.95 (m, 2H), 5.83 (dd, *J* = 8.5, 1.4 Hz, 1H), 5.43 (dd, *J* = 17.2, 1.6 Hz, 1H), 5.30 – 5.18 (m, 3H), 5.08 (dd, *J* = 13.4, 3.2 Hz, 1H), 4.97 (d, *J* = 1.9 Hz, 1H), 4.86 (s, 1H), 4.70 – 4.53 (m, 2H), 4.13 – 4.03 (m, 2H), 3.85 (d, *J* = 15.1 Hz, 1H), 3.26 – 3.14 (m, 2H), 2.73 – 2.56 (m, 2H), 2.53 (dd, *J* = 11.2, 6.1 Hz, 1H), 2.42 (tdd, *J* = 16.6, 10.2, 6.6 Hz, 2H), 2.30 (ddd, *J* = 12.2, 8.0, 6.0 Hz, 1H), 0.96 – 0.81 (m, 21H); ¹³C NMR (126 MHz) δ 172.47, 166.40, 157.09, 155.96, 136.13, 134.96, 134.60, 133.41, 131.50, 128.79, 128.65, 128.54, 127.59, 127.07, 126.66, 120.39, 118.92, 117.52, 117.25, 111.07, 109.81, 73.77, 73.55, 69.10, 67.47, 64.58, 61.51, 61.48, 55.37, 53.04, 33.77, 31.72, 17.83, 17.83, 17.82, 17.76, 12.31; HRMS (ESI) calcd for C₄₄H₅₉N₂O₇Si *m/z* 755.4092 ([M + H]⁺), found *m/z* 755.4101.

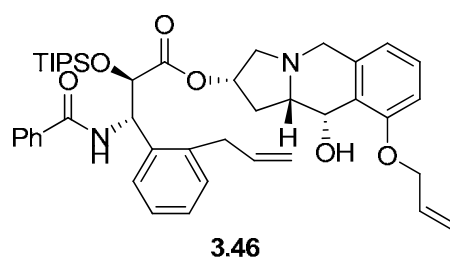
**(2*S*,10*S*,10*aS*)-9-Allyloxy-10-hydroxy-1,2,3,5,10,10*a*-hexahydropyrrolo[1,2-
b]isoquinolin-2-yl (2'*S*,3'*R*)-3'-benzoylamino-2'-triisopropylsilyloxy-3'-(2-
(allyloxy)phenyl)-propanoate (3.45)**



A solution of **3.34** (11.4 mg, 0.044 mmol) in THF (1.5 mL) was added into a stirred cold (0 °C) suspension of NaH (42 mg, 60 %, dispersed in mineral oil, 1.05 mmol, 24 equiv) in THF (1.5 mL) and the resulting mixture was stirred for 10 min at 0 °C. To this mixture was added a solution of **3.36** (22 mg, 0.046 mmol, 1.04 equiv) in THF (1.5 mL) and the reaction was allowed to continue for 20 min at 0 °C. Aqueous NaHCO₃ (5 mL) was added into the reaction mixture and the aqueous phase was extracted with EtOAc (10 mL × 3) and the combined organic phase was dried and concentrated. Purification by PTLC (hexanes:EtOAc = 3:1) yielded compound **3.45** as a yellowish oil (29 mg, 89 %). [α]_D²³ -14.3 (*c* 0.8, CHCl₃); ¹H NMR (500 MHz) δ 7.87 – 7.83 (m, 2H), 7.39 (dt, *J* = 2.4, 1.8 Hz, 1H), 7.34 (dd, *J* = 8.1, 6.4 Hz, 3H), 7.19 (dt, *J* = 16.0, 4.8 Hz, 3H), 6.89 – 6.83 (m, 2H), 6.75 (d, *J* = 8.1 Hz, 1H), 6.62 (d, *J* = 7.7 Hz, 1H), 6.18 – 6.03 (m, 2H), 5.89 – 5.82 (m, 1H), 5.57 – 5.51 (m, 1H), 5.48 – 5.40 (m, 1H), 5.35 – 5.20 (m, 4H), 4.98 (d, *J* = 2.0 Hz, 1H), 4.89 – 4.83 (m, 1H), 4.68 (ddt, *J* = 13.1, 4.9, 1.5 Hz, 1H), 4.63 – 4.53 (m, 3H), 3.86 (d, *J* = 15.0 Hz, 1H), 3.25 – 3.15 (m, 2H), 2.53 (dd, *J* = 11.3, 6.1 Hz, 1H), 2.48 – 2.36 (m, 2H), 2.33 – 2.26 (m, 1H), 2.21 (d, *J* = 9.8 Hz, 1H), 0.95 – 0.81 (m, 21H); ¹³C

NMR (126 MHz) δ 172.48, 166.35, 157.09, 155.72, 136.13, 134.56, 133.40, 133.09, 131.50, 128.79, 128.65, 128.56, 127.74, 127.06, 126.86, 126.63, 120.62, 118.93, 117.55, 117.53, 111.66, 109.83, 73.83, 73.57, 69.10, 68.92, 64.57, 61.51, 61.50, 55.40, 53.07, 31.68, 17.82, 17.81, 17.76, 12.31; HRMS (ESI) calcd for $C_{43}H_{57}N_2O_7Si$ m/z 741.3935 ($[M + H]^+$), found m/z 741.3915.

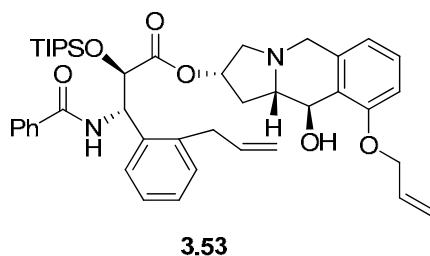
(2*S*,10*S*,10*aS*)-9-Allyloxy-10-hydroxy-1,2,3,5,10,10*a*-hexahydropyrrolo[1,2-*b*]isoquinolin-2-yl (2'*S*,3'*R*)-3'-benzoylamino-2'-triisopropylsilyloxy-3'-(2-allylphenyl)-propanoate (3.46)



A solution of **3.34** (18 mg, 0.069 mmol) in THF (1.5 mL) was added into a stirred cold (0 °C) suspension of NaH (66 mg, 60 %, dispersed in mineral oil, 1.65 mmol, 24 equiv) in THF (1.5 mL) and the resulting mixture was stirred for 10 min at 0 °C. To this mixture was added a solution of **3.37** (33.6 mg, 0.072 mmol, 1.05 equiv) in THF (1.5 mL) and the reaction was allowed to continue for 20 min at 0 °C. Aqueous NaHCO₃ (5 mL) was added into the reaction mixture and the aqueous phase was extracted with EtOAc (10 mL \times 3) and the combined organic phase was dried and concentrated. Purification by PTLC (hexanes:EtOAc = 3:1) yielded compound **3.46** as a yellowish oil

(46 mg, 92 %). $[\alpha]_D^{23}$ -14.9 (*c* 1.0, CHCl₃); ¹H NMR (500 MHz) δ 7.87 – 7.80 (m, 2H), 7.46 – 7.35 (m, 3H), 7.35 – 7.27 (m, 3H), 7.22 – 7.10 (m, 4H), 6.75 (d, *J* = 8.1 Hz, 1H), 6.62 (t, *J* = 9.9 Hz, 1H), 6.15 – 5.98 (m, 2H), 5.81 (d, *J* = 8.0 Hz, 1H), 5.47 – 5.41 (m, 1H), 5.32 – 5.26 (m, 2H), 5.22 – 5.16 (m, 1H), 5.16 – 5.12 (m, 1H), 4.88 (d, *J* = 4.2 Hz, 1H), 4.72 – 4.64 (m, 2H), 4.58 (m, 1H), 3.87 (d, *J* = 15.0 Hz, 1H), 3.74 – 3.53 (m, 2H), 3.27 – 3.14 (m, 2H), 2.52 (m, 2H), 2.38 (m, 2H), 0.99 – 0.83 (m, 21H); ¹³C NMR (126 MHz) δ 172.29, 166.26, 157.11, 137.15, 137.10, 136.82, 136.14, 134.31, 133.36, 131.57, 130.36, 128.74, 128.66, 128.60, 127.90, 127.13, 127.02, 126.96, 126.50, 126.26, 124.89, 118.95, 117.61, 116.67, 109.80, 74.79, 74.16, 69.10, 64.60, 61.52, 55.34, 53.27, 36.76, 31.69, 17.83, 17.79, 17.75, 12.46, 12.36, 0.08; HRMS (ESI) calcd for C₄₃H₅₇N₂O₆Si *m/z* 725.3986 ([M + H]⁺), found *m/z* 725.3967.

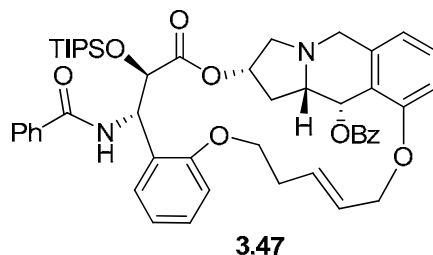
(2*S*,10*R*,10*aS*)-9-Allyloxy-10-hydroxy-1,2,3,5,10,10*a*-hexahydropyrrolo[1,2-*b*]isoquinolin-2-yl (2'*S*,3'*R*)-3'-benzoylamino-2'-triisopropylsilyloxy-3'-(2-allylphenyl)-propanoate (3.53)



A solution of **3.33** (24 mg, 0.092 mmol) in THF (1.5 mL) was added into a stirred cold (0 °C) suspension of NaH (44 mg, 60 %, dispersed in mineral oil, 1.1 mmol, 12

equiv) in THF (1.5 mL) and the resulting mixture was stirred for 10 min at 0 °C. To this mixture was added a solution of **3.37** (43 mg, 0.093 mmol, 1.01 equiv) in THF (1.5 mL) and the reaction was allowed to continue for 20 min at 0 °C. Aqueous NaHCO₃ (5 mL) was added into the reaction mixture and the aqueous phase was extracted with EtOAc (10 mL × 3) and the combined organic phase was dried and concentrated. Purification by PTLC (hexanes:EtOAc = 3:1) yielded compound **3.53** as a yellowish oil (49 mg, 73 %). $[\alpha]_D^{23}$ -8.5 (*c* 0.6, CHCl₃); ¹H NMR (500 MHz) δ 7.84 – 7.76 (m, 2H), 7.39 – 7.34 (m, 2H), 7.31 – 7.26 (m, 3H), 7.23 – 7.07 (m, 4H), 6.75 (dd, *J* = 10.6, 6.1 Hz, 1H), 6.64 (d, *J* = 7.7 Hz, 1H), 6.14 – 5.99 (m, 2H), 5.79 (d, *J* = 8.0 Hz, 1H), 5.48 – 5.41 (m, 1H), 5.37 – 5.28 (m, 2H), 5.19 (dd, *J* = 17.1, 1.6 Hz, 1H), 5.11 (dd, *J* = 10.1, 1.4 Hz, 1H), 4.89 (d, *J* = 8.5 Hz, 1H), 4.70 – 4.57 (m, 3H), 4.16 (s, 1H), 3.74 (d, *J* = 14.5 Hz, 1H), 3.70 – 3.54 (m, 2H), 3.29 (d, *J* = 14.4 Hz, 1H), 3.16 (d, *J* = 11.2 Hz, 1H), 2.90 – 2.78 (m, 1H), 2.52 (dd, *J* = 11.1, 5.8 Hz, 1H), 2.31 (dd, *J* = 16.0, 8.7 Hz, 1H), 2.00 – 1.90 (m, 1H), 1.01 – 0.82 (m, 21H); ¹³C NMR (126 MHz) δ 172.07, 166.33, 137.12, 137.04, 136.93, 136.71, 134.34, 132.64, 131.45, 130.22, 128.66, 128.55, 127.99, 127.90, 127.11, 127.06, 126.97, 126.62, 126.28, 119.59, 118.61, 116.72, 109.87, 74.80, 74.12, 72.07, 69.20, 65.65, 61.13, 55.28, 53.31, 37.51, 36.84, 17.83, 17.82, 17.80, 17.79, 12.38; HRMS (ESI) calcd for C₄₃H₅₇N₂O₆Si *m/z* 725.3922 ([M + H]⁺), found *m/z* 725.3986.

Protected macrocyclic paclitaxel mimic **3.47**

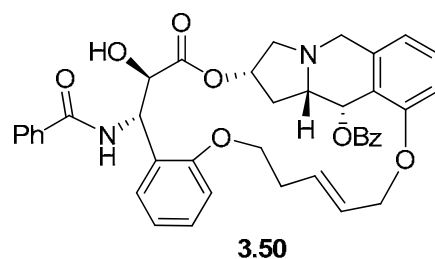


To a stirred solution of **3.44** (20 mg, 0.026 mmol, 1 equiv) in CH_2Cl_2 (25 mL) was added D-(-)-10-camphorsulphonic acid (18.5 mg, 0.079 mmol, 3 equiv) and the mixture was refluxed for 1 hour. The reaction mixture was cooled to rt and Grubbs 2nd generation catalyst (2.2 mg, 10 mol %) in CH_2Cl_2 (5 mL) was added slowly. The resulting solution was heated to reflux and continued stirring for 2 hours. The resulting light brown solution was washed with 1N aqueous NaOH (3 mL \times 2), dried with anhydrous Na_2SO_4 and concentrated under vacuum to yield a dark brown residue. The crude product was purified by PTLC (hexanes:EtOAc=2:1) and the spot with a $R_f = 0.3$ was collected (15.5 mg, with minor impurities) and used in the next step without further purification.

The product (5 mg) after the ring-closing metathesis was dissolved in dry THF (1 mL) and cooled to $-78\text{ }^\circ\text{C}$, followed by slow addition of lithium bis(trimethylsilyl)amide solution in THF (1M, 21 μL , 3 equiv). The resulting mixture was stirred at $-78\text{ }^\circ\text{C}$ for 10 min before the addition of benzoyl chloride (3.2 μL , 4 equiv) in one portion. The reaction was allowed to continue for another 3h at $-78\text{ }^\circ\text{C}$ before the addition of saturated aqueous NaHCO_3 (5 mL). The resulting solution was extracted with EtOAc (20 mL \times 3), washed with brine and dried. The crude product was purified with PTLC (5% MeOH in CH_2Cl_2)

to yield **3.47** (5 mg, 70% from **3.44**) as a colorless oil. $[\alpha]_D^{23}$ -27.2 (*c* 0.5, CHCl₃); ¹H NMR (500 MHz) δ 8.23 (d, *J* = 7.5 Hz, 2H), 7.83 (d, *J* = 7.5 Hz, 2H), 7.61 – 7.42 (m, 6H), 7.22 – 7.10 (m, 3H), 7.07 (d, *J* = 8.5 Hz, 1H), 6.91 – 6.83 (m, 2H), 6.80 – 6.72 (m, 2H), 6.09 (d, *J* = 7.0 Hz, 1H), 5.92 – 5.78 (m, 2H), 5.57 – 5.45 (m, 1H), 5.35 – 5.25 (m, 1H), 4.91 (d, *J* = 2.0 Hz, 1H), 4.42 (dd, *J* = 12.8, 7.9 Hz, 1H), 4.27 (dd, *J* = 12.7, 5.3 Hz, 1H), 3.98 (m, 1H), 3.90 – 3.74 (m, 3H), 3.59 (d, *J* = 15.2 Hz, 1H), 3.14 – 3.07 (m, 1H), 2.57 – 2.48 (m, 1H), 2.43 (m, 1H), 2.34 (m, 1H), 2.08 (m, 2H), 0.91 – 0.75 (m, 21H); ¹³C NMR (126 MHz) δ 171.63, 166.70, 166.41, 155.80, 155.67, 138.04, 136.25, 134.85, 133.55, 133.13, 131.61, 130.17, 128.79, 128.58, 127.55, 127.41, 127.09, 126.95, 126.71, 124.66, 122.52, 120.71, 111.57, 73.71, 73.12, 72.04, 70.26, 68.15, 58.43, 56.04, 52.34, 51.17, 33.79, 32.83, 29.78, 17.68, 17.65, 12.27, 1.10, 1.09; HRMS (ESI) calcd for C₄₉H₅₉N₂O₈Si *m/z* 831.4041 ([M + H]⁺), found *m/z* 831.4054.

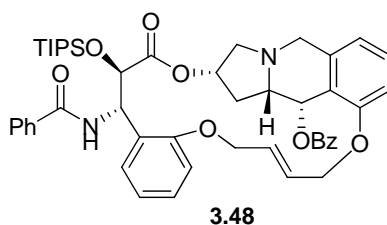
Macrocyclic paclitaxel mimic **3.50**



A solution of compound **3.47** (6 mg, 0.007 mmol) in THF (2 mL) was cooled to 0 °C with an ice bath and treated with HF (0.1 mL, 70% in pyridine). The ice bath was removed and the reaction was continued overnight. Saturated aqueous NaHCO₃ (10 mL)

was added slowly and the resulting solution was extracted with EtOAc (10 mL × 3). The EtOAc solution was washed, dried and concentrated. The crude product was purified by PTLC (1:1 EtOAc:hexanes) to yield compound **3.50** (4.3 mg, 88 %) as a colorless oil. $[\alpha]_D^{23} +20.2$ (*c* 0.5, MeOH); $^1\text{H NMR}$ (500 MHz) δ 8.27 (dd, *J* = 7.8, 1.8 Hz, 2H), 7.78 – 7.71 (m, 2H), 7.60 – 7.54 (m, 3H), 7.52 – 7.48 (m, 1H), 7.43 (t, *J* = 7.6 Hz, 2H), 7.31 (dd, *J* = 7.6, 1.4 Hz, 1H), 7.28 – 7.21 (m, 4H), 7.10 (t, *J* = 7.8 Hz, 1H), 6.94 (t, *J* = 7.5 Hz, 1H), 6.76 (d, *J* = 7.3 Hz, 1H), 6.73 (d, *J* = 8.3 Hz, 2H), 6.58 (d, *J* = 8.3 Hz, 1H), 6.26 (d, *J* = 6.0 Hz, 1H), 5.96 (dd, *J* = 8.3, 4.2 Hz, 1H), 5.81 – 5.68 (m, 1H), 5.38 (dt, *J* = 15.6, 5.7 Hz, 1H), 5.17 (dq, *J* = 10.1, 5.0 Hz, 1H), 4.63 (d, *J* = 4.2 Hz, 1H), 4.40 (dd, *J* = 13.8, 5.5 Hz, 1H), 4.31 (dd, *J* = 13.8, 6.0 Hz, 1H), 3.82 – 3.70 (m, 2H), 3.66 (d, *J* = 14.9 Hz, 1H), 3.49 – 3.38 (m, 3H), 2.89 – 2.76 (m, 1H), 2.44 (dt, *J* = 15.0, 7.7 Hz, 1H), 2.37 – 2.19 (m, 3H), 2.14 (ddd, *J* = 13.4, 6.5, 4.1 Hz, 1H); $^{13}\text{C NMR}$ (126 MHz) δ 172.05, 167.69, 166.66, 156.44, 156.40, 134.24, 133.17, 132.50, 131.88, 130.36, 130.19, 129.33, 128.77, 128.67, 127.37, 127.26, 127.15, 126.65, 126.55, 123.91, 120.88, 118.76, 112.45, 74.27, 71.04, 68.83, 68.52, 60.51, 57.93, 52.65, 51.23, 33.28, 32.57, 29.78; HRMS (ESI) calcd for $\text{C}_{40}\text{H}_{39}\text{N}_2\text{O}_8$ *m/z* 675.2706 ($[\text{M} + \text{H}]^+$), found *m/z* 675.2696.

Protected macrocyclic paclitaxel mimic **3.48**

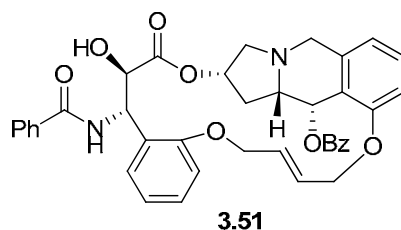


To a stirred solution of **3.45** (21 mg, 0.028 mmol, 1 equiv) in CH₂Cl₂ (25 mL) was added D-(-)-10-camphorsulphonic acid (19.7 mg, 0.085 mmol, 3 equiv) and the mixture was stirred under reflux for 1 hour. The reaction was cooled to rt and Grubbs 2nd generation catalyst (2.4 mg, 10 mol %) in CH₂Cl₂ (5 mL) was added slowly in 10 minutes. The resulting solution was heated to reflux and continued stirring for 2 hours. The resulting light brown solution was washed with 1 N aqueous NaOH (3 mL × 2), dried with anhydrous Na₂SO₄ and concentrated under vacuum to yield a dark brown residue. The crude product was purified by PTLC (hexanes:EtOAc=2:1) and the spot with a R_f = 0.35 was collected as the product (7 mg, with minor impurities) and used in the next step without further purification. Also collected was the unreacted starting material (5 mg).

The product (7 mg) from last step was completely dried and dissolved in dry THF (1 mL). The resulting solution was cooled to -78 °C, followed by slow addition of Lithium bis(trimethylsilyl)amide solution in THF (1M, 39 μL, 4 equiv). The reaction mixture was stirred at -78 °C for 10 min before the addition of benzoyl chloride (7.3 μL, 8 equiv) in one portion. The reaction was allowed to continue for another 3h at -78 °C and quenched by adding saturated aqueous NaHCO₃ (5 mL). To the resulting mixture was added EtOAc (20 mL). The organic solution was separated and the aqueous was extracted with EtOAc (20 mL × 3). The combined organic phase was washed with brine and dried. The crude product was purified with PTLC (hexanes:EtOAc = 6:5) to yield **3.48** (3.4 mg, 19% for two steps from **3.45**) as a colorless oil. $[\alpha]_D^{23}$ -34.6 (*c* 0.3, CHCl₃); ¹H NMR (500 MHz) δ 8.24 – 8.17 (m, 2H), 7.83 (d, *J* = 7.3 Hz, 2H), 7.62 – 7.48 (m, 4H), 7.44 (t, *J* = 7.4 Hz, 2H), 7.24 – 7.20 (m, 1H), 7.18 (d, *J* = 7.5 Hz, 2H), 7.13 (t, *J* = 7.8 Hz, 1H), 6.87 (t, *J* =

7.5 Hz, 1H), 6.81 (d, $J = 8.1$ Hz, 1H), 6.77 (d, $J = 7.3$ Hz, 1H), 6.73 (d, $J = 8.5$ Hz, 1H), 6.08 (d, $J = 7.1$ Hz, 1H), 5.87 – 5.79 (m, 2H), 5.74 (dt, $J = 16.4, 3.3$ Hz, 1H), 5.30 (p, $J = 7.8$ Hz, 1H), 4.63 – 4.45 (m, 4H), 4.10 (dt, $J = 16.3, 2.4$ Hz, 1H), 4.02 – 3.92 (m, 2H), 3.60 (d, $J = 15.2$ Hz, 1H), 3.31 (dd, $J = 9.4, 6.9$ Hz, 1H), 2.69 – 2.55 (m, 1H), 2.16 – 1.94 (m, 2H), 0.87 – 0.76 (m, 21H); ^{13}C NMR (126 MHz) δ 171.52, 166.84, 166.64, 155.68, 155.41, 138.75, 134.62, 132.98, 131.63, 130.53, 130.04, 128.79, 128.76, 128.57, 127.70, 127.48, 127.14, 126.10, 121.01, 120.87, 120.46, 112.33, 112.03, 77.29, 73.38, 72.65, 70.94, 69.11, 65.24, 59.11, 57.14, 51.51, 51.12, 43.06, 34.30, 17.74, 17.73, 17.72, 17.70, 12.29, 0.08, 0.08, 0.07, 0.06, 0.06, 0.05; HRMS (ESI) calcd for $\text{C}_{48}\text{H}_{57}\text{N}_2\text{O}_8\text{Si}$ m/z 817.3884 ($[\text{M} + \text{H}]^+$), found m/z 817.3815.

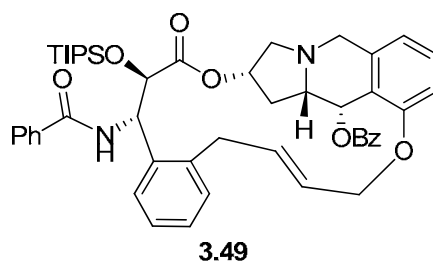
Macrocyclic paclitaxel mimic **3.51**



A solution of compound **3.48** (3 mg, 0.004 mmol) in THF (2 mL) was cooled to 0 °C with an ice bath and treated with HF (0.1 mL, 70% in pyridine). The ice bath was removed and the reaction was continued overnight. Saturated aqueous NaHCO_3 (10 mL) was added slowly and the resulting solution was extracted with EtOAc (10 mL \times 3). The EtOAc solution was washed, dried and concentrated. The crude product was purified by PTLC (1:1 EtOAc:hexanes) to yield the compound **3.51** (2.3 mg, 88 %) as a colorless oil.

$[\alpha]_D^{23}$ -27.5 (*c* 0.2, CHCl₃); ¹H NMR (500 MHz) δ 8.35 – 8.28 (m, 2H), 7.79 – 7.73 (m, 2H), 7.57 – 7.38 (m, 7H), 7.25 – 7.22 (m, 1H), 7.11 (t, *J* = 7.9 Hz, 1H), 6.95 (t, *J* = 7.5 Hz, 1H), 6.83 (d, *J* = 8.2 Hz, 1H), 6.76 (d, *J* = 7.3 Hz, 1H), 6.70 (t, *J* = 8.6 Hz, 2H), 6.14 (d, *J* = 7.2 Hz, 1H), 6.07 (d, *J* = 9.1 Hz, 1H), 5.96 – 5.86 (m, 1H), 5.80 (d, *J* = 16.1 Hz, 1H), 5.36 – 5.26 (m, 1H), 4.62 – 4.45 (m, 3H), 4.33 (d, *J* = 1.3 Hz, 1H), 4.16 – 4.06 (m, 2H), 3.96 (m, 1H), 3.62 (d, *J* = 15.2 Hz, 1H), 3.24 (dd, *J* = 9.2, 6.5 Hz, 1H), 2.71 – 2.63 (m, 1H), 2.27 (dt, *J* = 14.3, 8.1 Hz, 1H), 2.22 – 2.17 (m, 1H); ¹³C NMR (126 MHz) δ 173.03, 166.96, 166.45, 155.70, 155.33, 134.55, 132.86, 131.66, 130.65, 130.24, 129.16, 128.65, 128.48, 128.21, 127.95, 127.35, 127.24, 127.19, 126.42, 121.28, 121.14, 120.30, 112.91, 112.20, 74.00, 72.25, 70.46, 68.30, 66.14, 59.10, 56.62, 51.20, 48.91, 34.17; HRMS (ESI) calcd for C₃₉H₃₇N₂O₈ *m/z* 661.2550 ([M + H]⁺), found *m/z* 661.2485.

Protected macrocyclic paclitaxel mimic **3.49**



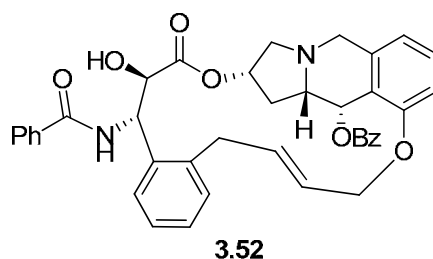
To a stirred solution of **3.46** (25 mg, 0.034 mmol, 1 equiv) in CH₂Cl₂ (25 mL) was added D-(-)-10-camphorsulphonic acid (24 mg, 0.103 mmol, 3 equiv) and the mixture was stirred under reflux for 1 hour. The reaction was cooled to rt and Grubbs 2nd generation catalyst (1.5 mg, 5 mol %) in CH₂Cl₂ (5 mL) was added slowly in 10 minutes.

The resulting solution was heated to reflux and continued overnight. The resulting light brown solution was washed with 1 N aqueous NaOH (3 mL × 2), dried with anhydrous Na₂SO₄ and concentrated under vacuum to yield a dark brown residue. The crude product was purified by PTLC (hexanes:EtOAc = 3:1) and the spot with a R_f = 0.3 was collected as the product (3.3 mg, with minor impurities) and used in the next step without further purification. Also collected was the unreacted starting material (10 mg).

The product (3.3 mg) from last step was completely dried and dissolved in dry THF (1 mL). The resulting solution was cooled to -78 °C, followed by slow addition of Lithium bis(trimethylsilyl)amide solution in THF (1M, 19 μL, 4 equiv). The reaction mixture was stirred at -78 °C for 10 min before the addition of benzoyl chloride (4.4 μL, 8 equiv) in one portion. The reaction was allowed to continue for another 3h at -78 °C and quenched by adding saturated aqueous NaHCO₃ (5 mL). To the resulting mixture was added EtOAc (20 mL). The organic solution was separated and the aqueous was extracted with EtOAc (20 mL × 3). The combined organic phase was washed with brine and dried. The crude product was purified with PTLC (hexanes:EtOAc = 1:1) to yield **3.49** (1.5 mg, 9% for two steps from **3.46**) as a colorless oil. $[\alpha]_D^{23} +11.0$ (c 0.3, CHCl₃); ¹H NMR (500 MHz) δ 8.30 – 8.26 (m, 2H), 7.83 – 7.79 (m, 2H), 7.59 – 7.46 (m, 4H), 7.46 – 7.40 (m, 2H), 7.39 – 7.35 (m, 1H), 7.19 – 7.07 (m, 4H), 7.01 (dd, *J* = 7.2, 1.7 Hz, 1H), 6.78 – 6.74 (m, 2H), 6.05 (d, *J* = 7.4 Hz, 1H), 5.95 – 5.88 (m, 1H), 5.83 – 5.75 (m, 1H), 5.65 (dd, *J* = 8.1, 1.7 Hz, 1H), 5.30 – 5.21 (m, 1H), 4.52 (dd, *J* = 13.7, 6.6 Hz, 1H), 4.33 (d, *J* = 1.9 Hz, 1H), 4.19 (dd, *J* = 14.3, 4.1 Hz, 1H), 4.05 – 3.94 (m, 2H), 3.61 (d, *J* = 15.4 Hz, 1H), 3.46 (d, *J* = 7.0 Hz, 2H), 3.20 (dd, *J* = 10.1, 5.8 Hz, 1H), 2.62 – 2.53 (m, 1H), 2.28 (dd, *J* = 9.8, 7.1 Hz, 1H), 2.10 (m, 1H), 1.08 – 0.79 (m, 21H); ¹³C NMR (126

MHz) δ 171.30, 166.87, 166.51, 155.35, 137.58, 137.23, 135.02, 134.67, 133.10, 132.93, 131.58, 130.45, 130.25, 129.95, 129.87, 128.73, 128.61, 128.15, 127.64, 127.26, 127.04, 126.96, 126.49, 126.43, 123.37, 120.63, 117.31, 74.61, 73.39, 70.23, 68.48, 59.30, 57.28, 52.37, 51.53, 35.72, 31.68, 17.86, 17.82, 12.40; HRMS (ESI) calcd for $C_{48}H_{57}N_2O_7Si$ m/z 801.3935 ($[M + H]^+$), found m/z 801.3917.

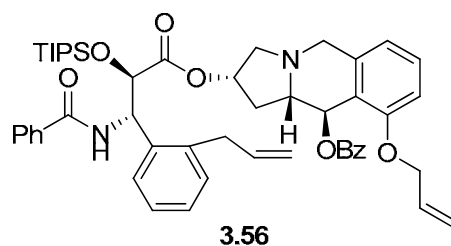
Macrocyclic paclitaxel mimic **3.52**



A solution of compound **3.49** (1.5 mg, 0.002 mmol) in THF (2 mL) was cooled to 0 °C with an ice bath and treated with HF (0.1 mL, 70% in pyridine). The ice bath was removed and the reaction was continued overnight. Saturated aqueous $NaHCO_3$ (10 mL) was added slowly and the resulting solution was extracted with EtOAc (10 mL \times 3). The EtOAc solution was washed, dried and concentrated. The crude product was purified by PTLC (75 % EtOAc in hexanes) to yield compound **3.52** (1 mg, 83 %) as a colorless oil. $[\alpha]_D^{23} +42.5$ (c 0.2, $CHCl_3$); 1H NMR (500 MHz) δ 8.19 (d, $J = 8.0$ Hz, 2H), 7.75 (d, $J = 14.8$ Hz, 1H), 7.63 (dt, $J = 9.0, 4.5$ Hz, 3H), 7.52 (t, $J = 7.7$ Hz, 2H), 7.49 – 7.42 (m, 1H), 7.37 (t, $J = 7.7$ Hz, 2H), 7.13 – 7.07 (m, 1H), 6.89 (s, 1H), 6.65 (s, 1H), 6.48 – 6.39 (m, 2H), 6.19 (d, $J = 4.5$ Hz, 1H), 5.90 – 5.76 (m, 1H), 5.59 – 5.50 (m, 1H), 5.39 (d, $J = 9.2$

Hz, 1H), 4.86 (s, 1H), 4.39 (dd, $J = 14.3, 7.3$ Hz, 1H), 4.08 (d, $J = 6.7$ Hz, 1H), 4.01 (d, $J = 14.2$ Hz, 1H), 3.89 (s, 1H), 3.72 – 3.44 (m, 3H), 3.21 (d, $J = 14.8$ Hz, 2H), 2.99 (s, 1H), 2.51 (s, 2H); HRMS (ESI) calcd for $C_{39}H_{37}N_2O_7Si$ m/z 645.2601 ($[M + H]^+$), found m/z 645.2570.

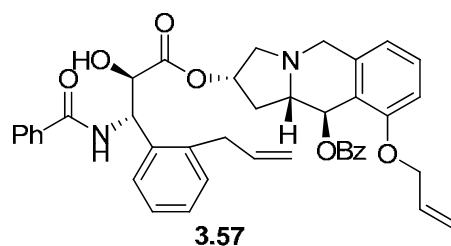
**(2*S*,10*R*,10*aS*)-9-Allyloxy-10-benzoyloxy-1,2,3,5,10,10*a*-hexahydropyrrolo[1,2-
b]isoquinolin-2-yl (2'*S*,3'*R*)-3'-benzoylamino-2'-triisopropylsilyloxy-3'-(2-
allylphenyl)-propanoate (3.56)**



A solution of **3.53** (8 mg, 0.011 mmol) in dry THF (2 mL) was cooled to -78 °C. To this solution was added slowly lithium bis(trimethylsilyl)amide solution in THF (1M, 44 μ L, 4 equiv). The reaction mixture was stirred at -78 °C for 10 min before the addition of benzoyl chloride (11 μ L, 8 equiv) in one portion. The reaction was allowed to continue for another 3h at -78 °C and quenched by adding saturated aqueous $NaHCO_3$ (5 mL). To the resulting mixture was added EtOAc (20 mL). The organic solution was separated and the aqueous was extracted with EtOAc (20 mL \times 3). The combined organic phase was washed with brine and dried. The crude product was purified with PTLC (hexanes:EtOAc = 4:1) to yield **3.56** (5.5 mg, 60%) as a colorless oil. $[\alpha]_D^{23} -20.9$ (c 0.6, $CHCl_3$); 1H NMR (500 MHz) δ 7.99 (d, $J = 8.0$ Hz, 2H), 7.80 (d, $J = 7.9$ Hz, 2H), 7.51 (t,

$J = 7.3$ Hz, 1H), 7.38 (dd, $J = 10.2, 4.9$ Hz, 3H), 7.33 (t, $J = 7.3$ Hz, 1H), 7.28 – 7.17 (m, 8H), 7.16 – 7.09 (m, 1H), 6.72 (d, $J = 8.2$ Hz, 1H), 6.63 (d, $J = 7.6$ Hz, 1H), 6.45 (d, $J = 8.2$ Hz, 1H), 6.08 (ddt, $J = 16.7, 10.2, 6.3$ Hz, 1H), 5.79 (d, $J = 8.0$ Hz, 1H), 5.66 (ddt, $J = 16.5, 10.7, 5.5$ Hz, 1H), 5.27 – 5.14 (m, 3H), 5.07 (d, $J = 17.3$ Hz, 1H), 4.96 (d, $J = 10.5$ Hz, 1H), 4.67 (s, 1H), 4.36 (ddd, $J = 60.8, 12.4, 5.4$ Hz, 2H), 3.77 – 3.55 (m, 3H), 3.34 (d, $J = 14.3$ Hz, 1H), 3.14 (d, $J = 11.3$ Hz, 1H), 2.73 – 2.61 (m, 1H), 2.58 – 2.40 (m, 2H), 1.03 – 0.77 (m, 21H); ^{13}C NMR (126 MHz) δ 172.28, 166.37, 165.98, 157.69, 138.03, 137.13, 136.66, 134.29, 132.82, 132.67, 131.42, 130.87, 130.33, 130.16, 129.84, 128.74, 128.52, 128.43, 128.20, 127.91, 127.05, 126.96, 126.26, 122.76, 118.84, 117.61, 116.84, 110.04, 75.01, 73.73, 71.57, 69.12, 65.21, 60.98, 60.49, 54.94, 53.38, 36.91, 36.82, 21.13, 17.83, 17.80, 14.28, 12.40; HRMS (ESI) calcd for $\text{C}_{43}\text{H}_{57}\text{N}_2\text{O}_6\text{Si}$ m/z 829.4248 ($[\text{M} + \text{H}]^+$), found m/z 829.4201.

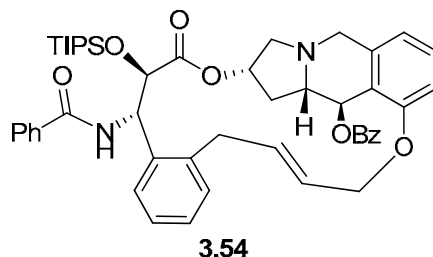
(2*S*,10*R*,10*aS*)-9-Allyloxy-10-benzoyloxy-1,2,3,5,10,10*a*-hexahydropyrrolo[1,2-*b*]isoquinolin-2-yl (2'*S*,3'*R*)-3'-benzoylamino-2'-hydroxy-3'-(2-allylphenyl)propanoate (3.57)



A solution of compound **3.56** (3.3 mg, 0.004 mmol) in THF (3 mL) was cooled to 0 °C with an ice bath and treated with HF (0.1 mL, 70% in pyridine). The ice bath was

removed and the reaction was continued overnight. Saturated aqueous NaHCO₃ (5 mL) was added slowly and the resulting solution was extracted with EtOAc (10 mL × 3). The EtOAc solution was washed, dried and concentrated. The crude product was purified by PTLC (50 % EtOAc in hexanes) to yield compound **3.57** (2.4 mg, 89 %) as a colorless oil. $[\alpha]_D^{23} +2.0$ (*c* 0.3, CHCl₃); ¹H NMR (500 MHz) δ 8.00 (d, *J* = 8.0 Hz, 2H), 7.75 (d, *J* = 8.0 Hz, 2H), 7.52 (dd, *J* = 11.5, 5.0 Hz, 2H), 7.39 (tt, *J* = 26.5, 7.8 Hz, 6H), 7.25 – 7.19 (m, 3H), 6.89 (d, *J* = 8.6 Hz, 1H), 6.72 (d, *J* = 8.0 Hz, 2H), 6.52 (d, *J* = 8.2 Hz, 1H), 6.06 (tt, *J* = 16.5, 6.2 Hz, 1H), 5.94 (dd, *J* = 8.6, 2.2 Hz, 1H), 5.64 (qd, *J* = 10.7, 5.5 Hz, 1H), 5.27 (t, *J* = 8.5 Hz, 1H), 5.17 – 5.01 (m, 3H), 4.95 (d, *J* = 10.5 Hz, 1H), 4.56 (d, *J* = 2.2 Hz, 1H), 4.34 (ddd, *J* = 17.9, 12.3, 5.1 Hz, 2H), 3.92 (d, *J* = 14.4 Hz, 1H), 3.69 – 3.53 (m, 2H), 3.46 (d, *J* = 14.3 Hz, 1H), 3.29 (d, *J* = 11.3 Hz, 1H), 2.80 – 2.67 (m, 1H), 2.62 – 2.50 (m, 2H), 2.33 (t, *J* = 7.5 Hz, 1H), 2.30 – 2.22 (m, 1H); ¹³C NMR (126 MHz) δ 172.94, 166.88, 165.99, 157.75, 138.21, 137.90, 137.08, 136.85, 134.15, 132.75, 132.72, 131.66, 130.81, 130.56, 129.85, 128.89, 128.61, 128.34, 128.23, 127.19, 126.95, 122.76, 118.80, 117.64, 116.71, 110.20, 74.90, 73.14, 71.65, 69.12, 65.39, 60.75, 55.23, 51.56, 37.25, 33.55, 32.01, 24.82, 22.78, 14.21, 0.08; HRMS (ESI) calcd for C₄₃H₅₇N₂O₆Si *m/z* 673.2914 ([M + H]⁺), found *m/z* 673.2876.

Protected macrocyclic paclitaxel mimic **3.54**



To a solution of **3.53** (48 mg, 0.066 mmol) in CH_2Cl_2 (50 mL) was added D-(-)-10-camphorsulfonic acid (76.6 mg, 0.33 mmol, 5 equiv) and the mixture was stirred under reflux for 1 hour. The reaction was cooled to rt and Grubbs 2nd generation catalyst (5.6 mg, 10 mol %) in CH_2Cl_2 (5 mL) was added slowly in 10 minutes. The resulting solution was heated to reflux and continued stirring overnight. The resulting light brown solution was washed with 1 N aqueous NaOH (3 mL \times 2), dried with anhydrous Na_2SO_4 and concentrated under vacuum to yield a dark brown residue. The crude product was purified by PTLC (hexanes:EtOAc = 1:2) to yield the bridged compound with a R_f = 0.25 (16 mg) together with unreacted starting material (12 mg).

The product (8 mg, 0.012 mmol) from the previous step was completely dried and dissolved in dry THF (2 mL). The resulting solution was cooled to -78°C , followed by slow addition of lithium bis(trimethylsilyl)amide solution in THF (1M, 46 μL , 4 equiv). The reaction mixture was stirred at -78°C for 10 min before the addition of benzoyl chloride (10.7 μL , 8 equiv) in one portion. The reaction was allowed to continue for another 3 h at -78°C and quenched by adding saturated aqueous NaHCO_3 (5 mL). To the resulting mixture was added EtOAc (20 mL). The organic solution was separated and the

A solution of compound **3.54** (5.5 mg, 0.007 mmol) in THF (3 mL) was cooled to 0 °C with an ice bath and treated with HF (0.1 mL, 70% in pyridine). The ice bath was removed and the reaction was continued overnight. Saturated aqueous NaHCO₃ (10 mL) was added slowly and the resulting solution was extracted with EtOAc (10 mL × 3). The EtOAc solution was washed, dried and concentrated. The crude product was purified by PTLC (3:1 EtOAc:hexanes) to yield compound **3.55** (3.5 mg, 85 %) as a colorless oil. $[\alpha]_D^{23} +2.6$ (*c* 0.3, CHCl₃); ¹H NMR (500 MHz) δ 8.03 – 7.96 (m, 2H), 7.83 (d, *J* = 8.2 Hz, 2H), 7.72 (d, *J* = 7.7 Hz, 1H), 7.66 (d, *J* = 7.5 Hz, 1H), 7.57 – 7.50 (m, 1H), 7.45 (dd, *J* = 11.1, 3.8 Hz, 1H), 7.40 (t, *J* = 7.3 Hz, 2H), 7.34 (t, *J* = 7.2 Hz, 2H), 7.24 (d, *J* = 4.0 Hz, 2H), 7.19 (t, *J* = 7.9 Hz, 1H), 7.12 (d, *J* = 6.0 Hz, 1H), 6.78 (d, *J* = 7.9 Hz, 2H), 6.59 (d, *J* = 5.4 Hz, 1H), 6.07 – 5.97 (m, 1H), 5.55 (dd, *J* = 15.6, 5.7 Hz, 2H), 5.36 (s, 1H), 4.55 (d, *J* = 5.3 Hz, 2H), 4.37 (d, *J* = 16.0 Hz, 1H), 4.28 (s, 1H), 3.77 (d, *J* = 15.8 Hz, 1H), 3.62 (dd, *J* = 14.6, 6.1 Hz, 2H), 3.49 – 3.31 (m, 2H), 2.86 (d, *J* = 11.6 Hz, 1H), 2.46 (dt, *J* = 14.8, 7.5 Hz, 1H), 2.15 (d, *J* = 14.2 Hz, 1H); ¹³C NMR (126 MHz) δ 172.46, 168.48, 166.92, 157.58, 137.43, 137.34, 134.03, 133.71, 133.12, 131.81, 130.61, 130.36, 129.88, 129.45, 128.60, 128.59, 128.40, 128.37, 127.39, 127.21, 126.36, 120.01, 114.46, 76.20, 72.89, 69.94, 68.15, 62.50, 58.17, 54.20, 51.21, 37.95, 36.09; HRMS (ESI) calcd for C₃₉H₃₇N₂O₇ *m/z* 645.2601 ([M + H]⁺), found *m/z* 645.2573.

References

1. Holton, R. A.; Somoza, C.; Kim, H.-B.; Liang, F.; Biediger, R. J.; Boatman, P. D.; Shindo, M.; Smith, C. C.; Kim, S.; Nadizadeh, H.; Suzuki, Y.; Tao, C.; Vu, P.; Tang, S.; Zhang, P.; Murthi, K. K.; Gentile, L. N.; Liu, J. H. First Total Synthesis

- of Taxol. 1. Functionalization of the B Ring. *J. Am. Chem. Soc.* **1994**, *116*, 1597-1598.
2. Holton, R. A.; Kim, H.-B.; Somoza, C.; Liang, F.; Biediger, R. J.; Boatman, P. D.; Shindo, M.; Smith, C. C.; Kim, S.; Nadizadeh, H.; Suzuki, Y.; Tao, C.; Vu, P.; Tang, S.; Zhang, P.; Murthi, K. K.; Gentile, L. N.; Liu, J. H. First Total Synthesis of Taxol. 2. Completion of the C and D Rings. *J. Am. Chem. Soc.* **1994**, *116*, 1599-1600.
3. Nicolaou, K. C.; Yang, Z.; Liu, J. J.; Ueno, H.; Nantermet, P. G.; Guy, R. K.; Claiborne, C. F.; Renaud, J.; Couladouros, E. A.; Paulvannan, K.; Sorensen, E. J. Total Synthesis of Taxol. *Nature* **1994**, *367*, 630-634.
4. Danishefsky, S. J.; Masters, J. J.; Young, W. B.; Link, J. T.; Snyder, L. B.; Magee, T. V.; Jung, D. K.; Isaacs, R. C. A.; Bornmann, W. G.; Alaimo, C. A.; Coburn, C. A.; Di Grandi, M. J. Total Synthesis of Baccatin III and Taxol. *J. Am. Chem. Soc.* **1996**, *118*, 2843-2859.
5. Wender, P. A.; Badham, N. F.; Conway, S. P.; Floreancig, P. E.; Glass, T. E.; Granicher, C.; Houze, J. B.; Janichen, J.; Lee, D.; Marquess, D. G.; McGrane, P. L.; Meng, W.; Mucciario, T. P.; Muhlebach, M.; Natchus, M. G.; Paulsen, H.; Rawlins, D. B.; Satkofsky, J.; Shuker, A. J.; Sutton, J. C.; Taylor, R. E.; Tommoka, K. The Pinene Path to Taxanes. 5. Stereocontrolled Synthesis of a Versatile Taxane Precursor. *J. Am. Chem. Soc.* **1997**, *119*, 2755-2756.
6. Wender, P. A.; Badham, N. F.; Conway, S. P.; Floreancig, P. E.; Glass, T. E.; Houze, J. B.; Krauss, N. E.; Lee, D.; Marquess, D. G.; McGrane, P. L.; Meng, W.; Natchus, M. G.; Shuker, A. J.; Sutton, J. C.; Taylor, R. E. The Pinene Path to

- Taxanes. 6. A Concise Stereocontrolled Synthesis of Taxol. *J. Am. Chem. Soc.* **1997**, *119*, 2757-2758.
7. Kusama, H.; Hara, R.; Kawahara, S.; Nishimori, T.; Kashima, H.; Nakamura, N.; Morihira, K.; Kuwajima, I. Enantioselective Total Synthesis of (-)-Taxol. *J. Am. Chem. Soc.* **2000**, *122*, 3811-3820.
 8. Mukaiyama, T.; Shiina, I.; Iwadare, H.; Saitoh, M.; Nishimura, T.; Ohkawa, N.; Sakoh, H.; Nishimura, K.; Tani, Y.-I.; Hasegawa, M.; Yamada, K.; Saitoh, K. Asymmetric Total Synthesis of Taxol. *Chem. Eur. J.* **1999**, *5*, 121-161.
 9. Blechert, S.; Kleine-Klausing, A. Synthesis of a Biologically Active Taxol Analogue *Angew. Chem. Int. Ed. Engl.* **1991** *30*, 412-414.
 10. Blechert, S.; Jansen, R.; Velder, J. Synthesis of New Taxoids. *Tetrahedron* **1994**, *50*, 9649-9656.
 11. Senilh, V.; Gueritte, F.; Guenard, D.; Colin, M.; Potier, P. Hemisynthese de Nouveaux Analogues du Taxol. Etude de Leur Interaction Avec la Tubuline. *C. R. Acad. Sc. Paris* **1984**, *299*, 1039-1043.
 12. Kingston, D. G. I.; Hawkins, D. R.; Ovington, L. New Taxanes from *Taxus brevifolia* *J. Nat. Prod.* **1982**, *45*, 466-470
 13. Klar, U.; Graf, H.; Schenk, O.; Rohr, B.; Schulz, H. New Synthetic Inhibitors of Microtubule Depolymerization. *Bioorg. Med. Chem. Lett.* **1998**, *8*, 1397-1402.
 14. Almqvist, F.; Manner, S.; Thornqvist, V.; Berg, U.; Wallin, M.; Frejd, T. Spirobicyclo[2.2.2]octane Derivatives: Mimetics of Baccatin III and Paclitaxel (Taxol). *Org. Biomol. Chem.* **2004**, *2*, 3085-3090.

15. Geng, X.; Geney, R.; Pera, P.; Bernacki, J.; Ojima, I. Design and Synthesis of de novo Cytotoxic Alkaloids through Mimicking Taxoid Skeleton. *Bioorg. Med. Chem. Lett.* **2004**, *14*, 3491-3494.
16. Li, Y.; Poliks, B.; Cegelski, L.; Poliks, M.; Cryczynski, Z.; Piszczek, G.; Jagtap, P., G.; Studelska, D. R.; Kingston, D. G. I.; Schaefer, J.; Bane, S. Conformation of Microtubule-Bound Paclitaxel Determined by Fluorescence Spectroscopy and REDOR NMR. *Biochemistry* **2000**, *39*, 281-291.
17. Paik, Y.; Yang, C.; Metaferia, B.; Tang, S.; Bane, S.; Ravindra, R.; Shanker, N.; Alcaraz, A. A.; Johnson, S. A.; Schaefer, J.; O'Connor, R. D.; Cegelski, L.; Snyder, J. P.; Kingston, D. G. I. Rotational-echo Double-resonance NMR Distance Measurements for the Tubulin-bound Paclitaxel Conformation. *J. Am. Chem. Soc.* **2007**, *129*, 361-370.
18. Ganesh, T.; Guza, R. C.; Bane, S.; Ravindra, R.; Shanker, N.; Lakdawala, A. S.; Snyder, J. P.; Kingston, D. G. I. The Bioactive Taxol conformation of β -tubulin: Experimental Evidence from Highly Active Constrained Analogs. *Proc. Natl. Acad. Sci. USA* **2004**, *101*, 10006-10011.
19. Ganesh, T.; Norris, A.; Sharma, S.; Bane, S.; Alcaraz, A. A.; Snyder, J. P.; Kingston, D. G. I. Design, Synthesis, and Bioactivity of Simplified Paclitaxel Analogs Based on the T-Taxol Bioactive Conformation. *Bioorg. Med. Chem.* **2006**, *14*, 3447-3454.
20. Kadlecíková, K.; Dalla, V.; Marchalín, S.; Decroix, B.; Baran, P. Diastereoselective Synthesis of New Polyhydroxylated Indolizidines from (l)-Glutamic Acid. *Tetrahedron* **2005**, *61*, 4743-4754.

21. Lee, G. S.; Cho, Y. S.; Shim, S. C.; Kim, W. J.; Eibler, E.; Wiegrebe, W. Stereospecific Synthesis of 2,3-Dimethoxy-naphtho[1,2-b]indolizidine. *Arch. Pharm. (Weinheim)* **1989**, *322*, 607-611.
22. Seto, M.; Morihira, K.; Horiguchi, Y.; Kuwajima, I. An Efficient Approach toward Taxane Analogs: Atrop- and Diastereoselective Eight-Membered B Ring Cyclizations for Synthesis of Aromatic C-Ring Taxinine Derivatives. *J. Org. Chem.* **1994**, *59*, 3165-3174.
23. Qiu, X.-l.; Qing, F.-l. Practical Synthesis of Boc-Protected cis-4-Trifluoromethyl and cis-4-Difluoromethyl-L-prolines. *J. Org. Chem.* **2002**, *67*, 7162-7164.
24. Markus, B.; Patrick, D.; Athanassios, G.; Herbert, W. Synthesis and Evaluation of Acyl Protein Thioesterase 1 (APT1) Inhibitors. *Chem.--Eur. J.* **2006**, *12*, 4121-4143.
25. Zhang, X.; Schmitt, A. C.; Jiang, W. A Convenient and High Yield Method to Prepare 4-Hydroxypyroglutamic Acids. *Tetrahedron Lett.* **2001**, *42*, 5335-5338.
26. Piers, E.; Harrison, C. L.; Zetina-Rocha, C. Intramolecular Conjugate Addition of Alkenyl and Aryl Functions to Enones Initiated by Lithium-Iodine Exchange. *Org. Lett.* **2001**, *3*, 3245-3247.
27. Ganesh, T.; Yang, C.; Norris, A.; Glass, T.; Bane, S.; Ravindra, R.; Banerjee, A.; Metaferia, B.; Thomas, S. L.; Giannakakou, P.; Alcaraz, A. A.; Lakdawala, A. S.; Snyder, J. P.; Kingston, D. G. I. Evaluation of the Tubulin-bound Paclitaxel Conformation: Synthesis, Biology, and SAR Studies of C-4 to C-3' Bridged Paclitaxel Analogues. *J. Med. Chem.* **2007**, *50*, 713-725.

28. Compain, P. Olefin Metathesis of Amine-containing Systems: Beyond the Current Consensus. *Adv. Synth. Catal.* **2007**, *349*, 1829-1846.

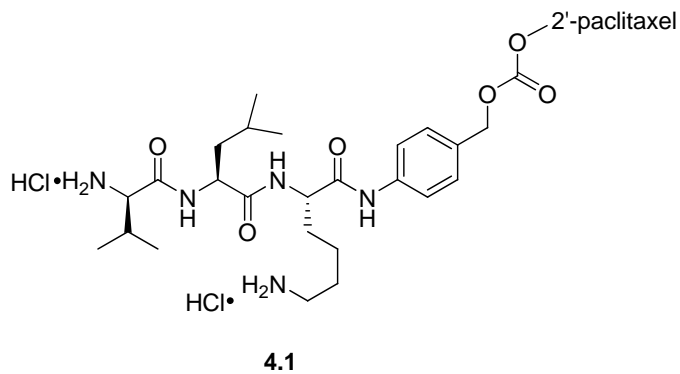
Chapter 4. Synthesis of Thiolated Paclitaxel Analogs for Reaction with Gold Nanoparticles as Drug Delivery Agents

4.1 Targeted Delivery of Paclitaxel to Tumor

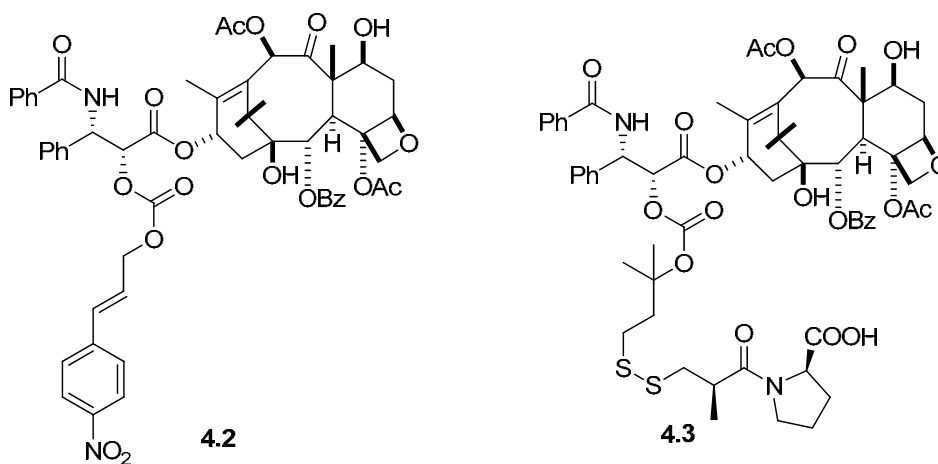
Despite its great success in clinical use, paclitaxel suffers from several major drawbacks such as poor water solubility, multidrug resistance (MDR), and dose-limiting toxicities.¹ Due to the poor water solubility of paclitaxel, the detergent Cremophor EL[®] is used in the drug formulation, which can cause severe adverse allergic reactions.² Moreover, systemic toxicity occurs due to the poor selectivity of the chemotherapeutic agent to tumor cells over normal cells causes, which often leads to severe adverse side effects such as mucositis, bone marrow suppression, febrile neutropenia, neurotoxicities, and ulceration.³ One solution to these problems is the development of prodrugs with greater water solubility and/or lower systemic toxicity. Improved water solubility can be achieved by introducing a hydrophilic moiety to the prodrug and toxicity can be lowered by tumor targeting prodrugs that only release paclitaxel at tumor sites.

4.1.1 Paclitaxel Prodrugs Designed to Target Tumor Tissue. Tumor-targeting prodrugs are designed to achieve selective delivery of chemotherapeutics to tumor tissues and thus reduce the toxicity to normal tissues. Such prodrugs are usually conjugates of a therapeutic agent and a tumor targeting agent. The latter could be hormones, peptides, polysaccharides, vitamins, nanoparticles, fatty acids and antibodies, etc. that have a certain affinity to tumor cells. Ideally, the drug conjugate should be stable and non-toxic

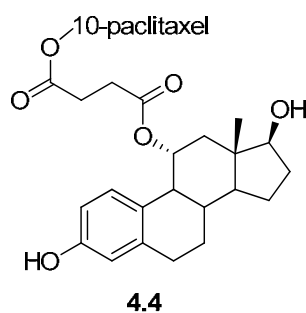
throughout the blood stream, bind selectively to cancer cells, and be cleaved readily to release the active drug upon reaching tumor cells.



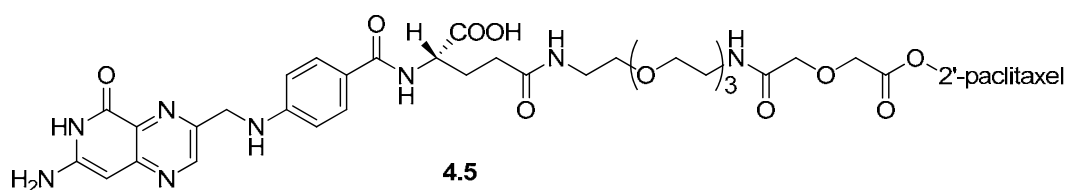
Prodrug **4.1** was designed to target the enzyme plasmin that is overproduced by tumor cells.⁴ The prodrug exhibited plasmin-dependent paclitaxel release with a half-life of 42 min, and was significantly less cytotoxic in various tumor cell lines without plasmin activation.



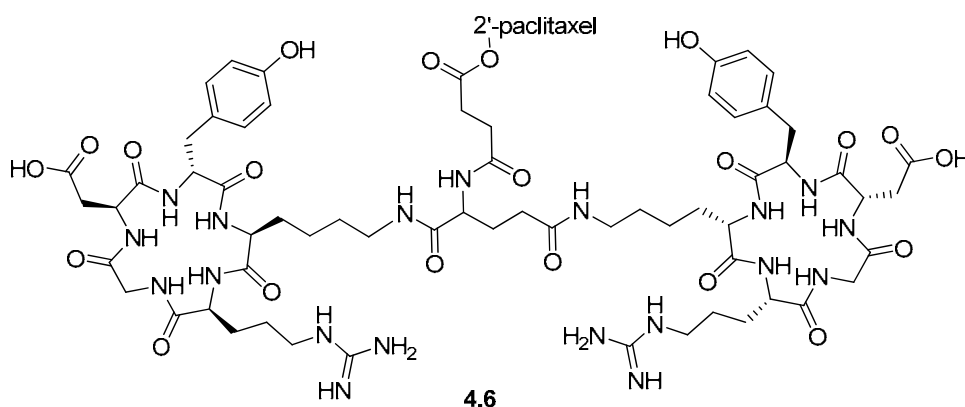
Bioreductive prodrugs **4.2** and **4.3** were designed to target the hypoxic environment of the tumor tissue, which is due to the rapid proliferation of tumor cells. It was demonstrated that compound **4.2** can release the parent drug by chemical reduction with sodium borohydride⁵ and it was significantly less cytotoxic than paclitaxel against several cancer cell lines. Compound **4.3** can produce paclitaxel by reduction with dithiothreitol, and showed 650-fold lower cytotoxicity than paclitaxel *in vitro* and superior tumor regression *in vivo*.⁶



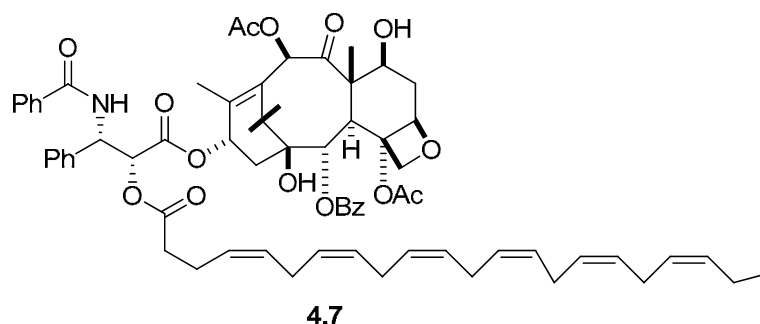
A series of estradiol-paclitaxel conjugates (represented by **4.4**) were designed to target the estrogen receptor (ER),⁷ which is overexpressed in breast, ovarian, and gonad cancer cells.⁸ Prodrug **4.4** was 3-fold more cytotoxic to the ER positive cell line than the ER negative cell line, although it was much less active than paclitaxel against both of the cell lines.



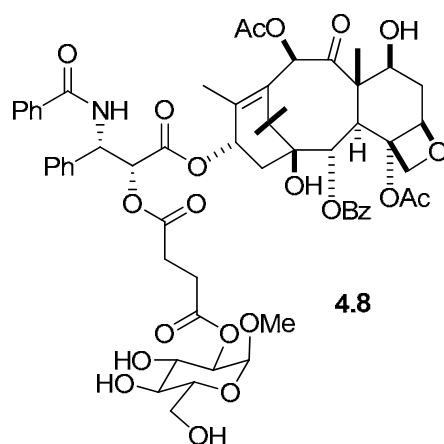
Several folic acid-paclitaxel conjugates such as **4.5** were designed to target the folate receptor (FR),⁹ which is significantly overexpressed in a broad spectrum of human cancers.¹⁰ The prodrugs retained the receptor-binding affinity of the folate ligand. However they did not show selective cytotoxicity against cancer cell lines that express the folate receptor and they were significantly less active *in vivo* compared to paclitaxel.



Prodrug **4.6** was designed to target the α_v integrin receptor which is highly overexpressed in metastatic cancer cells.^{11,12} Compound **4.6** demonstrated improved tumor specificity and cytotoxicity *in vivo* with mice bearing the MDA-MB-435 breast carcinoma, which is known to overexpress integrin $\alpha_v\beta_3$.

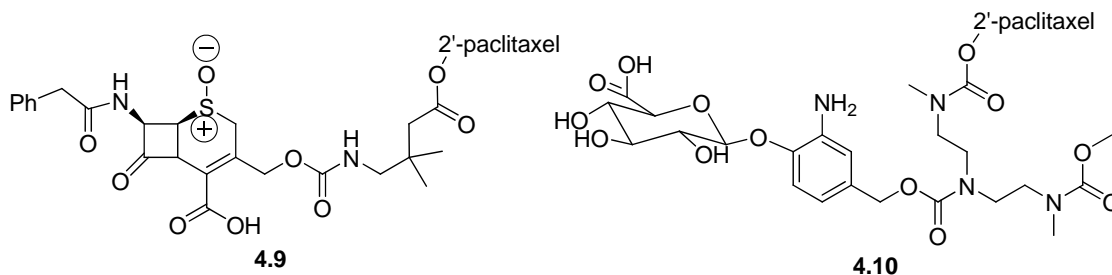


Prodrug **4.7** contained a docosahexaenoic acid (DHA) moiety as the targeting agent. It was designed based on the premise that tumor cells tend to uptake fatty acids as an energy source.^{13,14} Compound **4.7** showed no microtubule assembly activity and no cytotoxicity before it was converted to paclitaxel. It also exhibited better distribution and increased tolerance compared to paclitaxel. In several *in vivo* experiments, compound **4.7**, currently in clinical trials, demonstrated superior antitumor activity.



Glycan-paclitaxel conjugate **4.8** was designed to target tumor tissue via glucose transporters,¹⁵ a family of membrane proteins which are generally overexpressed in cancer cells compared with normal cells.¹⁶ Selective cytotoxicity of this compound was

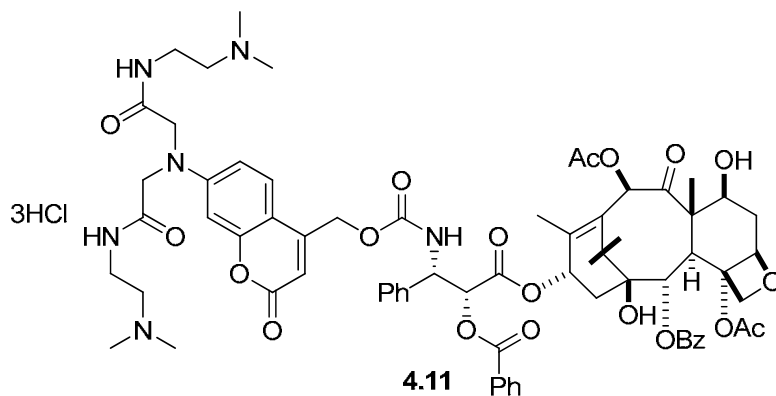
observed against cancer cells over normal cells. It was also less cytotoxic against cancer cell lines that express low levels of glucose transporters.



Prodrugs **4.9-4.10** were designed on the basis of antibody-directed enzyme prodrug therapy (ADEPT). In this technique, an antibody conjugated with a prodrug-activating enzyme is directed against a tumor-specific antigen located on the surface of tumor cells, followed by the administration of a non-toxic prodrug which can only be activated by the aforementioned enzyme. Compound **4.9**, which can be activated by β -lactamase,¹⁷ was developed by Bristol-Myers Squibb. This compound released paclitaxel 7-fold faster in the presence of β -lactamase than in human serum. The prodrug was 12-fold less active *in vitro* against 3667 melanoma cells compared to paclitaxel. However it was similarly active against cancer cells pre-saturated with monoclonal antibody- β -lactamase fusion protein L-49-sFv-bL. Prodrug **4.10** was designed to be activated by human β -glucuronidase.¹⁸ This compound showed enhanced water solubility and released paclitaxel with a half-life of 10 min at an enzyme concentration of 2.5 $\mu\text{g mL}^{-1}$.

Prodrug **4.11** contains a photolabile unit, 7-*N,N*-diethylamino-4-hydroxymethyl coumarin (DECM), which released paclitaxel by minimal tissue-damaging 365 nm UV

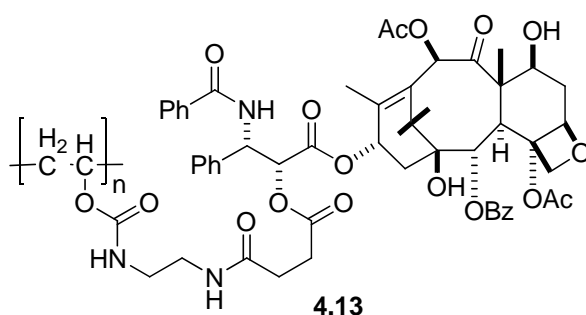
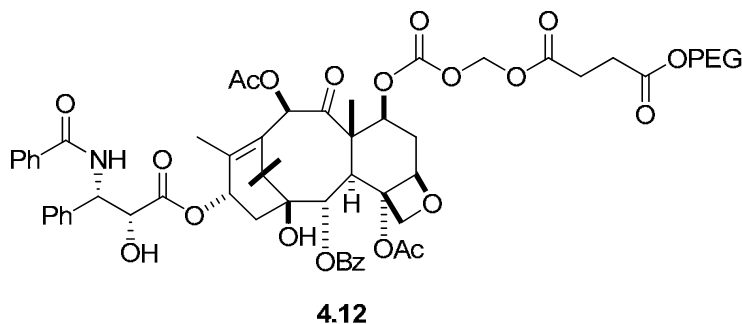
light irradiation at low power. Tumor targeting could be thus achieved by selective delivery of light to the tumor after administration.



4.1.2 Macromolecular Prodrugs of Paclitaxel. Macromolecules can serve as excellent promoieties for prodrug development. Macromolecules accumulate preferentially in tumor tissue through a mechanism called the enhanced permeability and retention (EPR) effect. When tumors reach a certain size they start to become dependent on blood supply produced by neovasculature for their nutritional and oxygen supply. These newly formed tumor vessels are usually abnormal in form and architecture. They are poorly-aligned defective endothelial cells with wide fenestrations, lacking a smooth muscle layer. Furthermore, tumor tissues usually lack effective lymphatic drainage. All these factors will lead to abnormal molecular and fluid transport dynamics, especially for macromolecular drugs. This phenomenon is called the “enhanced permeability and retention (EPR)-effect” of macromolecules and lipids in solid tumors.

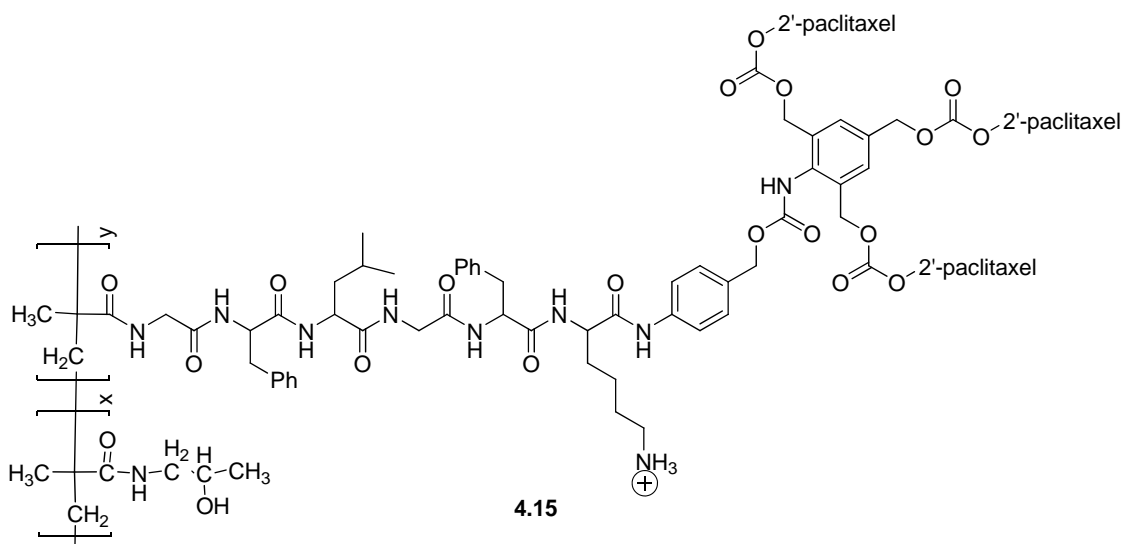
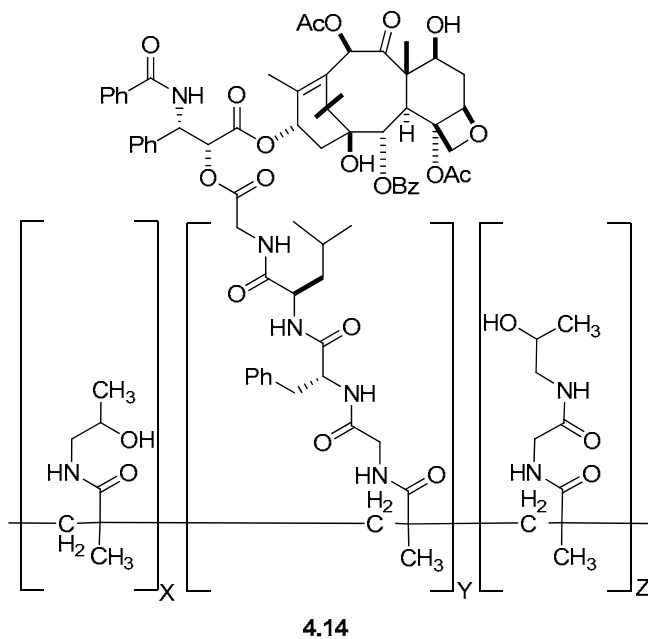
Besides this tumor targeting feature, some hydrophilic macromolecules can increase the water solubility and enhance the bioavailability of prodrugs. For example, prodrugs

4.12 and **4.13** contained highly hydrophilic polyethylene glycol (PEG)¹⁹ and poly(vinyl alcohol) (PVA) units.²⁰ In both cases, the water solubility was greatly enhanced and both prodrugs allowed fast release of the parent.

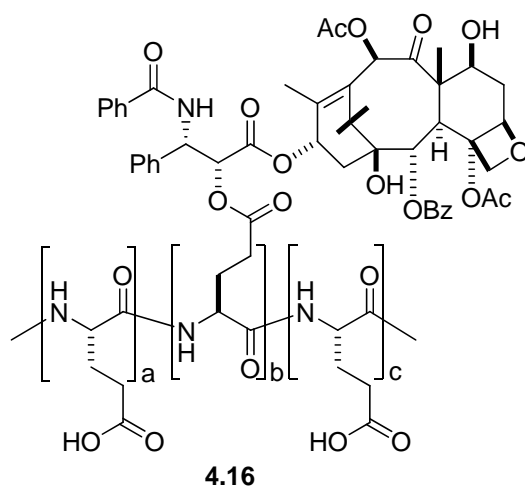


Another advantage of macromolecular prodrugs is that macromolecules can have multiple reaction sites. This feature allows a high load of active compound and makes possible the development of multifunctional prodrugs. Compounds **4.14** and **4.15** are water soluble conjugates^{21,22} of paclitaxel with N-(2-hydroxylpropyl)methacrylamide (HMPA) copolymer, which is biocompatible and nonimmunogenic. Paclitaxel was connected to the polymer through a peptide linker, which can be cleaved by lysosomal proteases.^{22,23} In the case of **4.14**, a Phase I clinical trial revealed that this water soluble conjugate had a high maximum tolerated dose (MTD) and superior activity in patients with advanced breast cancer. However further study was discontinued because of serious

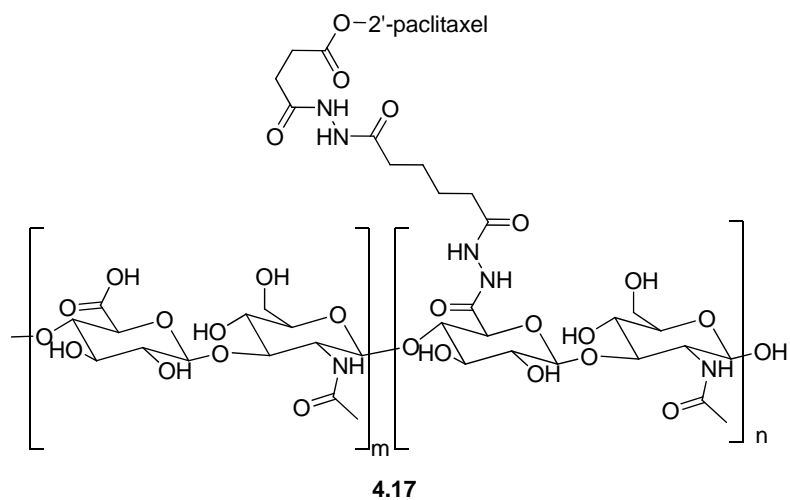
neurotoxicity. Compound **4.15** was designed as a triple-payload version through a self-immolative dendritic linker that acts as a molecular amplifier. It was reported to exhibit enhanced cytotoxicity compared to **4.14**.²²



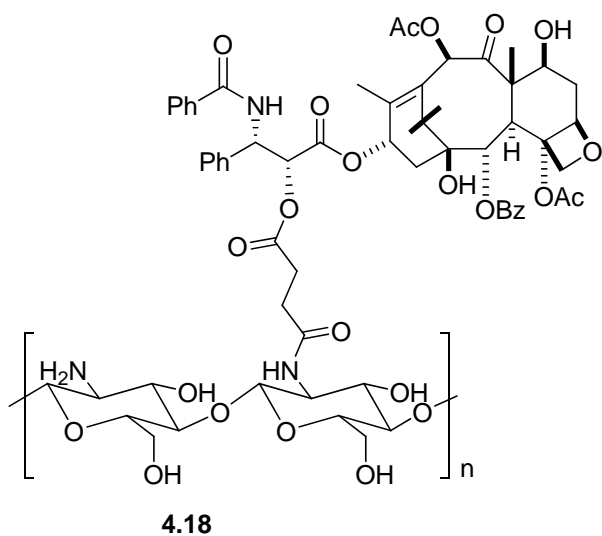
Compound **4.16** is another macromolecular prodrug that has also entered clinical trials.^{24,25} Paclitaxel was attached to a water-soluble and nonimmunogenic poly(L-glutamic acid) scaffold that can be degraded by cathepsin B to produce the parent drug and the non-toxic amino acid. The prodrug has shown comparable efficacy to paclitaxel and the non-toxic amino acid. The prodrug has shown comparable efficacy to paclitaxel with decreased side effects. The prodrug is currently in Phase III clinical trials.

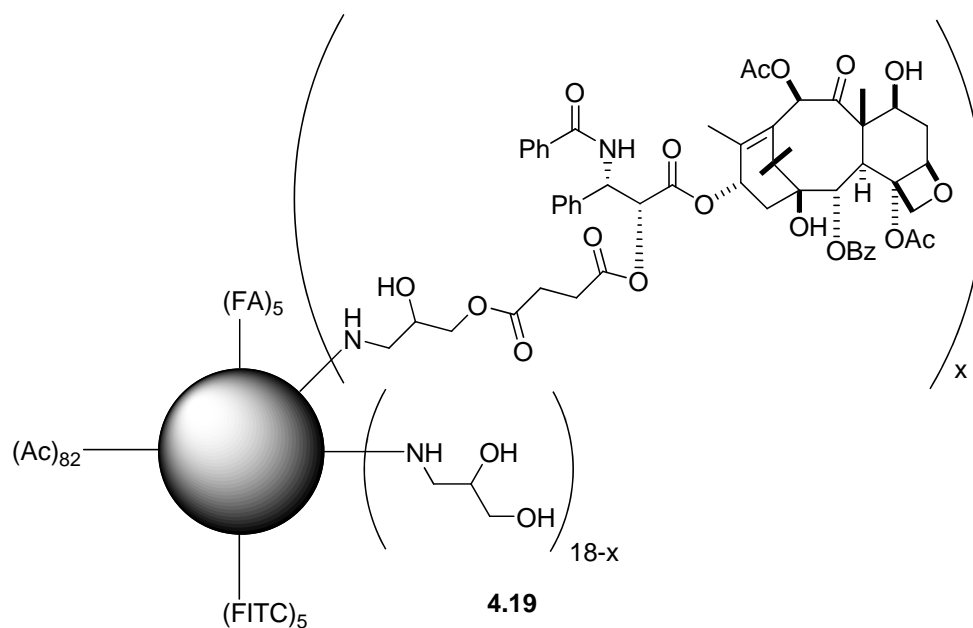


Compound **4.17** was synthesized as a conjugate of paclitaxel with hyaluronic acid (HA),²⁶ a naturally occurring linear polysaccharide which is often found in elevated levels in tumors.²⁷ In addition, most malignant cell types overexpress cell-membrane-localized HA receptors CD44 and RHAMM.^{28,29} The prodrug was internalized into cancer cells by receptor-mediated endocytosis and paclitaxel was then released inside. The compound showed selective cytotoxicity against cancer cells that overexpressed HA receptors.

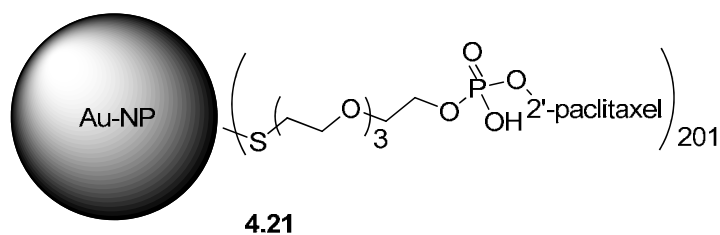
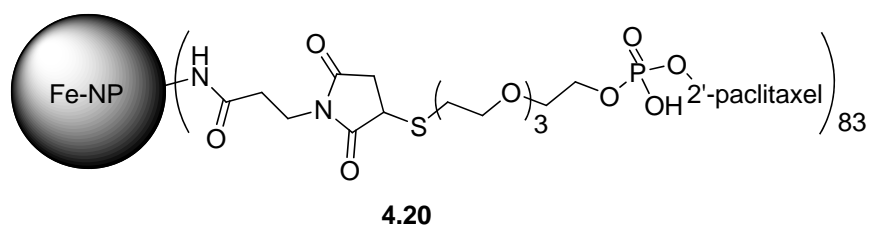


A potential oral delivery platform of paclitaxel (**4.18**) was developed recently through chemical conjugation of PTX to a low molecular weight chitosan (LMWC).³⁰ The water soluble prodrug contained ~12 wt % paclitaxel and showed comparable *in vitro* cytotoxicity and *in vivo* inhibition of tumor growth with the parent paclitaxel. Pharmacokinetic studies demonstrated high oral bioavailability of the prodrug, which was likely absorbed mainly from the ileum and reached the blood as the intact conjugate.



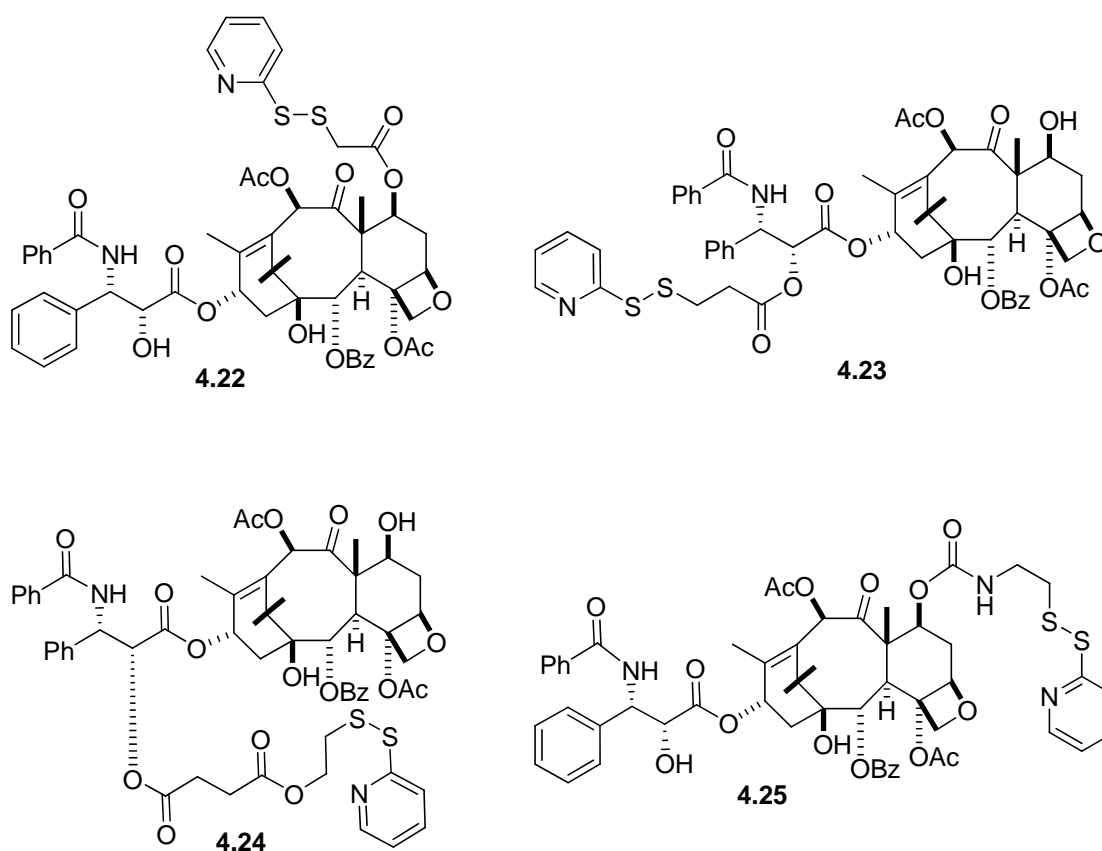


A poly(amidoamine) (PAMAM) dendrimer-based multifunctional conjugate **4.19** was designed and synthesized by Majoros et al.³¹ The PAMAM used contained 110 surface amine groups, which allowed the conjugation of multiple functional molecules including folic acid (FA, to target overexpressed folate receptors on specific cancer cells¹⁰), fluorescein isothiocyanate (FITC, an imaging agent), and paclitaxel (the chemotherapeutic drug) to the dendrimer. The average number of paclitaxel molecules loaded on one conjugate was determined to be 3 by gel permeation chromatography (GPC). Fluorescently traced assay showed that the conjugate was internalized only by the FR positive cancer cells. The conjugate was selectively cytotoxic to FR positive cancer cells at low concentrations (50 nM and 100 nM) *in vitro*. However, at high concentration (200 nM) it was equally active to both the PR positive and PR negative cancer cells. No *in vivo* data were reported.



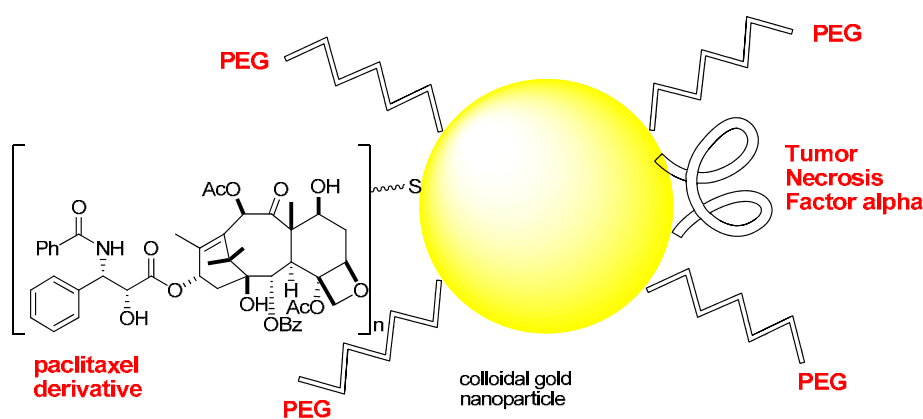
4.1.3 Paclitaxel-nanoparticle Conjugates The blending of material science and tumor biology makes possible the development of new vectors with the potential of achieving the goal of tumor-targeted drug delivery. Nanoparticle-drug conjugates share many advantages with previously discussed macromolecular prodrugs. The size of a nanoparticle is tunable. Nanoparticles can target tumor tissues by the EPR effect. In addition, the large surface area makes possible the installation of multiple components. They also have their own advantages depending on the material of the nanoparticles used. For example, Fe-NPs exhibit strong magnetization and little to no toxicity in vivo. Besides, the superparamagnetic Fe-NPs can be delivered to the desired target area by an external magnetic field. Au-NPs can serve as good drug delivery scaffolds because of their biocompatibility, tunable size, and strong reactivity with sulfur containing compounds, and controllable drug release. Recently, conjugates of paclitaxel with Fe-NPs (**4.20**) and Au-NPs (**4.21**) were reported.³² It was expected that hydrolysis of the phosphodiester moieties with phosphodiesterase could release paclitaxel from both

nanoparticles. Conjugate **4.20** indeed produced paclitaxel in the presence of phosphodiesterase in 10 days. However, in the case of conjugate **4.21**, less than 5 % of paclitaxel was liberated under the same conditions. It was demonstrated that conjugate **4.20** was 10^4 -fold more cytotoxic against the human cancer cell line (OECM1) than a human normal cell line (HUVEC).



In collaboration with Cytimmune Sciences, Inc., the Kingston group has been involved in the development of a colloidal gold nanoparticle-based drug delivery system (Scheme 4.1) with multiple components attached on the particle surface, which includes tumor necrosis factor alpha (TNF α) as a tumor targeting agent, polyethylene glycol

(PEG) to shield the system from being taken up by immune system, and paclitaxel as the anticancer therapeutic agent.³³ Previously, sulfur-containing paclitaxel analogs **4.22-4.25** were designed in order to attach paclitaxel to gold nanoparticles. It was demonstrated that the parent drug can be released in the presence of reducing agents such as dithiothreitol and cysteamine. However, these paclitaxel derivatives do not give the full therapeutic effect desired. It would be beneficial to develop paclitaxel derivatives with the desired properties to combine with gold nanoparticles, and which also exhibit the full therapeutic effects.

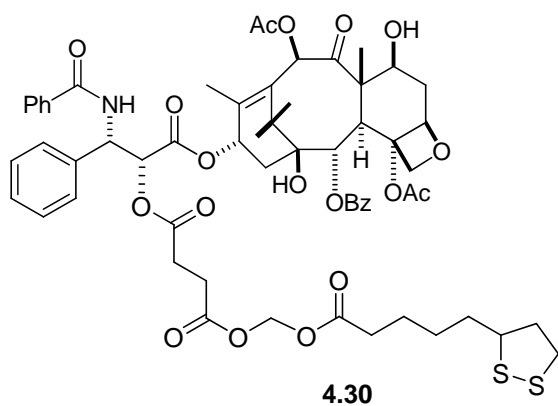
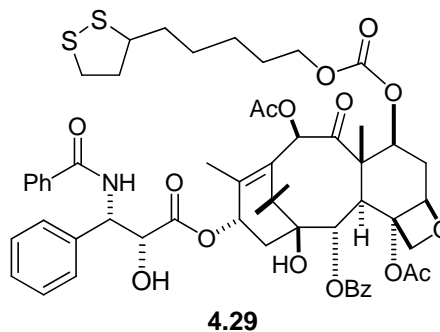
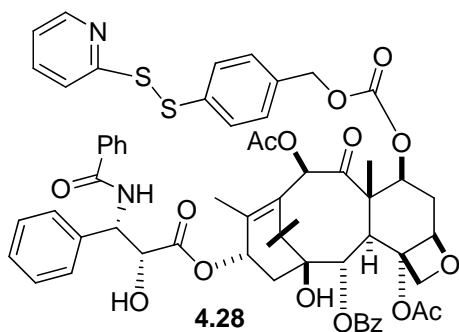
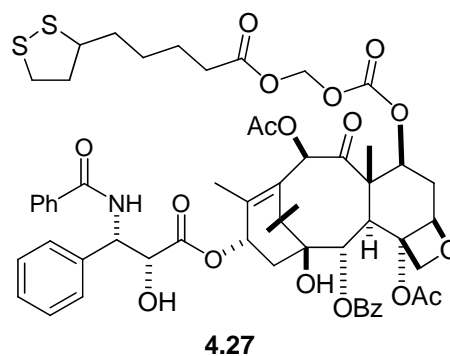
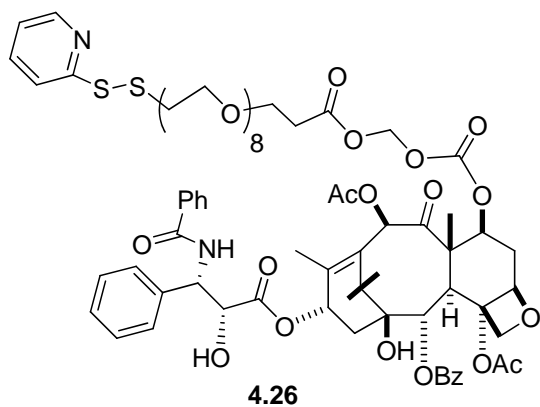


Scheme 4.1 Gold nanoparticle-based multifunctional anticancer drug delivery system

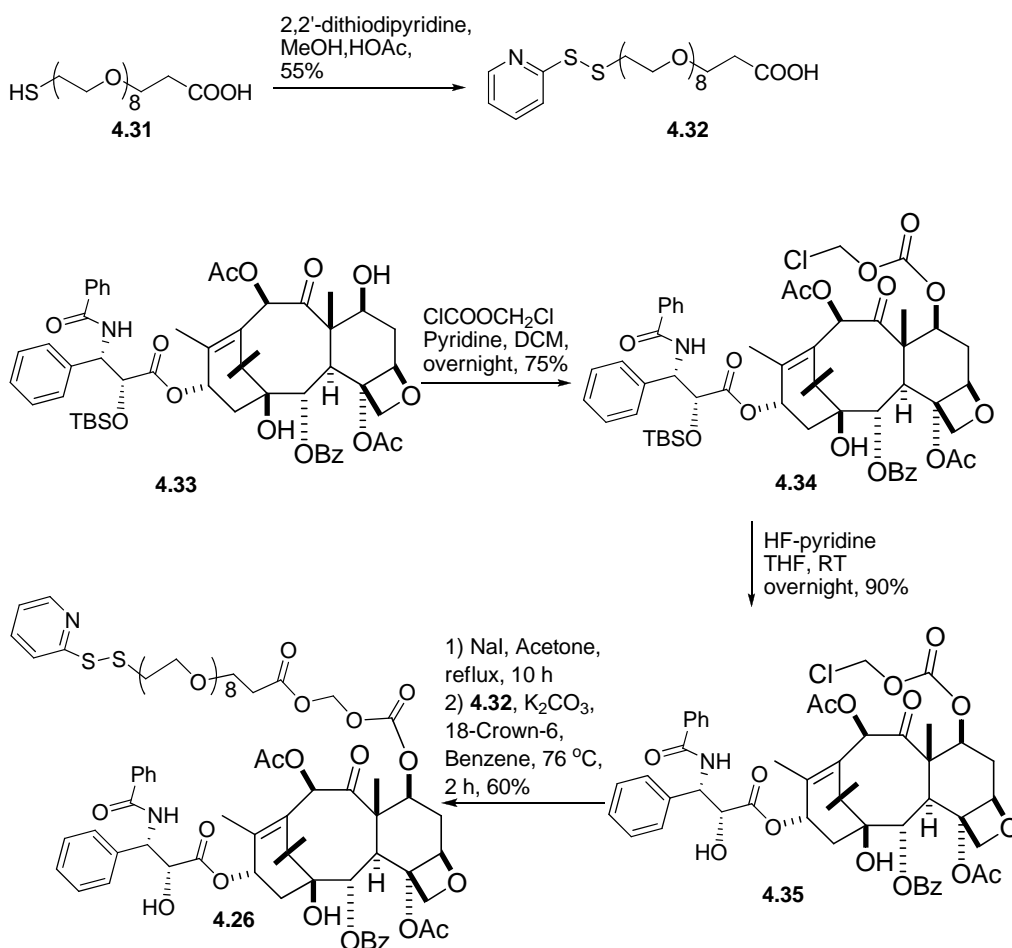
4.2 Synthesis of New Thiolated Paclitaxel Analogs for Reaction with Gold Nanoparticles as Drug Delivery Agents

To seek for paclitaxel analogs with the most suitable linkers for reaction with gold nanoparticles, a series of new paclitaxel analogs (**4.26-4.30**) with C-7 and C-2' thio-containing linkers were designed and synthesized. Pyridyl disulfide or lipoic acid moieties in the linkers enable the reaction of the analogs with the surface of the gold

nanoparticles due to the strong reactivity between gold and sulfur. The type of linkers seen in C-7 derivatives **4.26** and **4.27** was previously reported by Jo and coworkers¹⁹ in their development of a water soluble paclitaxel prodrug. Analogs **4.28** and **4.29** both contain a carbonate linkage.

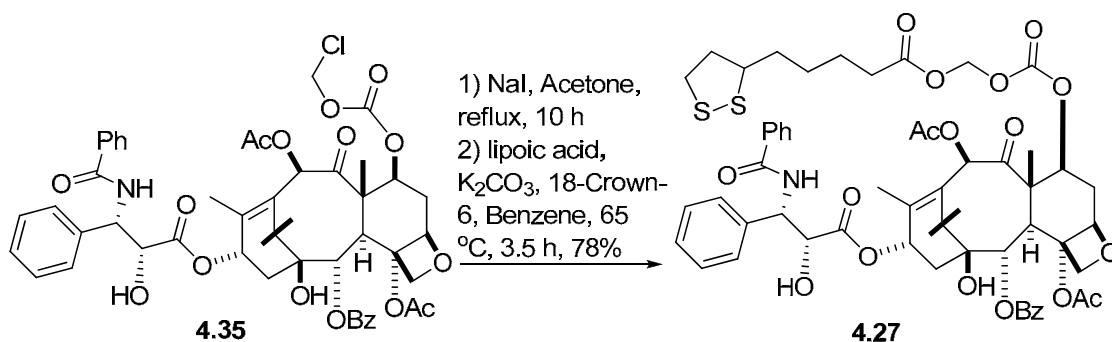


4.2.1 Synthesis of Analog 4.26. Compound **4.26** was prepared from paclitaxel derivative **4.35** and carboxylic acid **4.32** (Scheme 4.2) by the reported procedures.³⁴ Analog **4.35** was synthesized from the known compound **4.33**⁷ in two steps.³⁴ Acid **4.32** was prepared from commercially available acid **4.31** and 2,2'-dipyridyl disulfide in one step. Compound **4.35** was refluxed with NaI in acetone for a halogen exchange to facilitate subsequent S_N2 reaction with acid **4.32**, which produced the desired analog **4.26** with 60% yield.



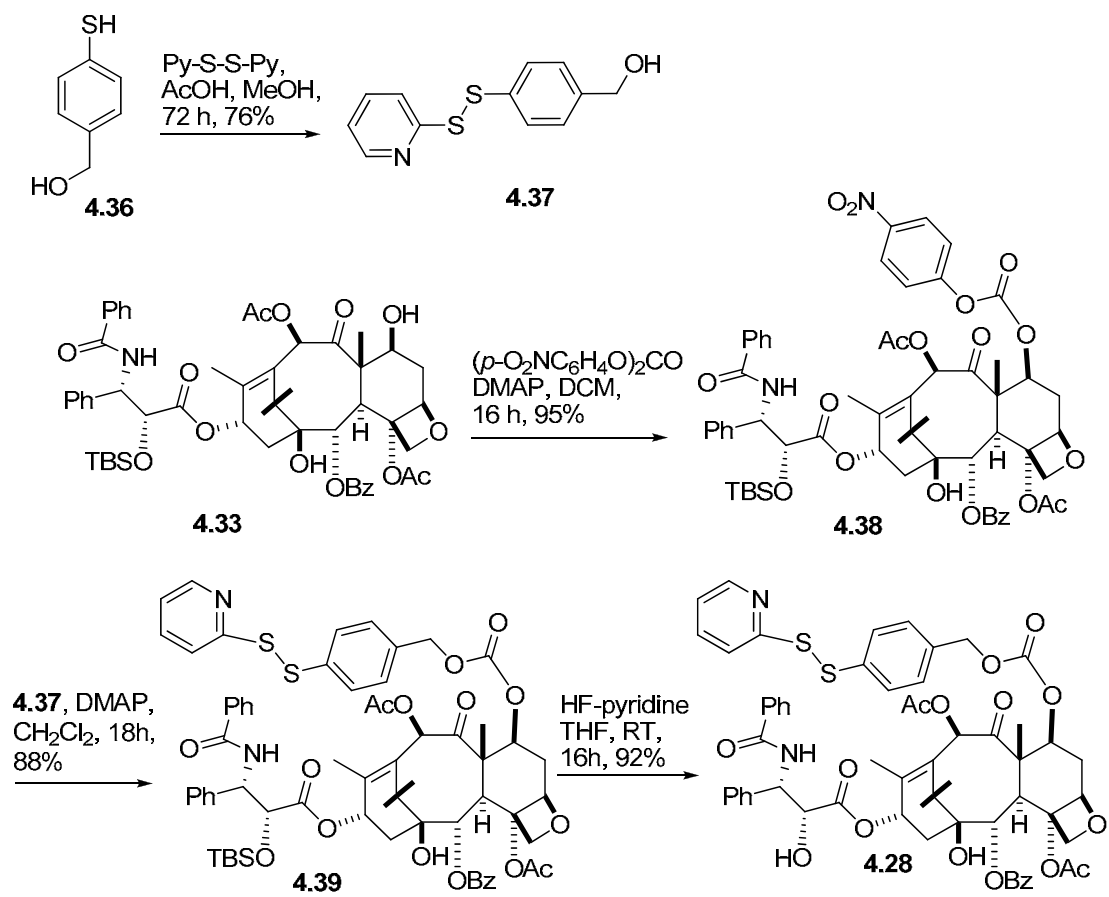
Scheme 4.2 Synthesis of **4.26**

4.2.2 Synthesis of Analog 4.27. Instead of the disulfide PEG acid moiety in analog **4.26**, lipoic acid was incorporated into analog **4.27** as a source of sulfur for reaction with gold nanoparticles. It is worth mentioning that lipoic is a natural product. The *R*-(+)-enantiomer exists in nature and is an essential cofactor of four mitochondrial enzyme complexes. Racemic lipoic acid was used as a preliminary test in this research for faster results and lower cost. As shown in Scheme 4.3, analog **4.27** was prepared from **4.35** and lipoic acid by the same procedure that was used to synthesize **4.26**.

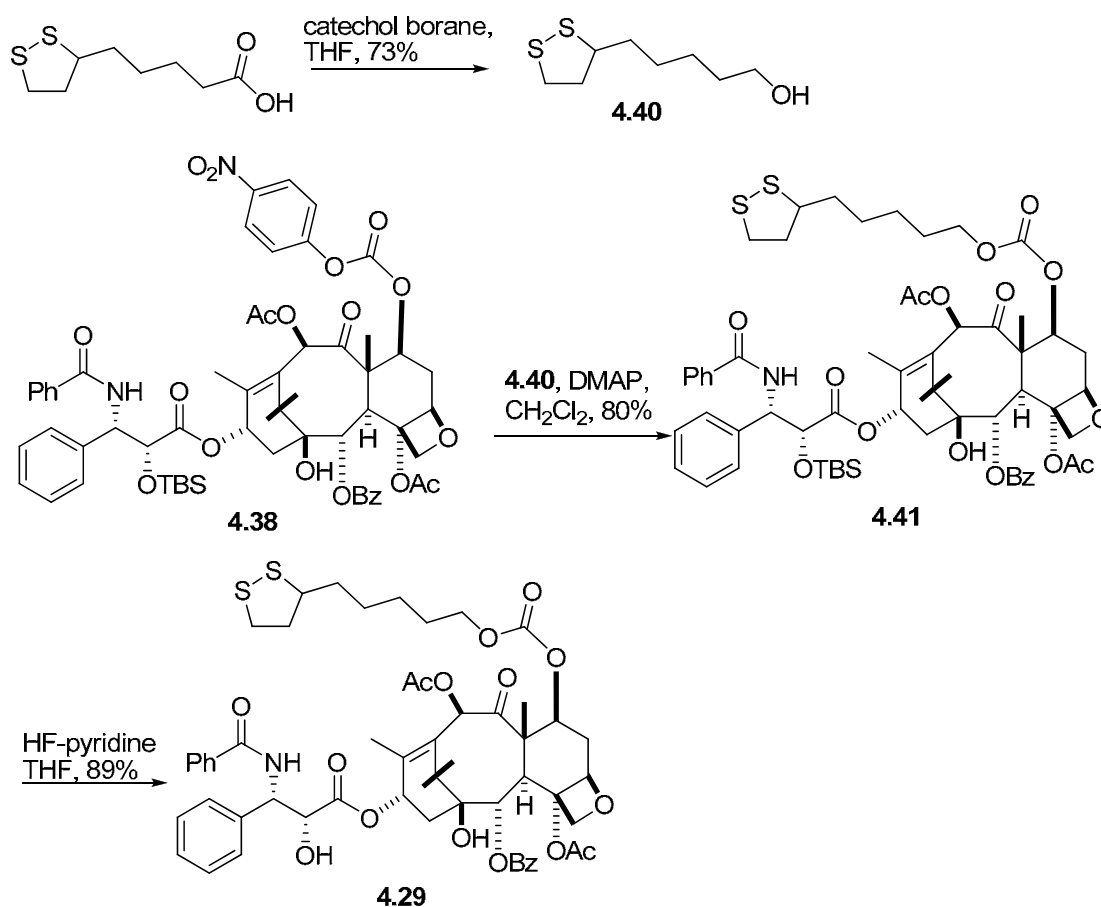


Scheme 4.3 Synthesis of **4.27**

4.2.3 Synthesis of Analogs 4.28 and 4.29. The carbonate derivatives **4.28** and **4.29** were prepared in a similar fashion (Schemes 4.4 and 4.5) by coupling precursor **4.38** with the corresponding known alcohols **4.37**³⁵ and **4.40**³⁶ respectively, followed by the deprotection of the resulting silyl ethers with HF.

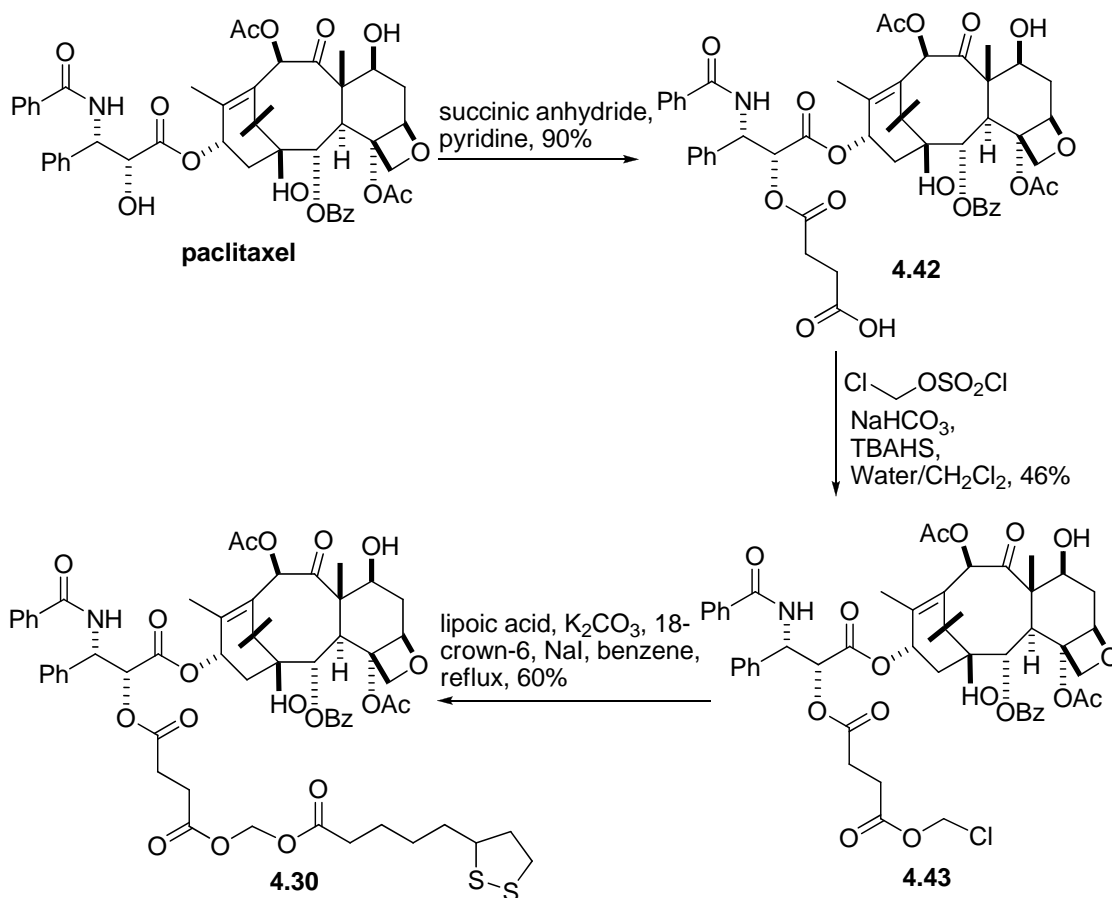


Scheme 4.4 Synthesis of 4.28



Scheme 4.5 Synthesis of **4.29**

4.2.4 Synthesis of Analog 4.30. Compound **4.30** is the only analog in this series that possesses a C-2' linker. This linker shares some similarities with the linkers seen in analogs **4.26** and **4.27**, although the synthesis is quite different (Scheme 4.6). Paclitaxel was reacted with succinic anhydride regioselectively at the C-2' position as previously reported.³⁷ The resulting acid **4.42** was reacted with chloromethyl chlorosulfate under phase-transfer conditions to generate the chloromethyl ester **4.43**. A similar strategy as used previously to incorporate lipoic acid to analogs **4.27** was applied here to furnish analog **4.30**.³⁴



Scheme 4.6 Synthesis of 4.30

4.2.5 Manufacture of a Gold-nanoparticle-based Multifunctional anticancer Drug Delivery System. The gold-nanoparticle-based multifunctional anticancer drug delivery system was manufactured in Cytimmune Sciences, Inc. by assembling the paclitaxel analogs, the tumor necrosis factor alpha (TNF α) and polyethylene glycol (PEG) onto the surface of gold nanoparticles. These are referred to as gold-bound analogs (Au-analogs) in the following sections. Gold-bound analogs Au-4.26, Au-4.27 and Au-4.28 were selected by Cytimmune for further studies.

4.2.6 Biological Evaluation of the Native Analogs and Gold-bound Analogs. The *in vitro* antiproliferative activities of the native analogs **4.26-4.28** and **4.30** against the A2780 cell line were evaluated in the Kingston group. Gold-bound analogs Au-**4.26** and Au-**4.28** were prepared by reacting native analogs **4.26** and **4.28** with gold nanoparticles and were evaluated by Cytimmune for their *in vitro* antiproliferative activities against the A2780 cell line. The results are shown in Table 4.1. All the native analogs and gold-bound analogs showed comparative or improved antiproliferative activities compared to paclitaxel.

Table 4.1 Antiproliferative activities (IC₅₀, ng/mL)^a of paclitaxel and analogs against A2780 cell line^b

Native Analogs					Gold-bound analogs	
4.26	4.27	4.28	4.30	paclitaxel	Au- 4.26	Au- 4.28
4.2±0.5	5.0±0.4	38.5±20.8	7.7±2.0	47.1±0.9	9.9±3.3	63.3±33.9

^a The concentration at which the compound inhibits 50% of the cell growth. ^b human ovarian cancer cell line.

Gold-bound analogs Au-**4.26** and Au-**4.28** were also evaluated for their *in vivo* efficacy by Cytimmune Sciences using paclitaxel as the positive control on mice bearing B16F10 tumors (Figure 4.1). Both of the gold-bound analogs showed higher efficacy than paclitaxel at the dose of 2.5 mg/Kg.

The stability of analog **4.27** in buffer solution at the physiological pH 7.4 was evaluated. Analog **4.27** was dissolved in a 3:1 mixture of methanol and 1xPBS buffer (pH = 7.4). Methanol was used to increase the solubility of the analog. Aliquots were taken at various time points and the concentrations of the analog and paclitaxel were determined by quantitative HPLC analyses. The analog was gradually hydrolyzed within 24 hours in the buffer solution and paclitaxel was generated slowly as the only product (Figure 4.2). A linear regression [Equation 4.1] was obtained plotting the logarithm of the concentration of **4.27** versus time, indicating pseudo 1st order kinetics (Figure 4.3). The rate constant was calculated, and the half life of analog **4.27** in the tested buffer solution was also obtained.

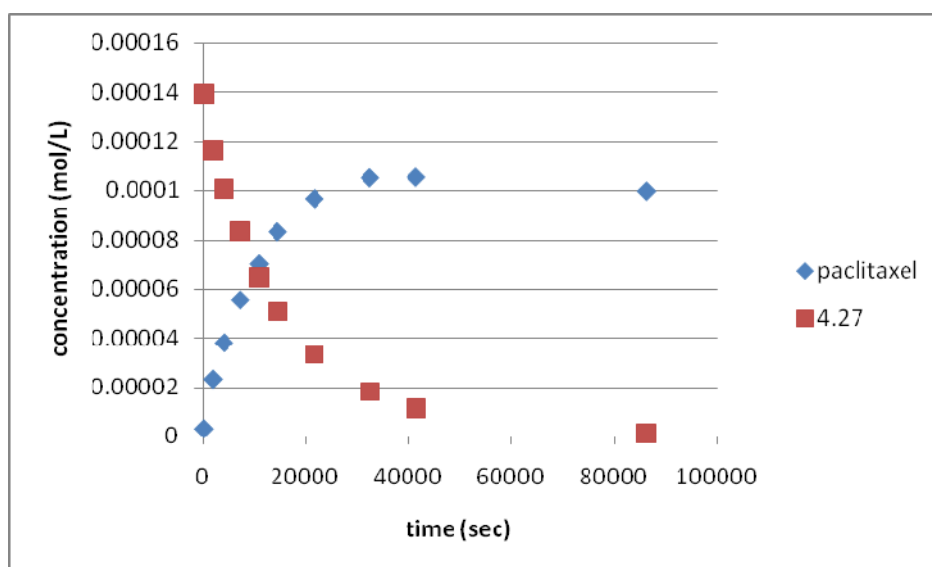


Figure 4.2 Hydrolytic conversion of **4.27** to paclitaxel

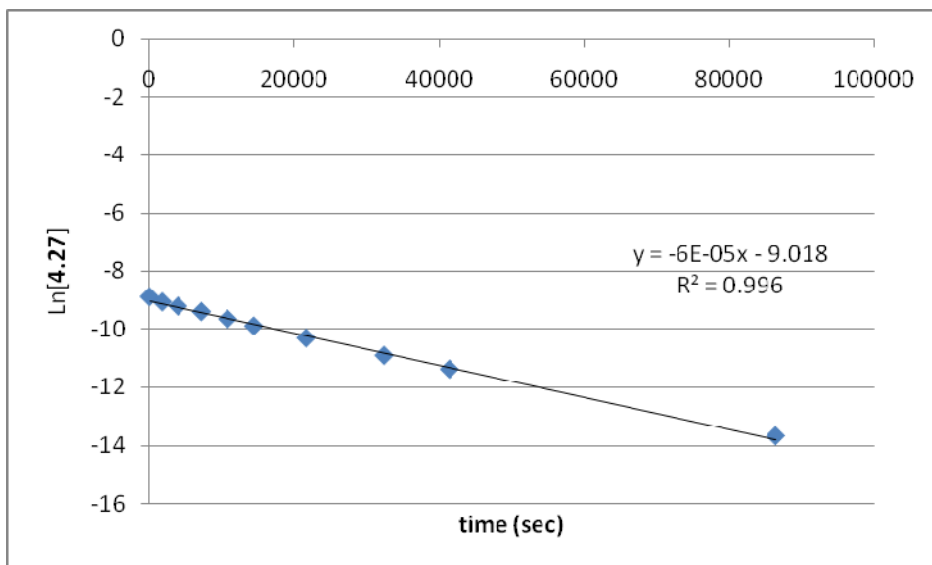


Figure 4.3 kinetics of the hydrolysis of **4.27** in buffer

$$\ln C_t = -k_{\text{obs}} \cdot t + \ln C_0 \quad [\text{Eq 4.1}]$$

$$k_{\text{obs}} = 6\text{E-}05 \text{ sec}^{-1}$$

$$T_{1/2} = 3.2 \text{ h}$$

Our collaborator, Cytimmune Sciences, recently conducted more stability studies on native analogs **4.26** and **4.28** and their corresponding gold-bound analogs Au-**4.26** and Au-**4.28** respectively. It was observed that the gold-bound analogs Au-**4.26** and Au-**4.28** are more stable to hydrolysis in buffer than their native counterparts (Figure 4.4).

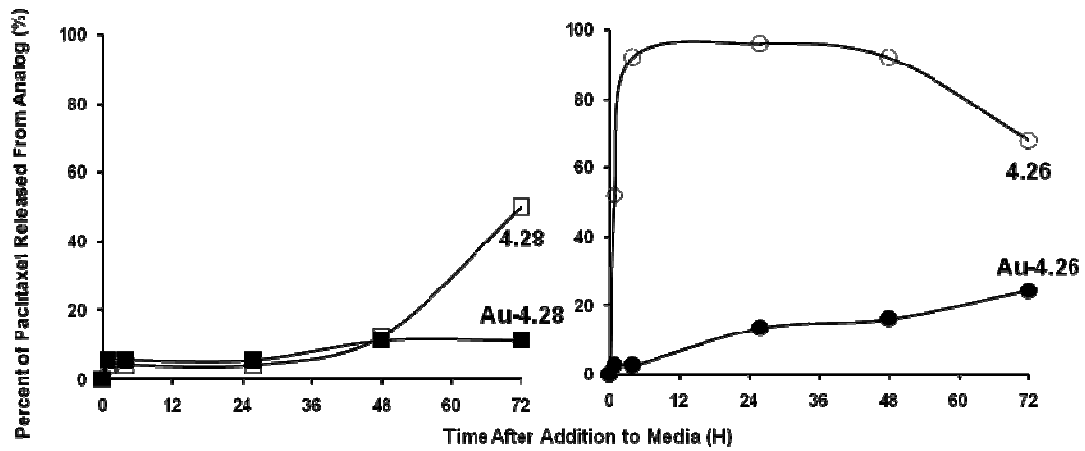


Figure 4.4 Comparison of the hydrolytic profiles of gold-bound analogs and native analogs in hydrolysis buffer (data from Cytimmune Sciences, Inc.)

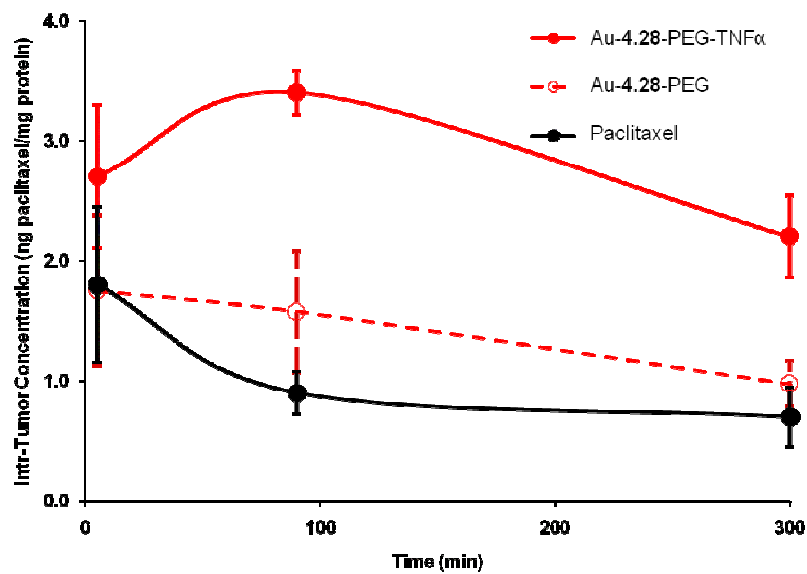


Figure 4.5 Delivery of paclitaxel to tumor by the gold nanoparticle-based drug delivery system (data from Cytimmune Sciences, Inc.)

The most recent data from Cytimmune showed that Au-**4.28** is effective in delivering paclitaxel to B16-F10 tumors implanted in C57/BL/6 mice with the help of TNF α (Figure 4.5), and maintains a higher level of paclitaxel in the tumor.

4.3 Conclusions

As part of the effort to develop a colloidal-gold-nanoparticle-based drug delivery system for the targeted delivery of paclitaxel to tumors, paclitaxel derivatives **4.26-4.30** with various sulfur containing linkers were synthesized. These paclitaxel analogs were reacted with gold nanoparticles whose surfaces were decorated with polyethylene glycol and Tumor Necrosis Factor Alpha (TNF α) to form the gold-bound analogs.

Native analogs **4.26-4.28** and **4.30** and gold-bound analogs Au-**4.26** and Au-**4.28** showed comparable antiproliferative activities with paclitaxel *in vitro*. Gold-bound analogs Au-**4.26** and Au-**4.28** showed higher efficacies than paclitaxel *in vivo* at the dose of 2.5 mg/Kg on tumor-bearing mice.

In the hydrolytic stability study of analog **4.27**, the paclitaxel derivative was slowly converted into paclitaxel within 24 hours in buffer solution with a half-life of 3.2 hours. Gold bound analogs Au-**4.26** and Au-**4.28** release paclitaxel much slower than their corresponding native analogs **4.26** and **4.28**, respectively in buffer.

Based on all these data, Au-**4.28** has been chosen as a lead by Cytimmune Sciences and is currently under further development.

4.4 Experimental Section

General experimental methods The following standard conditions apply unless otherwise stated. All reactions were performed under Ar or N₂ in oven-dried glassware using dry solvents and standard syringe techniques. Tetrahydrofuran (THF) was distilled from the sodium benzophenone ketyl radical ion. CH₂Cl₂ was distilled from CaH₂. HPLC grade methanol and water were purchased from Fisher Scientific. All reagents were of commercial quality and used as received. After workup, partitioned organic layers were washed with water and brine and dried over Na₂SO₄. Reaction progress was monitored using Al-backed thin layer chromatography (TLC) plates pre-coated with silica UV254. Purification by preparative thin layer chromatography (PTLC) was performed using glass-backed plates pre-coated with silica UV254. HPLC was conducted on a Shimadzu SCL-10AVP system using a column purchased from Phenomenex (Luna 5μ C18 (2) 25 × 4.6 mm). ¹H and ¹³C NMR spectra were recorded on a 400 MHz (400 MHz for ¹H and 100 MHz for ¹³C) spectrometer or a 500 MHz (500 MHz for ¹H and 126 MHz for ¹³C) spectrometer in CDCl₃ unless otherwise stated. All chemical shifts (δ) were referenced to the solvent peaks of CDCl₃ (7.26 ppm for ¹H, 77.0 ppm for ¹³C).

Synthesis of 1-(pyridin-2-yl)disulfanyl-3,6,9,12,15,18,21,24-octaoxaheptacosan-27-oic acid (4.32).³⁸ A 25 mL round bottom flask was dried in oven overnight, cooled to rt and equipped with a magnet stirring bar and a rubber septum. The flask was evacuated for 5 min and flushed with Ar. A solution of acid **17** (194mg, 0.423 mmol) in dry THF (2 mL) was added into the flask via syringe in the presence of an Ar atmosphere (balloon). The solution was stirred vigorously at rt and 30 L of glacial acetic acid was added via

syringe. The resulting solution was stirred at rt for 48 h. The resulted light yellow solution was concentrated by rotary evaporation (35 °C) to yield a yellow oil. This sample was applied to column chromatography (silica gel, 50 g) eluting with a mixture of hexane and EtOAc (1:3, 60 mL) and then methanol. The fraction eluted by methanol was concentrated by rotary evaporation (35 °C) to give a yellow oil, which was then purified by preparative TLC (developed with CH₂Cl₂:MeOH = 10:1) to produce **4.32** (200 mg, 0.35 mmol) as a colorless oil (82 %).

Synthesis of chloromethyl 7-((2'-*tert*-butyldimethylsiloxy)paclitaxel) carbonate (4.34).³⁶ To a 25 mL round bottom flask containing a magnetic stirring bar was charged compound **4.33**⁷ (399 mg, 0.41 mmol). The flask was then equipped with a rubber septum, evacuated and flushed with Ar. Dry CH₂Cl₂ (5 mL) was added to dissolve the solid and the resulting solution was cooled to 0 °C with an ice bath. To the mixture was added chloromethyl chloroformate (40.3 μL, 0.45 mmol) dropwise via syringe. After the solution was stirred for 5 min at 0 °C, pyridine (40.3 μL, 0.49 mmol) was added over a period of 5 min via syringe. The resulting mixture was allowed to warm to rt and stir for 15 h under an Ar atmosphere (balloon). The reaction was diluted with EtOAc (100 mL), washed with water (2 × 5 mL) and brine (2 × 5 mL) and dried with anhydrous Na₂SO₄. Rotary evaporation (35 °C) of the organic extract gave **4.34** (445 mg, crude) as a white powder, which was used in the next step without further purification. ¹H NMR (CDCl₃, 400 MHz) δ 8.12 (2H, d, *J* = 8.5 Hz), 7.74 (2H, d, *J* = 8.5 Hz), 7.25-7.65 (11H, m), 7.08 (1H, d, *J* = 9.0 Hz), 6.32 (1H, s), 6.26 (1H, t, *J* = 8.5 Hz), 5.98 (1H, d, *J* = 6.5 Hz), 5.73 (1H, d, *J* = 8.5 Hz), 5.69 (1H, d, *J* = 6.5 Hz), 5.57, 5.51 (1H, d, *J* = 6.5 Hz), 4.98 (1H, d, *J*

= 9.5 Hz), 4.67 (1H, d, $J = 2.5$ Hz), 4.35 (1H, d, $J = 8.0$ Hz), 4.20 (1H, d, $J = 8.5$ Hz), 3.96 (1H, d, $J = 7.0$ Hz), 2.66 (1H, m), 2.58 (3H, s), 2.41 (1H, dd, $J = 15, 8.5$ Hz), 2.14 (3H, s), 2.04 (3H, s), 1.99 (3H, s), 1.82 (3H, s), 1.21 (3H, s), 1.15 (3H, s), 0.80 (9H, s), -0.03 (3H, s), -0.30 (3H, s); HRFABMS m/z 1060.3853 [$M + H$]⁺ (calcd for C₅₅H₆₇ClNO₁₆Si, 1060.3918).

Synthesis of chloromethyl 7-paclitaxel carbonate (4.35).³⁶ A plastic vial (25 mL) equipped with a magnetic stirring bar was charged with a solution of **4.34** (445 mg, crude) in THF (10 mL). To the solution was added HF-pyridine (0.6 mL) dropwise at 0 °C. The resulting mixture was allowed to warm up to rt and stir for 10 h. The reaction mixture was diluted with EtOAc (100 mL), washed with saturated aqueous NaHCO₃ (2 × 5 mL), water (2 × 5 mL) and brine (2 × 5 mL) and dried with anhydrous Na₂SO₄. Rotary evaporation (35 °C) gave a light brown residue, which was then purified by column chromatography (silica gel, 150 g, eluted with hexanes:EtOAc, 3:2~2:3) to yield **4.35** (298 mg, 0.32 mmol) as a white powder (77 % for two steps from **4.33**). ¹H NMR (500 MHz) δ 8.11 (d, $J = 7.4$ Hz, 2H), 7.76 (d, $J = 7.4$ Hz, 2H), 7.62 (t, $J = 7.4$ Hz, 1H), 7.55 – 7.46 (m, 6H), 7.41 (m, 4H), 7.35 (t, $J = 7.3$ Hz, 1H), 7.04 (d, $J = 8.9$ Hz, 1H), 6.28 (s, 1H), 6.18 (t, $J = 8.5$ Hz, 1H), 5.97 (d, $J = 6.5$ Hz, 1H), 5.80 (dd, $J = 8.9, 2.4$ Hz, 1H), 5.67 (d, $J = 6.9$ Hz, 1H), 5.51 (q, $J = 5.7$ Hz, 2H), 4.95 (d, $J = 8.4$ Hz, 1H), 4.80 (dd, $J = 4.7, 2.5$ Hz, 1H), 4.32 (d, $J = 8.5$ Hz, 1H), 4.18 (d, $J = 8.5$ Hz, 1H), 3.92 (d, $J = 6.9$ Hz, 1H), 3.60 (d, $J = 4.9$ Hz, 1H), 2.65 (ddd, $J = 14.5, 9.5, 7.3$ Hz, 1H), 2.38 (s, 3H), 2.36 – 2.30 (m, 2H), 2.15 (s, 3H), 2.04 – 1.97 (m, 1H), 1.85 (s, 3H), 1.81 (s, 3H), 1.21 (s, 3H), 1.15 (s, 3H); ¹³C NMR (100 MHz) δ 201.54, 172.59, 170.53, 169.29, 167.12, 166.92,

152.71, 140.80, 138.10, 133.91, 133.74, 132.96, 132.04, 130.26, 129.09, 128.84, 128.80, 128.43, 127.16, 127.15, 83.78, 80.92, 78.62, 76.64, 76.47, 75.49, 74.26, 73.29, 73.06, 72.23, 56.25, 55.04, 47.00, 43.29, 35.63, 33.32, 26.61, 22.62, 20.98, 20.86, 14.72, 10.72; HRMS (ESI) calcd for C₄₉H₅₃ClNO₁₆ *m/z* 946.3053 ([M + H]⁺), found *m/z* 946.3022.

Synthesis of ((7-paclitaxel)-oxy-carbonyloxy)methyl 1-(pyridin-2-ylidysulfanyl)-3,6,9,12,15,18,21,24-octaohaheptacosan-27-oate (4.26).³⁶ A dry 25 mL round bottom flask was charged with a magnetic stirring bar, compound **4.35** (140 mg, 0.15 mmol) and NaI (33.3 mg, 0.22 mmol). Acetone (5 mL) was added via syringe to dissolve the solid. The flask was then equipped with a water condenser and the reaction mixture was allowed to reflux (~62 °C, oil bath) for 10 h. The resulting yellow solution was concentrated by rotary evaporation (35 °C) to give a yellow residue. To the flask was introduced a solution of **4.32** (128 mg, 0.22 mmol) in benzene (5 mL). After K₂CO₃ (61.3 mg, 0.44 mmol) and 18-crown-6 (235 mg, 0.89 mmol) were added, the flask was capped with a water condenser, warmed up to 75 °C and stirred for 2 h. The reaction solution was allowed to cool down to rt and diluted with EtOAc (100 mL), washed with saturated aqueous NaHCO₃ (2 × 5 mL), water (2 × 5 mL) and brine (2 × 5 mL) and dried with anhydrous Na₂SO₄. Rotary evaporation (35 °C) gave a yellowish oil. This was applied to preparative TLC (developed with 5 % MeOH in CH₂Cl₂) to yield **4.26** (136 mg, 0.092 mmol, 62 %). ¹H NMR (500 MHz) δ 8.44 (1H, d, *J* = 4.8 Hz), 8.11 (2H, d, *J* = 7.6 Hz), 7.25-7.80 (15H, m), 7.10 (2H, m), 6.30 (1H, s), 6.18 (1H, dd, *J* = 8.0, 8.0 Hz), 5.90 (1H, d, *J* = 6.0 Hz), 5.79 (1H, dd, *J* = 9.2, 2.4 Hz), 5.71 (1H, d, *J* = 6.0 Hz), 5.67 (1H, d, *J* = 6.8 Hz), 5.48 (1H, dd, *J* = 10.8, 6.8 Hz), 5.30 (1H, s), 4.94 (1H, d, *J* = 8.4 Hz), 4.80 (1H,

dd, $J = 6.4, 4.0$ Hz), 4.31 (1H, d, $J = 8.4$ Hz), 4.19 (1H, d, $J = 7.6$ Hz), 3.91 (1H, d, $J = 6.8$ Hz), 3.55-3.80 (33H, m), 2.99 (2H, dd, $J = 6.4, 6.4$ Hz), 2.67 (2H, dd, $J = 6.4, 6.4$ Hz), 2.64 (1H, m), 2.38 (3H, s), 2.32 (2H, d, $J = 9.2$ Hz), 2.16 (3H, s), 2.01 (1H, m), 1.85 (3H, s), 1.80 (3H, s), 1.21 (3H, s), 1.16 (3H, s); ^{13}C NMR (126 MHz) δ 201.4, 172.6, 170.5, 170.1, 169.1, 167.0, 166.8, 153.3, 149.6, 140.7, 138.1, 137.2, 133.9, 133.0, 132.0, 130.3, 129.1, 129.1, 128.8, 128.8, 128.4, 127.1, 127.1, 120.7, 119.7, 84.5, 83.8, 82.6, 81.2, 81.0, 79.2, 78.7, 76.5, 76.2, 75.7, 75.4, 74.3, 73.2, 72.5, 72.2, 70.6, 70.5, 69.0, 66.1, 65.5, 56.2, 54.9, 47.0, 43.3, 38.5, 35.6, 34.8, 33.4, 29.8, 27.0, 26.6, 22.6, 21.0, 20.8, 14.8, 10.7; HRFABMS m/z 1477.5421 $[\text{M} + \text{H}]^+$ (calcd for $\text{C}_{73}\text{H}_{93}\text{N}_2\text{O}_{26}\text{S}_2$, 1477.5458).

Synthesis of (7-paclitaxel)-oxy-carbonyloxy)methyl 5-(1,2-dithiolan-3-yl)pentanoate (4.27). A dry 25 mL round bottom flask was charged with a magnetic stirring bar, compound **4.35** (40 mg, 42.3 μmol) and NaI (9.5 mg, 63.5 μmol). Acetone (2 mL) was added via syringe to dissolve the solid. The flask was then equipped with a water condenser and the reaction mixture was allowed to reflux (~ 62 $^\circ\text{C}$, oil bath) for 10 h. The resulting yellow solution was concentrated by rotary evaporation (35 $^\circ\text{C}$) to give a yellow residue. To the flask was added lipoic acid (17.0 mg, 82.6 μmol) and benzene (2 mL). After K_2CO_3 (17.5 mg, 126.9 μmol) and 18-crown-6 (67.1 mg, 253.8 μmol) was added, the flask was capped with a water condenser, warmed to 65 $^\circ\text{C}$ and stirred for 3.5 h. TLC was used to examine the reaction progress. Decomposed product could be detected with prolonged reaction times. The reaction solution was allowed to cool down to rt and diluted with EtOAc (75 mL), washed with saturated aqueous NaHCO_3 (2×4 mL), water (2×4 mL) and brine (2×4 mL) and dried with anhydrous Na_2SO_4 . Rotary

evaporation (35 °C) gave a yellowish oily residue, which was purified by preparative TLC (developed with hexanes:EtOAc, 1:1) to yield **4.27** (36 mg, 32.2 μ mol, 76 %). ^1H NMR (400 MHz) δ 8.10 (2H, dd, $J = 7.5, 1.5$ Hz), 7.76 (2H, d, $J = 7.0, 1.5$ Hz), 7.62 (1H, m), 7.47-7.52 (5H, m), 7.33-7.43 (4H, m), 7.04 (1H, d, $J = 9.0$ Hz), 6.30 (1H, s), 6.18 (1H, dd, $J = 8.0, 8.0$ Hz), 5.90 (1H, d, $J = 6.0$ Hz), 5.79 (1H, dd, $J = 9.0, 2.0$ Hz), 5.70 (1H, d, $J = 6.0$ Hz), 5.66 (1H, d, $J = 7.0$ Hz), 5.48 (1H, dd, $J = 10.0, 7.0$ Hz), 4.94 (1H, d, $J = 8.0$ Hz), 4.79 (1H, d, $J = 2.5$ Hz), 4.31 (1H, d, $J = 8.5$ Hz), 4.17 (1H, d, $J = 8.5$ Hz), 3.91 (1H, d, $J = 7.5$ Hz), 3.56 (2H, m), 3.08-3.18 (2H, m), 2.62 (1H, m), 2.45 (1H, m), 2.38 (3H, s), 2.31 (2H, dd, $J = 9.0, 4.0$ Hz), 2.15 (3H, s), 1.96 (1H, m), 1.89 (1H, m), 1.84 (3H, s), 1.80 (3H, s), 1.67 (6H, m), 1.46 (2H, m), 1.21 (3H, s), 1.18 (3H, s); ^{13}C NMR (126 MHz) δ 201.44, 172.59, 172.00, 170.52, 169.11, 167.10, 166.92, 153.28, 140.66, 138.08, 133.90, 133.73, 133.05, 132.06, 130.26, 129.10, 128.84, 128.81, 128.44, 127.17, 127.14, 83.81, 82.65, 80.97, 78.62, 76.49, 76.22, 75.40, 74.27, 73.27, 72.29, 56.35, 56.34, 56.19, 55.01, 47.02, 43.31, 40.28, 38.57, 35.61, 34.64, 33.74, 33.38, 28.71, 28.70, 26.64, 24.29, 22.64, 20.98, 20.87, 14.75, 10.73; HRMS (ESI) calcd for $\text{C}_{57}\text{H}_{66}\text{NO}_{18}\text{S}_2$ m/z 1116.3687 ($[\text{M} + \text{H}]^+$), found m/z 1116.3721.

Synthesis of 2'-(tert-butyldimethylsiloxy)-7-((4-nitrophenoxy)carbonyloxy)-paclitaxel (4.38). To a stirred solution of bis(4-nitrophenyl) carbonate (123 mg, 0.40 mmol) and DMAP (49 mg, 0.40 mmol) in CH_2Cl_2 (3 mL) was added slowly (over 30 min) a solution of compound **4.33** (78 mg, 0.081 mmol) in CH_2Cl_2 (2 mL). After being stirred at rt for 16 h, the reaction mixture was concentrated under reduced pressure and the crude product was purified by preparative TLC (50% EtOAc in hexanes) afforded

compound **4.38** (87 mg, 95%): ^1H NMR (400 MHz) δ 8.27 (2H, d, $J = 9.2$ Hz), 8.13 (2H, d, $J = 7.9$ Hz), 7.75 (2H, d, $J = 7.3$ Hz), 7.30-7.65 (11H, m), 7.10 (1H, d, $J = 9.0$ Hz), 6.39 (1H, s), 6.28 (1H, dd, $J = 9.0, 8.7$ Hz), 5.73 (1H, br d, $J = 7.1$ Hz), 5.73 (1H, d, $J = 7.1$ Hz), 5.57 (1H, dd, $J = 10.5, 7.1$), 5.01 (1H, br d, $J = 8.7$ Hz), 4.67 (1H, d, $J = 2.1$ Hz), 4.37 (1H, d, $J = 8.5$ Hz), 4.24 (1H, d, $J = 8.5$ Hz), 4.00 (1H, d, $J = 6.7$ Hz), 2.73 (1H, ddd, $J = 16.5, 9.4, 7.1$ Hz), 2.58 (3H, s), 2.43 (1H, dd, $J = 13.4, 9.6$ Hz), 2.20 (3H, s), 2.18 (1H, dd, $J = 15.4, 8.9$ Hz), 2.08 (1H, ddd, $J = 13.4, 10.5, 1.6$ Hz), 1.96 (3H, s), 1.88 (3H, s), 1.24 (3H, s), 1.19 (3H, s), 0.80 (9H, s), -0.04 (3H, s), -0.30 (3H, s); ^{13}C NMR (100 MHz) δ 201.3, 171.4, 170.1, 169.3, 167.2, 166.9, 162.0, 155.7, 151.8, 145.5, 141.4, 138.1, 134.0, 133.8, 132.7, 131.9, 130.2, 129.0, 128.8, 128.8, 128.0, 127.0, 126.4, 126.0, 125.0, 122.6, 115.5, 83.7, 80.8, 78.7, 77.1, 76.4, 75.2, 75.1, 74.4, 71.3, 60.4, 55.9, 55.7, 46.8, 43.4, 35.6, 33.2, 26.4, 25.5, 22.9, 21.5, 21.0, 20.8, 18.1, 14.6, 14.2, 10.7, -5.2, -5.8; HRFABMS m/z 1133.4362 [$\text{M} + \text{H}$] $^+$ (calcd for $\text{C}_{60}\text{H}_{69}\text{N}_2\text{O}_{18}\text{Si}$, 1133.4315).

Synthesis of 2'-(tert-butyldimethylsiloxy)-7-(((4-(pyridin-2-yl)disulfanyl)-benzyloxy)-carbonyloxy)-paclitaxel (4.39). To a stirred solution of compounds **4.38** (48.5 mg, 0.043 mmol) and **4.37**³⁵ (16 mg, 0.064 mmol) in dry CH_2Cl_2 (2 mL) was added 4-(dimethylamino) pyridine (15.6 mg, 0.128 mmol), and the mixture was stirred at rt for 18 h. The resulting mixture was diluted with CH_2Cl_2 (40 mL) and washed with water (2 \times 2 mL) and brine (2 \times 2 mL). The solution was dried with anhydrous Na_2SO_4 and concentrated in vacuo. The crude product was purified by preparative TLC (50% EtOAc in hexanes) to afford compound **4.39** (47 mg, 88%): ^1H NMR (500 MHz) δ 8.46 (1H, d, $J = 4.9$ Hz), 8.11 (2H, d, $J = 7.3$ Hz), 7.76 (2H, d, $J = 7.6$ Hz), 7.25-7.55 (17 H, m), 7.10

(1H, d, $J = 8.7$ Hz), 6.39 (1H, s), 6.26 (1H, dd, $J = 9.2, 8.1$ Hz), 5.73 (1H, d, $J = 8.7$ Hz), 5.70 (1H, br d, $J = 6.7$ Hz), 5.54 (1H, dd, $J = 10.1, 6.9$), 5.16 (2H, br s), 4.97 (1H, d, $J = 9.2$ Hz), 4.67 (1H, br s), 4.34 (1H, d, $J = 8.5$ Hz), 4.20 (1H, d, $J = 8.5$ Hz), 3.97 (1H, d, $J = 6.7$ Hz), 2.60 (1H, m), 2.58 (3H, s), 2.42 (1H, dd, $J = 15.1, 9.4$ Hz), 2.15 (3H, s), 2.15 (1H, dd, $J = 15.4, 8.9$ Hz), 2.00 (1H, m), 2.00 (3H, s), 1.80 (3H, s), 1.22 (3H, s), 1.16 (3H, s), 0.80 (9H, s), -0.03 (3H, s), -0.30 (3H, s); ^{13}C NMR (126 MHz) δ 201.6, 171.4, 170.0, 169.1, 167.1, 166.9, 159.0, 154.0, 149.0, 141.1, 138.2, 136.6, 135.7, 134.0, 133.7, 132.7, 131.8, 130.2, 129.7, 129.0, 128.8, 128.3, 128.0, 127.0, 126.3, 126.0, 121.5, 120.5, 115.7, 83.8, 80.9, 78.7, 76.3, 75.5, 75.3, 75.0, 74.4, 71.3, 69.2, 56.0, 55.7, 46.8, 43.3, 35.5, 33.3, 26.4, 25.5, 23.0, 21.4, 20.8, 18.1, 14.6, 10.7, -5.2, -5.8; HRFABMS m/z 1243.4370 $[\text{M} + \text{H}]^+$ (calcd for $\text{C}_{66}\text{H}_{75}\text{N}_2\text{O}_{16}\text{S}_2\text{Si}$, 1243.4327).

Synthesis of 7-(((4-(pyridin-2-yl)disulfanyl)benzyloxy)carbonyloxy)-paclitaxel (4.28). A plastic vial was charged with a solution of compound **4.39** (45 mg, 0.036 mmol) in 4.5 mL of dried THF and cooled to 0 °C. To this solution was added 0.15 mL of HF-pyridine. The mixture was allowed to warm to rt and stirred for 16 h. The reaction was quenched by careful addition of saturated aqueous NaHCO_3 until no bubbles were formed. The resulting solution was extracted with EtOAc (3×15 mL). The organic solution was washed with water (2×2 mL) and brine (2×2 mL), dried with anhydrous Na_2SO_4 and concentrated in vacuo. The residue was purified by preparative TLC (1:1 EtOAc:hexanes) to give **7** (35 mg, 92 % based on 93 % conversion), together with 3 mg unreacted compound **4.28**. ^1H NMR (500 MHz) δ 8.46 (1H, d, $J = 4.9$ Hz), 8.11 (2H, d, $J = 7.2$ Hz), 7.76 (2H, d, $J = 8.0$ Hz), 7.25-7.65 (17H, m), 7.10 (1H, br dd, $J = 7.0, 4.1$ Hz),

7.04 (1H, d, $J = 8.8$ Hz), 6.36 (1H, s), 6.19 (1H, dd, $J = 6.9, 6.9$ Hz), 5.80 (1H, dd, $J = 8.8, 2.5$ Hz), 5.67 (1H, d, $J = 6.8$ Hz), 5.47 (1H, dd, $J = 10.7, 7.5$), 5.17 (1H, d, $J = 12.3$ Hz), 5.13 (1H, d, $J = 12.3$ Hz), 4.93 (1H, d, $J = 8.8$ Hz), 4.80 (1H, dd, $J = 5.0, 2.5$ Hz), 4.31 (1H, d, $J = 8.7$ Hz), 4.18 (1H, d, $J = 8.7$ Hz), 3.93 (1H, d, $J = 6.8$ Hz), 3.65 (1H, d, $J = 5.0$ Hz), 2.58 (1H, m), 2.38 (3H, s), 2.33 (2H, d, $J = 6.9$ Hz), 2.15 (3H, s), 1.95 (1H, m), 1.85 (3H, s), 1.80 (3H, s), 1.22 (3H, s), 1.17 (3H, s); ^{13}C NMR (126 MHz) δ 201.5, 172.5, 170.4, 169.0, 167.0, 166.8, 159.0, 153.8, 149.0, 140.5, 138.0, 137.8, 133.8, 133.8, 133.6, 133.0, 131.9, 130.1, 129.6, 129.0, 128.7, 128.7, 128.4, 127.7, 127.0, 127.0, 127.0, 121.5, 120.5, 83.8, 80.9, 78.5, 76.4, 75.6, 75.3, 74.2, 73.1, 72.2, 69.3, 56.1, 54.9, 46.9, 43.2, 35.5, 33.4, 26.5, 22.5, 20.9, 20.8, 14.6, 10.6; HRFABMS m/z 1129.3464 $[\text{M} + \text{H}]^+$ (calcd for $\text{C}_{60}\text{H}_{61}\text{N}_2\text{O}_{16}\text{S}_2$, 1129.3463).

Synthesis of 5-(1,2-dithiolan-3-yl)pentan-1-ol (4.40).³⁶ To a stirred solution of lipoic acid (41.2 mg, 0.2 mmol) in THF (2 mL) at rt was added slowly a solution of catecholborane (107 μL , 1.0 mmol) in THF. The mixture was heated to 55 $^\circ\text{C}$ and stirred for 12 hours. Cold water was added slowly to the mixture and the resulting solution was extracted with CH_2Cl_2 (10 mL \times 3) and the organic phase was washed with 1 M NaOH solution (2 mL \times 3). The solution was dried, filtered, and evaporated under reduced pressure. The residue was separated by PTLC with hexanes and EtOAc (2:1) as developing solvent to yield compound **4.40** (28 mg, 73% yield). ^1H NMR (500 MHz) δ 3.55 – 3.46 (m, 4H), 3.13 – 3.00 (m, 2H), 2.38 (dtd, $J = 11.9, 6.5, 5.4$ Hz, 1H), 1.83 (dq, $J = 12.8, 7.0$ Hz, 1H), 1.68 – 1.52 (m, 2H), 1.47 (dt, $J = 10.7, 7.0$ Hz, 3H), 1.43 – 1.23 (m,

5H); ^{13}C NMR (126 MHz) δ 62.22, 56.66, 40.27, 38.42, 34.87, 32.31, 29.11, 25.56. Data of the title compound were identical to those of the reported compound.³⁶

Synthesis of 5-(1,2-dithiolan-3-yl)pentyl (2'-(*tert*-butyldimethylsiloxy)-paclitaxel-7-yl) carbonate (4.41). To a stirred solution of **4.38** (40 mg, 0.044 mmol) and **4.40** (13 mg, 0.066 mmol) in CH_2Cl_2 (2 mL) at rt was added 4-dimethylaminopyridine (16 mg, 0.13 mmol). The resulting yellow solution was stirred for 18 hours at rt. Usual workup and purification by PTLC (hexanes:EtOAc, 2:1) gave compound **4.41** as a white solid (33 mg, 80%). ^1H NMR (500 MHz) δ 8.12 (d, $J = 7.4$ Hz, 2H), 7.74 (d, $J = 7.4$ Hz, 2H), 7.60 (t, $J = 7.4$ Hz, 1H), 7.50 (dd, $J = 15.0, 7.6$ Hz, 3H), 7.46 – 7.35 (m, 4H), 7.35 – 7.27 (m, 3H), 7.09 (d, $J = 8.9$ Hz, 1H), 6.38 (s, 1H), 6.25 (t, $J = 8.9$ Hz, 1H), 5.73 (d, $J = 9.0$ Hz, 1H), 5.70 (d, $J = 7.0$ Hz, 1H), 5.50 (dd, $J = 10.7, 7.1$ Hz, 1H), 4.98 (d, $J = 8.5$ Hz, 1H), 4.66 (d, $J = 2.0$ Hz, 1H), 4.34 (d, $J = 8.5$ Hz, 1H), 4.24 – 4.14 (m, 3H), 3.97 (d, $J = 6.9$ Hz, 1H), 3.56 (m, 1H), 3.21 – 3.06 (m, 2H), 2.65 – 2.59 (m, 1H), 2.57 (s, 3H), 2.49 – 2.36 (m, 2H), 2.14 (s, 4H), 2.03 (s, 3H), 1.99 (s, 4H), 1.92 – 1.86 (m, 2H), 1.81 (s, 3H), 1.77 (s, 2H), 1.73 – 1.60 (m, 5H), 1.55 – 1.31 (m, 5H), 1.20 (s, 3H), 1.16 (s, 3H), 0.79 (s, 9H), -0.04 (s, 3H), -0.24 – -0.39 (m, 3H); ^{13}C NMR (126 MHz) δ 201.80, 171.57, 170.03, 168.93, 167.18, 166.96, 154.39, 141.03, 138.32, 134.16, 133.81, 132.92, 131.93, 130.29, 129.17, 128.86, 128.85, 128.08, 127.08, 126.48, 84.03, 81.03, 78.73, 76.49, 75.30, 75.23, 75.16, 74.56, 71.49, 68.56, 56.63, 56.61, 56.16, 55.77, 46.95, 43.43, 40.32, 38.54, 35.66, 34.88, 33.49, 28.99, 28.37, 26.46, 25.62, 25.61, 23.08, 21.56, 20.84, 18.21, 14.71, 10.87, -5.10, -5.73; HRMS (ESI) calcd for $\text{C}_{62}\text{H}_{80}\text{NO}_{16}\text{S}_2\text{Si}$ m/z 1186.4688 ($[\text{M} + \text{H}]^+$), found m/z 1186.4634.

Synthesis of 5-(1,2-dithiolan-3-yl)pentyl (paclitaxel-7-yl) carbonate (4.29). To a solution of **4.41** (30 mg, 0.025 mol) in THF at 0 °C was added 60 % HF in pyridine (0.1 mL) dropwise. The resulting solution was warmed up to rt and stirred overnight. Saturated NaHCO₃ solution was added to the reaction carefully to quench the unreacted HF until no effervescence was observed. The resulting solution was extracted with EtOAc (10 mL × 3) and the combined organic layers were washed, dried and concentrated. The residue was purified by PTLC (hexanes:EtOAc, 1:1) to yield **4.29** as a white power (24 mg, 89%). ¹H NMR (500 MHz) δ 8.10 (d, *J* = 8.4 Hz, 2H), 7.75 (d, *J* = 8.4 Hz, 2H), 7.61 (t, *J* = 7.4 Hz, 1H), 7.54 – 7.30 (m, 10H), 7.08 (d, *J* = 9.0 Hz, 1H), 6.34 (s, 1H), 6.17 (t, *J* = 8.8 Hz, 1H), 5.79 (dd, *J* = 8.9, 2.4 Hz, 1H), 5.66 (d, *J* = 6.9 Hz, 1H), 5.44 (dd, *J* = 10.5, 7.2 Hz, 1H), 4.93 (d, *J* = 9.4 Hz, 1H), 4.78 (dd, *J* = 4.8, 2.6 Hz, 1H), 4.30 (d, *J* = 8.4 Hz, 1H), 4.22 – 4.13 (m, 3H), 3.91 (d, *J* = 6.9 Hz, 1H), 3.66 (d, *J* = 5.0 Hz, 1H), 3.60 – 3.49 (m, 1H), 3.22 – 3.06 (m, 2H), 2.66 – 2.54 (m, 1H), 2.46 (qt, *J* = 12.4, 6.1 Hz, 1H), 2.37 (s, 3H), 2.35 – 2.27 (m, 2H), 2.15 (s, 3H), 1.99 – 1.89 (m, 2H), 1.84 (s, 3H), 1.80 (s, 3H), 1.70 – 1.61 (m, 4H), 1.52 – 1.33 (m, 4H), 1.19 (s, 3H), 1.16 (s, 3H); ¹³C NMR (126 MHz) δ 201.70, 172.55, 170.46, 168.92, 167.08, 166.94, 154.32, 140.49, 138.10, 133.87, 133.76, 133.21, 132.03, 130.26, 129.15, 129.08, 128.82, 128.80, 128.42, 127.16, 127.14, 83.95, 81.07, 78.63, 76.52, 75.36, 75.27, 74.37, 73.28, 72.31, 68.56, 56.63, 56.62, 56.28, 54.98, 47.06, 43.32, 40.32, 38.54, 35.63, 34.88, 33.53, 29.00, 28.38, 26.63, 25.62, 25.60, 22.64, 20.97, 20.87, 14.72, 10.79, 0.08; HRMS (ESI) calcd for C₅₆H₆₆NO₁₆S₂ *m/z* 1072.3823 ([M + H]⁺), found *m/z* 1072.3772.

Synthesis of paclitaxel-2'-monosuccinate (4.42).³⁶ A dry round bottom flask was equipped with a magnet stirring bar and a rubber septum. After being evacuated for 5 min and flushed with N₂, the flask was charged with paclitaxel (50 mg, 59 μmol). Dry pyridine (4 mL) was added via syringe to dissolve the paclitaxel solid. To the resulting solution was added succinic anhydride (90 mg, 0.9 mmol) while stirring. The resulting mixture was stirred for 3 h under a N₂ atmosphere. The extra solvent was evaporated under vacuum and the residue was applied to a silica gel column eluted with was purified with a silica gel column using CH₂Cl₂ and 6 % methanol to afford the compound **4.42** as a white solid (55 mg, 92%). ¹H NMR (500 MHz): 1.13 (s, 3H), 1.12 (s, 3H), 1.65 (s, 3H), 1.86 (m, 1H), 1.91 (s, 3H), 2.16 (s, 3H), 2.17 (m, 1H), 2.38 (s, 3H), 2.46 (m, 1H), 2.55 (m, 1H), 2.62 (m, 2H), 2.74 (m, 2H), 3.80 (d, J = 7.5 Hz, 1H), 4.18 (AB, J = 7.0 Hz, 1H), 4.33 (dd, J = 9.0 Hz, 4.5 Hz, 1H), 4.99 (dd, J = 9.5 Hz, 9.5 Hz, 1H), 5.47 (d, J = 5.0 Hz), 5.63 (d, J = 7.5 Hz, 1H), 5.84 (d, J = 7.0 Hz, 1H), 6.07 (t, J = 9.0 Hz, 1H), 6.44 (s, 1H), 7.26 (m, 1H), 7.41-7.60 (m, 9H), 7.66 (m, 1H), 7.81 (m, 2H), 8.11 (m, 2H); Data were identical with those reported in the literature.³⁶

Synthesis of succinic acid, chloromethyl 2'-paclitaxel ester (4.43). A mixture of CH₂Cl₂ (2 mL) and 2 mL of aqueous solution containing compound **4.42** (20.8 mg, 0.022 mmol), NaHCO₃ (9 mg, 0.11 mmol), and tetrabutylammonium bisulfate (1 mg, 0.003 mmol) was stirred for 10 min at rt. Chloromethyl chlorosulfate (4.6 mg, 0.028 mmol) was added. The reaction mixture was vigorously stirred at rt for 2 h. The reaction mixture was diluted with 10 mL CH₂Cl₂, washed with brine (2 × 1 mL), dried over anhydrous Na₂SO₄, filtered, and evaporated under reduced pressure. The residue was separated by PTLC with

hexanes and EtOAc (1:2) as developing solvent to yield compound **4.43** (10 mg, 46% yield). ¹H NMR (500 MHz): 1.12 (s, 3H), 1.23 (s, 3H), 1.67 (s, 3H), 1.87 (m, 1H), 1.92 (s, 3H), 2.15 (m, 1H), 2.22 (s, 3H), 2.37 (m, 1H), 2.44 (s, 3H), 2.55 (m, 1H), 2.68 (m, 2H), 2.78 (m, 2H), 3.80 (d, J = 7.0 Hz, 1H), 4.19 (d, J = 8.5 Hz, 1H), 4.31 (d, J = 8.5 Hz, 1H), 4.43 (m, 1H), 4.96 (d, J = 7.5 Hz, 1H), 5.50 (d, J = 3.0 Hz), 5.57 (s, 2H), 5.68 (d, J = 7.0 Hz, 1H), 5.98 (dd, J = 6.5, 3.0 Hz, 1H), 6.23 (t, 9.0 Hz, 1H), 6.28 (s, 1H), 6.94 (d, J = 9.0 Hz, 1H), 7.34-7.45 (m, 7H), 7.52 (m, 3H), 7.60 (m, 1H), 7.77 (m, 2H), 8.14 (m, 2H); ¹³C NMR (126 MHz) δ 203.91, 171.37, 170.83, 170.38, 169.91, 169.17, 167.89, 167.16, 167.15, 153.29, 142.85, 138.91, 136.93, 133.79, 133.59, 132.85, 132.15, 130.33, 129.24, 129.21, 128.84, 128.80, 128.60, 127.28, 127.27, 126.59, 84.52, 81.15, 79.27, 77.30, 76.80, 75.68, 75.16, 74.45, 72.24, 72.00, 68.94, 62.97, 58.61, 52.74, 45.64, 43.25, 35.58, 29.09, 28.71, 26.89, 22.78, 22.20, 20.91, 14.91, 9.67; HRMS (ESI) calcd for C₅₂H₅₇ClNO₁₇ *m/z* 1002.3315 ([M + H]⁺), found *m/z* 1002.3276.

Synthesis of succinic acid, (5-(1,2-dithiolane-3-yl)pentanoyloxy)methyl 2'-paclitaxel ester (4.30). A mixture of **4.43** (10 mg, 0.01 mmol), lipoic acid (4.4 mg, 0.02 mmol), K₂CO₃ (4.4 mg, 0.03 mmol), 18-crown-6 (16.8 mg, 0.06 mmol) and NaI (cat.) was refluxed in benzene for 5 hr. The reaction mixture was diluted with ether (10 mL) and washed with water (2 × 1 mL) and brine (2 × 1 mL). The resulting crude product was purified by PTLC (1:2 hexanes:EtOAc) to give compound **4.30** as a white solid (7 mg, 60% yield). ¹H NMR (500 MHz): 1.12 (s, 3H), 1.23 (s, 3H), 1.40-1.50 (m, 2H), 1.64 (m, 2H), 1.67 (s, 3H), 1.87 (m, 1H), 1.92 (s, 3H), 2.15 (m, 1H), 2.22 (s, 3H), 2.30-2.40 (m, 3H), 2.44 (s, 3H), 2.45 (m, 2H), 2.55 (m, 1H), 2.68 (m, 2H), 2.78 (m, 2H), 3.06-3.18 (m,

2H), 3.54 (m, 1H), 3.80 (d, J = 7.0 Hz, 1H), 4.19 (d, J = 8.5 Hz, 1H), 4.31 (d, J = 8.5 Hz, 1H), 4.43 (m, 1H), 4.96 (d, J = 7.5 Hz, 1H) 5.50 (d, J = 3.0 Hz), 5.64 (m, 2H), 5.68 (d, J = 7.0 Hz, 1H), 5.98 (dd, J = 6.5, 3.0 Hz, 1H), 6.23 (t, 9.0 Hz, 1H) 6.28 (s, 1H), 6.98 (d, J = 9.0 Hz, 1H), 7.34-7.45 (m, 7H), 7.52 (m, 3H), 7.60 (m 1H), 7.77 (m, 2H), 8.14 (m, 2H); HRMS (ESI) calcd for C₆₀H₇₀NO₁₉S₂ *m/z* 1172.3983 ([M + H]⁺), found *m/z* 1172.3849.

Hydrolytic release of paclitaxel by compound 4.27 in buffer. Concentrations of **4.27** and paclitaxel were determined by quantitative HPLC with a Shimadzu SCL-10AVP system. Reverse phase C18 column was purchased from Phenomenex (Luna 5 μ C18 (2) 25 \times 4.6 mm). HPLC analyses were run with MeOH/water a linear gradient elution (50% MeOH \sim 100% MeOH in 20 min, followed by 100% MeOH for 10 min) with a flow rate of 1 mL/min. Fresh stock solution of **4.27** was prepared by dissolving 5.20 mg **4.27** into 25 mL methanol. To a small vial equipped with cap and magnetic stirring bar was charged 3 mL of the above solution. To this solution was added 1 mL 1 \times PBS buffer (pH = 7.4) quickly in one portion. 50 μ L of this solution was taken out immediately and injected immediately into the HPLC system. The vial was then capped and sealed well with parafilm. Aliquots (50 μ L) were continuously taken out at 30 min, 60 min, 120 min, 180 min, 240 min, 360 min, 540 min, 690 min and 1440 min, and were injected into the HPLC immediately after taken out from the vial. Concentrations of paclitaxel and **4.27** in each aliquot were determined based on previously prepared standard curves of paclitaxel and **4.27**.

References

1. Giannakakou, P.; Sackett, D. L.; Kang, Y.-K.; Zhang, Z.; Buters, J. T. M.; Fojo, T.; Poruchynsky, M. S. Paclitaxel-resistant Human Ovarian Cancer Cells Have Mutant β -Tubulins That Exhibit Impaired Paclitaxel-driven Polymerization. *J. Biol. Chem.* **1997**, *272*, 17118-17125.
2. Sharma, A.; Mayhew, E.; Bolcsak, L.; Cavanaugh, C.; Harmon, P.; Janoff, A.; Bernacki, R. J. Activity of Paclitaxel Liposome Formulations Against Human Ovarian Tumor Xenografts. *Int. J. Cancer* **1997**, *71*, 103-107.
3. Michaud, L. B.; Valero, V.; Hortobagyi, G. Risks and Benefits of Taxanes in Breast and Ovarian Cancer. *Drug Saf.* **2000**, *23*, 401-428.
4. de Groot, F. M. H.; van Berkom, L. W. A.; Scheeren, H. W. Synthesis and Biological Evaluation of 2'-Carbamate-Linked and 2'-Carbonate-Linked Prodrugs of Paclitaxel: Selective Activation by the Tumor-Associated Protease Plasmin. *J. Med. Chem.* **2000**, *43*, 3093-3102.
5. Damen, E. W. P.; Nevalainen, T. J.; van den Bergh, T. J. M.; de Groot, F. M. H.; Scheeren, H. W. Synthesis of Novel Paclitaxel Prodrugs Designed for Bioreductive Activation in Hypoxic Tumour Tissue. *Bioorg. Med. Chem. Lett.* **2002**, *10*, 71-77.
6. Vrudhula, V. M.; MacMaster, J. F.; Li, Z.; Kerr, D. E.; Senter, P. D. Reductively Activated Disulfide Prodrugs of Paclitaxel. *Bioorg. Med. Chem. Lett.* **2002**, *12*, 3591-3594.
7. Liu, C.; Strobl, J. S.; Bane, S.; Schilling, J. K.; McCracken, M.; Chatterjee, S. K.; Rahim-Bata, R.; Kingston, D. G. I. Design, Synthesis, and Bioactivities of Steroid-

- Linked Taxol Analogues as Potential Targeted Drugs for Prostate and Breast Cancer. *J. Nat. Prod.* **2003**, *67*, 152-159.
8. Park, W.-C.; Jordan, V. C. Selective Estrogen Receptor Modulators (SERMS) and Their Roles in Breast Cancer Prevention. *Trends Mol. Med.* **2002**, *8*, 82-88.
 9. Lee, J. W.; Lu, J. Y.; Low, P. S.; Fuchs, P. L. Synthesis and Evaluation of Taxol-Folic Acid Conjugates as Targeted Antineoplastics. *Bioorg. Med. Chem.* **2002**, *10*, 2397-2414.
 10. Wang, S.; Low, P. S. Folate-mediated Targeting of Antineoplastic Drugs, Imaging Agents, and Nucleic Acids to Cancer Cells. *J. Control. Release* **1998**, *53*, 39-48.
 11. Chen, X.; Plasencia, C.; Hou, Y.; Neamati, N. Synthesis and Biological Evaluation of Dimeric RGD Peptide-Paclitaxel Conjugate as a Model for Integrin-Targeted Drug Delivery. *J. Med. Chem.* **2005**, *48*, 1098-1106.
 12. Ryppa, C.; Mann-Steinberg, H.; Biniossek, M. L.; Satchi-Fainaro, R.; Kratz, F. In vitro and In vivo Evaluation of A Paclitaxel Conjugate with the Divalent Peptide E-[c(RGDfK)₂] that Targets Integrin $\alpha v \beta 3$. *Int. J. Pharm.* **2009**, *368*, 89-97.
 13. Bradley, M. O.; Swindell, C. S.; Anthony, F. H.; Witman, P. A.; Devanesan, P.; Webb, N. L.; Baker, S. D.; Wolff, A. C.; Donehower, R. C. Tumor Targeting by Conjugation of DHA to Paclitaxel. *J. Control. Release* **2001**, *74*, 233-236.
 14. Bradley, M. O.; Webb, N. L.; Anthony, F. H.; Devanesan, P.; Witman, P. A.; Hemamalini, S.; Chander, M. C.; Baker, S. D.; He, L.; Horwitz, S. B.; Swindell, C. S. Tumor Targeting by Covalent Conjugation of a Natural Fatty Acid to Paclitaxel. *Clin. Cancer Res.* **2001**, *7*, 3229-3238.

15. Lin, Y.-S.; Tungpradit, R.; Sinchaikul, S.; An, F.-M.; Liu, D.-Z.; Phutrakul, S.; Chen, S.-T. Targeting the Delivery of Glycan-Based Paclitaxel Prodrugs to Cancer Cells via Glucose Transporters. *J. Med. Chem.* **2008**, *51*, 7428-7441.
16. Nguyen, X. C.; Lee, W. W.; Chung, J. H.; Park, S. Y.; Sung, S. W.; Kim, Y. K.; So, Y.; Lee, D. S.; Chung, J. K.; Lee, M. C.; Kim, S. E. FDG Uptake, Glucose Transporter Type 1, and Ki-67 Expressions in Non-small-cell Lung Cancer: Correlations and Prognostic Values. *Eur. J. Radiol.* **2007**, *62*, 214-219.
17. Vrudhula, V. M.; Kerr, D.; Siemers, O.; Dubowchik, G. M.; Senter, P. D. Cephalosporin Prodrugs of Paclitaxel for Immunologically Specific Activation by L-49-sFv- β -Lactamase Fusion Protein. *Bioorg. Med. Chem. Lett.* **2003**, *13*, 539-542.
18. Bouvier, E.; Thiroit, S.; Schmidt, F.; Monneret, C. A New Paclitaxel Prodrug for use in ADEPT Strategy. *Org. Biomol. Chem.* **2003**, *1*, 3343-3352.
19. Ryu, B.-Y.; Sohn, J.-S.; Hess, M.; Choi, S.-K.; Choi, J.-K.; Jo, B.-W. Synthesis and Anti-cancer Efficacy of Rapid Hydrolysed Water-soluble Paclitaxel Pro-drugs. *J. Biomater. Sci., Polym. Ed.* **2008**, *19*, 311-324.
20. Kakinoki, A.; Kaneo, Y.; Tanaka, T.; Hosokawa, Y. Synthesis and Evaluation of Water-Soluble Poly(vinyl alcohol)-paclitaxel Conjugate as a Macromolecular Prodrug. *Biol. Pharm. Bull.* **2008**, *31*, 963-969.
21. Terwogt, J. M. M.; Huinink, W. W. T. B.; Schellens, J. H. M.; Schot, M.; Mandjes, I. A. M.; Zurio, M. G.; Rocchetti, M.; Rosing, H.; Koopman, F. J.; Beijnen, J. H. Phase I Clinical and Pharmacokinetic Study of PNU166945, a Novel Water-soluble Polymer-Conjugated Prodrug of Paclitaxel. *Anti-Cancer Drugs* **2001**, *12*, 315-323.

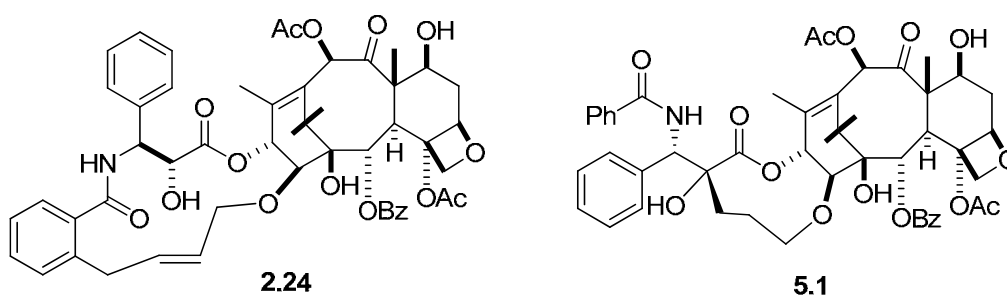
22. Erez, R.; Segal, E.; Miller, K.; Satchi-Fainaro, R.; Shabat, D. Enhanced Cytotoxicity of A Polymer-drug Conjugate with Triple Payload of Paclitaxel. *Bioorg. Med. Chem.* **2009**, *17*, 4327-4335.
23. Rihova, B.; Kubackova, K. Clinical Implications of N-(2-Hydroxypropyl)methacrylamide Copolymers. *Curr. Pharm. Biotechnol.* **2003**, *4*, 311-322.
24. Veronese, M. L.; Flaherty, K.; Kramer, A.; Konkle, B. A.; Morgan, M.; Stevenson, J. P.; O'Dwyer, P. J. Phase I Study of the Novel Taxane CT-2103 in Patients with Advanced Solid Tumors. *Cancer Chemother. Pharmacol.* **2005**, *55*, 497-501.
25. Singer, J. W. Paclitaxel Poliglumex (XYOTAX(TM), CT-2103): A Macromolecular Taxane. *J. Control. Release* **2005**, *109*, 120-126.
26. Luo, Y.; Ziebell, M. R.; Prestwich, G. D. A Hyaluronic Acid-Taxol Antitumor Bioconjugate Targeted to Cancer Cells. *Biomacromolecules* **2000**, *1*, 208-218.
27. Yeo, T.; Nagy, J.; Yeo, K.; Dvorak, H.; Toole, B. Increased Hyaluronan at Sites of Attachment to Mesentery by CD44- Positive Mouse Ovarian and Breast Tumor Cells. *Am. J. Pathol.* **1996**, *148*, 1733-1740.
28. Toole, B. P. Hyaluronan in Morphogenesis. *J. Intern. Med.* **1997**, *242*, 35-40.
29. Turley, E. A.; Belch, A. J.; Poppema, S.; Pilarsk, L. M. Expression and Function of a Receptor for Hyaluronan-Mediated Motility on Normal and Malignant B Lymphocytes *Blood* **1993** *81*, 446-453.
30. Lee, E.; Lee, J.; Lee, I.-H.; Yu, M.; Kim, H.; Chae, S. Y.; Jon, S. Conjugated Chitosan as a Novel Platform for Oral Delivery of Paclitaxel. *J. Med. Chem.* **2008**, *51*, 6442-6449.

31. Majoros, I. J.; Myc, A.; Thomas, T.; Mehta, C. B.; Baker, J. R. PAMAM Dendrimer-Based Multifunctional Conjugate for Cancer Therapy: Synthesis, Characterization, and Functionality. *Biomacromolecules* **2006**, *7*, 572-579.
32. Hwu, J. R.; Lin, Y. S.; Josephrajan, T.; Hsu, M.-H.; Cheng, F.-Y.; Yeh, C.-S.; Su, W.-C.; Shieh, D.-B. Targeted Paclitaxel by Conjugation to Iron Oxide and Gold Nanoparticles. *J. Am. Chem. Soc.* **2009**, *131*, 66-68.
33. Paciotti, G. F.; Kingston, D. G. I.; Tamarkin, L. Colloidal Gold Nanoparticles: A Novel Nanoparticle Platform for Developing Multifunctional Tumor-Targeted Drug Delivery Vectors. *Drug Dev. Res.* **2006**, *67*, 47-54.
34. Lee, K. H.; Chung, Y. J.; Kim, Y.-C.; Song, S. J. Anti-tumor Activity of Paclitaxel Prodrug Conjugated with Polyethylene Glycol. *Bull. Korean Chem. Soc.* **2005**, *26*, 1079-1082.
35. Senter, P. D.; Pearce, W. E.; Greenfield, R. S. Development of a Drug-release Strategy Based on the Reductive Fragmentation of Benzyl Carbamate Disulfides. *J. Org. Chem.* **1990**, *55*, 2975-2978.
36. Kabalka, G. W.; Baker, J. D.; Neal, G. W. Catecholborane (1,3,2-Benzodioxaborole). A Versatile Reducing Agent. *J. Org. Chem.* **1977**, *42*, 512-517.
37. Magri, N. F.; Kingston, D. G. I. Modified Taxols, 4. Synthesis and Biological Activity of Taxols Modified in the Side Chain. *J. Nat. Prod.* **1988**, *51*, 298-306.
38. Ebright, Y. W.; Chen, Y.; Kim, Y.; Ebright, R. H. S-[2-(4-Azidosalicylamido)ethylthio]-2-thiopyridine: Radioiodinatable, Cleavable, Photoactivatable Cross-Linking Agent. *Bioconjugate Chem.* **1996**, *7*, 380-384.

Chapter 5. Approaches to the Synthesis of a Conformationally Constrained Paclitaxel Analog

5.1 Introduction

As discussed in Chapter 2, T-taxol has been proposed as the bioactive conformation of paclitaxel on tubulin by Snyder and co-workers based on computational studies and data obtained from the electron density map of paclitaxel-bound tubulin from the electron crystallography studies.¹ The T-taxol model was supported experimentally by the REDOR-determined intramolecular distances^{2,3} and by the synthesis of constrained paclitaxel analogs which showed improved bioactivities compared to paclitaxel itself.⁴ However, there have been other opinions on the biological conformation of paclitaxel. A different conformation, namely the “REDOR-taxol” conformation, was proposed by the Ojima group⁵ in an effort to identify a bioactive paclitaxel geometry that is consistent with the interatomic distances determined by the first REDOR experiment.² The macrocyclic paclitaxel analog **2.24** was synthesized by the same group to mimic this conformation.⁵ However, the bridged compound proved to be less active than paclitaxel against all cancer cell lines tested.⁵



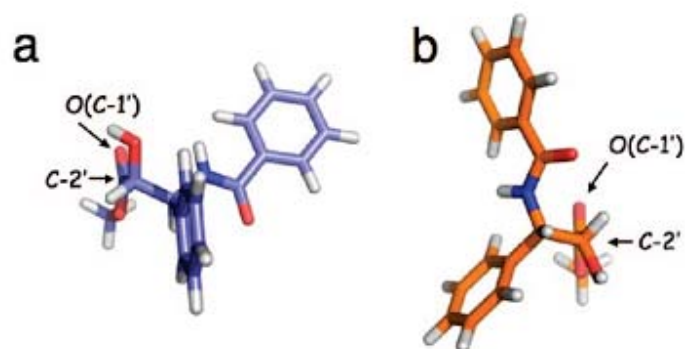


Figure 5.1 Comparison of the C-13 side chains of a) T-taxol and b) REDOR-taxol by looking down the C2'-C1' bonds⁶

The structural difference between T-taxol and REDOR-taxol resides mainly in the C-1' to C-3' region of the C-13 side chain.⁶ In REDOR-Taxol the 2'-hydroxyl group is H-bonded to His²²⁷, while in T-taxol similar bonding occurs with Arg³⁵⁹.⁵ The key differences of the C-13 side chains of T-taxol and REDOR-taxol can be illustrated by Figure 5.1. The two conformations differ by an approximate 165° rotation around the C2'-C1' bond. As a result, the C-13 terminal aromatic rings also participate in the change.⁶ Looking down the T-taxol C-2', C-1' bond in a Newman projection suggests that the C2'-OH and C1'=O have a gauche-like relationship. The C2'-OH and C1'=O bonds are gauche but linked by a hydrogen bond (Figure 5.1a). In the REDOR-taxol conformer, on the other hand, the C2'-OH and C1'=O groups are almost anti to one another. It has been pointed out by Snyder that this spatial arrangement incorporates a repulsive O---O interaction between the C2'-OH and ether oxygen of the ester group.⁶

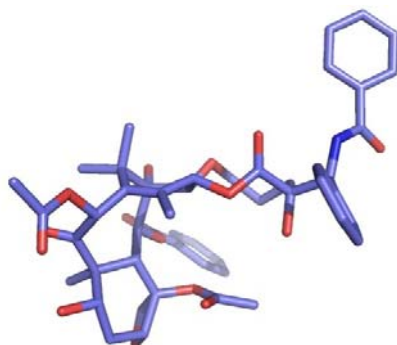
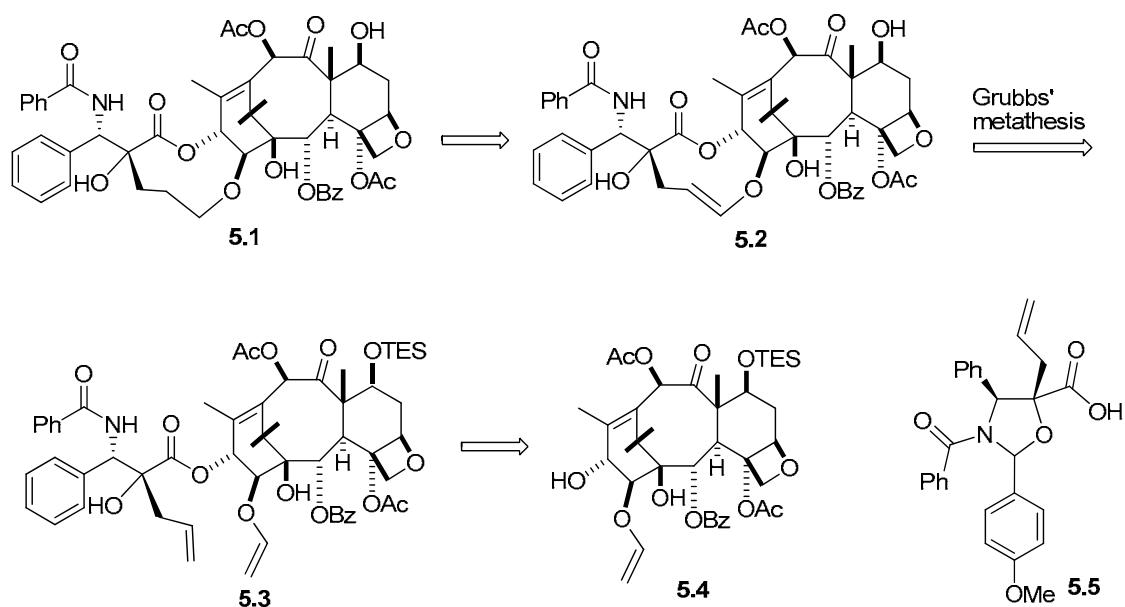


Figure 5.2 Optimized 3-D structure of analog **5.1**

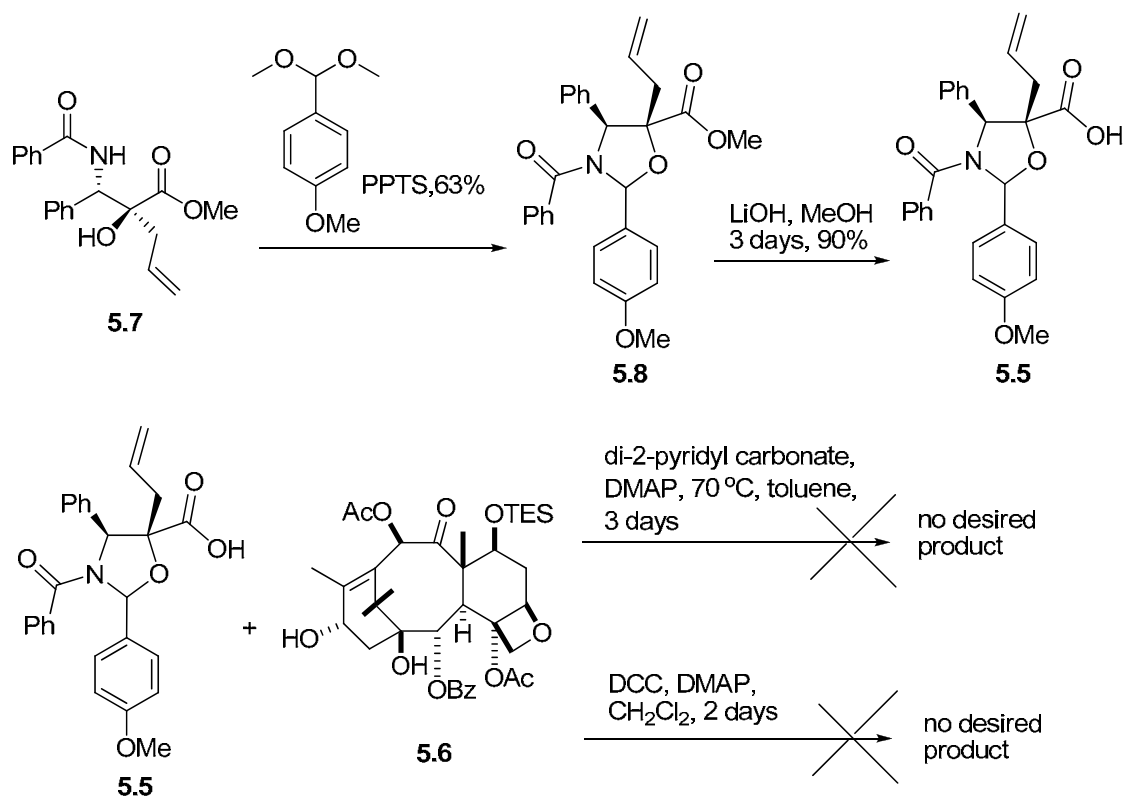
In a recent computer modeling study by our collaborators, the Snyder group at Emory University designed a macrocyclic paclitaxel analog **5.1** with a 4-membered bridge between C-2' and C-14. Computer modeling showed that the tether forces the paclitaxel molecule to adopt the REDOR-taxol conformation, where the C1'-O, C2'=O of the optimized structure are in an anti relationship (Figure 5.2). It was thus proposed that the synthesis and biological evaluation of the bridged analog **5.1** would provide a way of distinguishing between the T-taxol and REDOR-taxol structures. If the REDOR-taxol structure is correct, the bridged analog **5.1** should be at least as bioactive as its open-chain form **5.3**. If analog **5.1** is significantly less bioactive than **5.3**, then this would be strong evidence in support of the T-taxol conformation.



Scheme 5.1 Retrosynthesis of analog 5.1

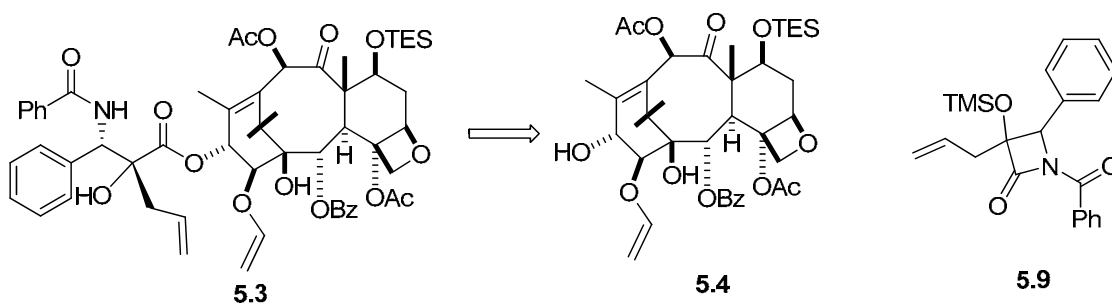
5.2 Synthesis of 5.1

The retrosynthesis of analog 5.1 is shown in Scheme 5.1. The bridge between C-2' and C-14 can be constructed by Grubbs' metathesis of the key intermediate 5.3 followed by hydrogenation. Compound 5.3 can be prepared from the 14 β -hydroxybaccatin III derivative 5.4 and side chain precursor 5.5.



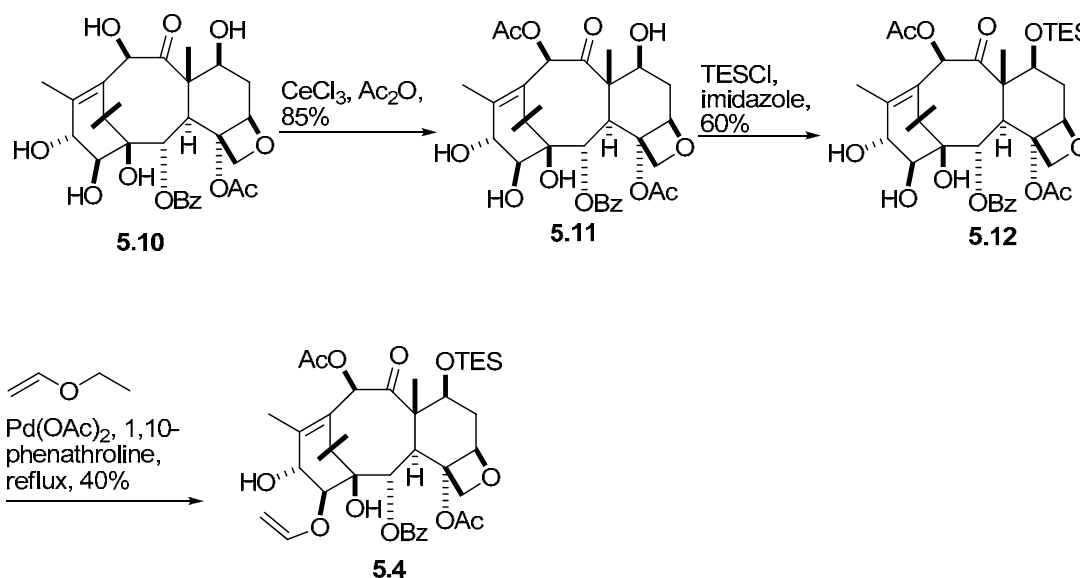
Scheme 5.2 Coupling of **5.5** and **5.6**

It was recognized that the coupling of intermediates **5.4** and **5.5** might be impeded by the steric bulk of both substrates. To test the plausibility of the proposed reaction route, a model reaction was performed by using racemic **5.5** and the known baccatin derivative **5.6**^{7,8} as model compounds. Side chain moiety **5.5** was synthesized from the known compound **5.7**⁹ in two steps with 57% yield. As feared, the esterification reaction between **5.5** and **5.6** could not be accomplished. Both the traditional dicyclohexylcarbodiimide-mediated reaction and the modified condition using di-2-pyridyl carbonate as the coupling reagent^{10,11} failed to produce any desired ester (Scheme 5.2).



Scheme 5.3 Modified retrosynthesis of **5.3**

The synthetic route for the preparation of the key intermediate **5.3** was thus modified as seen in Scheme 5.3, where the β -lactam derivative **5.9** was proposed as the side chain precursor, which can in principle be coupled with **5.4** in the presence of a strong base.

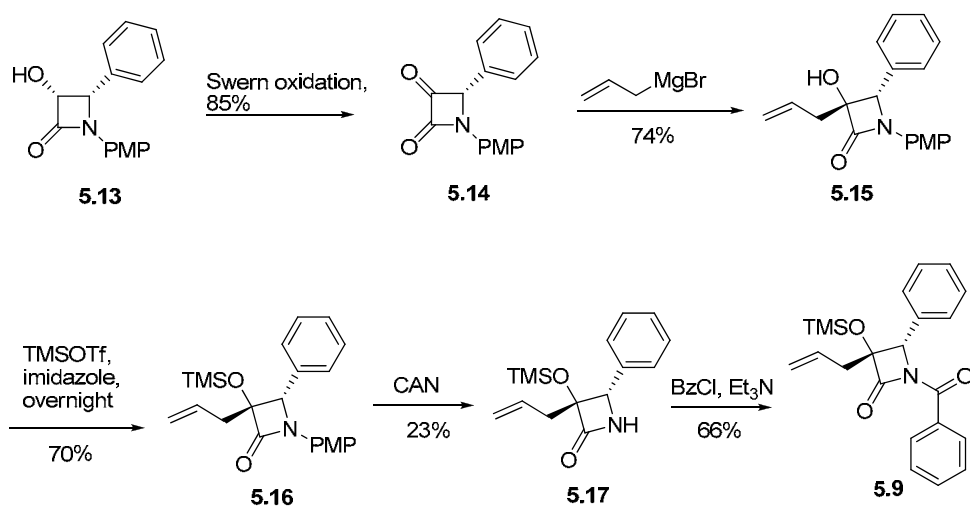


Scheme 5.4 Synthesis of compound **5.4**

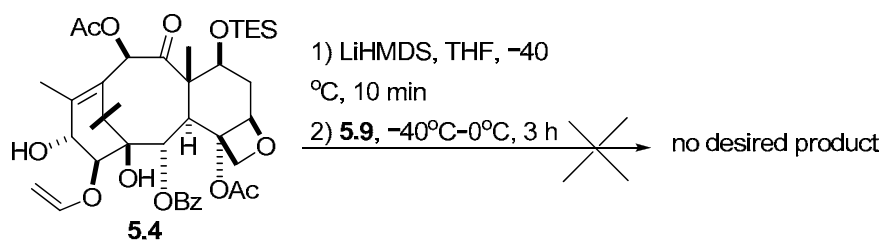
Compound **5.4** was prepared (scheme 5.4) by vinylation¹² of the C-14 hydroxyl group of the known 14 β -hydroxy-baccatin III derivative **5.12**, which was synthesized from 14 β -

hydroxy-10-deacetyl baccatin III (**5.10**) in 2 steps with procedures reported in the literature.¹³

Compound **5.9** can be synthesized from the optically pure, known β -lactam¹⁴ **5.13** in 5 straightforward steps (Scheme 5.5). Swern oxidation of **5.13** produced ketone **5.14**. The subsequent allylic addition to the ketone group took place from the opposite side of the large phenyl ring, leading to alcohol **5.15** with the desired stereochemistry. Silyl ether formation followed by oxidative deprotection of **5.15** produced compound **5.17**, which was acylated to yield the side chain precursor **5.9**. Disappointingly, attempts to couple **5.4** and **5.9** mediated by LiHMDS (Scheme 5.6) failed to generate the desired compound **5.3**.



Scheme 5.5 Synthesis of **5.9**



Scheme 5.6 Coupling of **5.4** with **5.9**

5.3 Conclusions

In order to synthesize the conformationally constrained paclitaxel analog **5.1** to mimic the REDOR-taxol conformation, two proposed synthetic routes were attempted for the preparation of the key intermediates **5.3**. However, both routes failed to yield the desired products under current reaction conditions (see experimental part for detail). The failure was conceivably due to the massive steric hindrance present in both the baccatin precursor and the side chain precursor. The C-13 hydroxyl group of baccatin III is known to be in a hindered environment since it is located on the concave face of the baccatin ring system. The chemical environment becomes even bulkier in our case with an extra vinyloxy substitution at the C-14 position. In addition, the reaction sites of the side chain precursors **5.5** and **5.9** are adjacent to quaternary carbons. The steric hindrance significantly lowers the possibility of successful coupling reactions.

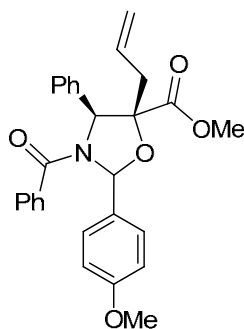
However, we believe that both of the synthetic routes are worthy of further optimization. More vigorous reaction conditions can be tried to overcome the steric hindrance. This project has recently been taken over by our collaborators, the Snyder group at Emory University.

5.4 Experimental Section

General experimental methods The following standard conditions apply unless otherwise stated. All reactions were performed under Ar or N₂ in oven-dried glassware using dry solvents and standard syringe techniques. Tetrahydrofuran (THF) was distilled from the sodium benzophenone ketyl radical ion. CH₂Cl₂ was distilled from CaH₂. All reagents were of commercial quality and used as received. After workup, partitioned

organic layers were washed with water and brine and dried over Na₂SO₄. Reaction progress was monitored using Al-backed thin layer chromatography (TLC) plates pre-coated with silica UV254. Purification of products by column chromatography was conducted using a column filled with silica gel 60 (220-240 mesh) using eluting solvent systems as indicated. Purification by preparative thin layer chromatography (PTLC) was performed using glass-backed plates pre-coated with silica UV254. ¹H and ¹³C NMR spectra were recorded on a 500 MHz (500 MHz for ¹H and 126 MHz for ¹³C) spectrometer. All chemical shifts (δ) were referenced to the solvent peaks of Chloroform-D (7.26 ppm for ¹H, 77.0 ppm for ¹³C). Optical rotation was measured on a polarimeter operating at the sodium D-line. 14-Hydroxy-10-deacetylbaccatin III was a generous gift of Dr. Giovanni Appendino, University of Turin, Italy.

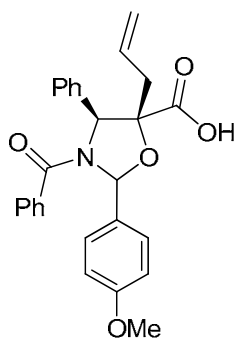
(±)-Methyl 5-allyl-3-benzoyl-2-(4-methoxyphenyl)-4-phenyloxazolidine-5-carboxylate (5.8).



To a solution of compound **5.7**⁹ (34 mg, 0.1 mmol) in toluene (1 mL) was added 4-methoxybenzaldehyde dimethyl acetal (36.4 mg, 0.2 mmol) and pyridinium *p*-toluenesulfonate (2.5 mg, 0.01 mmol) at rt. The mixture was stirred for 4 hours and water

was added. The solution was extracted three times with EtOAc. The organic layers were dried and concentrated. The crude product was purified with PTLC (1:3 EtOAc:hexanes) to yield compound **5.8** as a yellowish powder (29 mg, 63%). ^1H NMR (500 MHz) δ 7.64 (d, $J = 6.7$ Hz, 2H), 7.38 (t, $J = 6.9$ Hz, 1H), 7.34 – 7.16 (m, 7H), 7.07 (d, $J = 6.3$ Hz, 2H), 6.95 (d, $J = 8.4$ Hz, 2H), 6.82 (s, 1H), 5.62 (m, 1H), 5.21 (s, 1H), 4.99 (d, $J = 10.2$ Hz, 1H), 4.91 (d, $J = 17.1$ Hz, 1H), 3.85 (s, 3H), 3.80 (s, 3H), 2.16 (dd, $J = 14.1, 8.2$ Hz, 1H), 2.00 (dd, $J = 14.2, 6.2$ Hz, 1H); ^{13}C NMR (126 MHz) δ 172.64, 159.84, 137.45, 135.91, 130.96, 130.86, 129.78, 128.70, 128.64, 128.56, 128.36, 128.19, 127.50, 119.40, 113.65, 89.25, 88.91, 68.74, 55.39, 52.90, 39.08; HRMS (ESI) calcd for $\text{C}_{28}\text{H}_{28}\text{NO}_5$ m/z 458.1967 ($[\text{M} + \text{H}]^+$), found m/z 458.1917

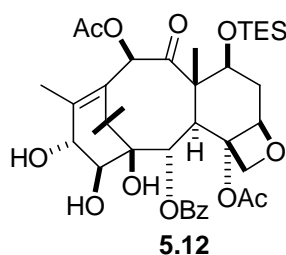
(±)-5-Allyl-3-benzoyl-2-(4-methoxyphenyl)-4-phenyloxazolidine-5-carboxylic acid (5.5).



To a solution of compound **5.8** (28 mg, 0.06 mmol) in methanol (2 mL) was added lithium hydroxide monohydrate (5.1 mg, 0.12 mmol) and the resulting suspension was stirred vigorously for 2 days. The reaction mixture was filtered and the filtrate was

concentrated in vacuo. The crude acid was used in the next step without further purification.

14 β -Hydroxy baccatin III (5.12).¹³

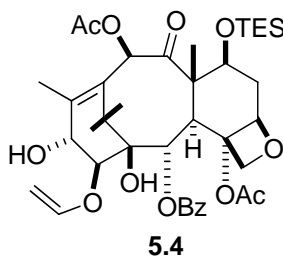


To a solution of 14-hydroxy-10-deacetyl baccatin III (158 mg, 0.282 mmol) in THF (6 mL) at rt was added anhydrous CeCl_3 (15 mg, 0.061 mmol). The resulting mixture was stirred for 5 min and acetic anhydride (0.5 mL, 5.30 mmol) was added. The resulting mixture was stirred for 4 h at rt. Saturated NaHCO_3 solution was added to quench the unreacted acetic anhydride. The resulting mixture was extracted with EtOAc (3×10 mL). The combined organic solution was washed, dried and concentrated under reduced pressure to give the crude product, which was purified with PTLC (3:2 EtOAc:hexanes) to yield **5.11** as a colorless powder (122 mg, 71%).

To a solution of **5.11** (120 mg, 0.199 mmol) in dry CH_2Cl_2 (5 mL) was added chlorotriethylsilane (67 μL , 0.39 mmol) and imidazole (54 mg, 0.796 mmol) at 0 °C. The resulting solution was warmed up to rt and stirred overnight. The reaction mixture was diluted with CH_2Cl_2 (50 mL) and washed with water (3×5 mL) and brine (2×3 mL). The organic solution was dried and concentrated under reduced pressure. The crude

product was purified by PTLC (1:1 EtOAc:hexanes) to yield compound **5.12** as a white powder (54.3 mg, 38%). ^1H NMR (500 MHz) δ 8.03 (d, $J = 7.2$ Hz, 2H), 7.55 (t, $J = 7.4$ Hz, 1H), 7.42 (t, $J = 7.8$ Hz, 2H), 6.43 (s, 1H), 5.78 (d, $J = 7.3$ Hz, 1H), 4.97 – 4.88 (m, 1H), 4.73 – 4.63 (m, 1H), 4.45 (dd, $J = 10.5, 6.7$ Hz, 1H), 4.25 (d, $J = 8.4$ Hz, 1H), 4.20 – 4.13 (m, 1H), 4.00 (t, $J = 9.1$ Hz, 1H), 3.80 (d, $J = 7.2$ Hz, 1H), 3.53 (s, 1H), 2.50 (ddd, $J = 14.3, 9.7, 6.7$ Hz, 1H), 2.28 (s, 3H), 2.17 (d, $J = 1.1$ Hz, 3H), 2.15 (s, 3H), 1.85 (ddd, $J = 10.7, 7.7, 2.0$ Hz, 1H), 1.67 (s, 3H), 1.22 (s, 3H), 1.02 (d, $J = 6.8$ Hz, 3H), 0.94 – 0.87 (m, 9H), 0.63 – 0.49 (m, 6H); ^{13}C NMR (126 MHz) δ 202.18, 170.50, 169.45, 166.52, 141.25, 133.69, 129.99, 129.49, 128.72, 84.20, 80.89, 76.85, 76.41, 76.02, 75.60, 74.38, 74.22, 72.30, 58.71, 46.47, 42.89, 37.20, 26.36, 22.45, 21.93, 20.97, 14.70, 10.10, 6.83, 6.82, 6.81, 5.33; HRMS (ESI) calcd for $\text{C}_{37}\text{H}_{53}\text{O}_{12}\text{Si}$ m/z 717.3306 ($[\text{M} + \text{H}]^+$), found m/z 717.3308. The above data are identical with those reported in the literature.¹³

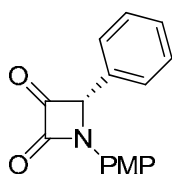
14 β -vinyloxy baccatin III (5.4).



A mixture of **5.12** (50 mg, 0.069 mmol), 1,10-phenanthroline-palladium acetate complex (2.5 mg), and ethyl vinyl ether (2 mL) was heated to reflux and stirred for 4 days. The reaction mixture was concentrated and the crude product was purified by PTLC

(hexanes:EtOAc, 1:1) to yield compound **5.4** as a white solid (21 mg, 40%). ¹H NMR (500 MHz) δ 8.06 (d, J = 7.9 Hz, 2H), 7.59 (t, J = 7.4 Hz, 1H), 7.46 (t, J = 7.8 Hz, 2H), 6.51 (dt, J = 18.7, 9.3 Hz, 1H), 6.43 (s, 1H), 5.81 (d, J = 7.3 Hz, 1H), 4.95 (d, J = 9.4 Hz, 1H), 4.78 (d, J = 6.4 Hz, 1H), 4.45 (m, 2H), 4.27 (d, J = 8.4 Hz, 1H), 4.18 (d, J = 8.5 Hz, 1H), 4.16 – 4.12 (m, 2H), 3.76 (d, J = 7.2 Hz, 1H), 3.39 (s, 1H), 2.56 – 2.46 (m, 1H), 2.20 (d, J = 3.2 Hz, 1H), 2.17 (s, 3H), 2.13 (s, 3H), 1.90 – 1.84 (m, 1H), 1.69 (s, 3H), 1.09 (s, 3H), 0.94 – 0.84 (m, 9H), 0.62 – 0.50 (m, 6H); ¹³C NMR (126 MHz) δ 201.52, 170.16, 169.39, 166.34, 153.09, 139.70, 134.66, 133.70, 130.01, 129.51, 128.79, 128.40, 89.61, 85.05, 84.13, 80.92, 76.57, 76.36, 75.24, 74.21, 72.72, 72.26, 60.50, 58.69, 46.43, 43.00, 37.21, 29.78, 26.43, 22.44, 21.93, 21.14, 20.97, 14.82, 14.28, 10.07, 6.82, 5.36, 5.34, 0.08; HRMS (ESI) calcd for C₃₉H₅₅O₁₂Si m/z 743.3463 ([M + H]⁺), found m/z 743.3457

(S)-1-(4-Methoxyphenyl)-4-phenylazetidine-2,3-dione (5.14).

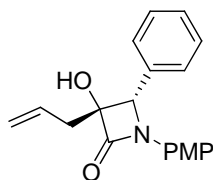


5.14

Compound **5.13**¹⁴ (1.76 g, 6.54 mmol) was dissolved in a 1:1 mixture of CH₂Cl₂ and DMSO (35 mL). To the solution at 0 °C was added triethylamine (4.5 mL, 32.7 mmol) and then sulfur trioxide pyridine complex (5.2 g, 32.7 mmol). The resulting solution was stirred for 2 hours at 0 °C. EtOAc (100 mL) was added to dilute the reaction mixture. The organic solution was washed with water and brine, dried and concentrated under reduced

pressure. The crude product was purified by PTLC (1:2 EtOAc:hexanes) to yield compound **5.14** as a yellowish powder (1.5 g, 85%). ¹H NMR (500 MHz) δ 7.49 – 7.42 (m, 3H), 7.43 – 7.36 (m, 3H), 7.34 – 7.28 (m, 2H), 6.88 (d, J = 9.1 Hz, 2H), 5.55 (s, 1H), 3.78 (s, 3H); ¹³C NMR (126 MHz) δ 190.70, 160.08, 158.07, 131.80, 130.02, 129.59, 129.51, 126.43, 119.83, 114.84, 74.98, 55.59; HRMS (ESI) calcd for C₁₆H₁₄NO₃ m/z 268.0974 ([M + H]⁺), found m/z 268.1818

(3R,4S)-3-Allyl-3-hydroxy-1-(4-methoxyphenyl)-4-phenylazetidin-2-one (5.15).

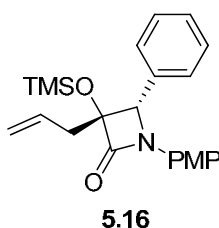


5.15

To a solution of **5.14** (267 mg, 1 mmol) in THF (8 mL) was added 1M solution of allylmagnesium bromide in THF (1 mL, 1 mmol) slowly at -40 °C. The resulting solution was stirred for 1 hour at -40 °C and brought to rt. The reaction was quenched by adding aqueous ammonium chloride solution and the mixture was extracted with EtOAc (30 mL \times 3). The organic solution was washed, dried and concentrated and the crude product was purified to yield compound **5.15** as a yellowish solid (229 mg, 74%). ¹H NMR (500 MHz) δ 7.43 – 7.35 (m, 3H), 7.29 – 7.25 (m, 4H), 6.82 – 6.79 (m, 2H), 5.98 (ddt, J = 17.1, 10.1, 7.2 Hz, 1H), 5.33 (d, J = 17.1 Hz, 1H), 5.29 (d, J = 10.1 Hz, 1H), 5.05 (s, 1H), 3.75 (s, 3H), 2.83 (dd, J = 14.2, 6.8 Hz, 1H), 2.71 (dd, J = 14.1, 7.7 Hz, 1H); ¹³C NMR (126 MHz) δ 156.46, 133.82, 131.63, 130.60, 129.18, 128.85, 127.40, 120.39, 119.00,

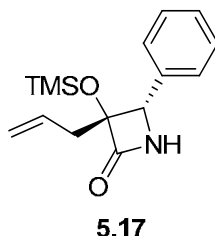
114.46, 114.40, 85.30, 66.62, 55.55, 39.91; HRMS (ESI) calcd for C₁₉H₂₀NO₃ *m/z* 310.1443 ([M + H]⁺), found *m/z* 310.1419

(3*R*,4*S*)-3-Allyl-1-(4-methoxyphenyl)-4-phenyl-3-(trimethylsilyloxy)azetidin-2-one
(5.16).



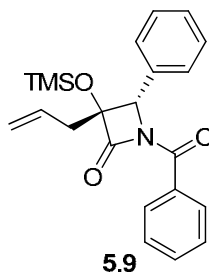
To a solution of **5.16** (309 mg, 1 mmol) in dry CH₂Cl₂ (5 mL) at 0 °C was added imidazole (408 mg, 6.0 mmol) and trimethylsilyl trifluoromethanesulfonate (0.6 mL, 3 mmol). The resulting mixture was stirred for 15 min at 0 °C before the addition of aqueous ammonium chloride (10 mL). The mixture was extracted with CH₂Cl₂ (20 mL × 3). The combined organic solution was washed, dried and concentrated under reduced pressure. The residue was purified by silica gel column (1:6 EtOAc:hexanes) to yield compound **5.16** as a colorless solid (220 mg, 58%). ¹H NMR (500 MHz) δ 7.35 – 7.28 (m, 5H), 7.22 – 7.15 (m, 2H), 6.85 – 6.75 (m, 2H), 6.00 – 5.83 (m, 1H), 5.27 (m, 1H), 5.24 – 5.19 (m, 1H), 4.94 (s, 1H), 3.75 (s, 3H), 2.73 (ddd, *J* = 14.1, 6.6, 1.0 Hz, 1H), 2.64 (ddd, *J* = 14.1, 7.6, 0.9 Hz, 1H); ¹³C NMR (126 MHz) δ 166.79, 156.32, 134.89, 132.37, 131.04, 128.19, 127.94, 127.77, 119.44, 118.87, 114.41, 87.37, 66.39, 55.55, 41.46, 29.79, 1.18, 1.11; HRMS (ESI) calcd for C₂₂H₂₇NO₃Si *m/z* 382.1838 ([M + H]⁺), found *m/z* 382.1818.

(3*R*,4*S*)-3-Allyl-4-phenyl-3-(trimethylsilyloxy)azetidin-2-one (5.17).



To a stirred solution of **5.16** (34 mg, 0.1 mmol) in CH₃CN (3 mL) and water (0.5 mL) at -5 °C was added a solution of cerium ammonium nitrate (164 mg, 0.3 mmol) in water (3 mL) dropwise. The resulting orange solution was stirred for 1 hour at -5 °C. The reaction mixture was treated with excess aqueous Na₂SO₃ and stirred for an additional 1 hour. The resulting solution was extracted with EtOAc (10 mL × 5). The combined organic solution was washed, dried and concentrated to give the crude product, which was purified by PTLC (1:2 EtOAc:hexanes) to yield compound **5.17** as a yellowish solid (6.3 mg, 23%). ¹H NMR (500 MHz) δ 7.38 – 7.31 (m, 2H), 7.31 – 7.26 (m, 1H), 7.24 – 7.19 (m, 2H), 6.24 (s, 1H), 6.00 – 5.88 (m, 1H), 5.31 – 5.20 (m, 2H), 4.62 (s, 1H), 2.74 – 2.56 (m, 2H), -0.06 (s, 9H); ¹³C NMR (126 MHz) δ 170.70, 136.96, 132.52, 128.05, 127.78, 127.35, 119.25, 89.52, 62.72, 41.48, 1.13; HRMS (ESI) calcd for C₁₅H₂₂NO₂Si *m/z* 276.1420 ([M + H]⁺), found *m/z* 276.1414

(3*R*,4*S*)-3-allyl-1-benzoyl-4-phenyl-3-(trimethylsilyloxy)azetidin-2-one (5.9).



To a solution of **5.17** (30 mg, 0.109 mmol) in dry CH₂Cl₂ (3 mL) at 0 °C was added benzoyl chloride (38 μL, 0.327 mmol), triethylamine (45.5 μL, 0.327 mmol) and 4-dimethylaminopyridine (5 mg, 0.041 mmol). The reaction mixture was stirred for 2 hours at 0 °C and then diluted with CH₂Cl₂ (30 mL). The resulting solution was washed with saturated aqueous NaHCO₃ solution, water and brine and concentrated under reduced pressure. The residue was purified by PTLC (1:4 EtOAc:hexanes) to yield compound **5.9** as a white solid (27 mg, 65%). ¹H NMR (500 MHz) δ 8.06 – 8.02 (m, 2H), 7.65 – 7.58 (m, 1H), 7.55 – 7.47 (m, 2H), 7.38 – 7.31 (m, 2H), 7.32 – 7.27 (m, 1H), 7.24 – 7.20 (m, 2H), 5.97 – 5.84 (m, 1H), 5.35 – 5.25 (m, 3H), 2.72 (dd, *J* = 14.0, 6.4 Hz, 1H), 2.63 (dd, *J* = 14.0, 7.9 Hz, 1H), -0.01 (s, 8H); ¹³C NMR (126 MHz) δ 166.81, 166.61, 134.43, 133.61, 132.20, 131.15, 130.04, 128.35, 128.16, 127.95, 127.28, 120.46, 86.18, 64.40, 41.57, 1.17, 1.17, 1.16, 1.15; HRMS (ESI) calcd for C₂₂H₂₆NO₃Si *m/z* 380.1682 ([M + H]⁺), found *m/z* 380.1676

References

1. Snyder, J. P.; Nettles, J. H.; Cornett, B.; Downing, K. H.; Nogales, E. The Binding Conformation of Taxol in Beta Tubulin: A Model Based on the Electron Crystallographic Density. *Proc. Natl. Acad. Sci. USA* **2001**, *98*, 5312-5316.
2. Li, Y.; Poliks, B.; Cegelski, L.; Poliks, M.; Cryczynski, Z.; Piszczek, G.; Jagtap, P., G.; Studelska, D. R.; Kingston, D. G. I.; Schaefer, J.; Bane, S. Conformation of Microtubule-Bound Paclitaxel Determined by Fluorescence Spectroscopy and REDOR NMR. *Biochemistry* **2000**, *39*, 281-291.
3. Paik, Y.; Yang, C.; Metaferia, B.; Tang, S.; Bane, S.; Ravindra, R.; Shanker, N.; Alcaraz, A. A.; Johnson, S. A.; Schaefer, J.; O'Connor, R. D.; Cegelski, L.; Snyder, J. P.; Kingston, D. G. I. Rotational-echo Double-resonance NMR Distance Measurements for the Tubulin-bound Paclitaxel Conformation. *J. Am. Chem. Soc.* **2007**, *129*, 361-370.
4. Ganesh, T.; Guza, R. C.; Bane, S.; Ravindra, R.; Shanker, N.; Lakdawala, A. S.; Snyder, J. P.; Kingston, D. G. I. The Bioactive Taxol conformation of β -tubulin: Experimental Evidence from Highly Active Constrained Analogs. *Proc. Natl. Acad. Sci. USA* **2004**, *101*, 10006-10011.
5. Geney, R.; Sun, L.; Pera, P.; Bernacki, R. J.; Xia, S.; Horwitz, S. B.; Simmerling, C. L.; Ojima, I. Use of the Tubulin Bound Paclitaxel Conformation for Structure-Based Rational Drug Design. *Chem. Biol.* **2005**, *12*, 339-348.
6. Yang, Y.; Alcaraz, A. A.; Snyder, J. P. The Tubulin-Bound Conformation of Paclitaxel: T-Taxol vs "PTX-NY". *J. Nat. Prod.* **2009**, *72*, 422-429.

7. Georg, G. I.; Harriman, G. C. B.; Hepperle, M.; Clowers, J. S.; Vander Velde, D. G.; Himes, R. H. Synthesis, Conformational Analysis, and Biological Evaluation of Heteroaromatic Taxanes. *J. Org. Chem.* **1996**, *61*, 2664-2676.
8. Damen, E. W. P.; Braamer, L.; Scheeren, H. W. Lanthanide Trifluoromethanesulfonate Catalysed Selective Acylation of 10-Deacetylbaaccatin III. *Tetrahedron Lett.* **1998**, *39*, 6081-6082.
9. Nocioni, A. M.; Papa, C.; Tomasini, C. A facile and stereocontrolled synthesis of syn- α -alkyl α -hydroxy β -amino acids. *Tetrahedron Lett.* **1999**, *40*, 8453-8456.
10. Kim, S.; Jae, I. L.; Young, K. K. Di-2-pyridyl Carbonate: a New Efficient Coupling Agent for the Direct Esterification of Carboxylic Acids. *Tetrahedron Lett.* **1984**, *25*, 4943-4946.
11. Denis, J.-N.; Greene, A. E.; Guenard, D.; Gueritte-Voegelein, F.; Mangatal, L.; Potier, P. A Highly Efficient, Practical Approach to Natural Taxol. *J. Am. Chem. Soc.* **1988**, *110*, 5917-5919.
12. Weintraub, P. M.; King, C.-H. R. Syntheses of Steroidal Vinyl Ethers Using Palladium Acetate-Phenanthroline as Catalyst. *J. Org. Chem.* **1997**, *62*, 1560-1562.
13. Barboni, L.; Giarlo, G.; Ballini, R.; Fontana, G. 14 β -Hydroxy-10-deacetylbaaccatin III As a Convenient, Alternative Substrate for the Improved Synthesis of Methoxylated Second-generation Taxanes. *Bioorg. Med. Chem. Lett.* **2006**, *16*, 5389-5391.
14. Brieva, R.; Crich, J. Z.; Sih, C. J. Chemoenzymic Synthesis of the C-13 Side Chain of Taxol: Optically Active 3-Hydroxy-4-phenyl β -Lactam Derivatives. *J. Org. Chem.* **1993**, *58*, 1068-1075.

APPENDIX

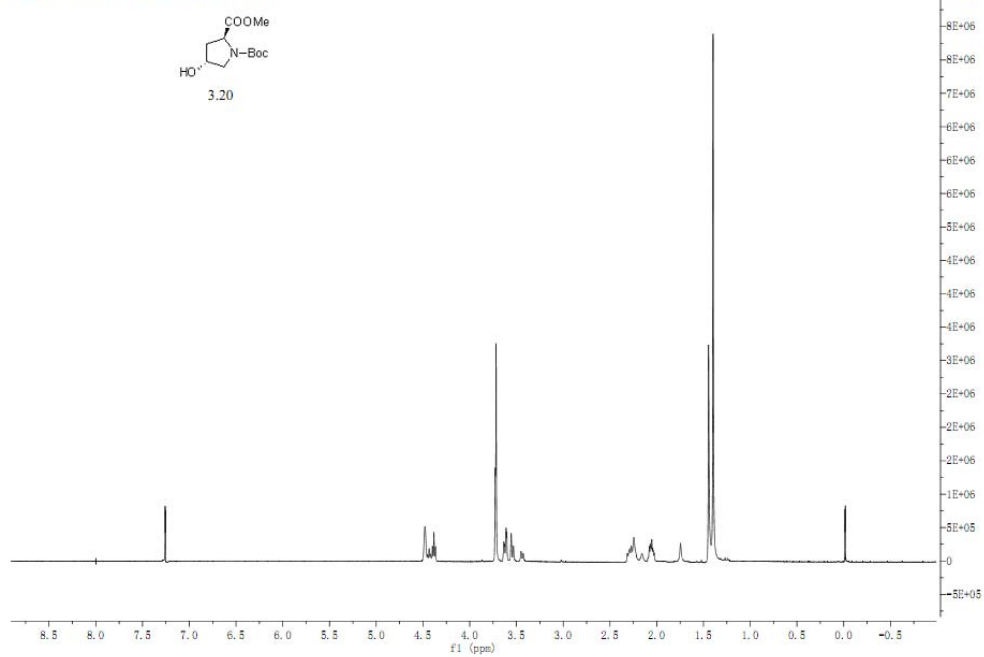
(NMR spectra of compounds)

^1H NMR and ^{13}C NMR spectra of 3.20	175
^1H NMR and ^{13}C NMR spectra of 3.21	176
^1H NMR and ^{13}C NMR spectra of 3.22	177
^1H NMR and ^{13}C NMR spectra of 3.24	178
^1H NMR and ^{13}C NMR spectra of 3.25	179
^1H NMR and ^{13}C NMR spectra of 3.18	180
^1H NMR and ^{13}C NMR spectra of 3.19	181
^1H NMR and ^{13}C NMR spectra of 3.29	182
^1H NMR and ^{13}C NMR spectra of 3.31	183
^1H NMR and ^{13}C NMR spectra of 3.32	184
^1H NMR and ^{13}C NMR spectra of 3.33	185
^1H NMR and ^{13}C NMR spectra of 3.34	186
^1H NMR and ^{13}C NMR spectra of 3.39	187
^1H NMR and ^{13}C NMR spectra of 3.38	188
^1H NMR and ^{13}C NMR spectra of 3.40	189
^1H NMR and ^{13}C NMR spectra of 3.42	190
^1H NMR and ^{13}C NMR spectra of 3.41	191
^1H NMR and ^{13}C NMR spectra of 3.43	192
^1H NMR and ^{13}C NMR spectra of 3.44	193
^1H NMR and ^{13}C NMR spectra of 3.45	194
^1H NMR and ^{13}C NMR spectra of 3.46	195

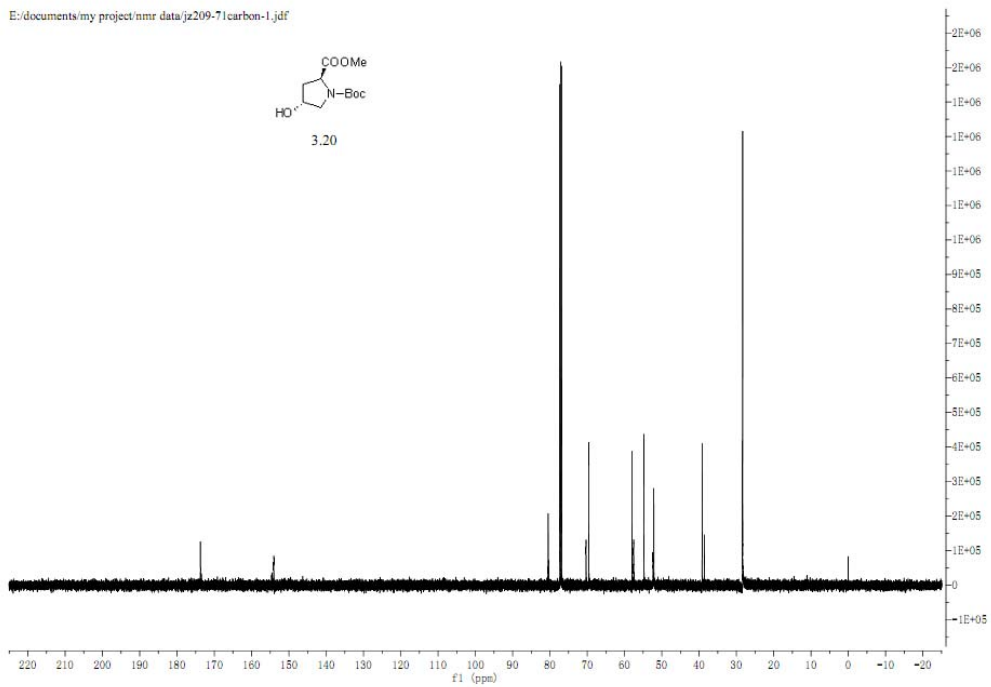
^1H NMR and ^{13}C NMR spectra of 3.53	196
^1H NMR and ^{13}C NMR spectra of 3.47	197
^1H NMR and ^{13}C NMR spectra of 3.50	198
^1H NMR and ^{13}C NMR spectra of 3.48	199
^1H NMR and ^{13}C NMR spectra of 3.51	200
^1H NMR spectrum of 3.49	201
^1H NMR spectrum of 3.52	201
^1H NMR and ^{13}C NMR spectra of 3.56	202
^1H NMR and ^{13}C NMR spectra of 3.57	203
^1H NMR and ^{13}C NMR spectra of 3.54	204
^1H NMR and ^{13}C NMR spectra of 3.55	205
^1H NMR spectrum of 4.34	206
^1H NMR and ^{13}C NMR spectra of 4.35	207
^1H NMR spectrum of 4.26	208
^1H NMR and ^{13}C NMR spectra of 4.27	209
^1H NMR and ^{13}C NMR spectra of 4.38	210
^1H NMR and ^{13}C NMR spectra of 4.39	211
^1H NMR and ^{13}C NMR spectra of 4.28	212
^1H NMR and ^{13}C NMR spectra of 4.41	213
^1H NMR and ^{13}C NMR spectra of 4.29	214
^1H NMR and ^{13}C NMR spectra of 4.43	215
^1H NMR spectrum of 4.30	216
^1H NMR and ^{13}C NMR spectra of 5.8	217

^1H NMR and ^{13}C NMR spectra of 5.12	218
^1H NMR and ^{13}C NMR spectra of 5.4	219
^1H NMR and ^{13}C NMR spectra of 5.14	220
^1H NMR and ^{13}C NMR spectra of 5.15	221
^1H NMR and ^{13}C NMR spectra of 5.16	222
^1H NMR and ^{13}C NMR spectra of 5.17	223
^1H NMR and ^{13}C NMR spectra of 5.9	224

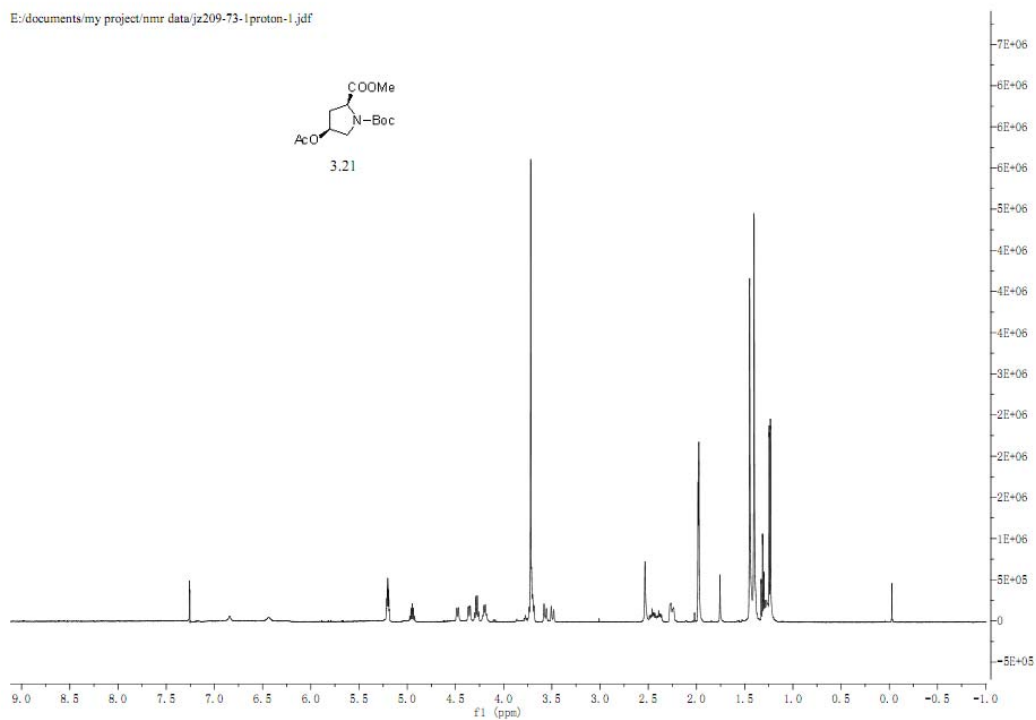
E:/documents/my project/nmr data/jz209-71proton-1.jdf



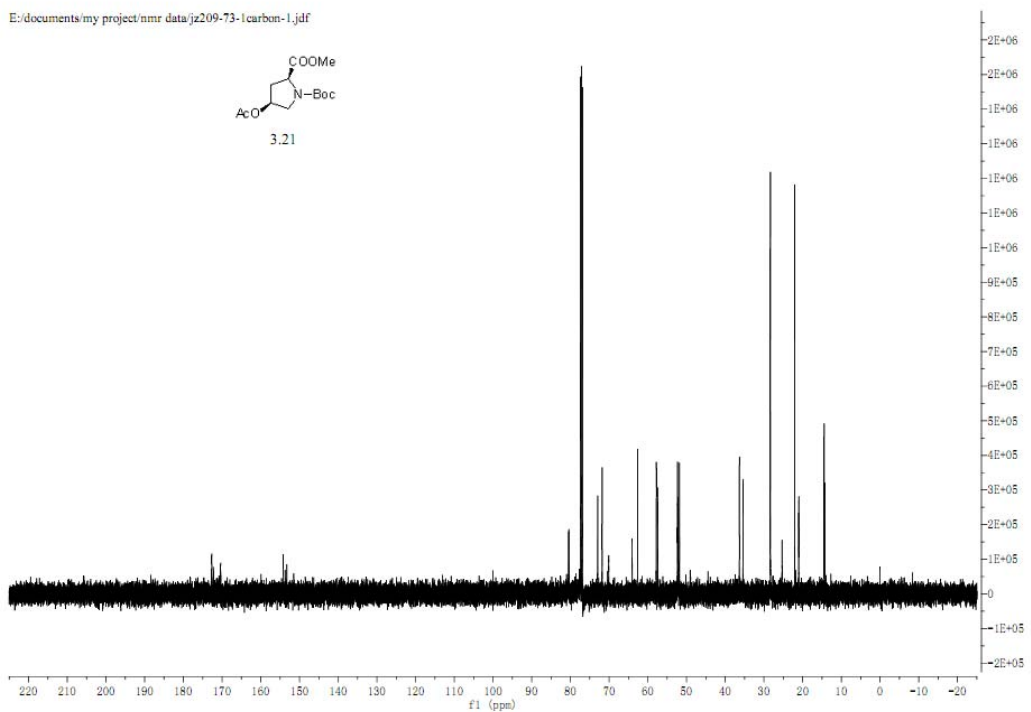
E:/documents/my project/nmr data/jz209-71carbon-1.jdf



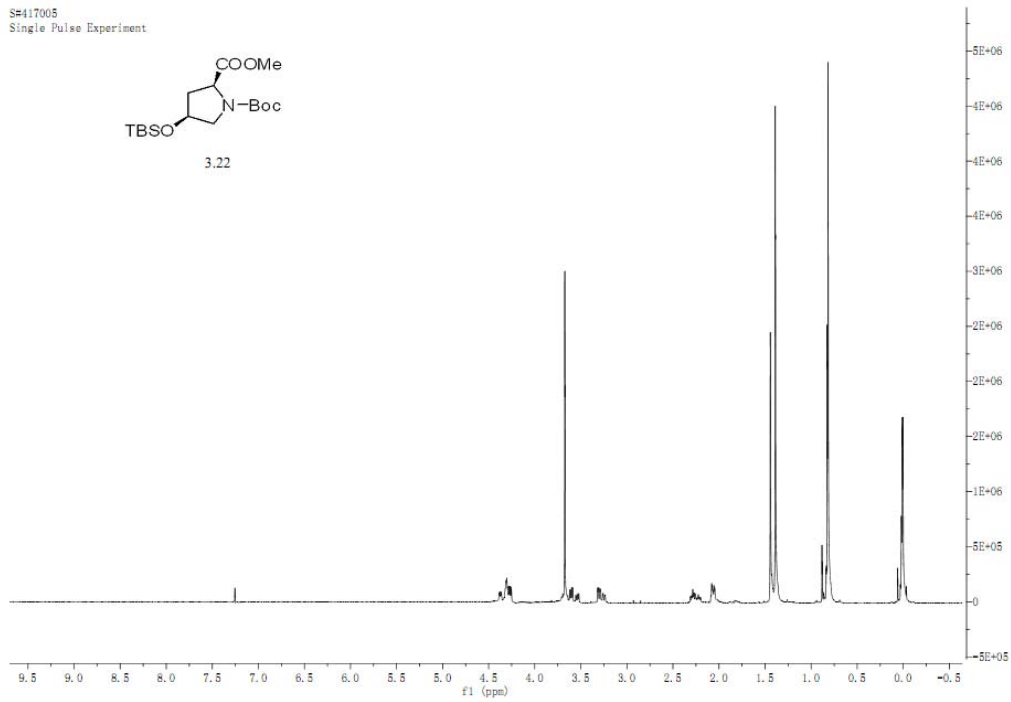
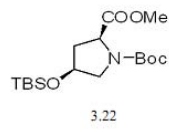
E:/documents/my project/nmr data/jz209-73-1proton-1.jdf



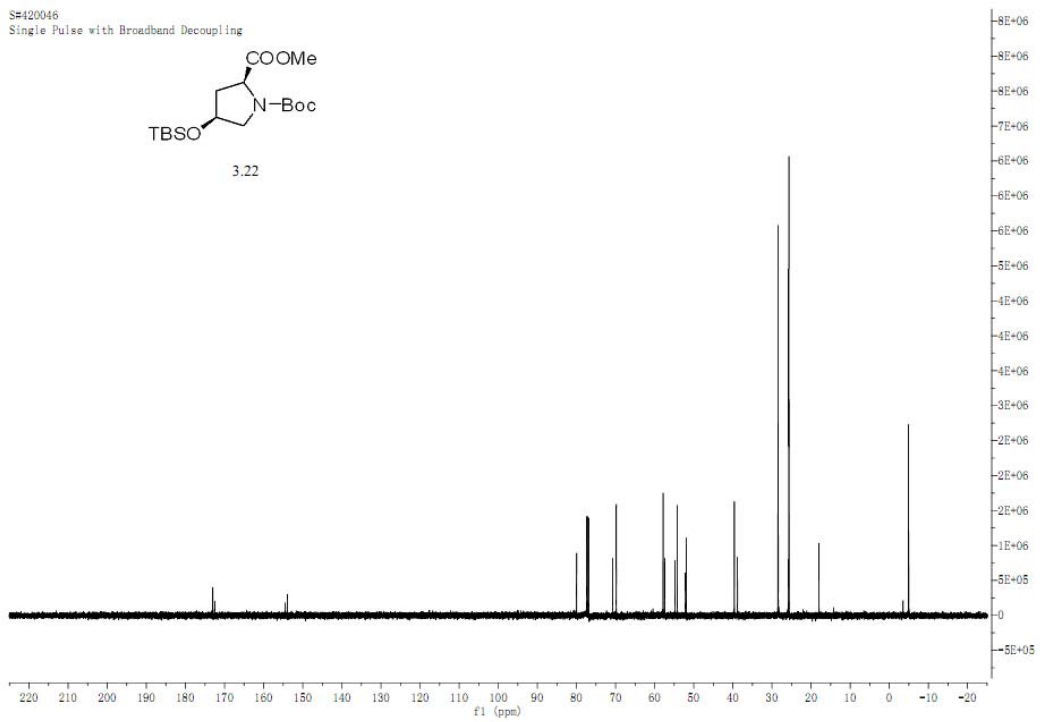
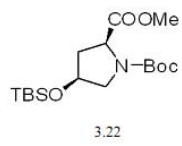
E:/documents/my project/nmr data/jz209-73-1carbon-1.jdf



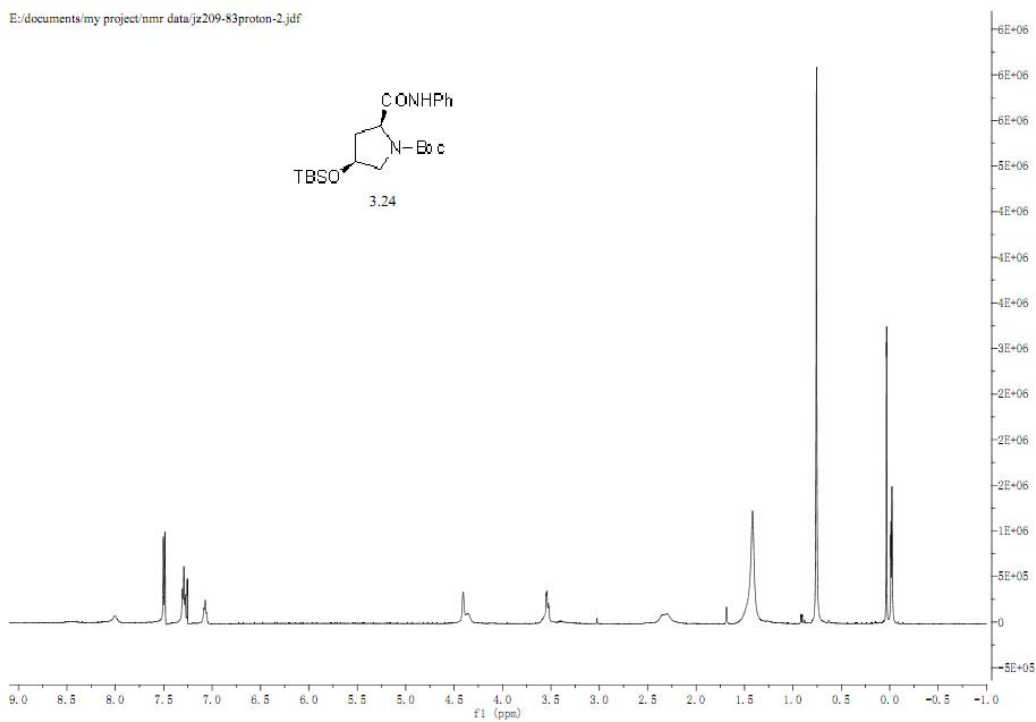
S#417005
Single Pulse Experiment



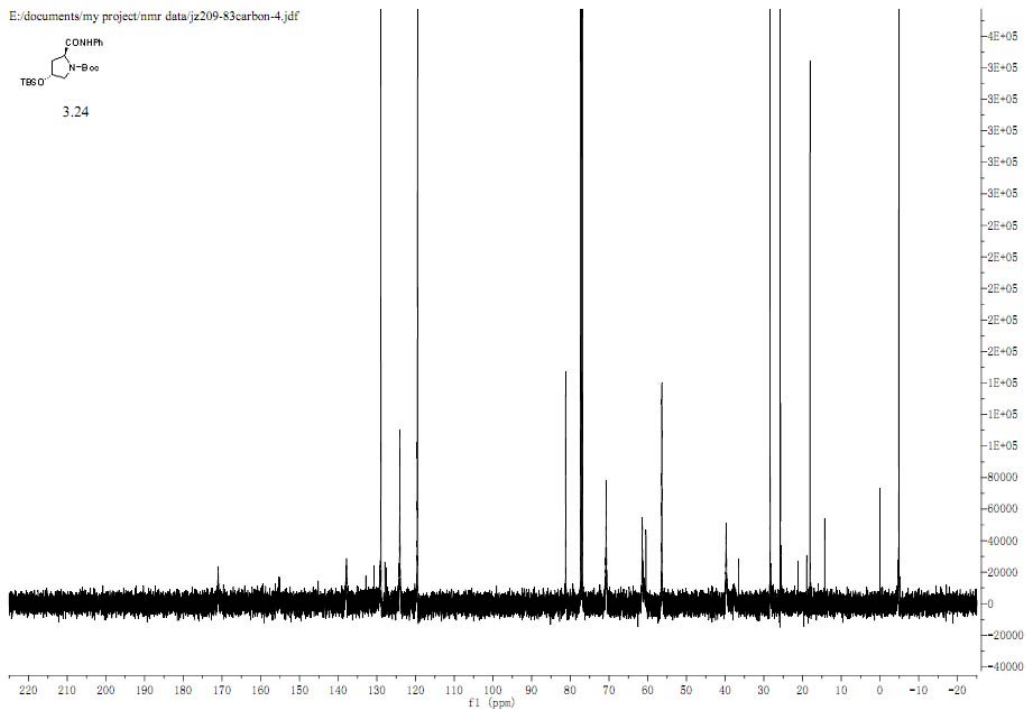
S#420046
Single Pulse with Broadband Decoupling



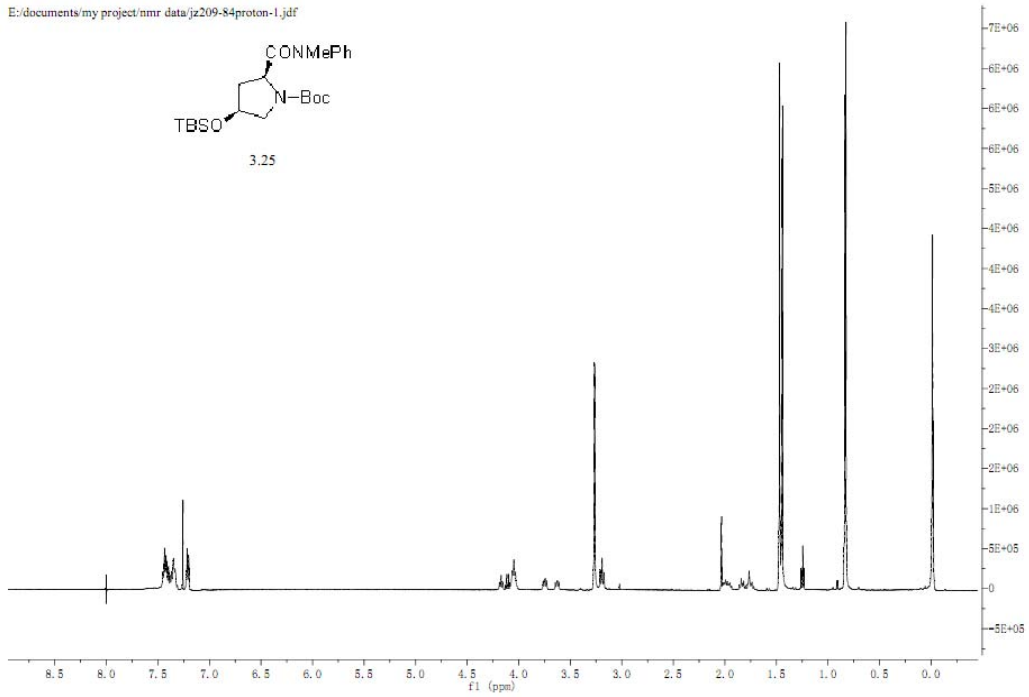
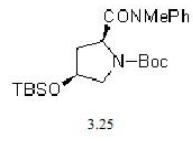
E:/documents/my project/nmr data/jz209-83proton-2.jdf



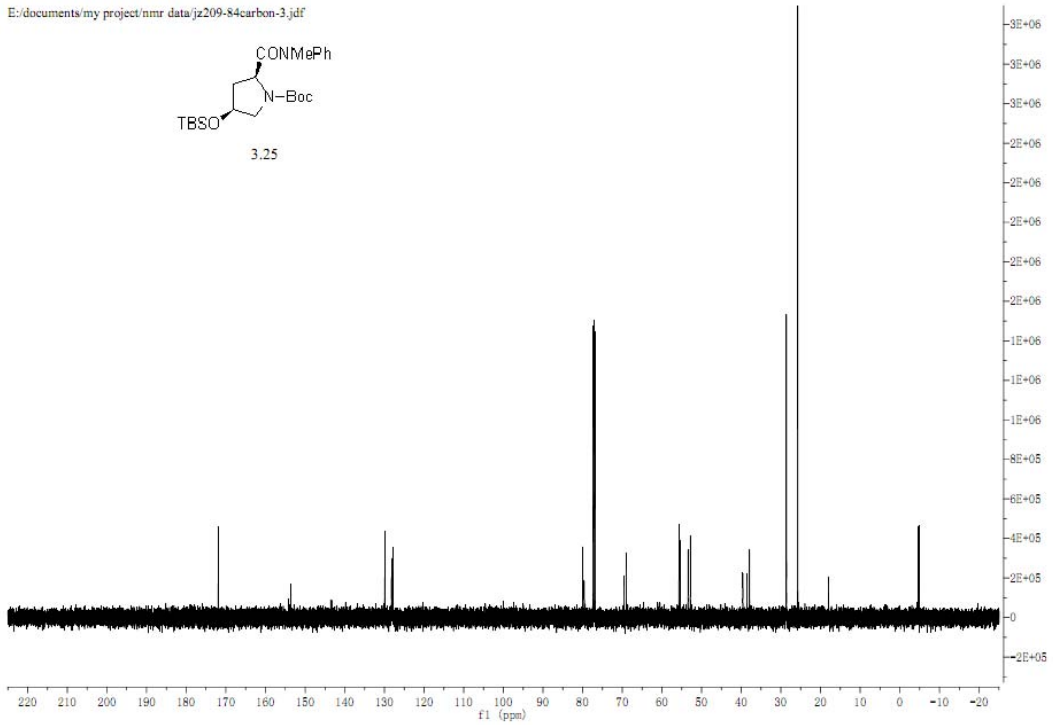
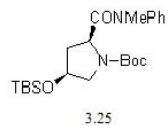
E:/documents/my project/nmr data/jz209-83carbon-4.jdf



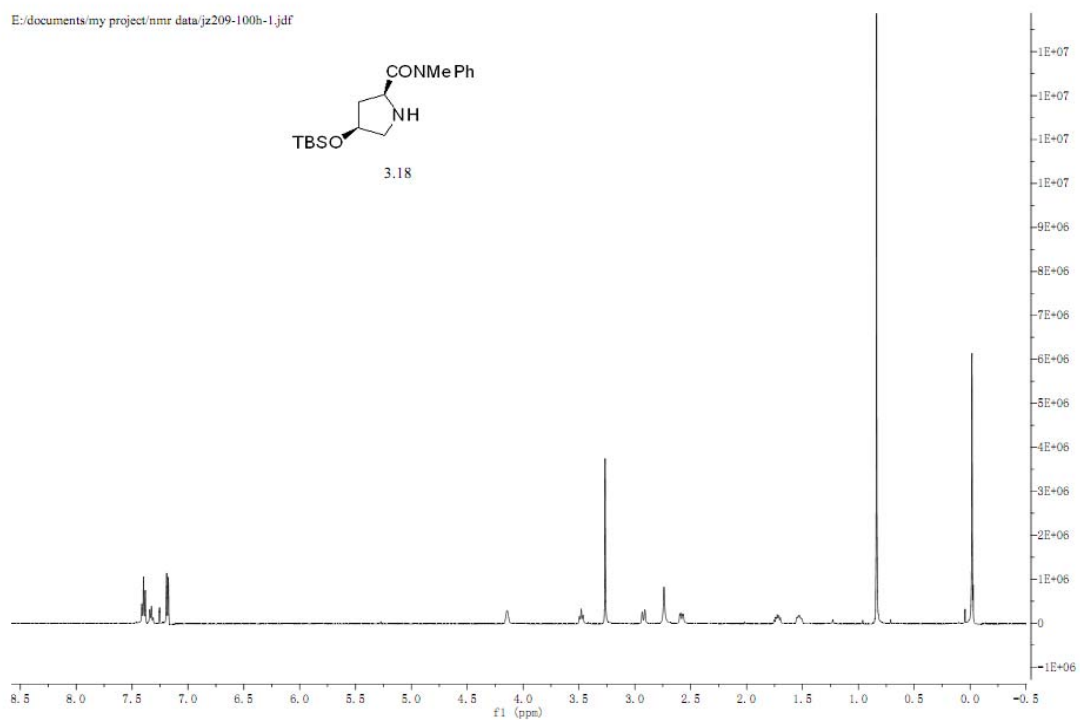
E:/documents/my project/nmr data/jz209-84proton-1.jdf



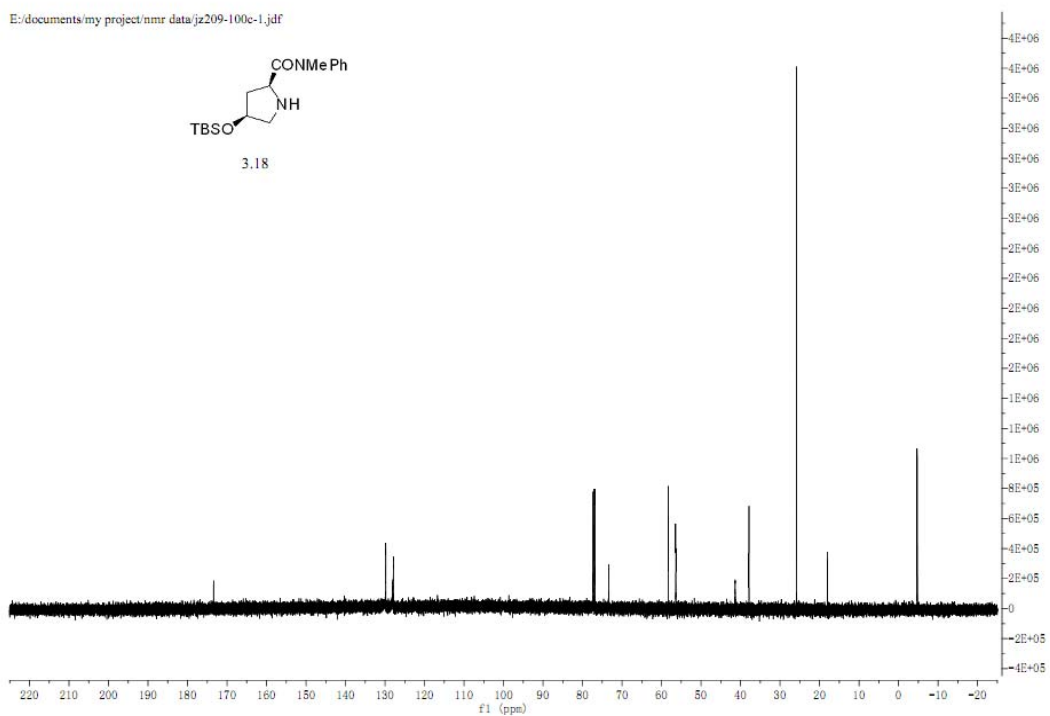
E:/documents/my project/nmr data/jz209-84carbon-3.jdf



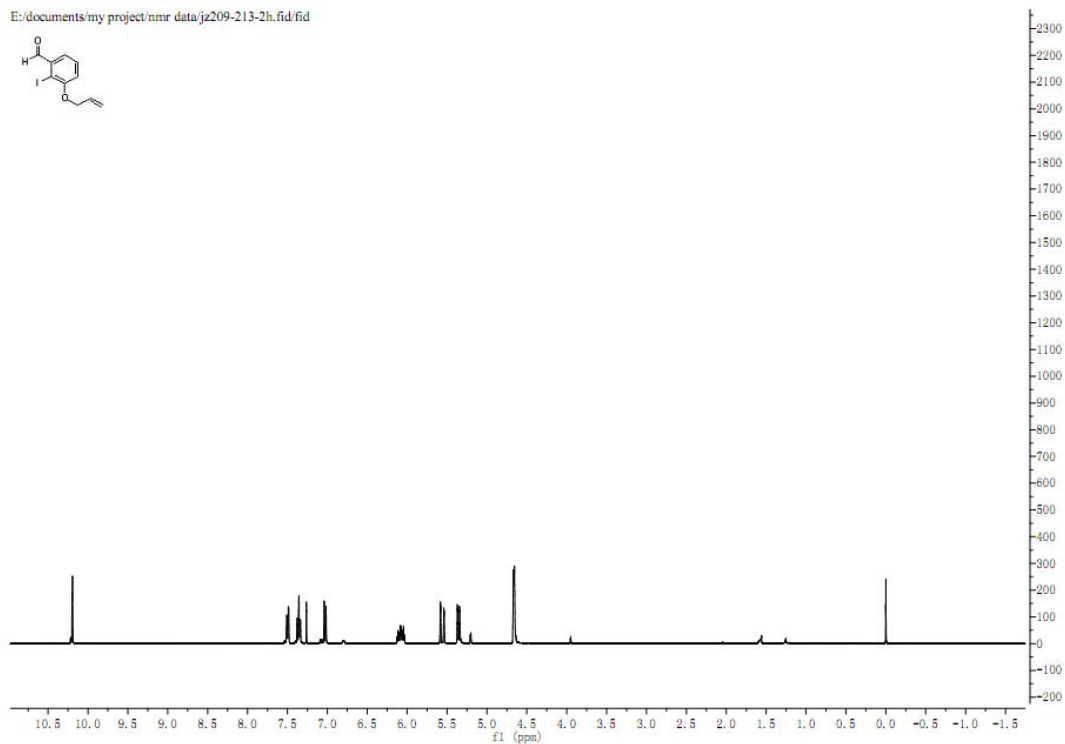
E:/documents/my project/nmr data/jz209-100b-1.jdf



E:/documents/my project/nmr data/jz209-100c-1.jdf

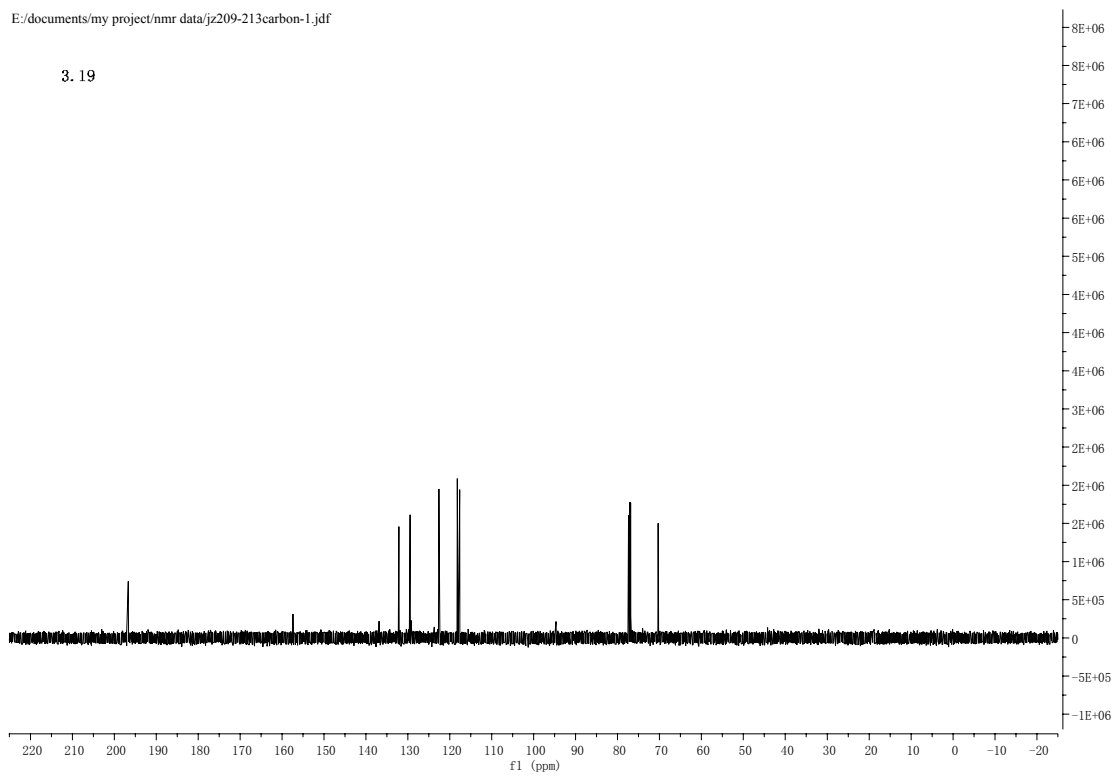


E:/documents/my project/nmr data/jz209-213-2h.fid/fid

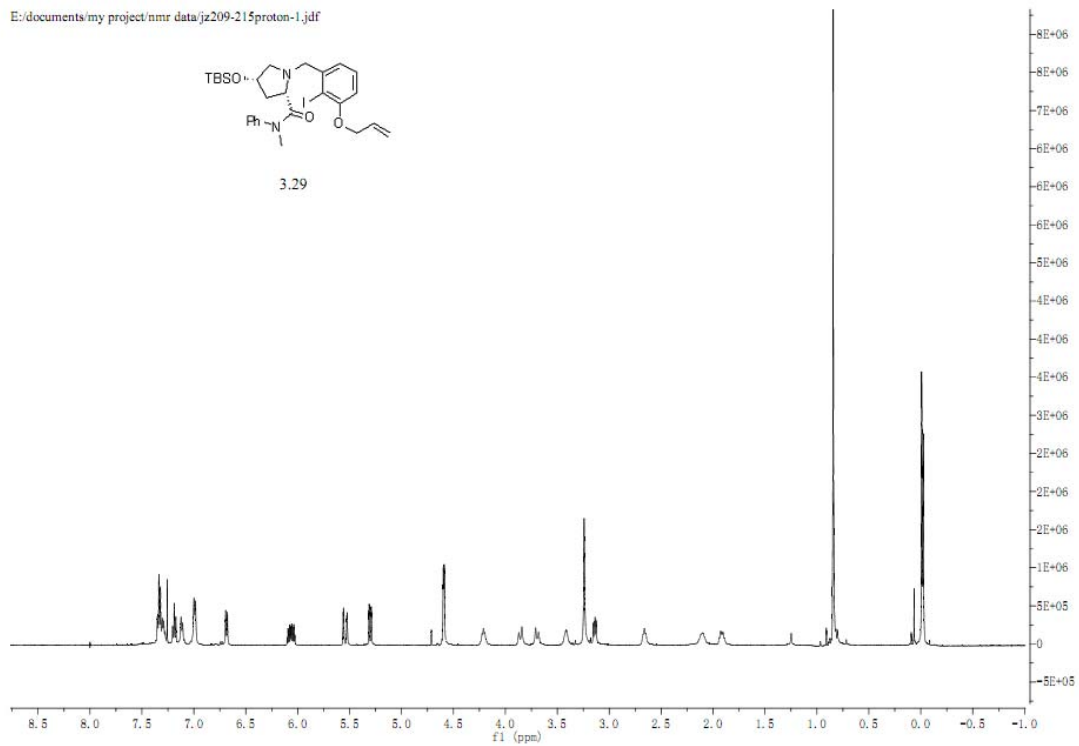


E:/documents/my project/nmr data/jz209-213carbon-1.jdf

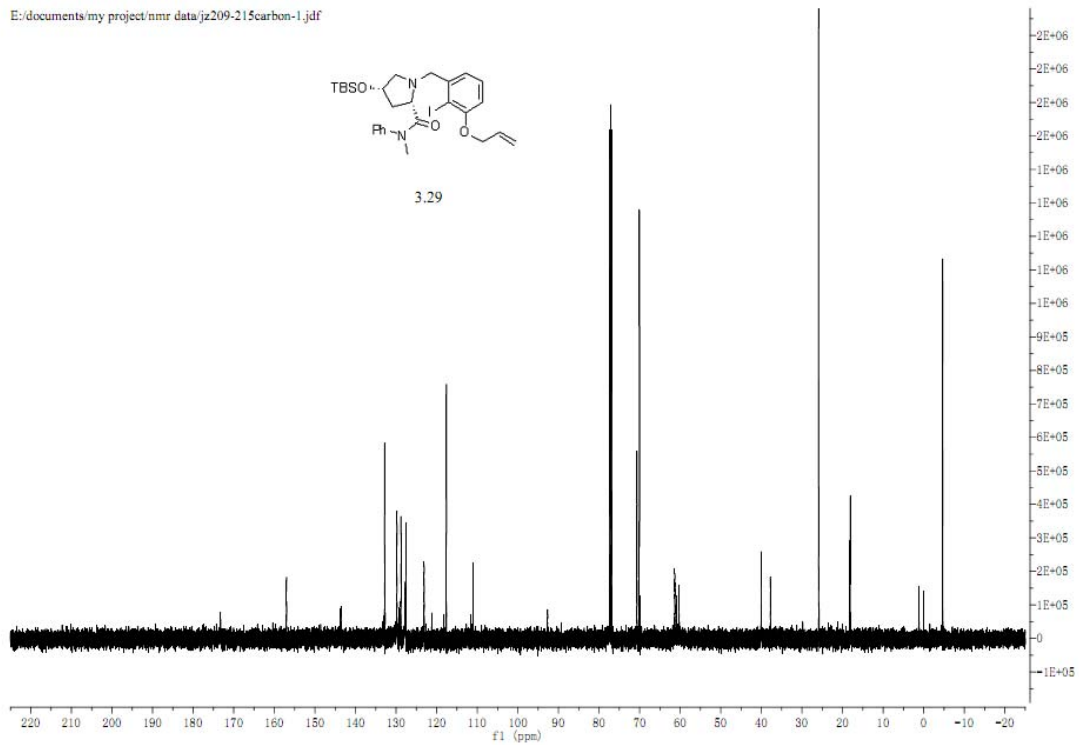
3.19



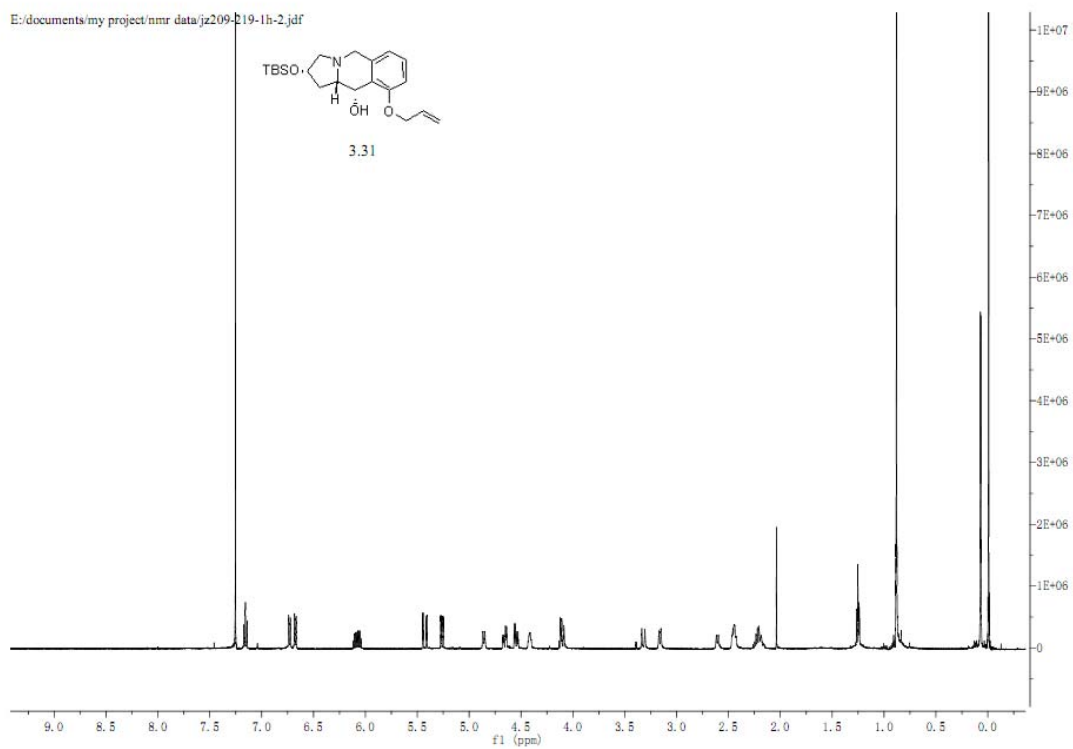
E:/documents/my project/nmr data/jz209-215proton-1.jdf



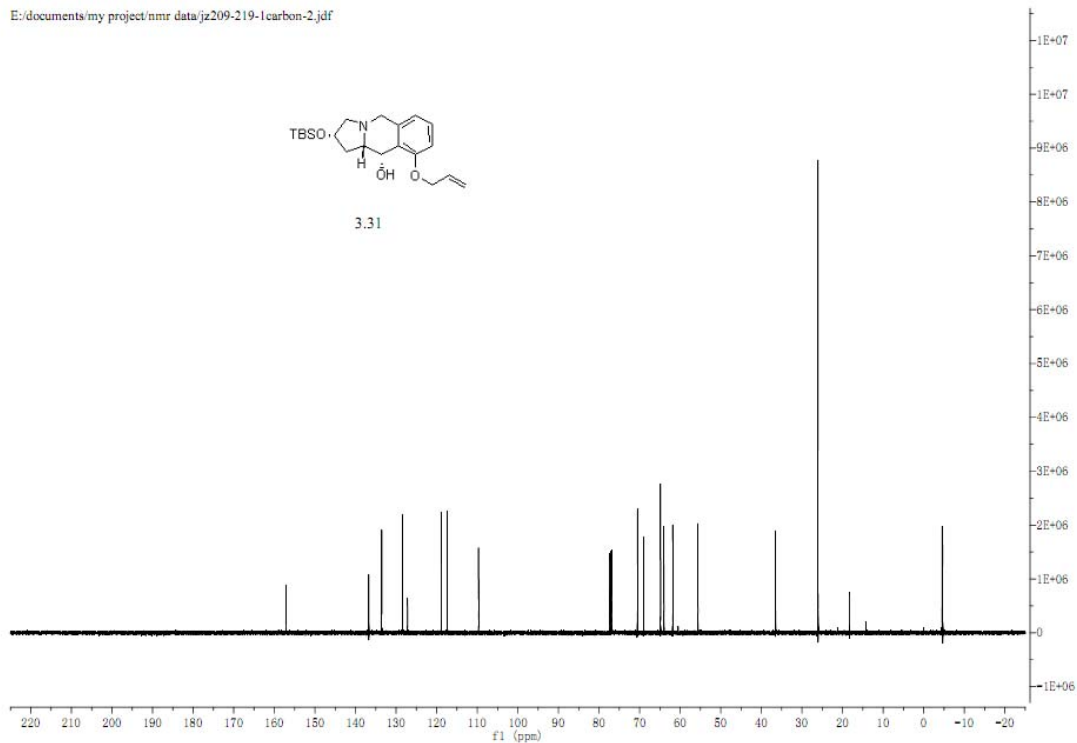
E:/documents/my project/nmr data/jz209-215carbon-1.jdf



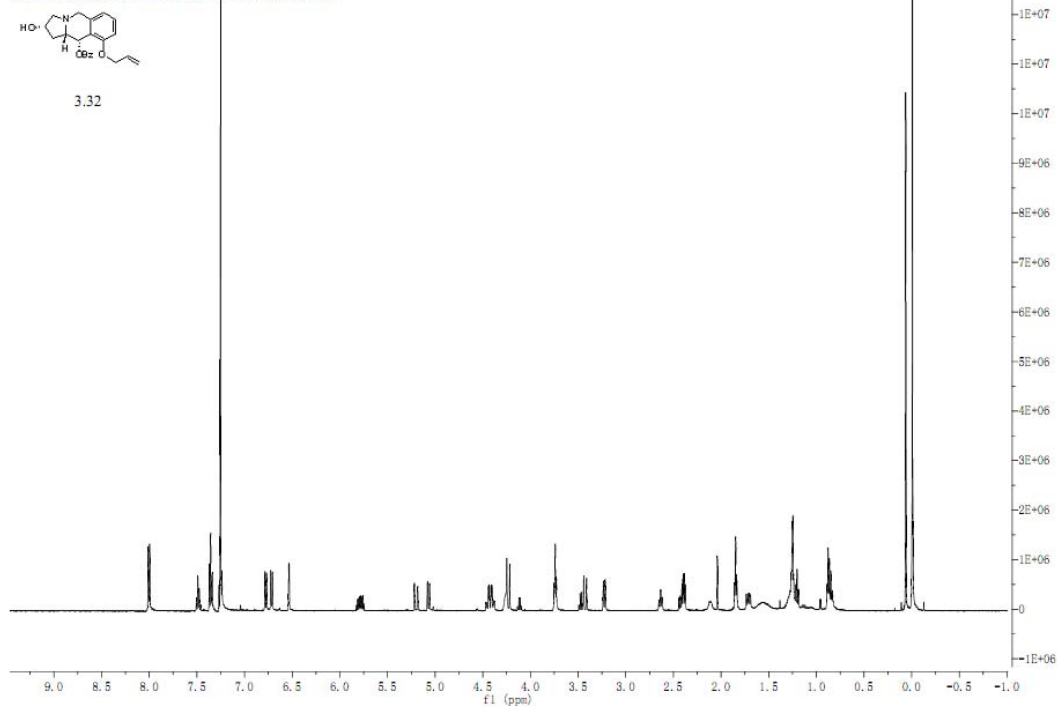
E:/documents/my project/nmr data/jz209-219-1h-2.jdf



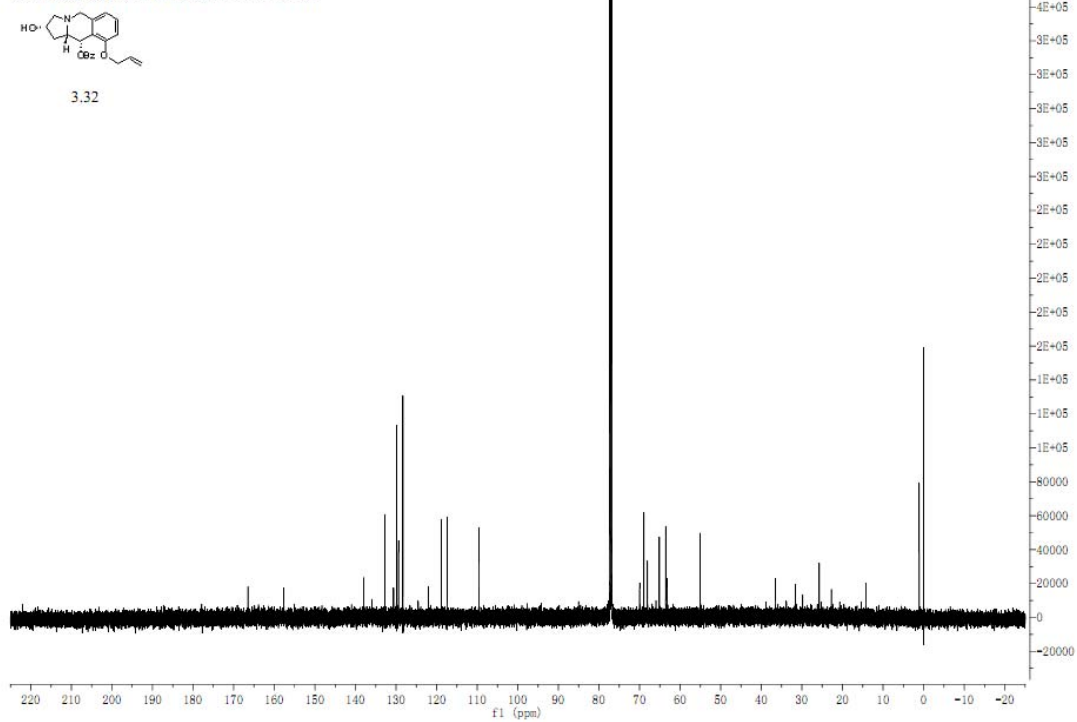
E:/documents/my project/nmr data/jz209-219-1carbon-2.jdf



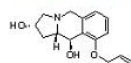
E:/documents/my project/nmr data/jz20p-225dry-proton-3.jdf



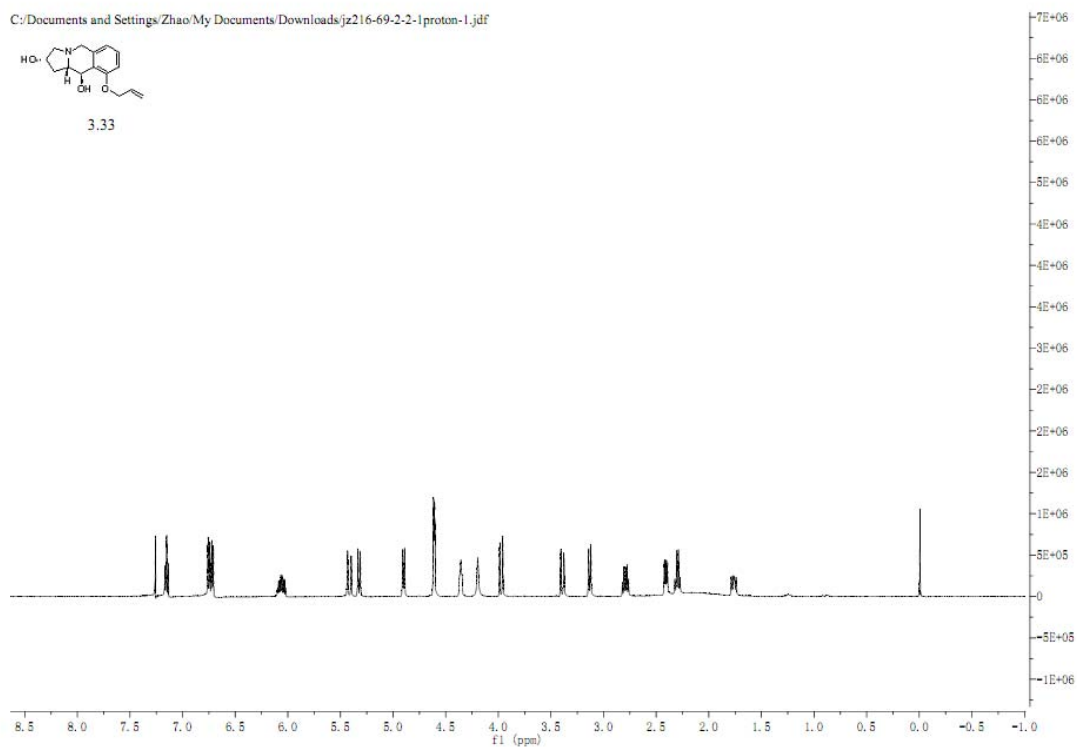
E:/documents/my project/nmr data/jz209-225carbon-1.jdf



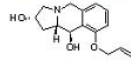
C:\Documents and Settings\Zhao\My Documents\Downloads\jz216-69-2-2-1proton-1.jdf



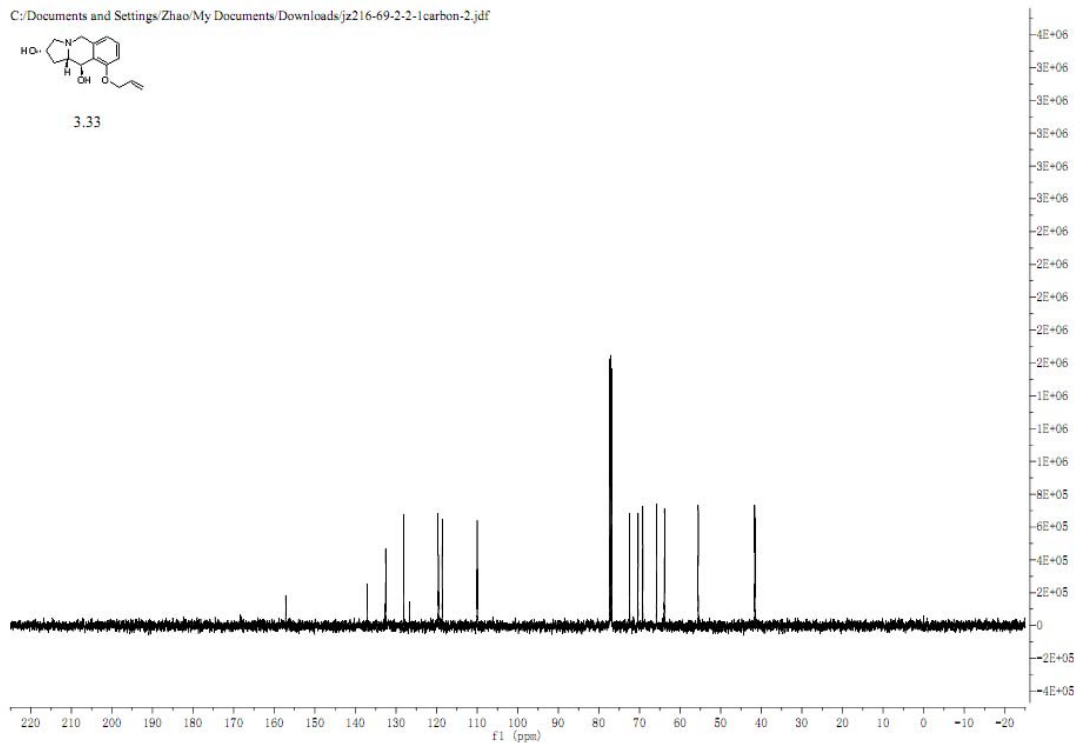
3.33



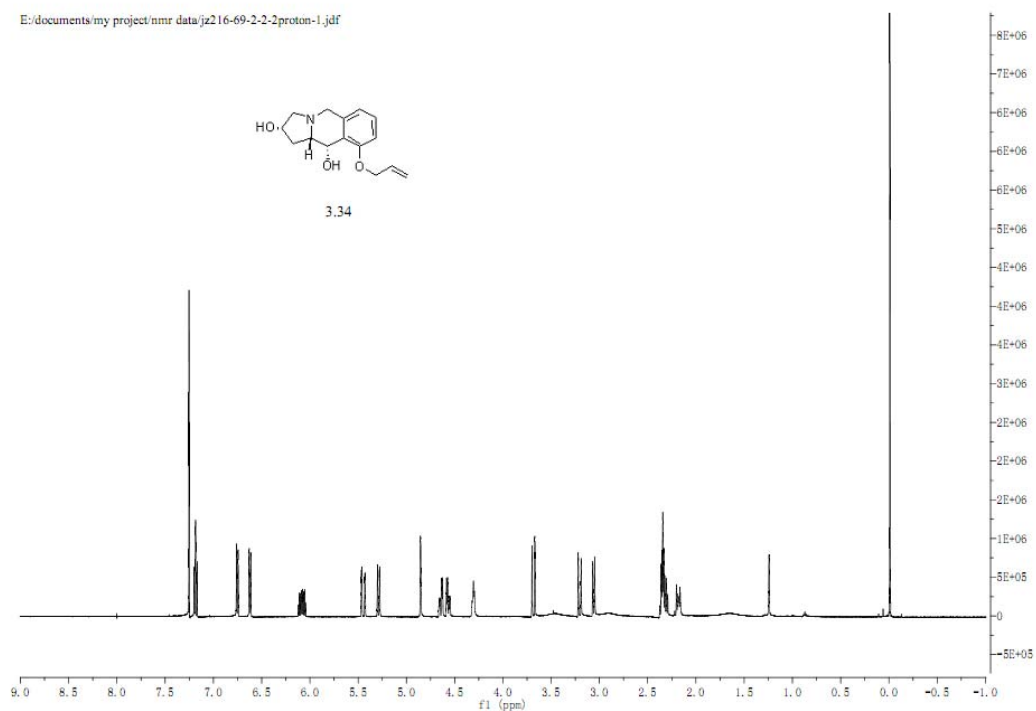
C:\Documents and Settings\Zhao\My Documents\Downloads\jz216-69-2-2-1carbon-2.jdf



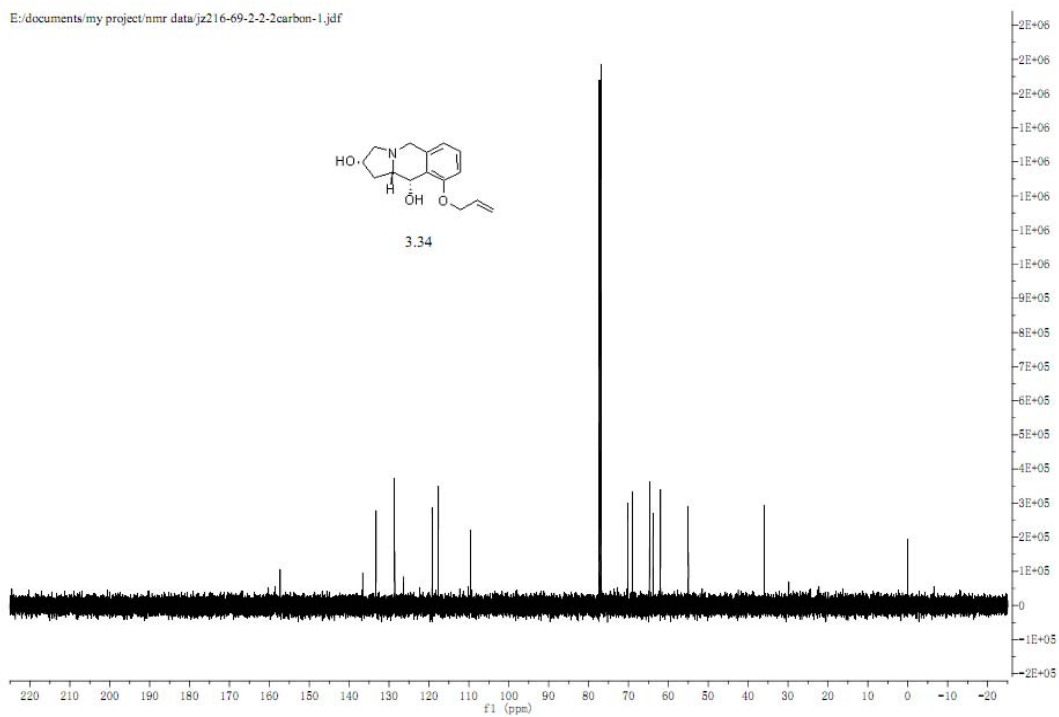
3.33



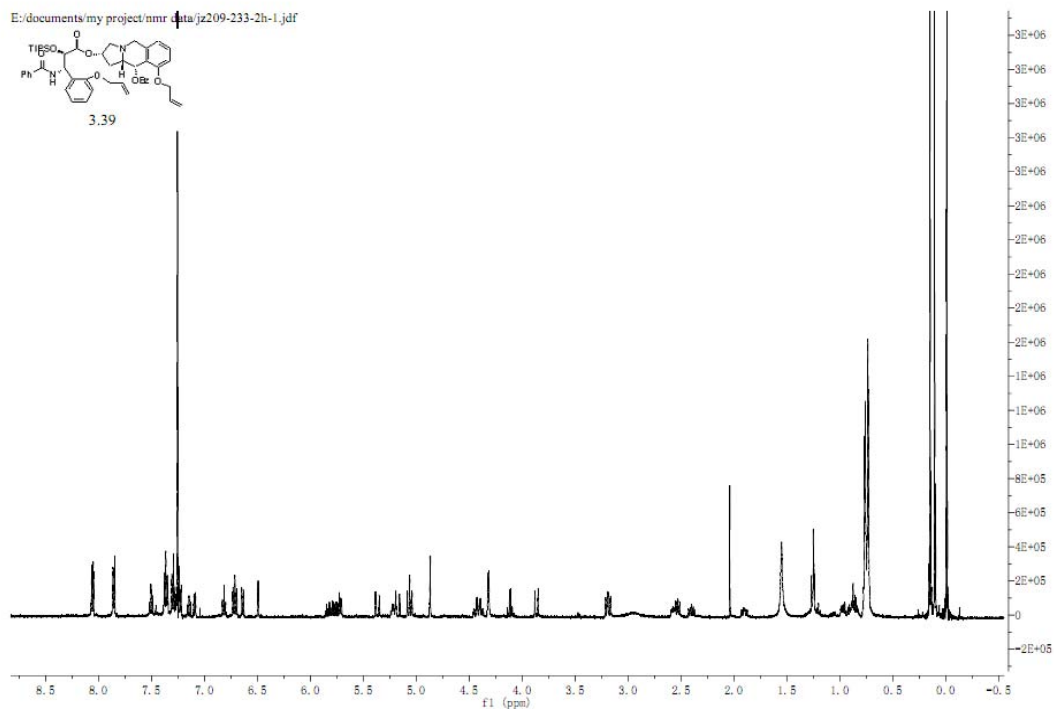
E:/documents/my project/nmr data/jz216-69-2-2-proton-1.jdf



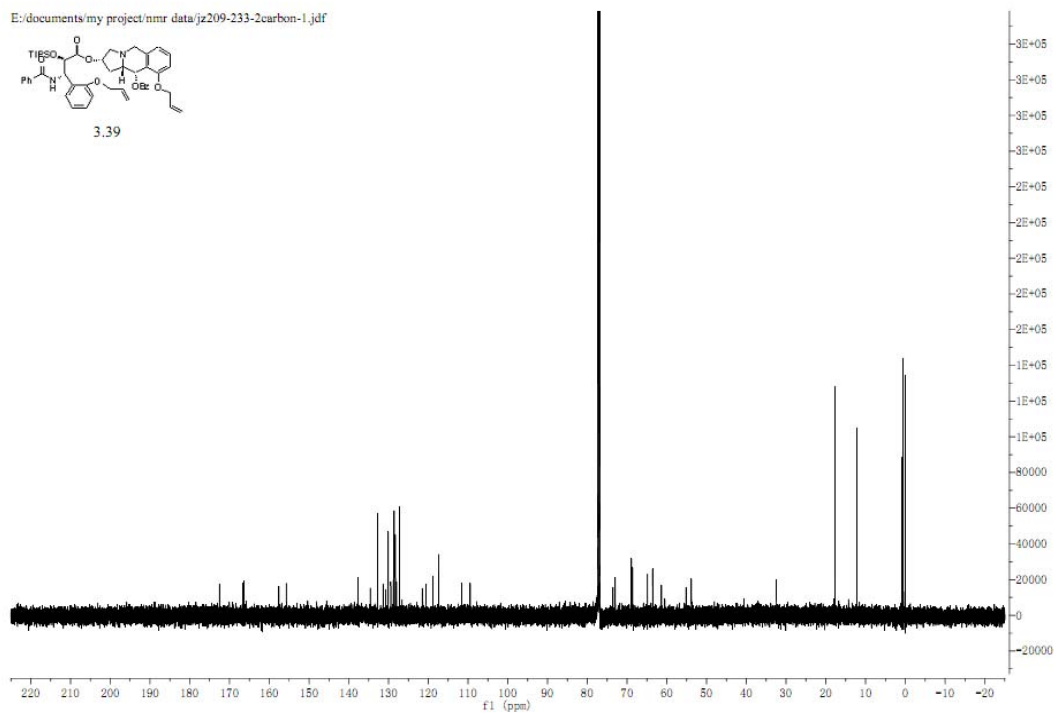
E:/documents/my project/nmr data/jz216-69-2-2-carbon-1.jdf



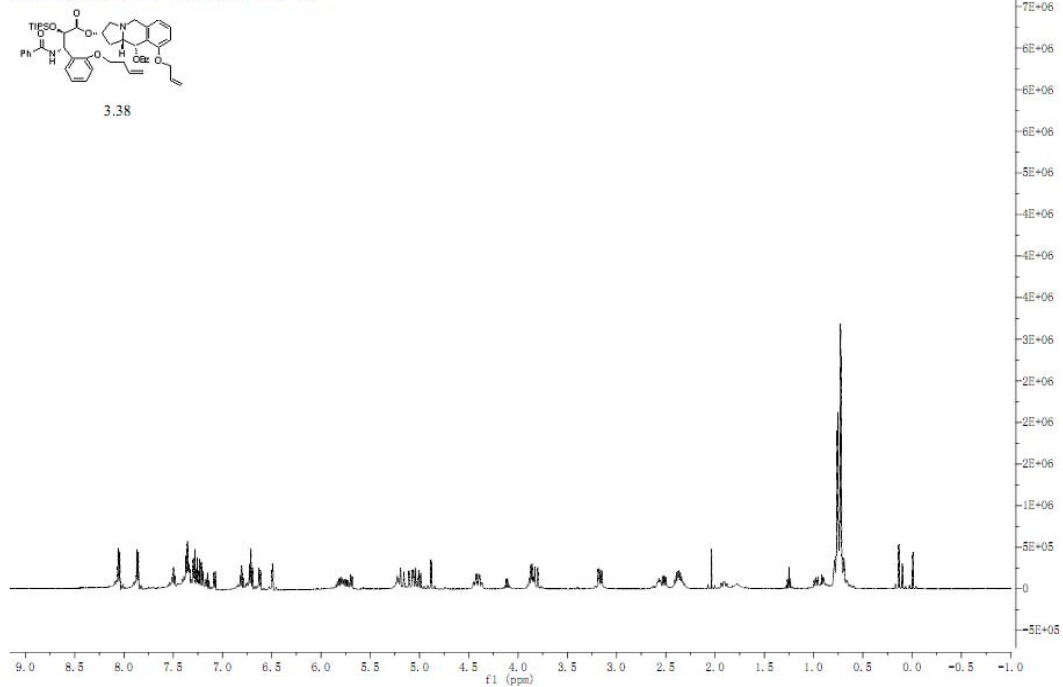
E:/documents/my project/nmr data/jz209-233-2h-1.jdf



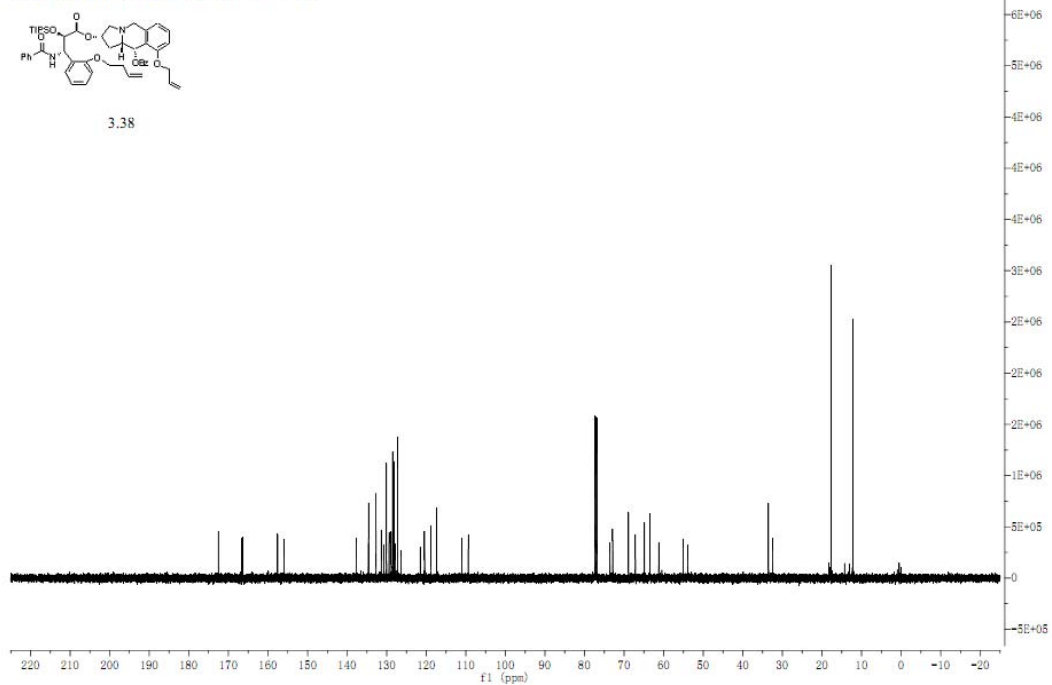
E:/documents/my project/nmr data/jz209-233-2carbon-1.jdf



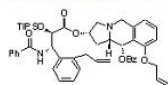
E:/documents/my project/nmr data/jz216-50-2proton-1.jdf



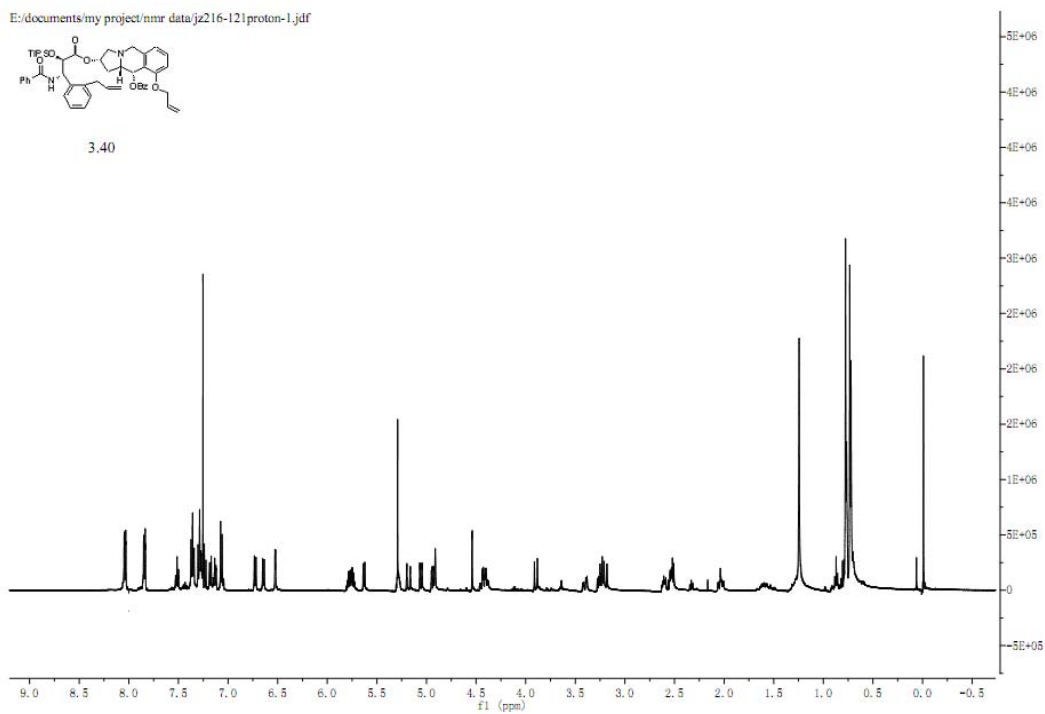
E:/documents/my project/nmr data/jz216-50-2carbon-1.jdf



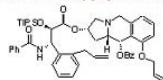
E:/documents/my project/nmr data/jz216-121proton-1.jdf



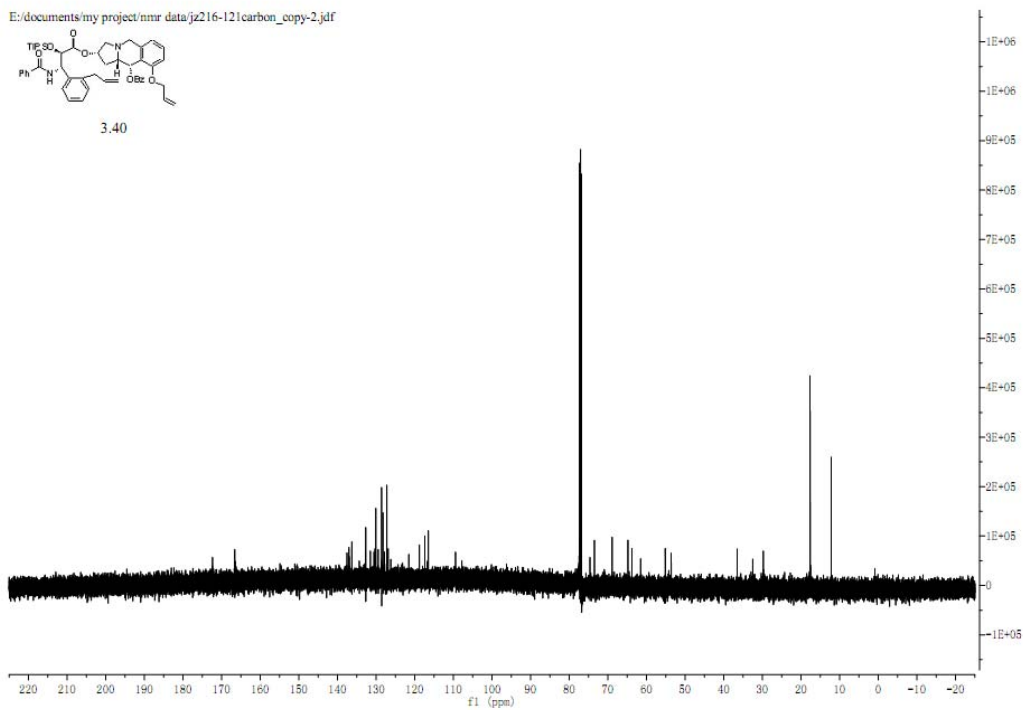
3.40



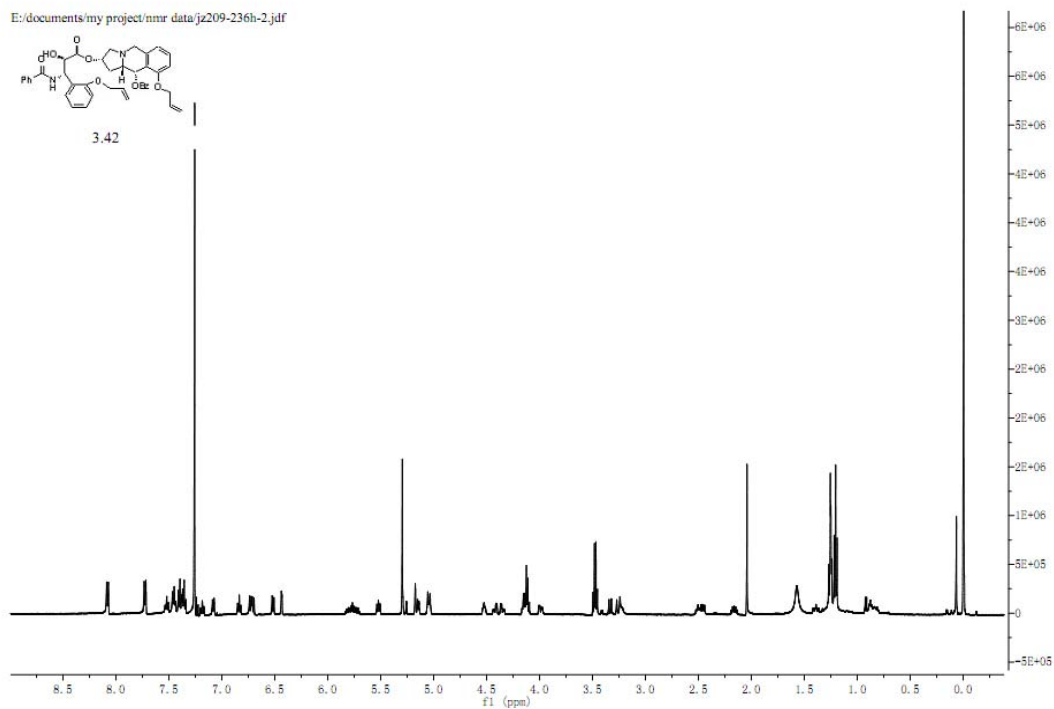
E:/documents/my project/nmr data/jz216-121carbon_copy-2.jdf



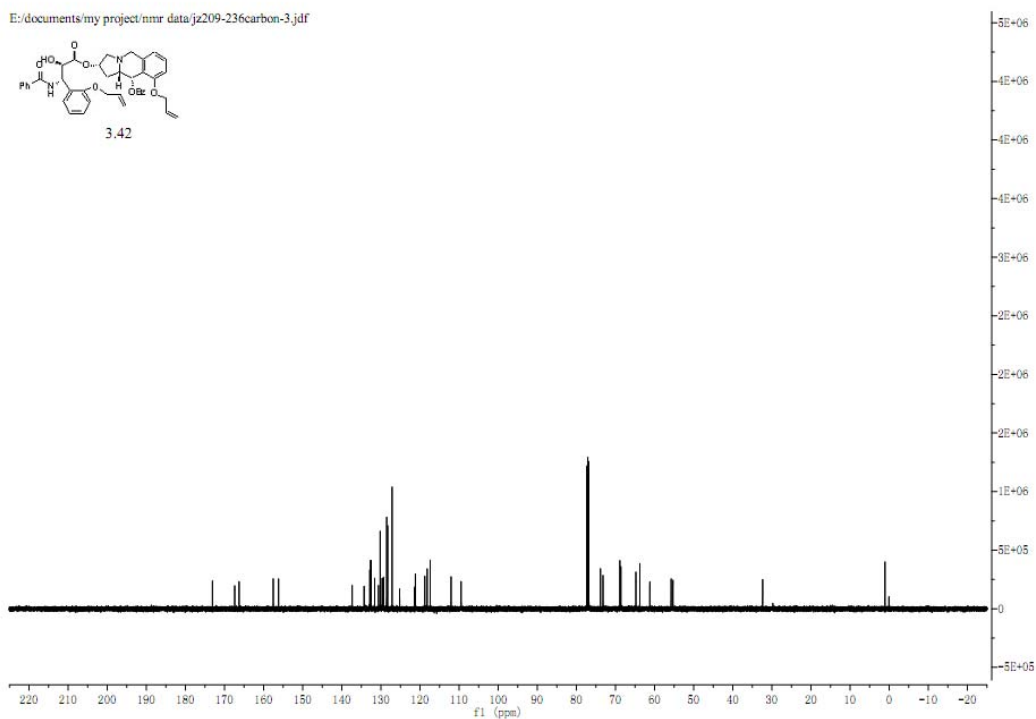
3.40



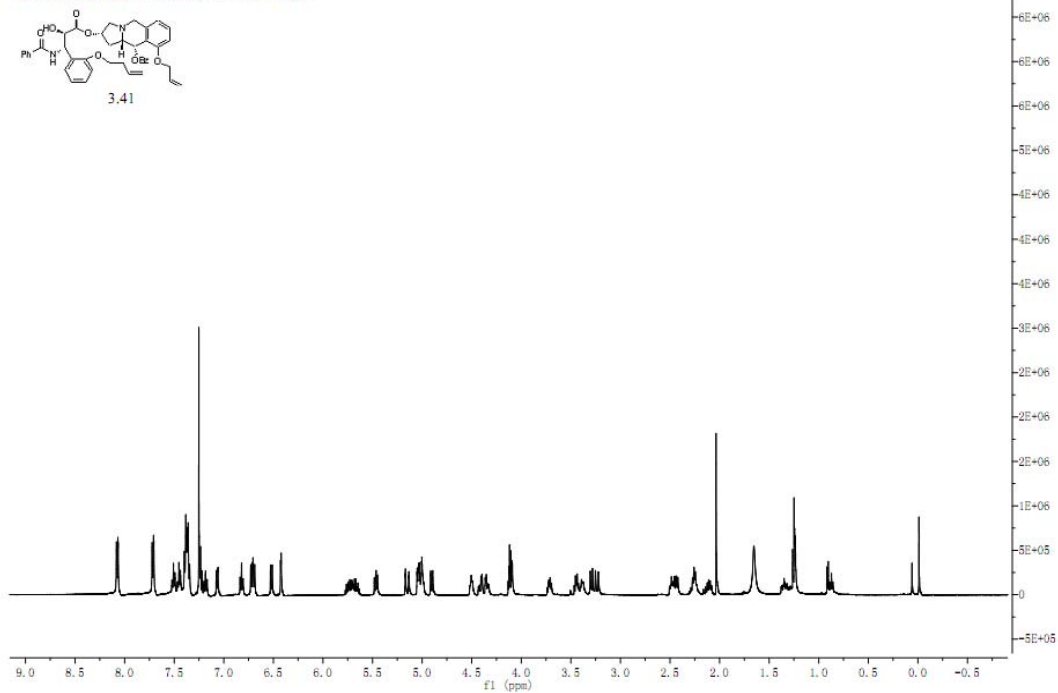
E:/documents/my project/nmr data/jz209-236h-2.jdf



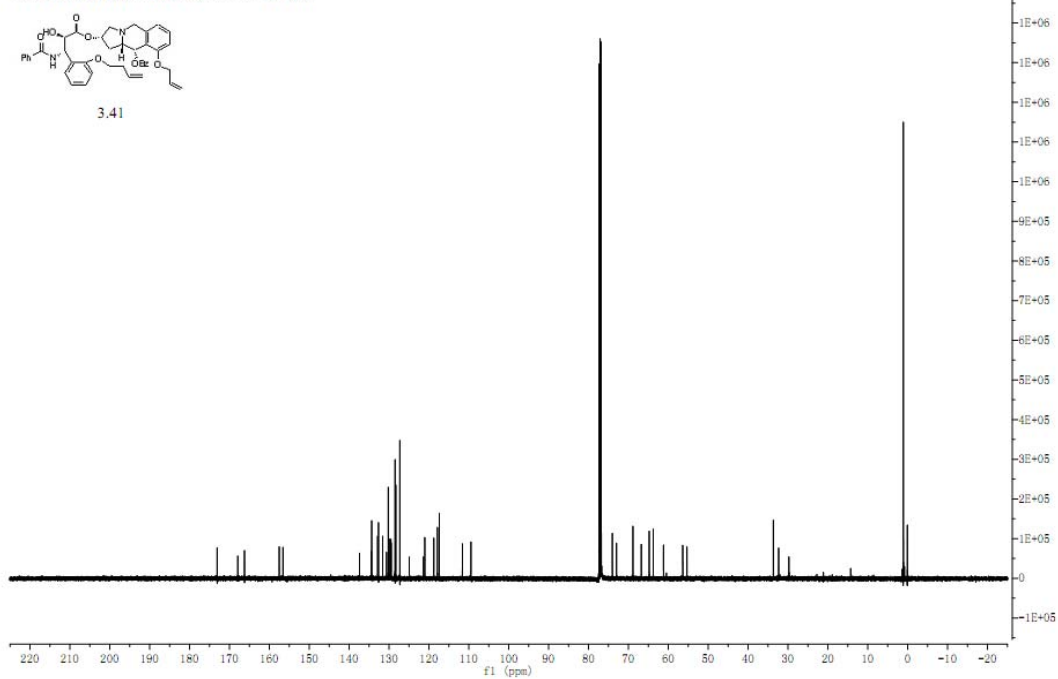
E:/documents/my project/nmr data/jz209-236carbon-3.jdf



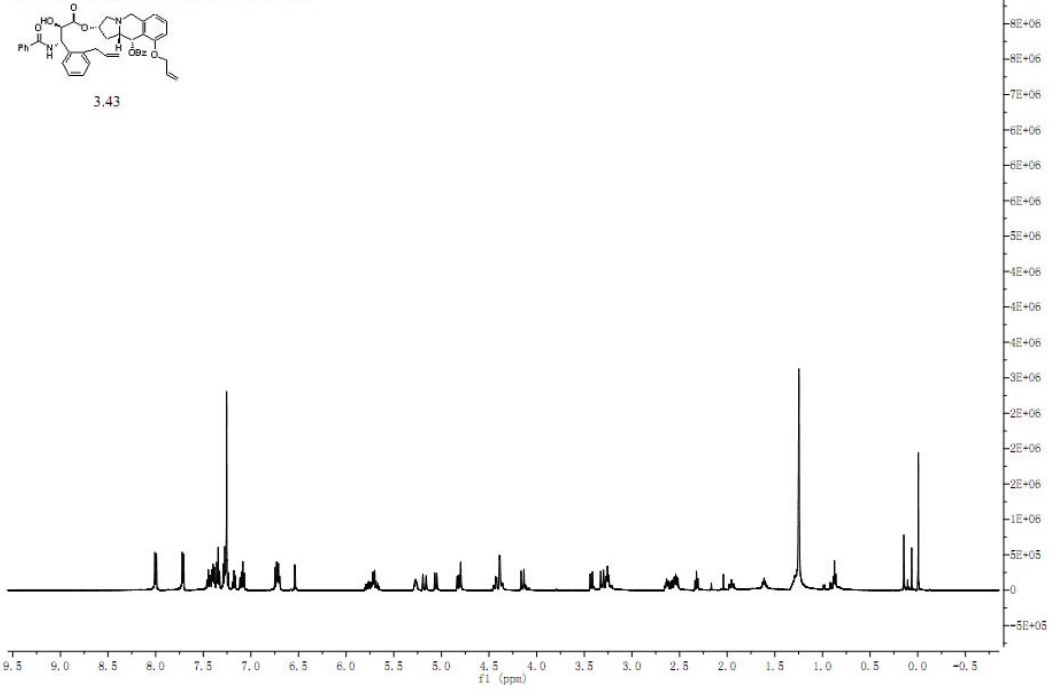
E:/documents/my project/nmr data/jz216-77proton-1.jdf



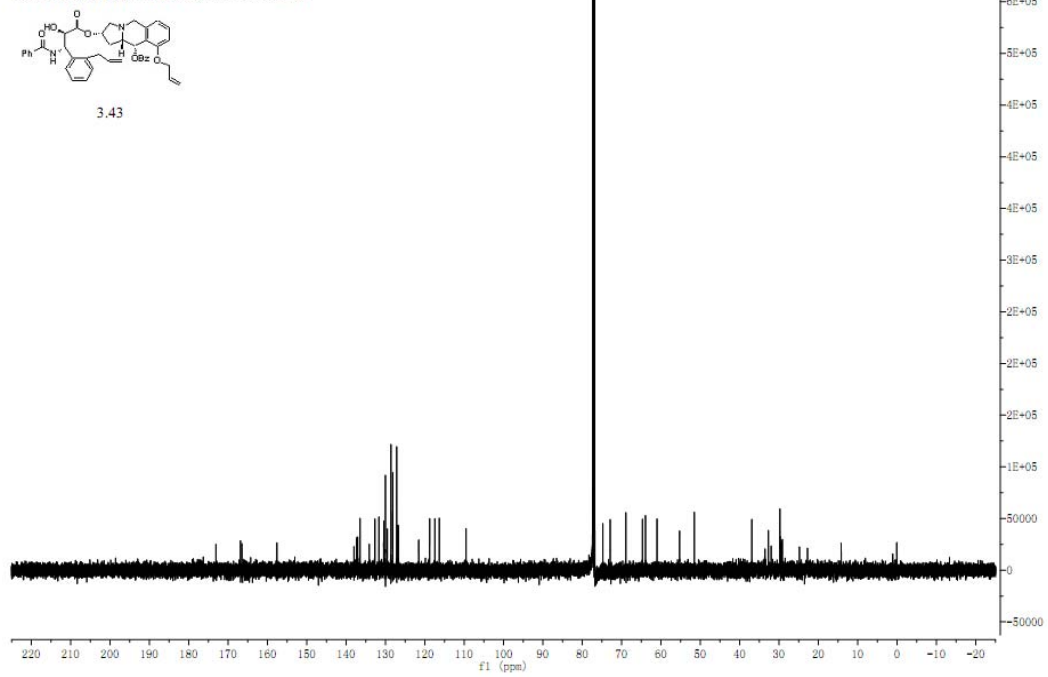
E:/documents/my project/nmr data/jz216-77carbon-2.jdf



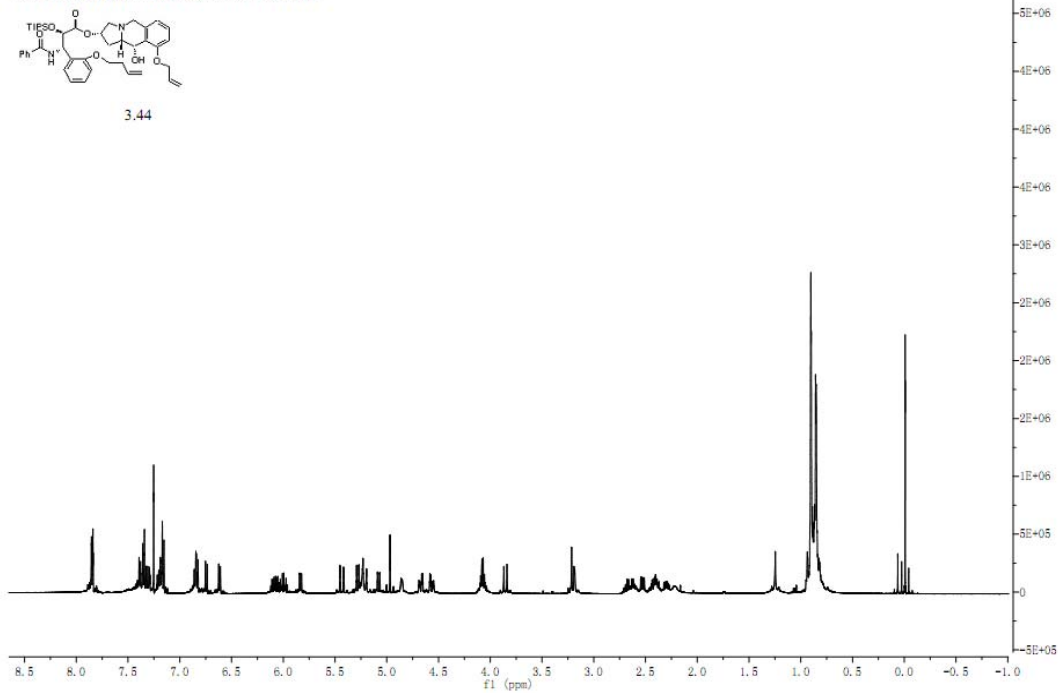
E:/documents/my project/nmr data/jz216-125proton-1.jdf



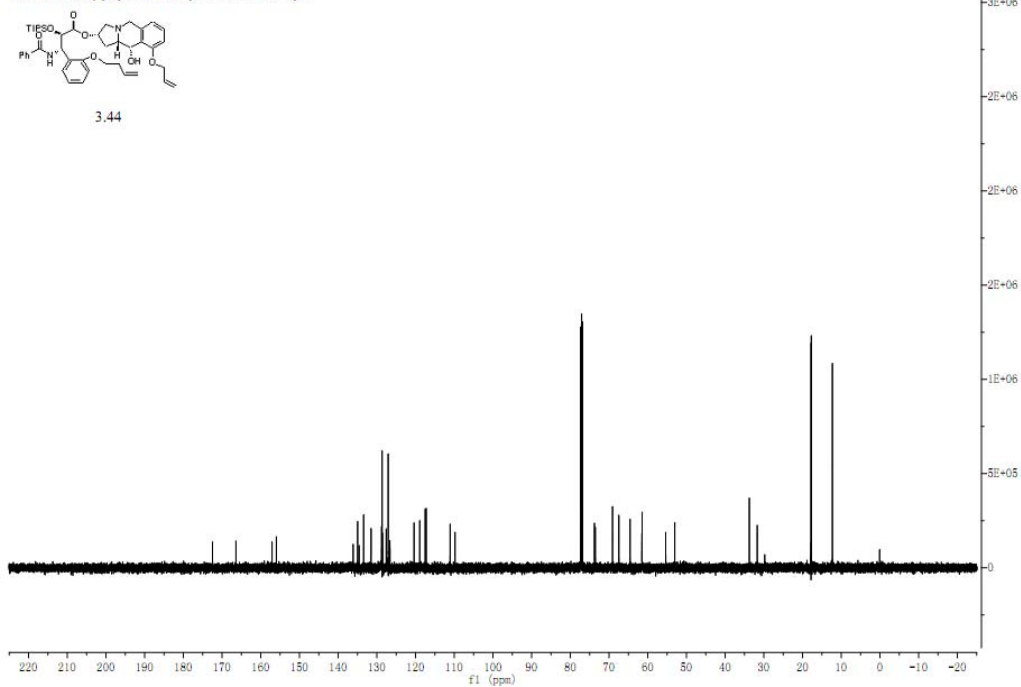
E:/documents/my project/nmr data/jz216-125carbon-1.jdf



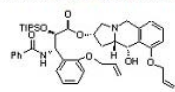
E:/documents/my project/nmr data/jz216-58-2proton-2.jdf



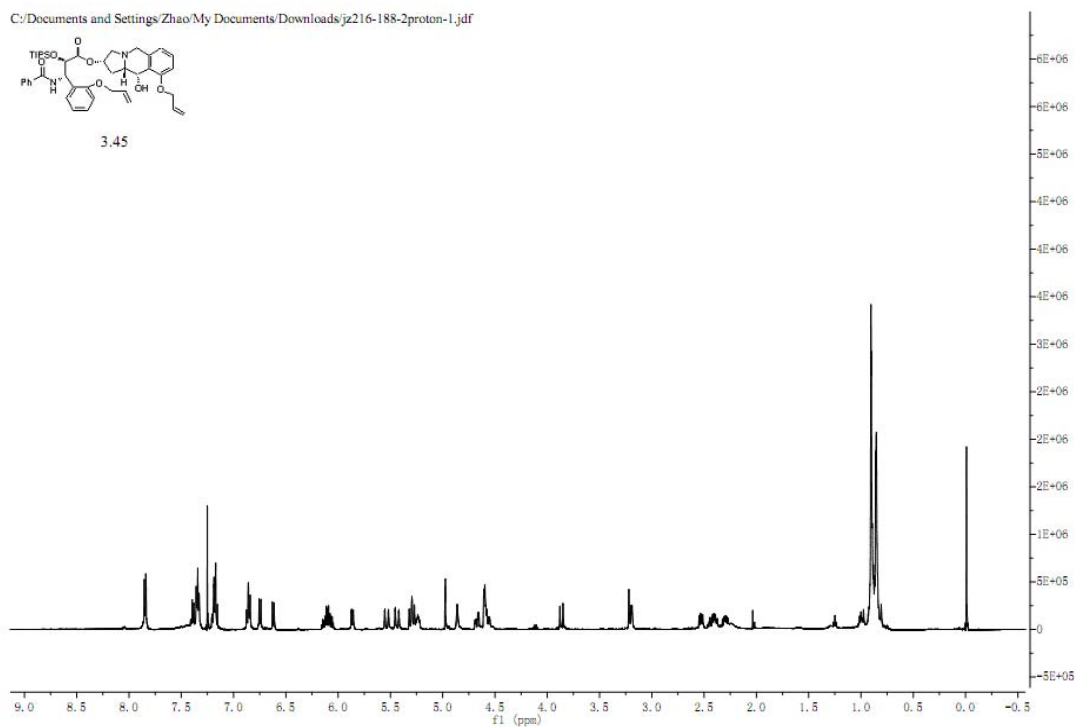
E:/documents/my project/nmr data/jz216-58-2carbon-1.jdf



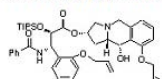
C:/Documents and Settings/Zhao/My Documents/Downloads/jz216-188-2proton-1.jdf



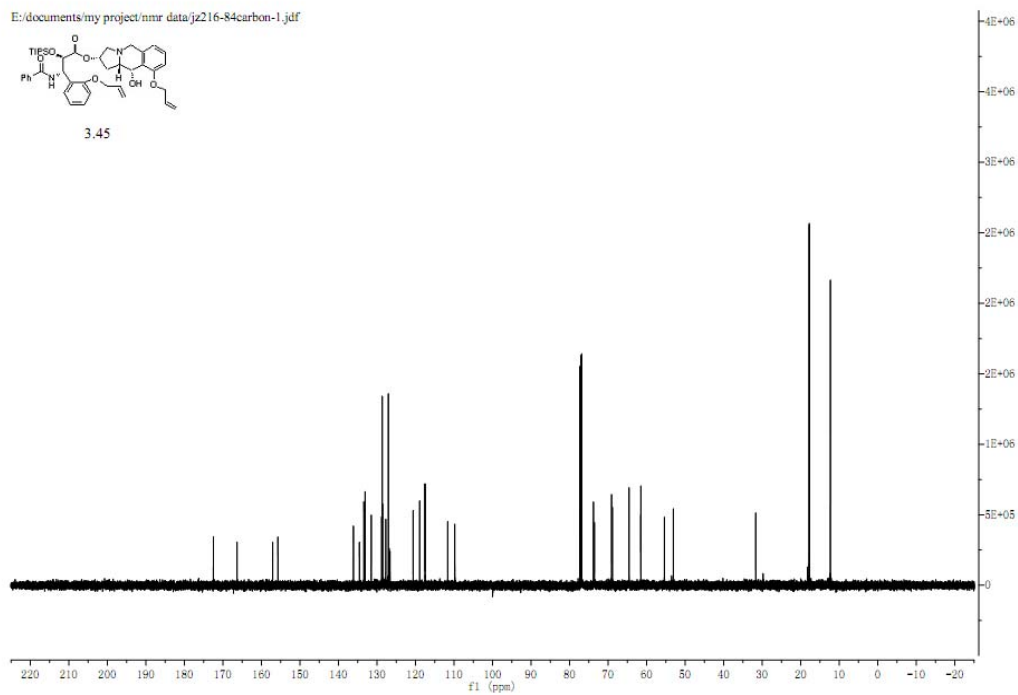
3.45



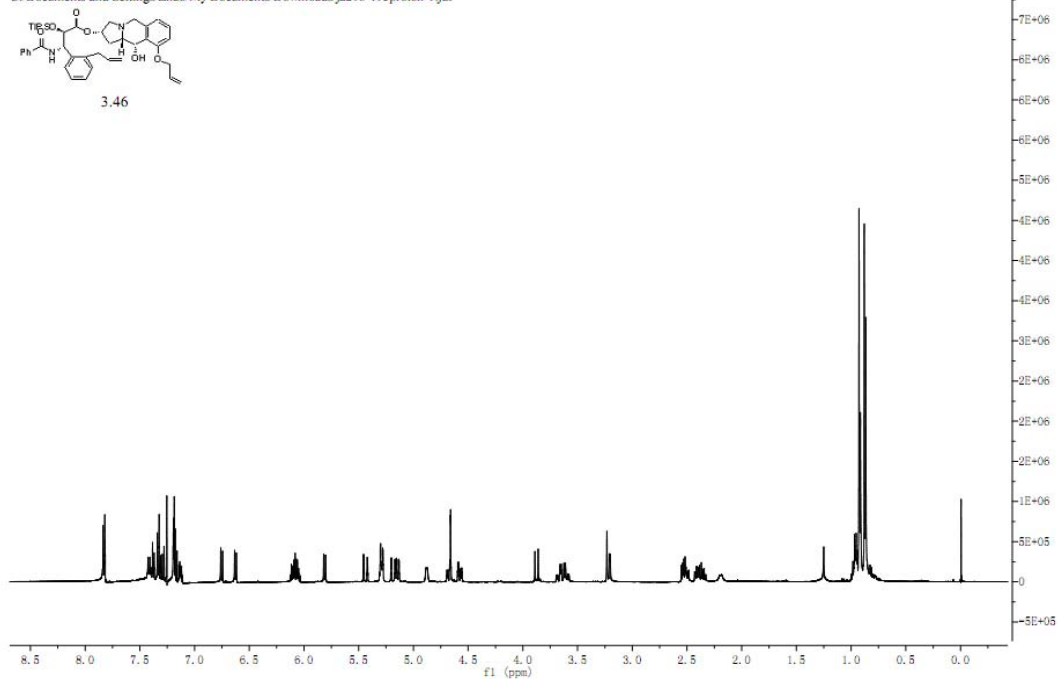
E:/documents/my project/nmr data/jz216-84carbon-1.jdf



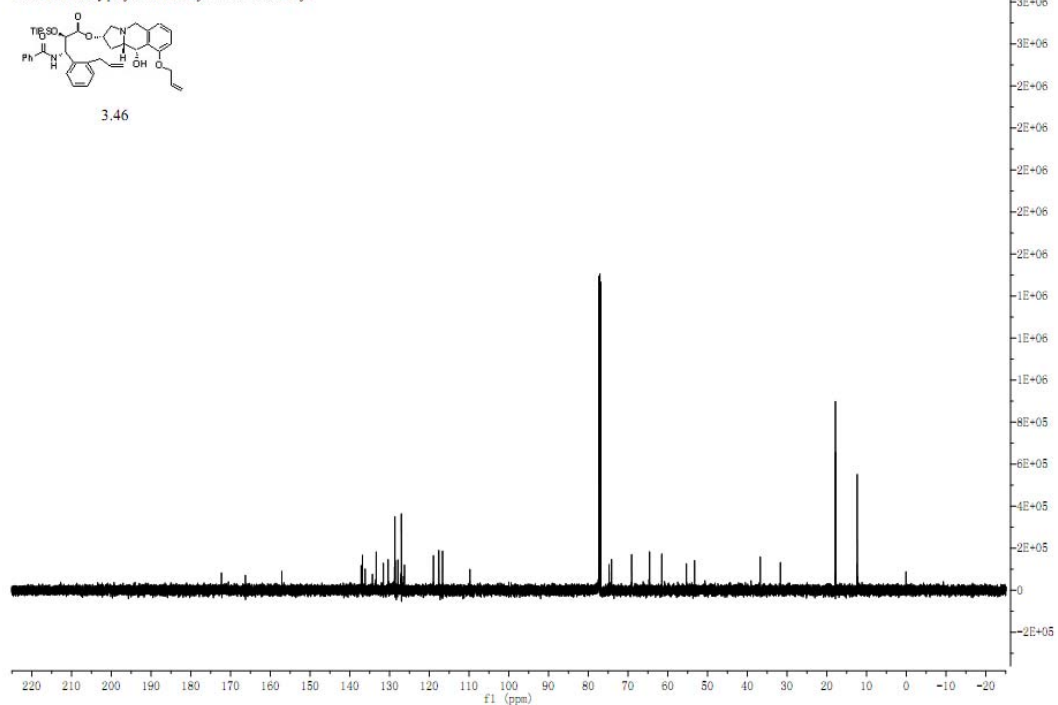
3.45



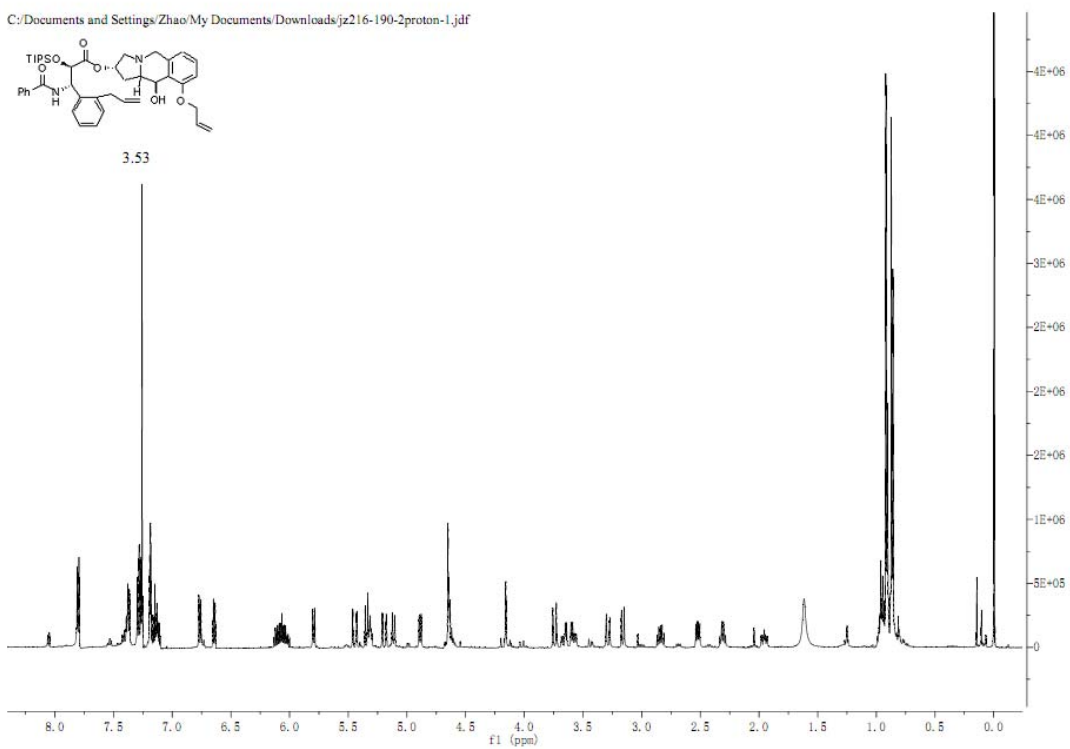
C:/Documents and Settings/Zhao/My Documents/Downloads/jz216-195proton-1.jdf



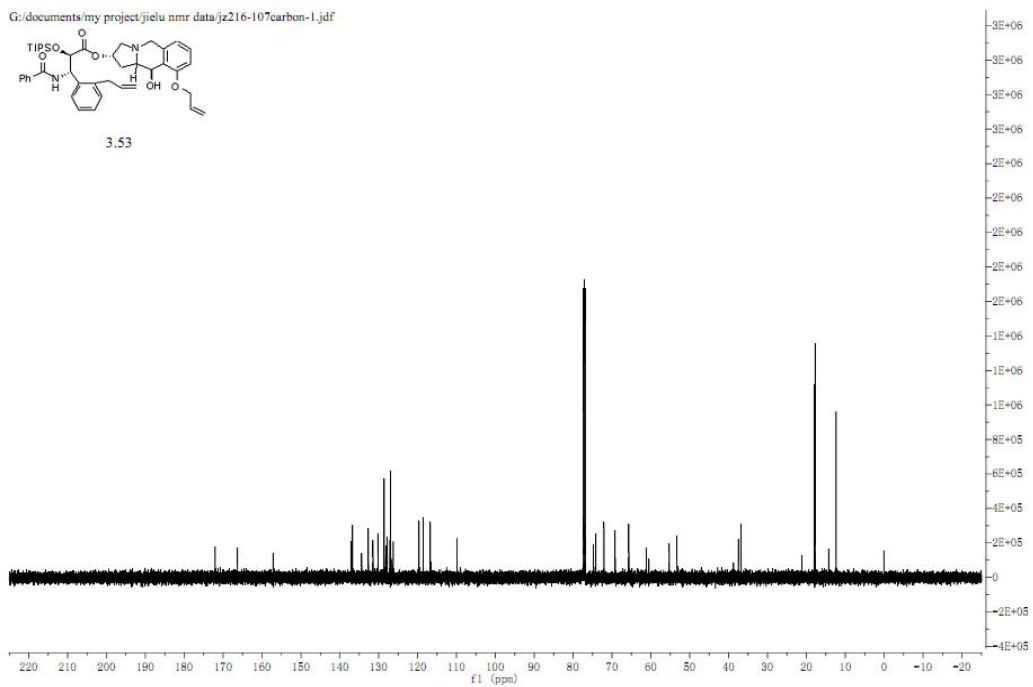
E:/documents/my project/nmr_data/jz216-104carbon-2.jdf



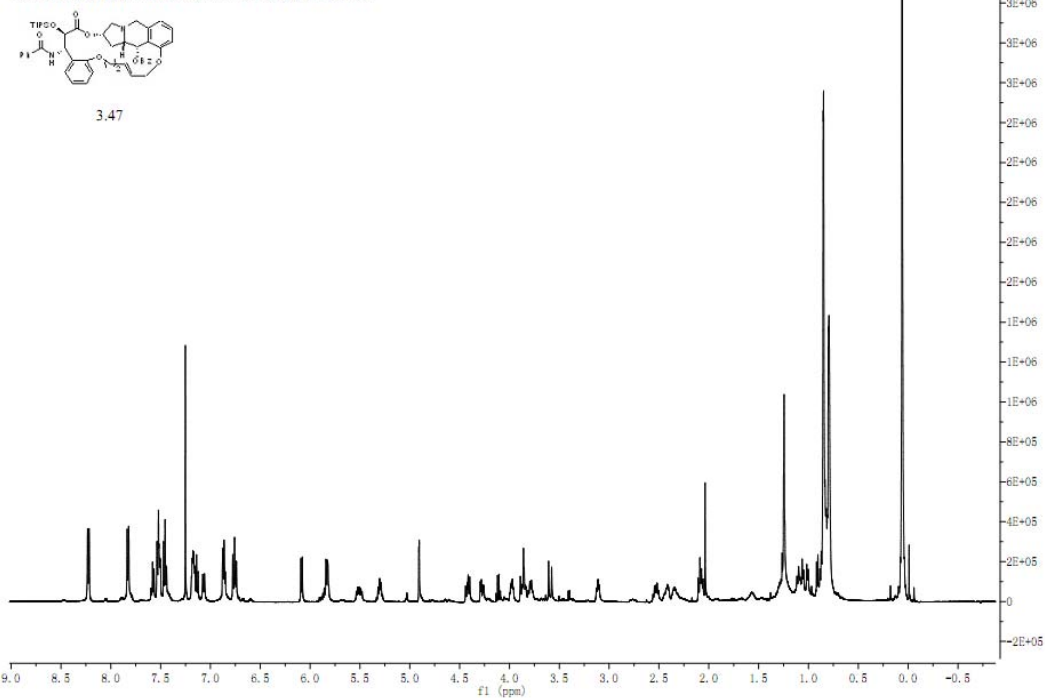
C:\Documents and Settings\Zhao\My Documents\Downloads\jz216-190-2proton-1.jdf



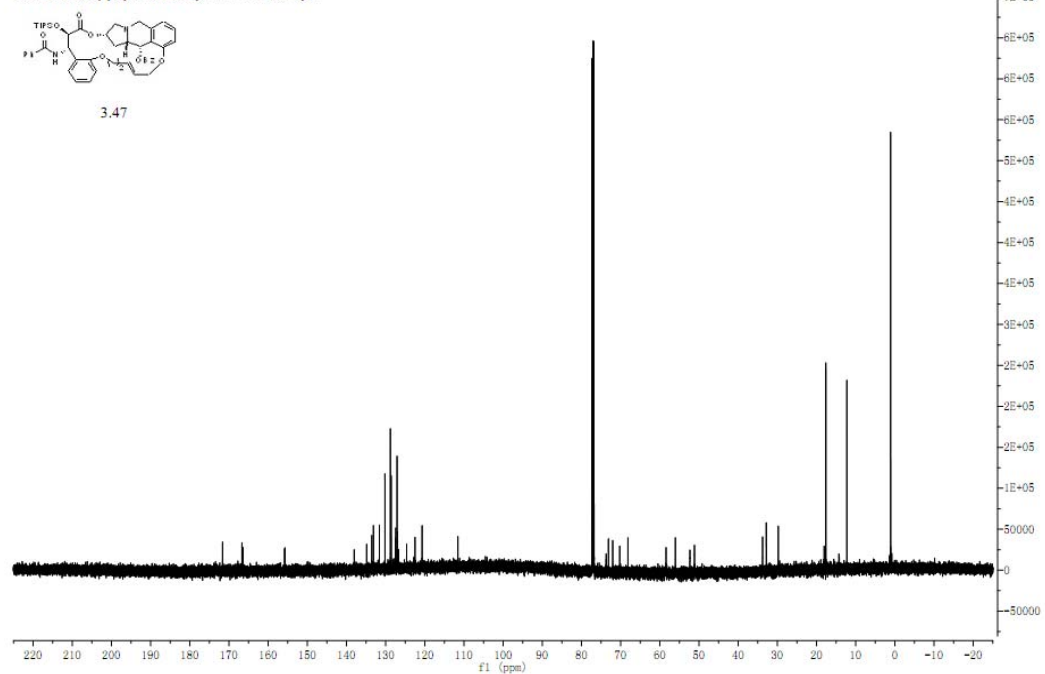
G:\documents\my project\jielu nmr data\jz216-107carbon-1.jdf



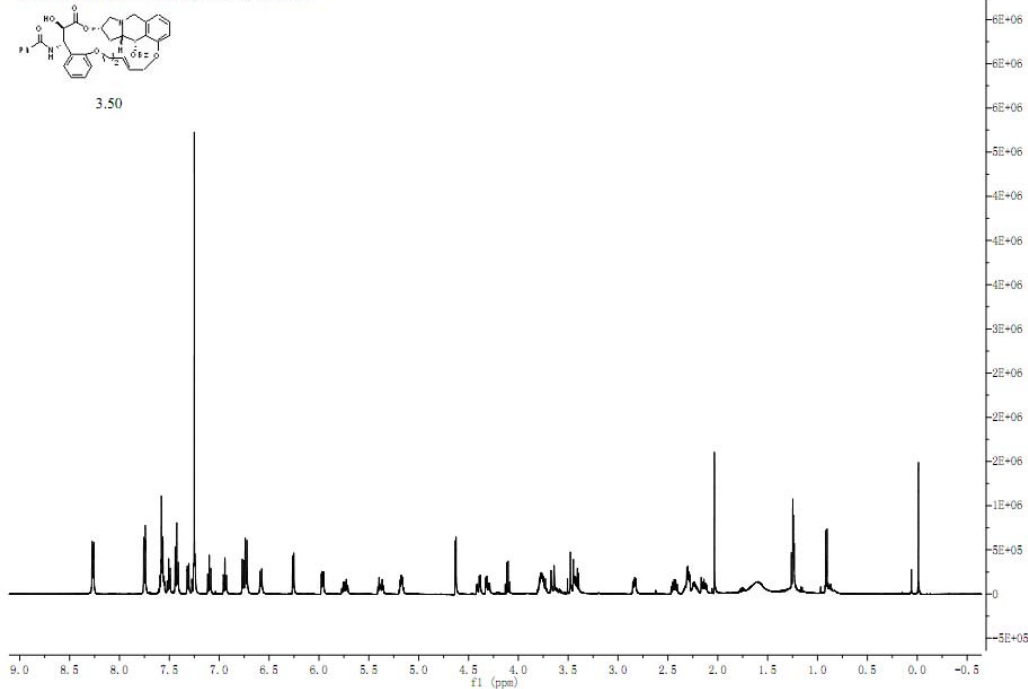
E:/documents/my project/nmr data/jz216-72-2proton-largeamount.jdf



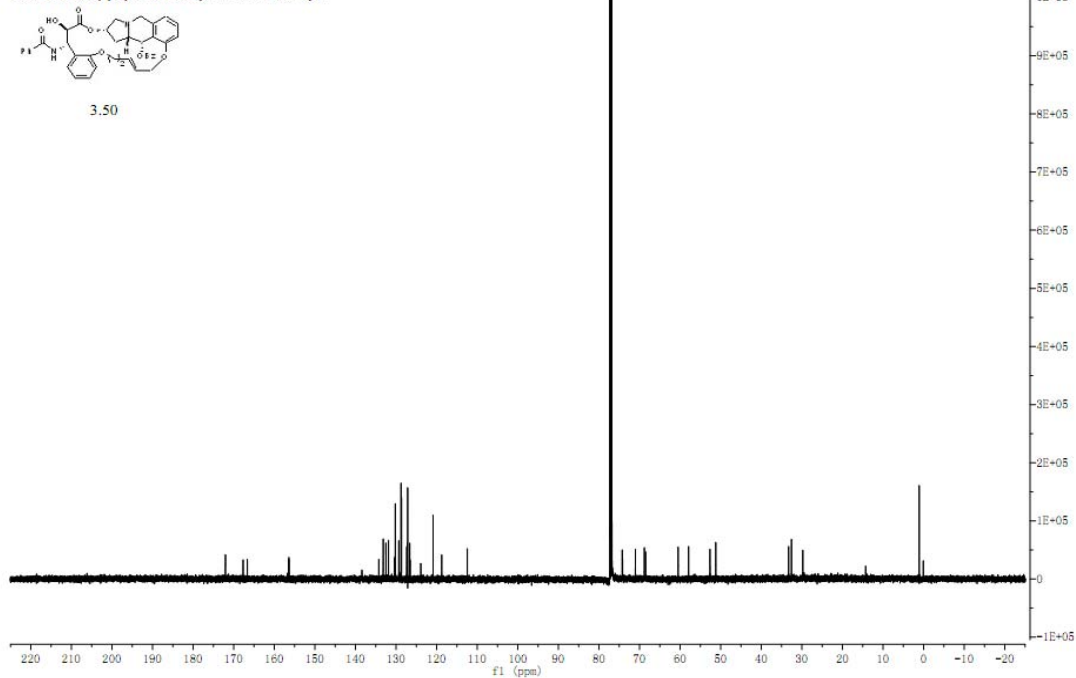
E:/documents/my project/nmr data/jz216-72-2carbon-1.jdf



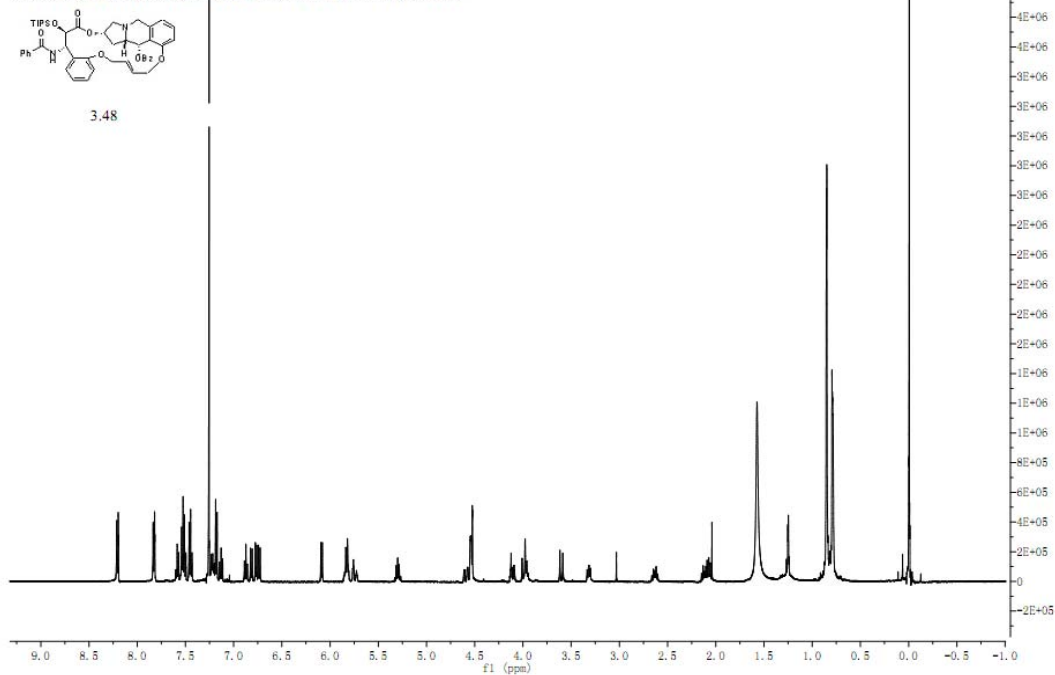
E:/documents/my project/nmr data/jz216-78-3proton-1.jdf



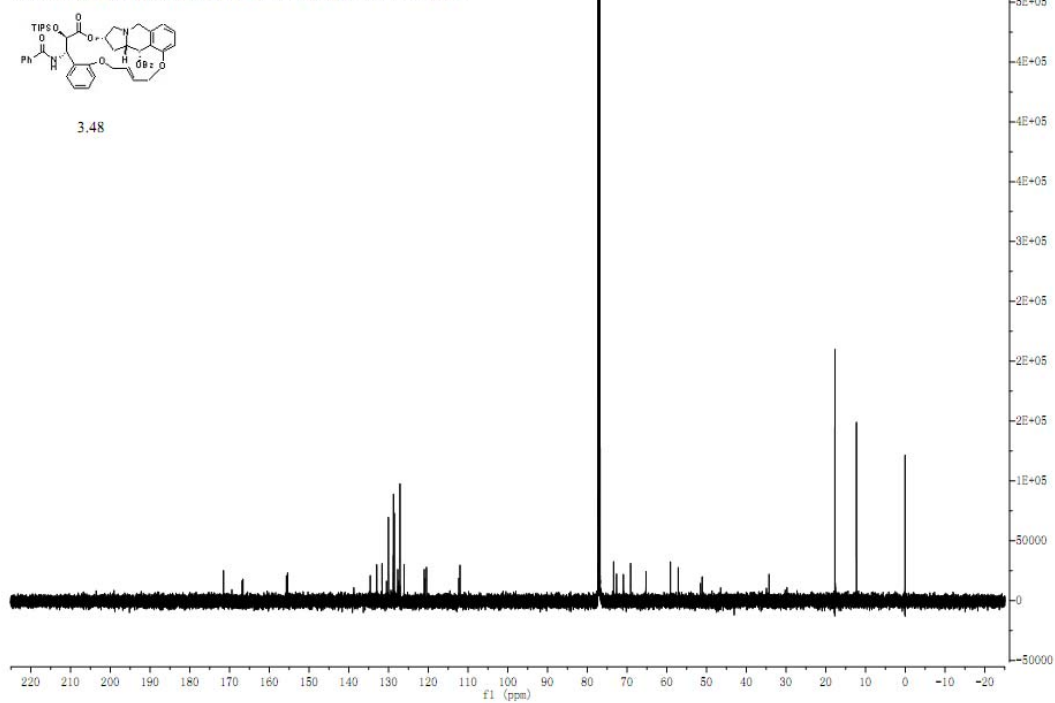
E:/documents/my project/nmr data/jz216-78-3carbon-1.jdf



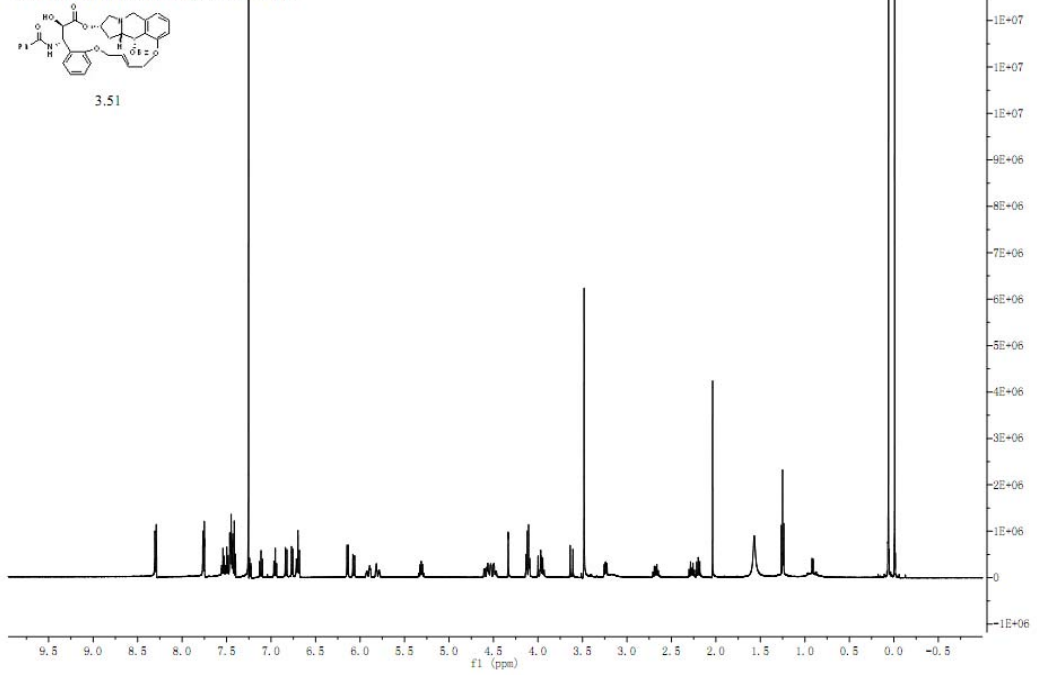
C:/Documents and Settings/Zhao/My Documents/Downloads/jz216-193-2proton-1.jdf



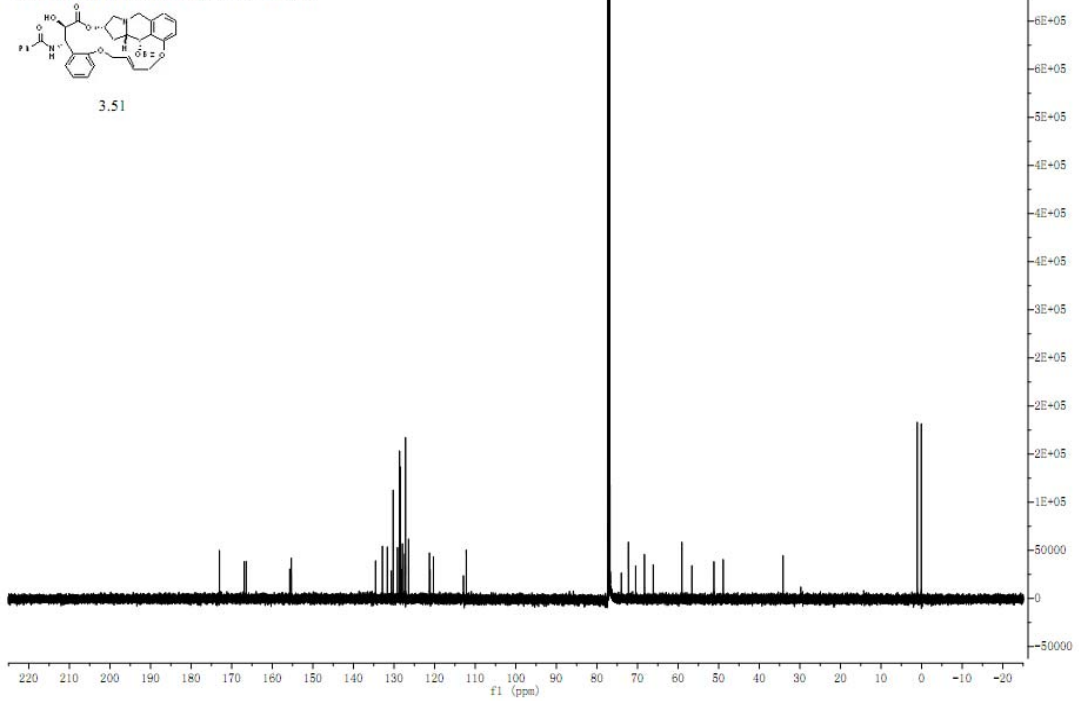
C:/Documents and Settings/Zhao/My Documents/Downloads/jz216-193-2carbon-1.jdf

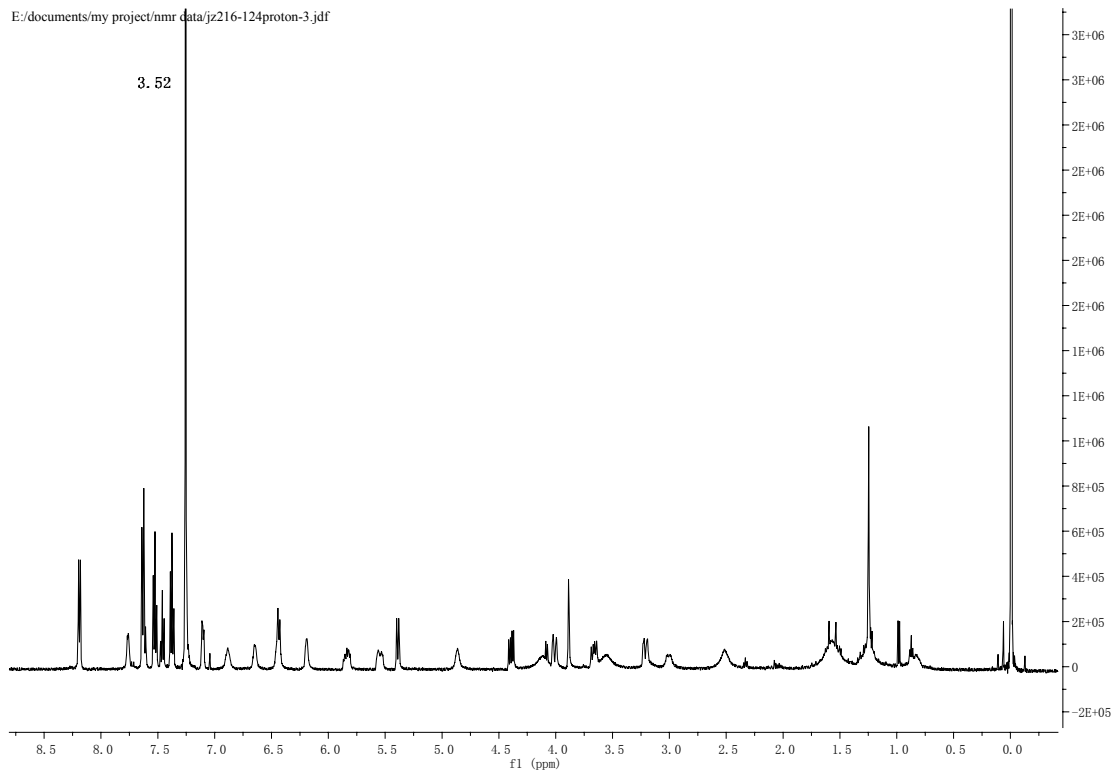
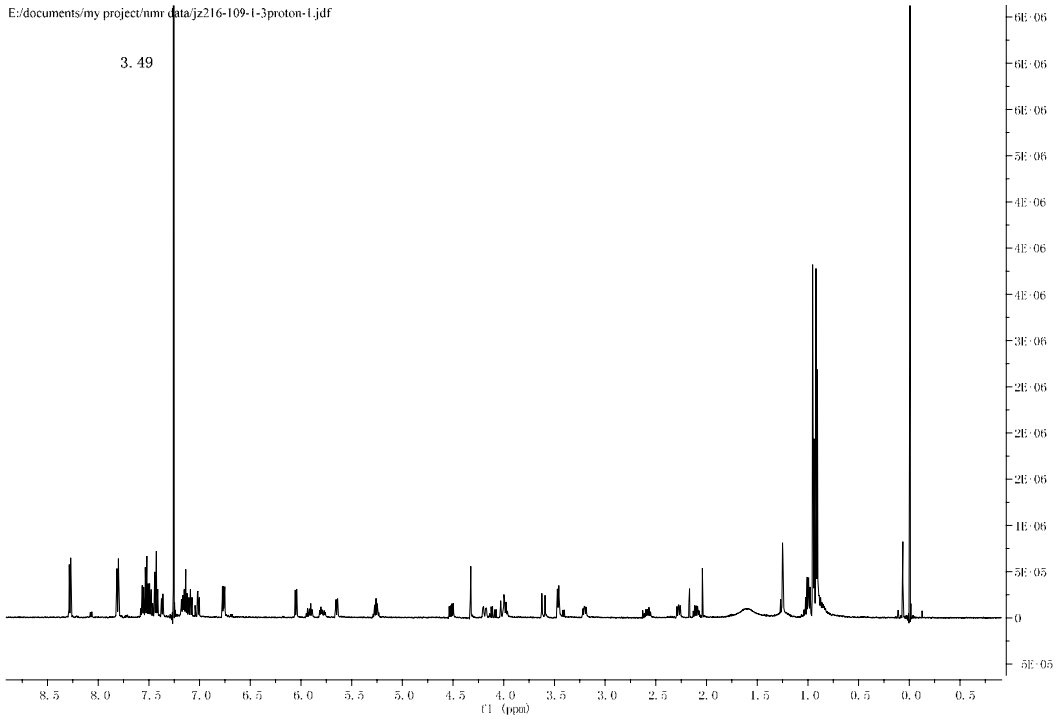


E:/documents/my project/nmr data/jz216-87ppmton-1.jdf

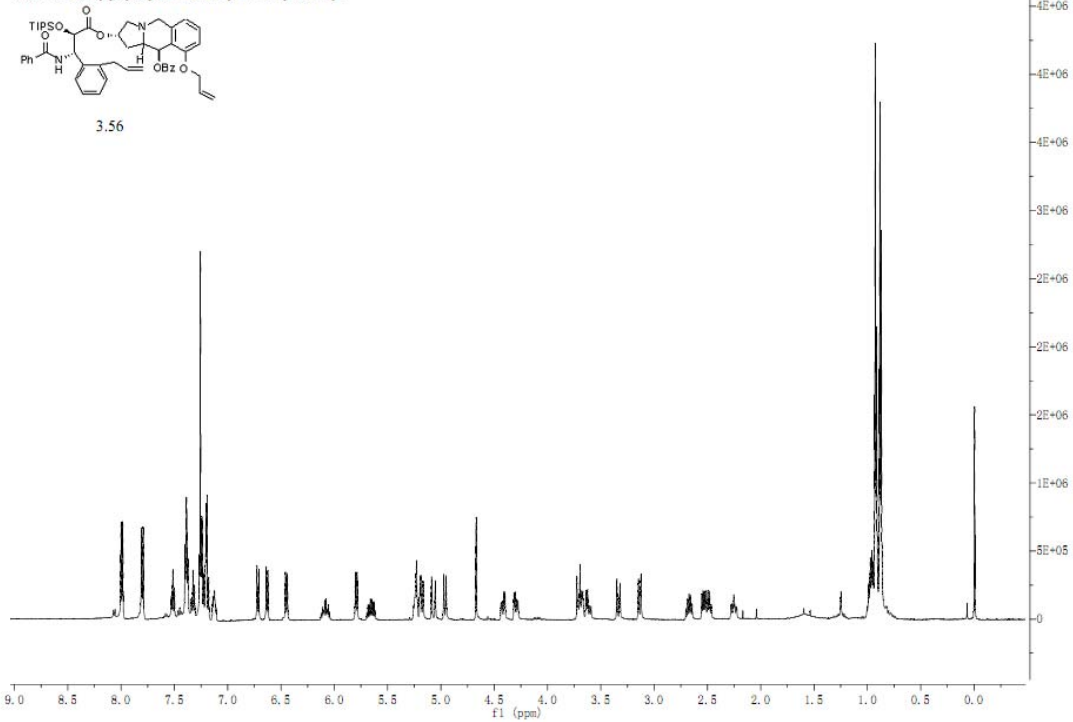


E:/documents/my project/nmr data/jz216-87carbon-1.jdf

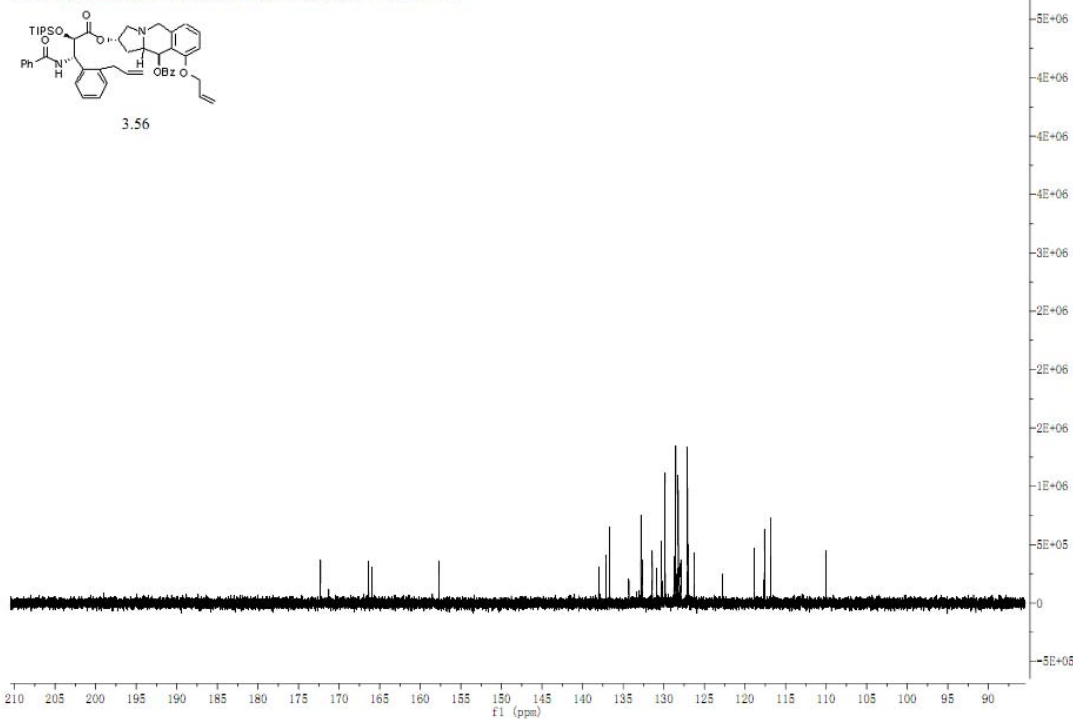




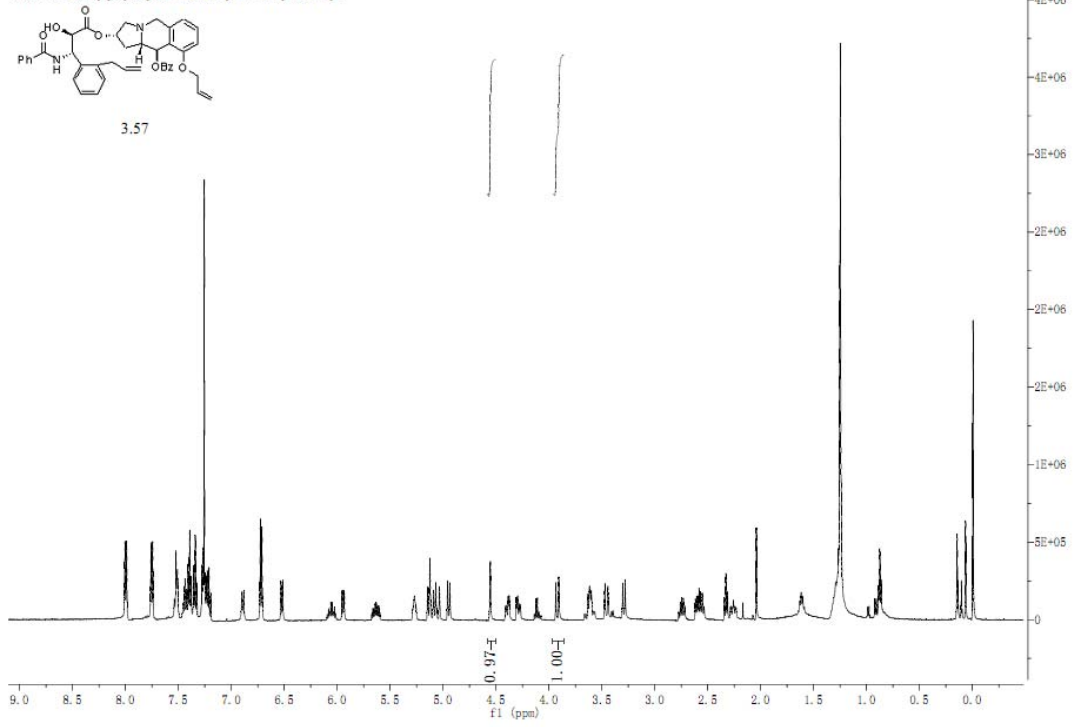
G:/documents/my project/jielu nmr data/jz216-122proton-1.jdf



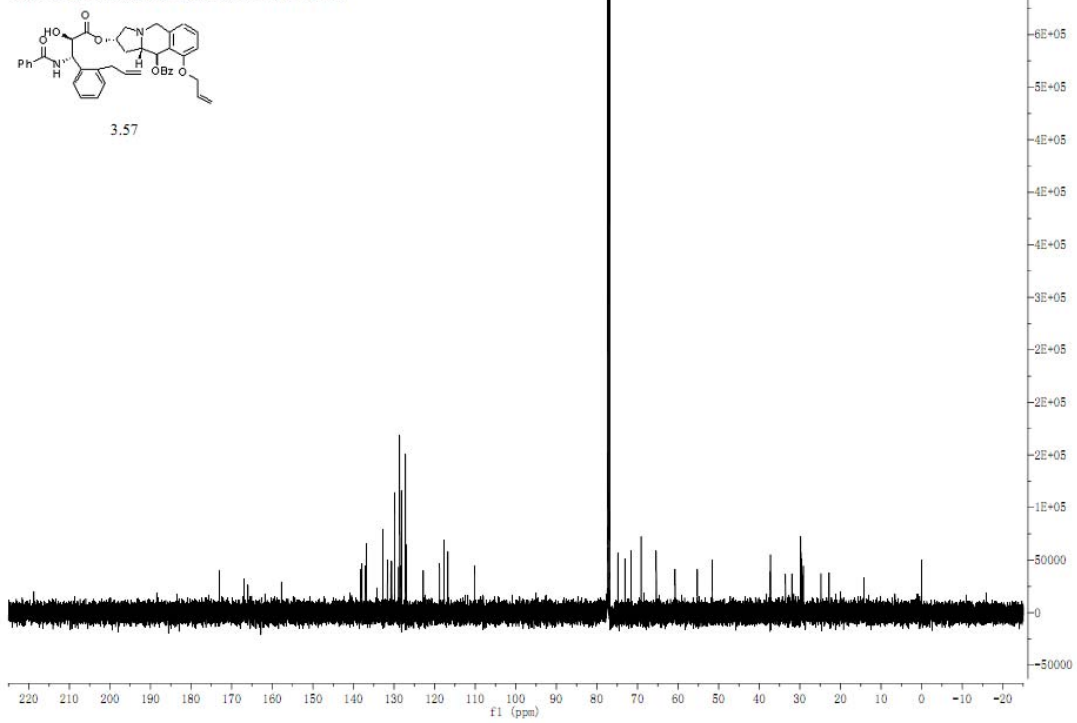
C:/Documents and Settings/Zhao/My Documents/Downloads/jz216-196carbon-1.jdf



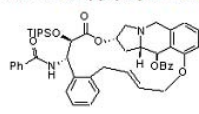
G:/documents/my project/jielu nmr data/jz216-126proton-1.jdf



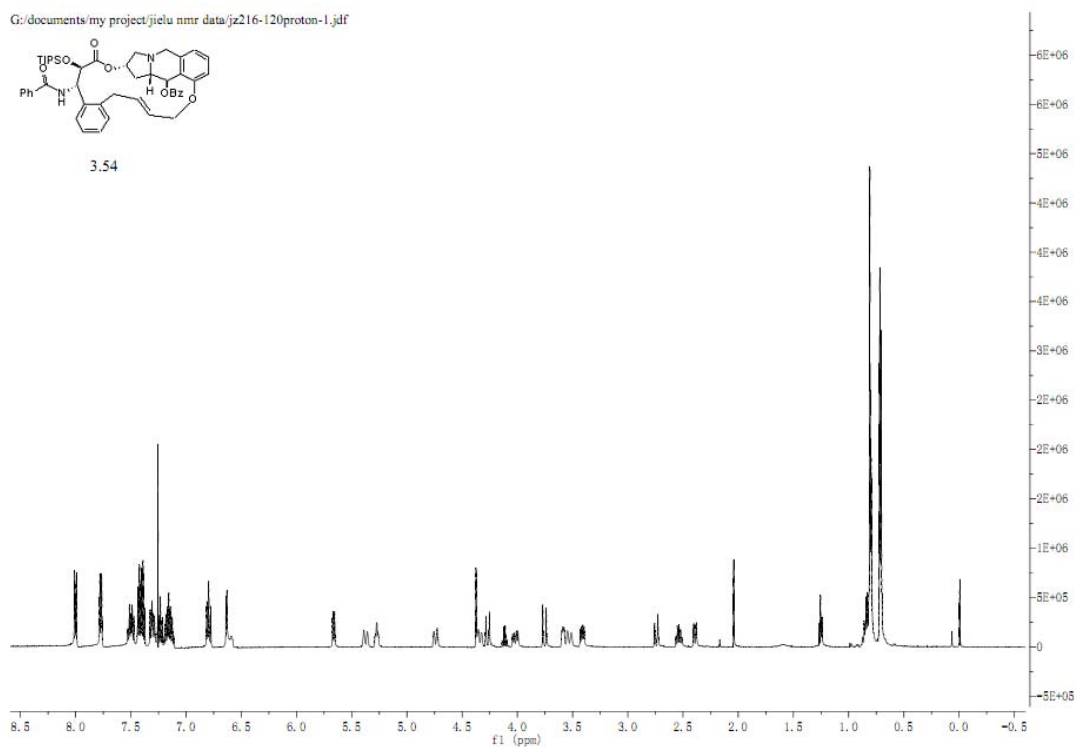
G:/documents/my project/jielu nmr data/jz216-126carbon-1.jdf



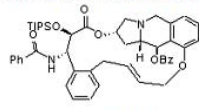
G:/documents/my project/jielu nmr data/jz216-120proton-1.jdf



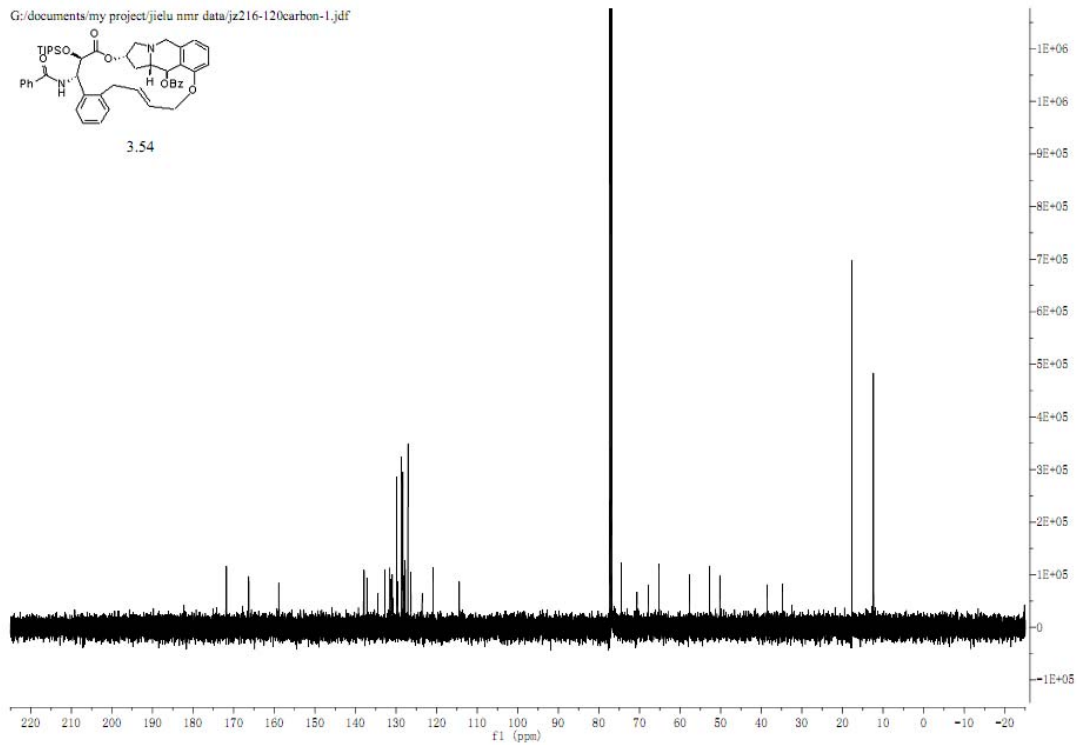
3.54



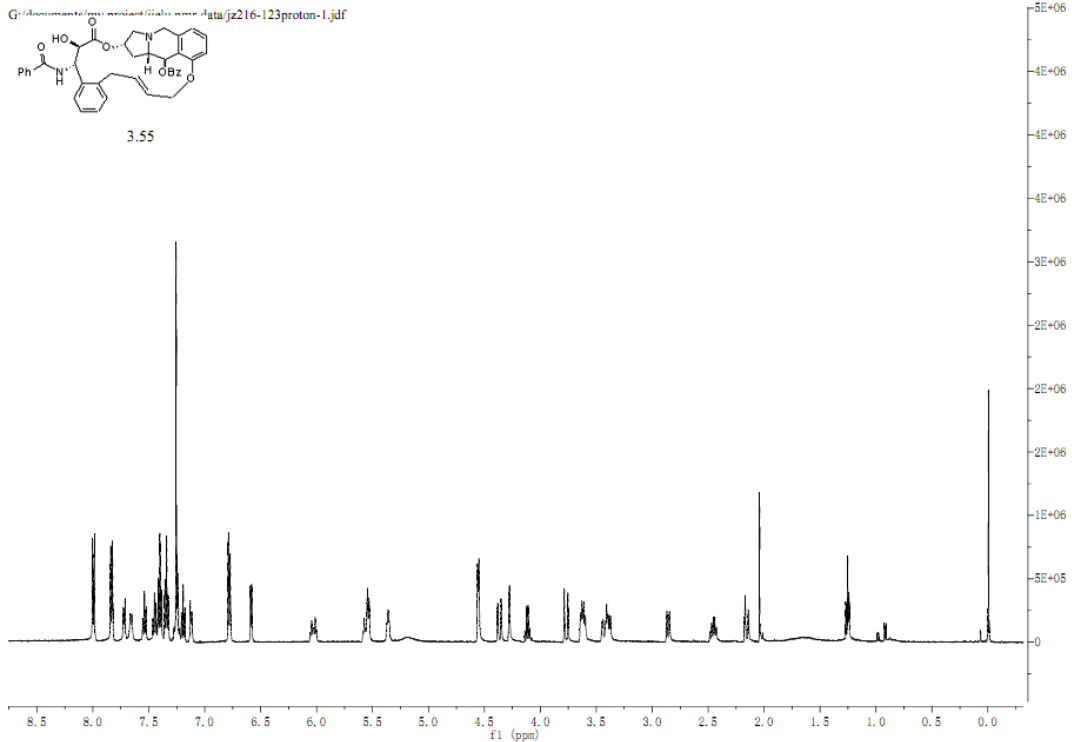
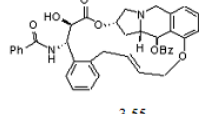
G:/documents/my project/jielu nmr data/jz216-120carbon-1.jdf



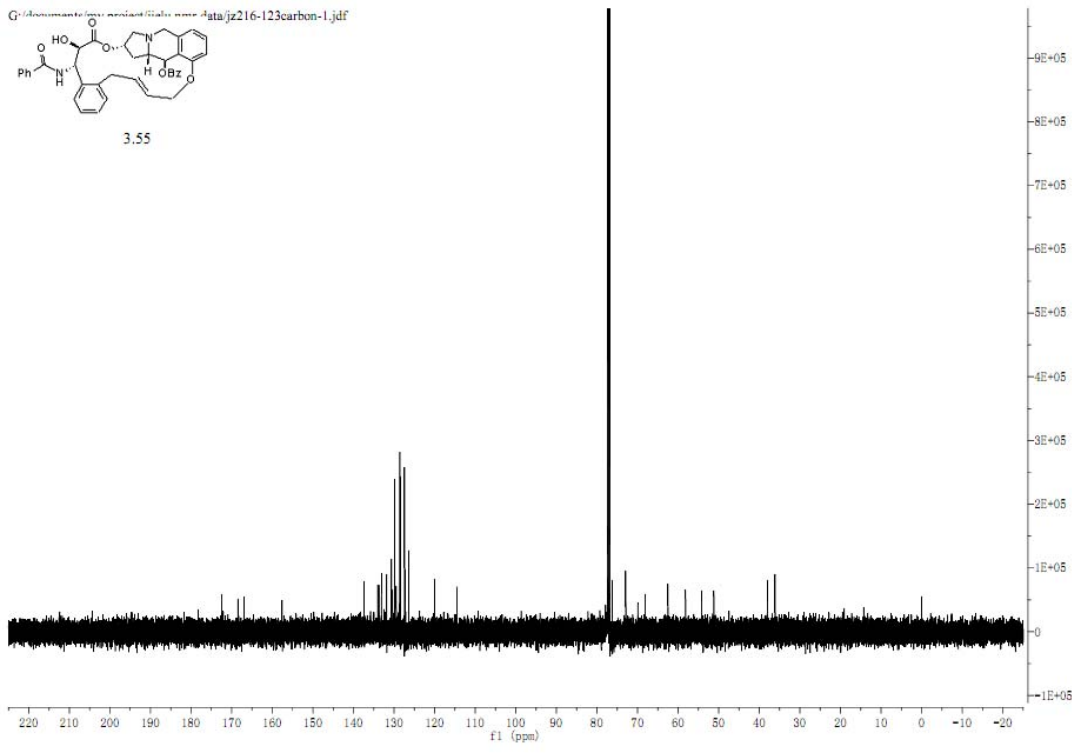
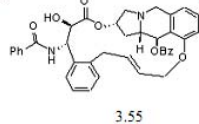
3.54



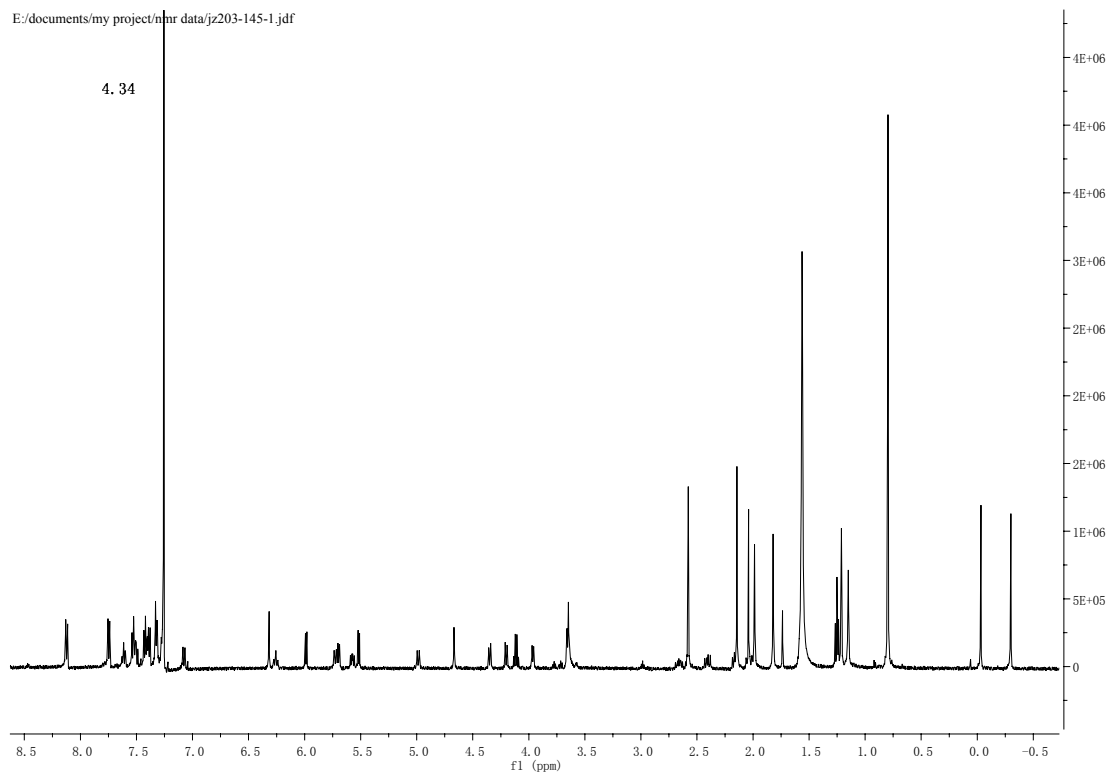
G:\Anonimato\files\residuo\files\nmr\data\jz216-123proton-1.jdf



G:\Anonimato\files\residuo\files\nmr\data\jz216-123carbon-1.jdf

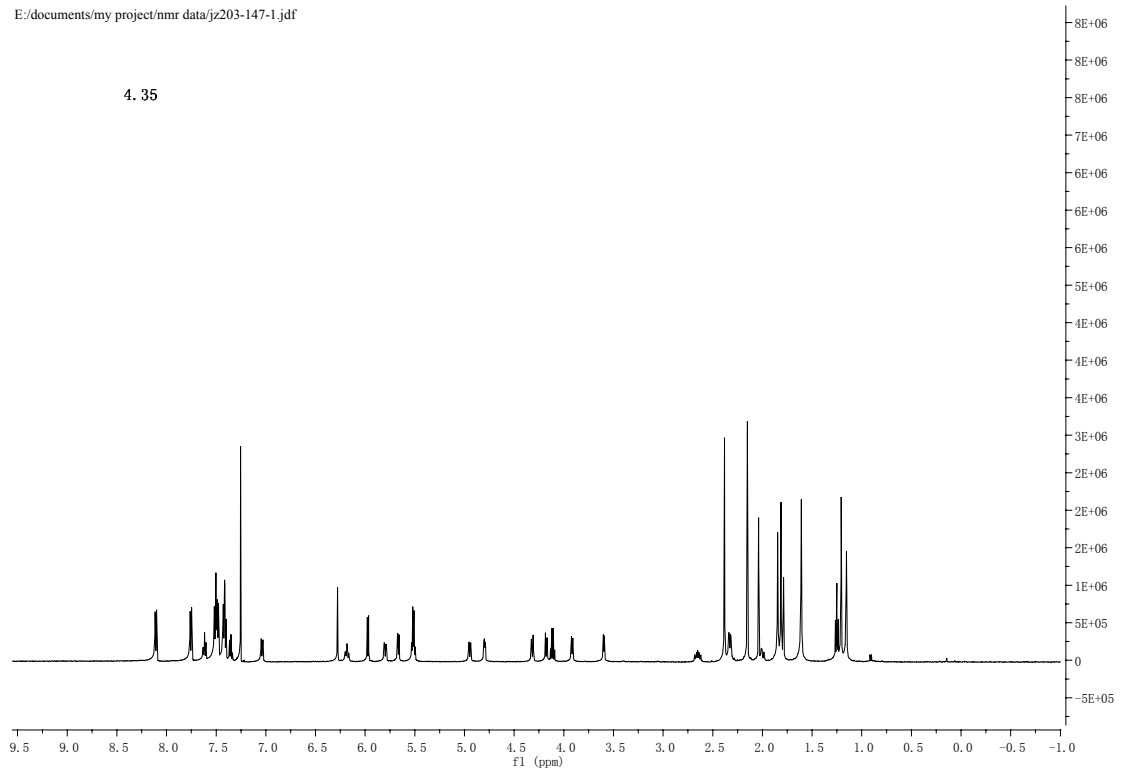


E:/documents/my project/nmr data/jz203-145-1.jdf



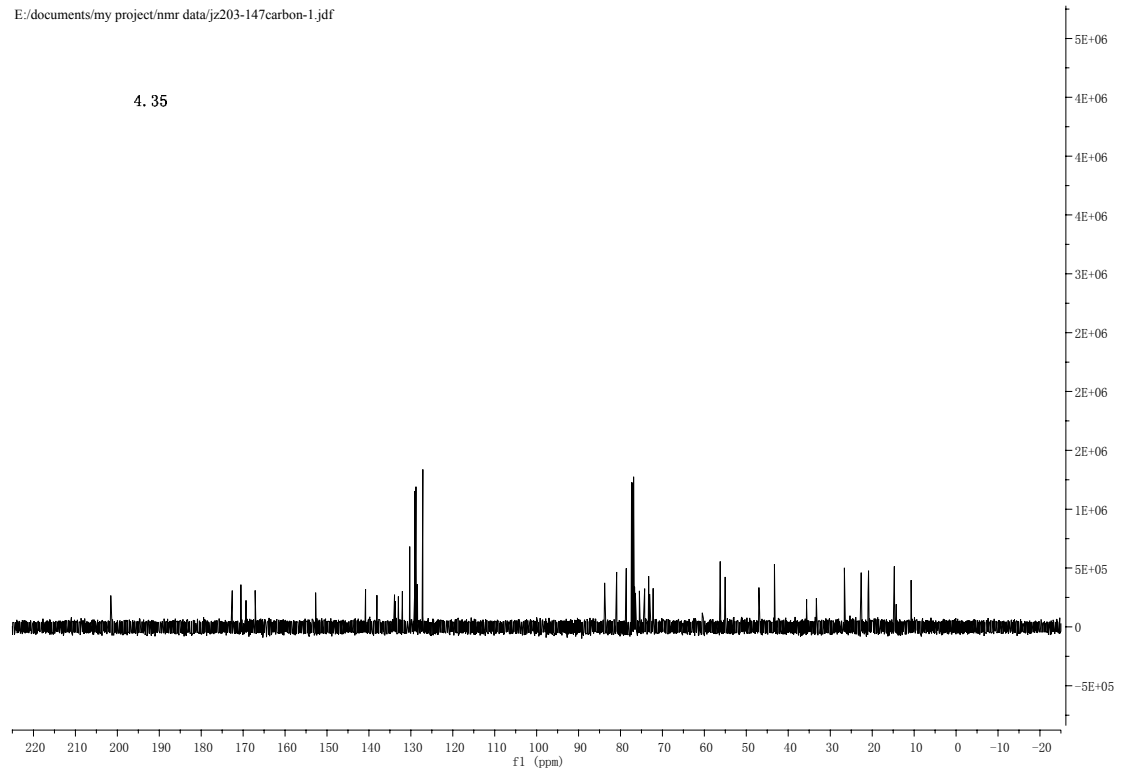
E:/documents/my project/nmr data/jz203-147-1.jdf

4.35

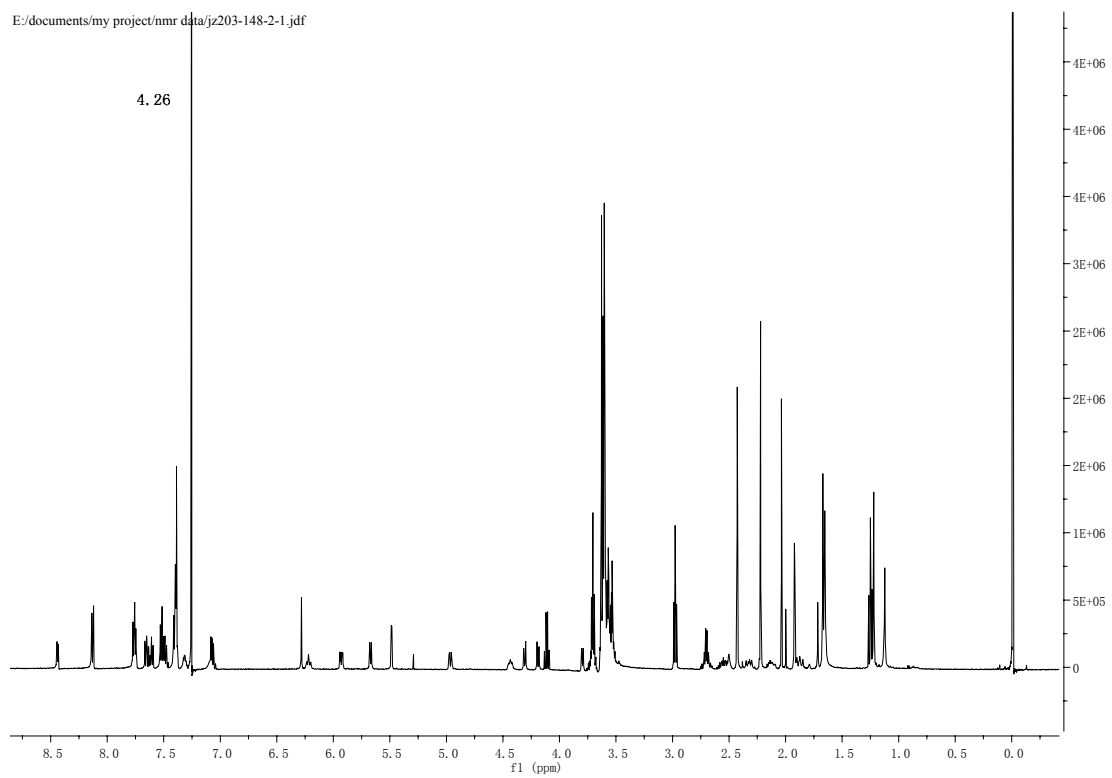


E:/documents/my project/nmr data/jz203-147carbon-1.jdf

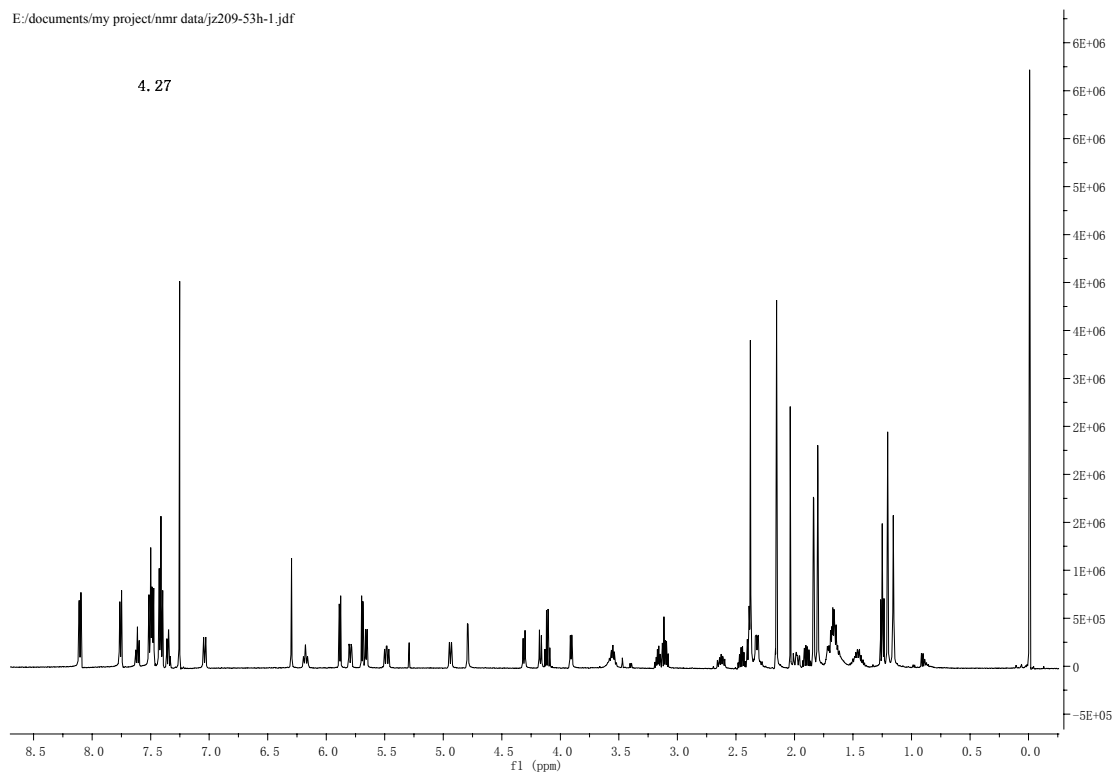
4.35



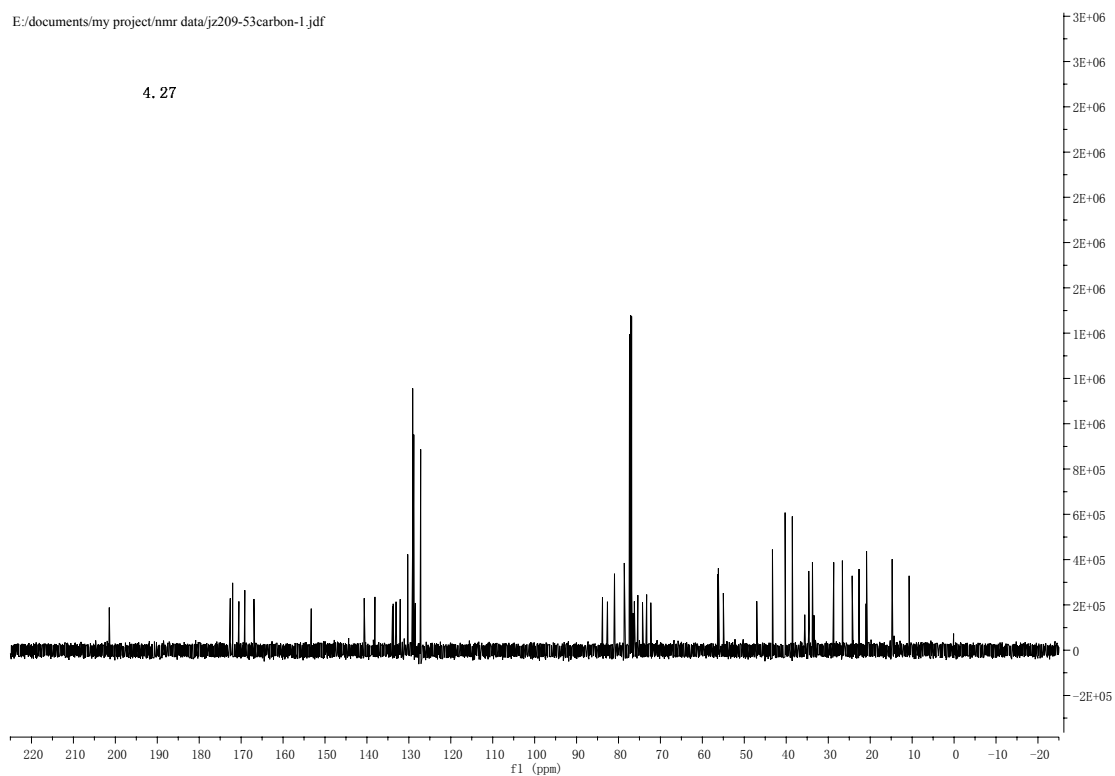
E:/documents/my project/nmr data/jz203-148-2-1.jdf



E:/documents/my project/nmr data/jz209-53h-1.jdf

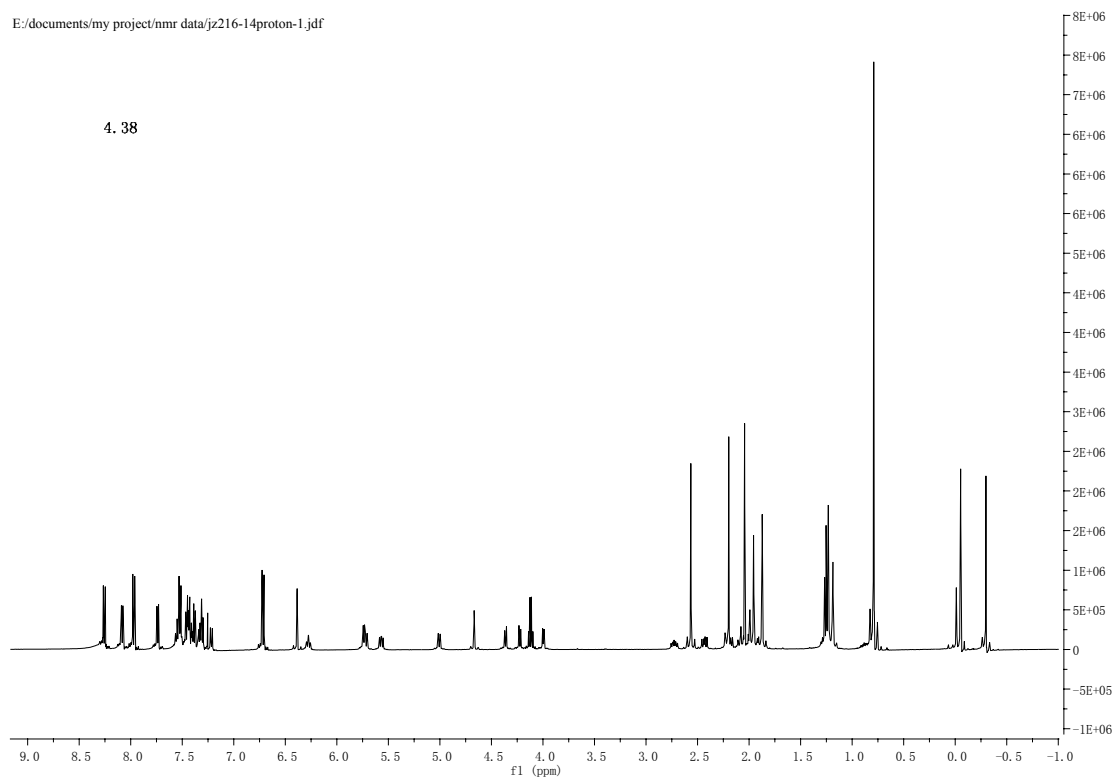


E:/documents/my project/nmr data/jz209-53carbon-1.jdf



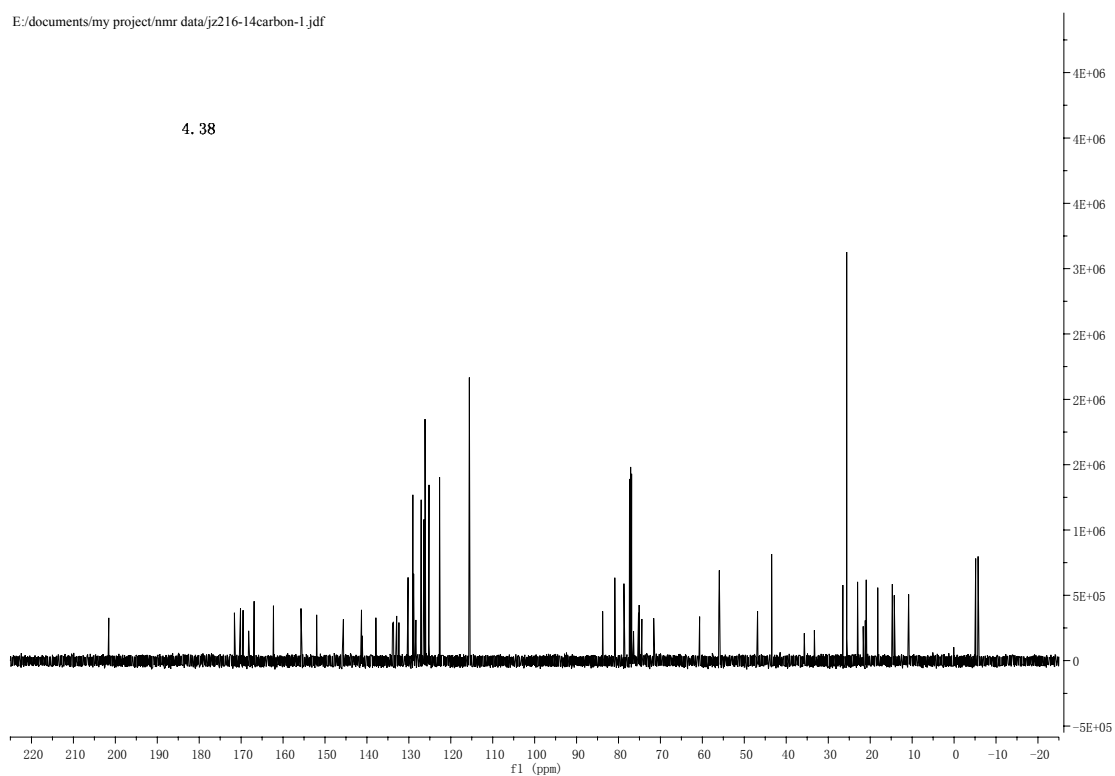
E:/documents/my project/nmr data/jz216-14proton-1.jdf

4. 38



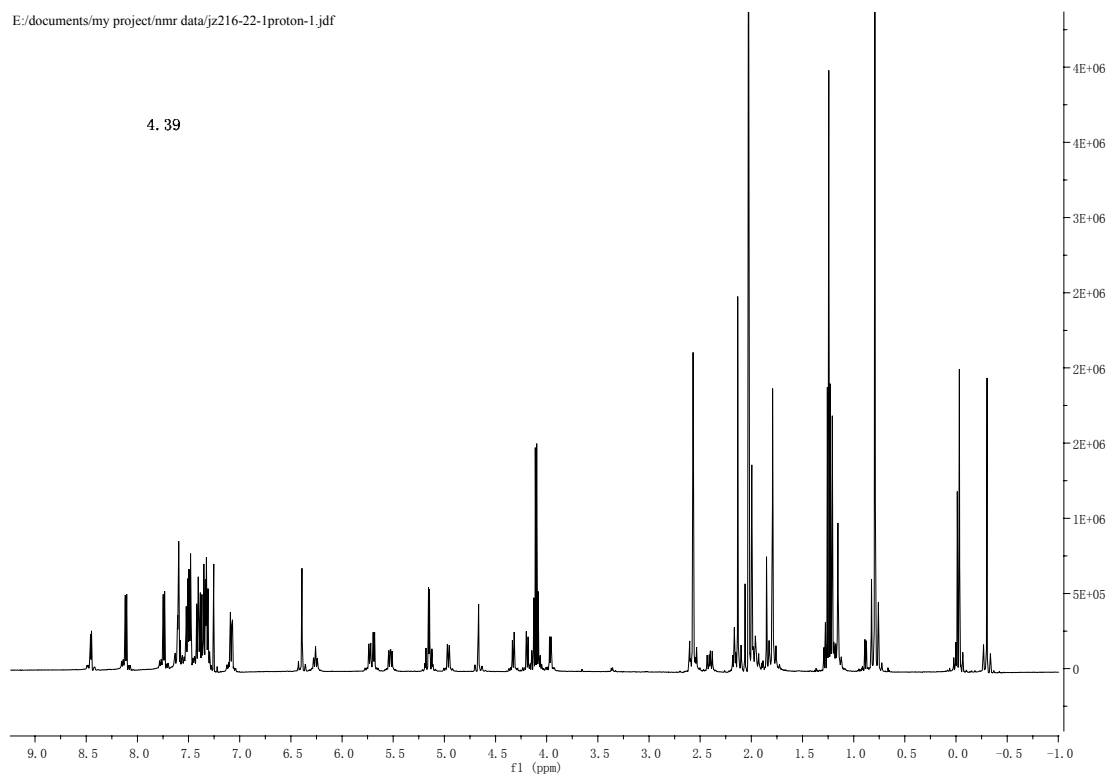
E:/documents/my project/nmr data/jz216-14carbon-1.jdf

4. 38



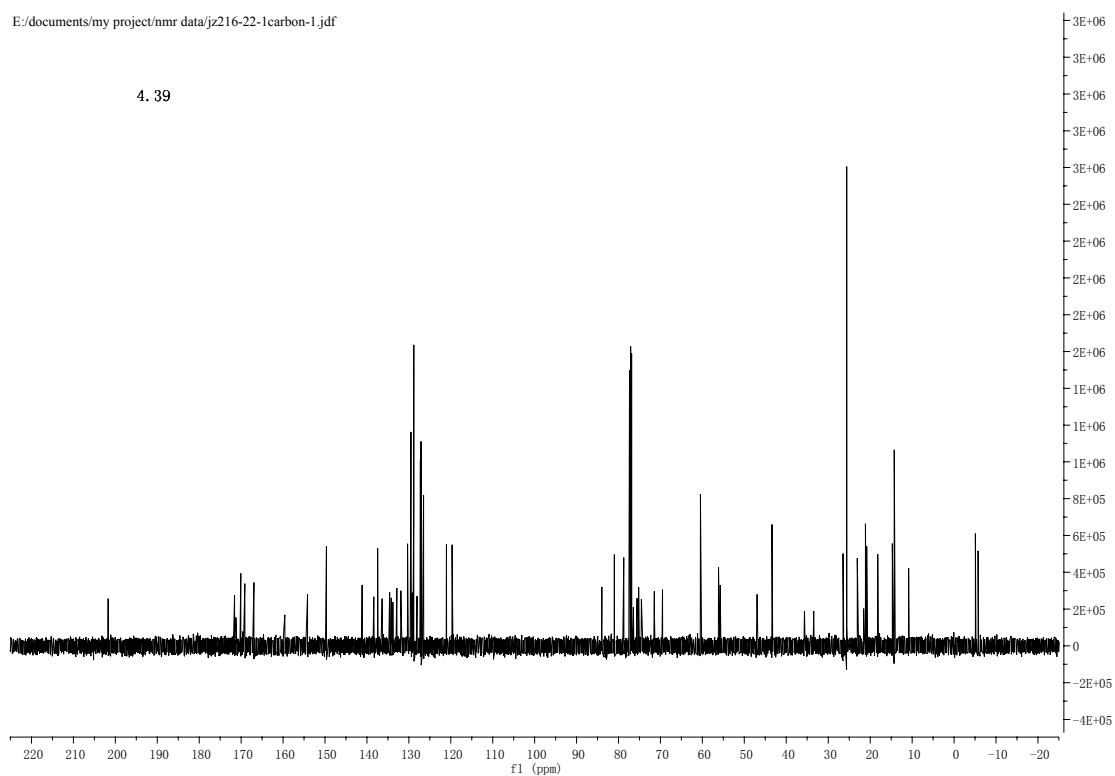
E:/documents/my project/nmr data/jz216-22-1proton-1.jdf

4.39



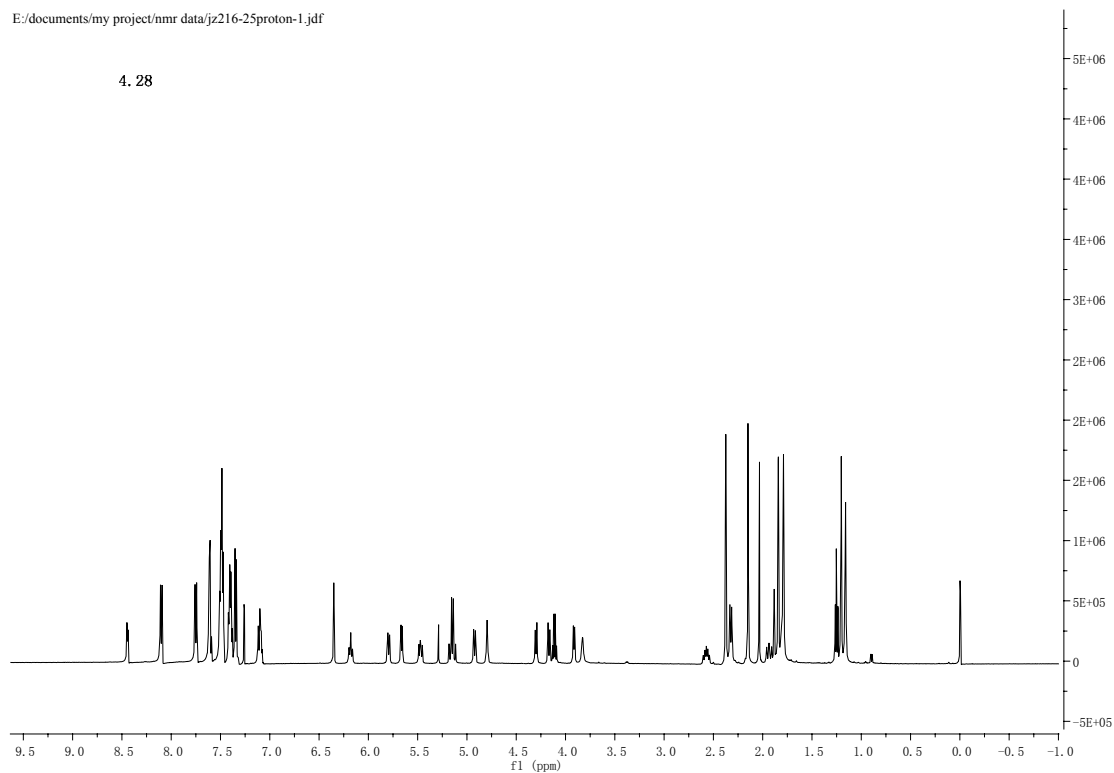
E:/documents/my project/nmr data/jz216-22-1carbon-1.jdf

4.39



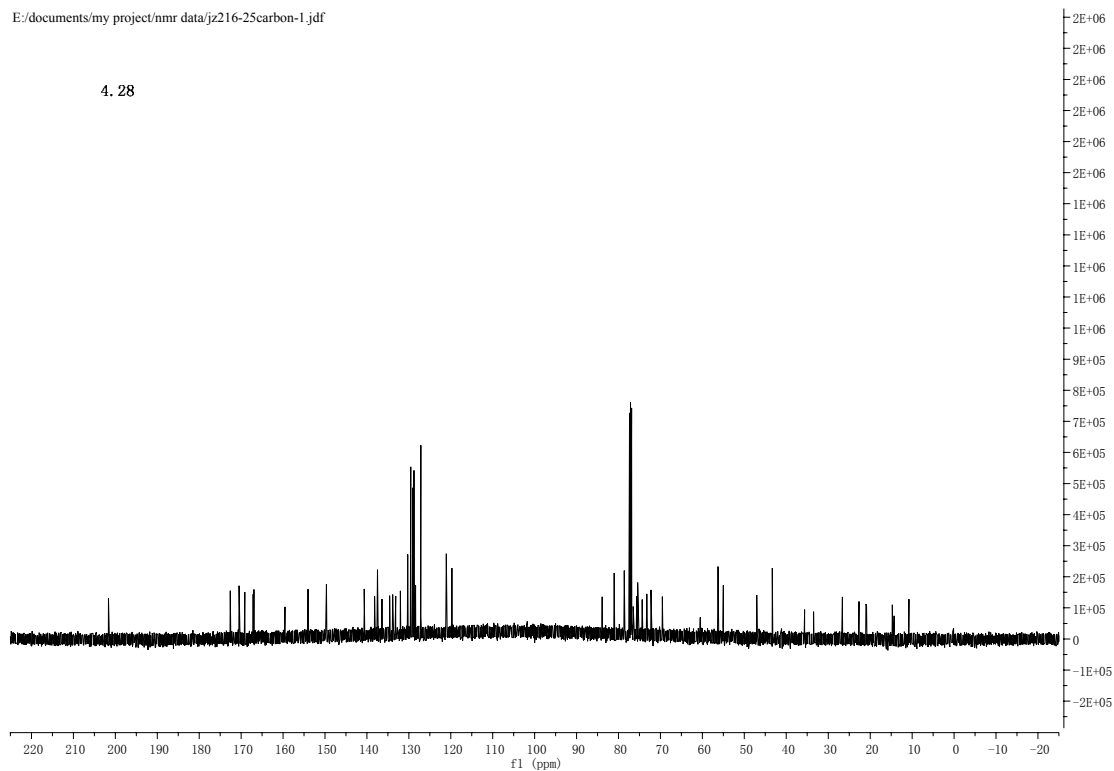
E:/documents/my project/nmr data/jz216-25proton-1.jdf

4.28



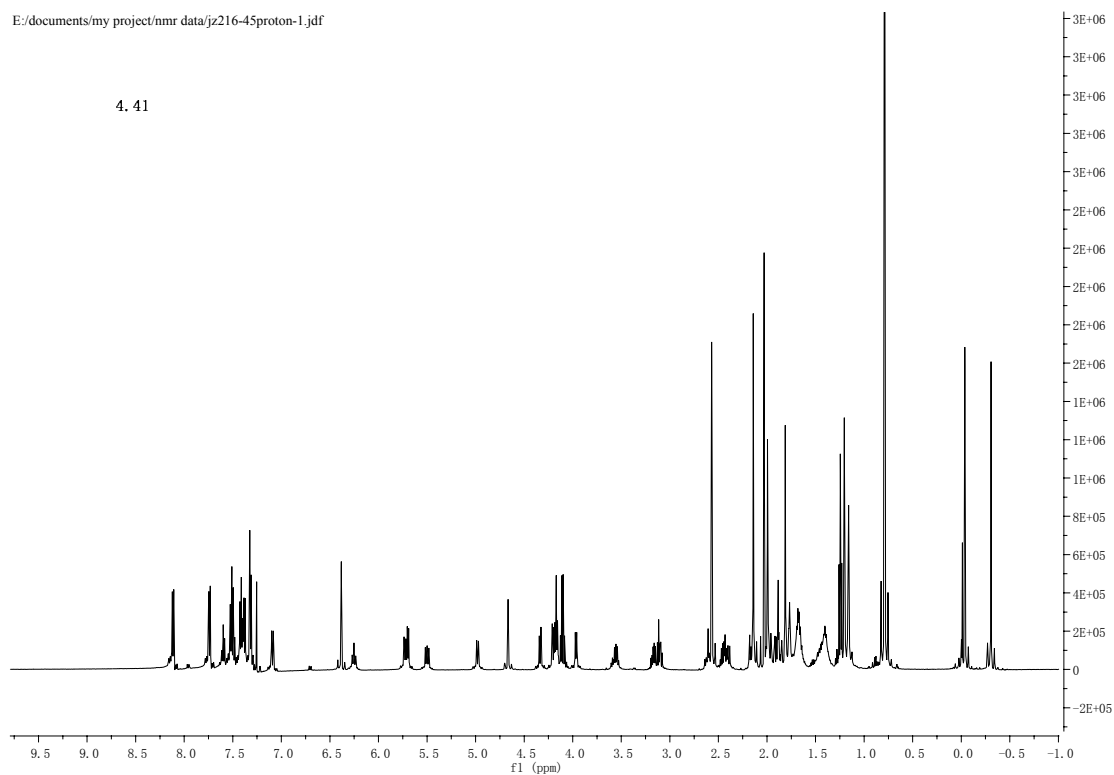
E:/documents/my project/nmr data/jz216-25carbon-1.jdf

4.28



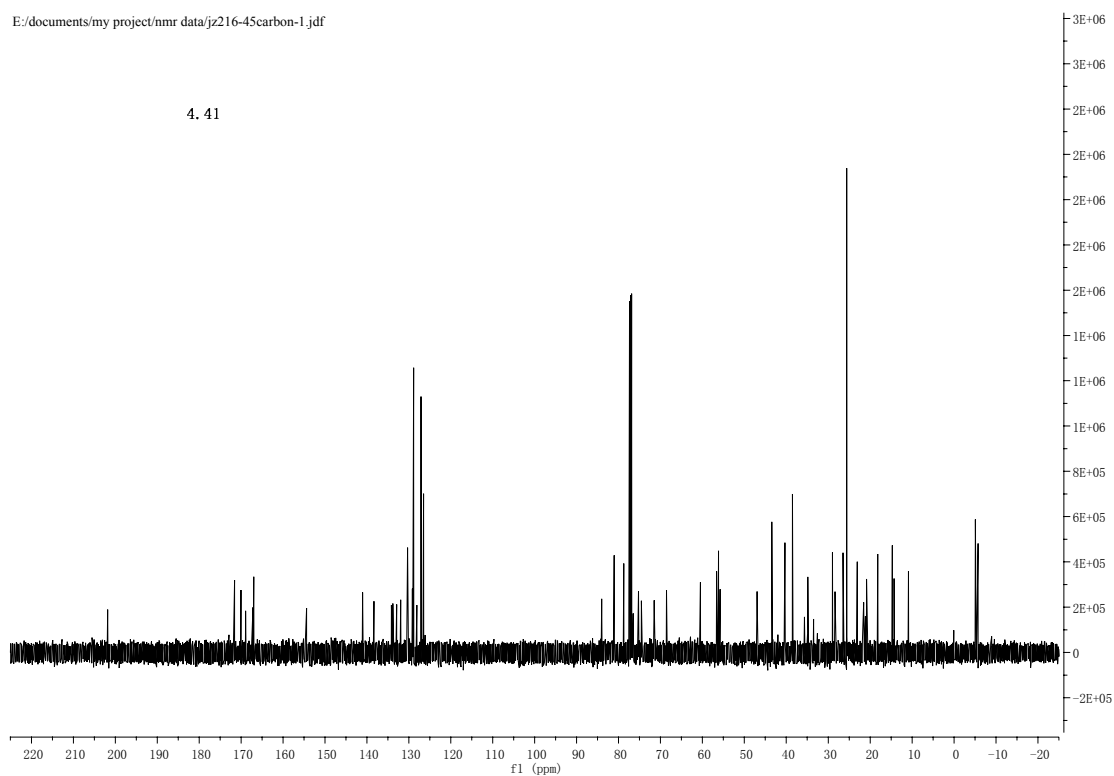
E:/documents/my project/nmr data/jz216-45proton-1.jdf

4.41



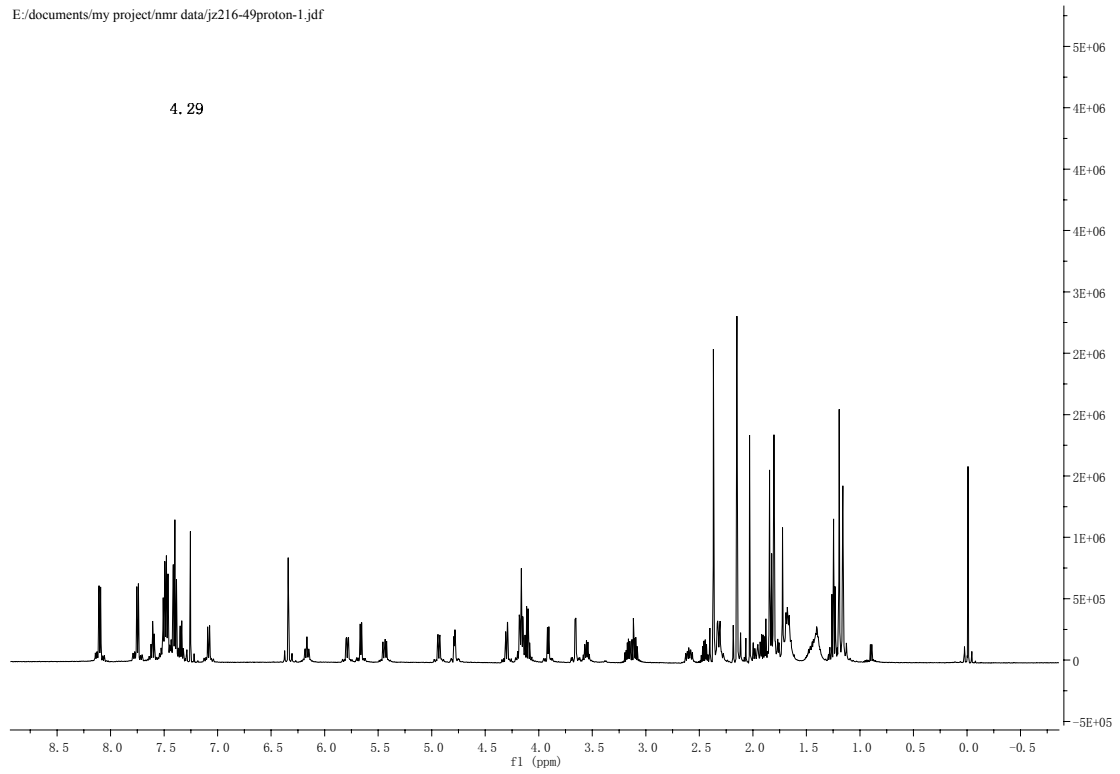
E:/documents/my project/nmr data/jz216-45carbon-1.jdf

4.41



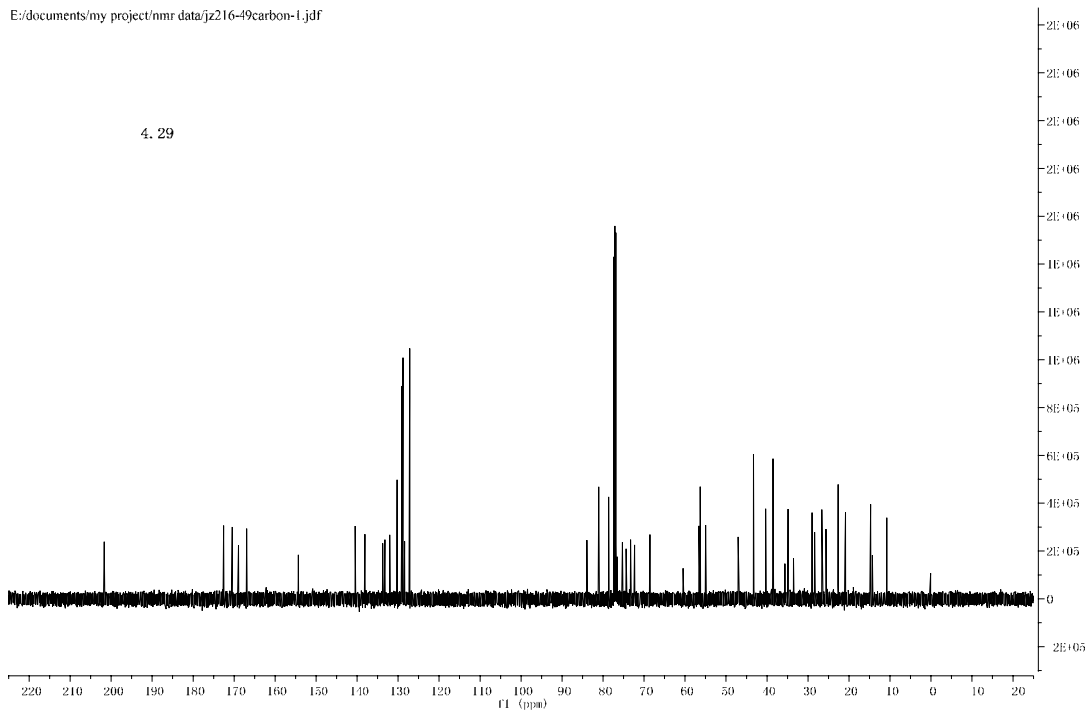
E:/documents/my project/nmr data/jz216-49proton-1.jdf

4. 29



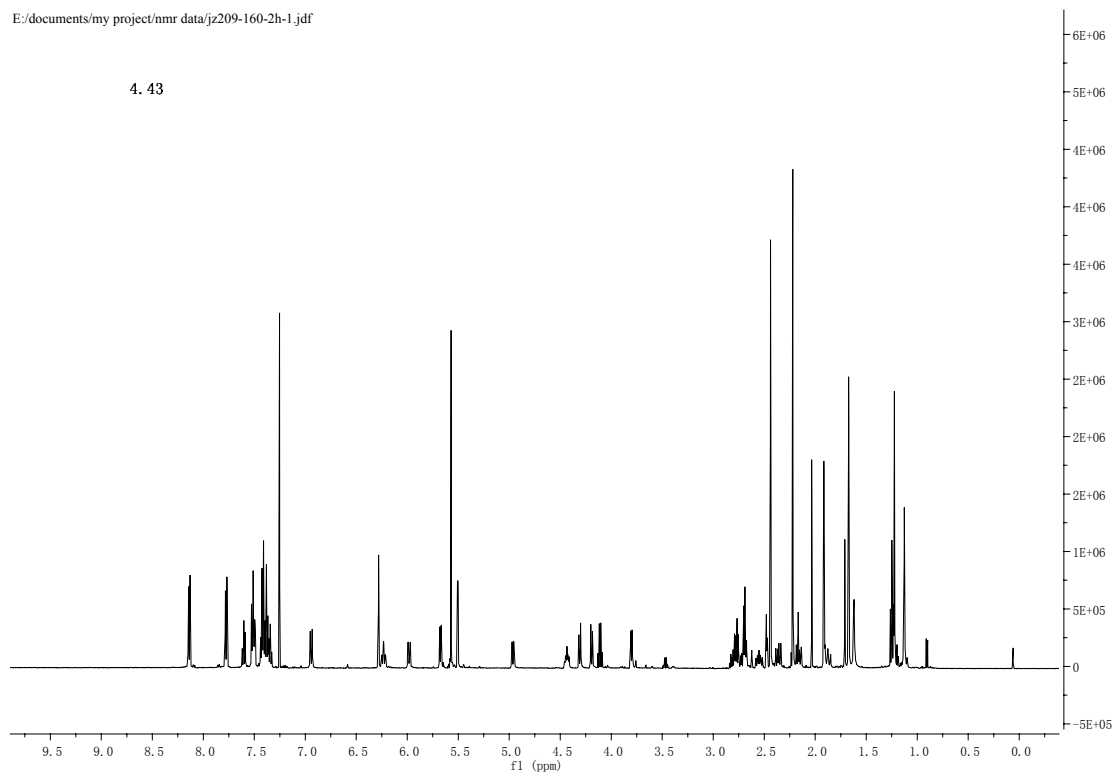
E:/documents/my project/nmr data/jz216-49carbon-1.jdf

4. 29



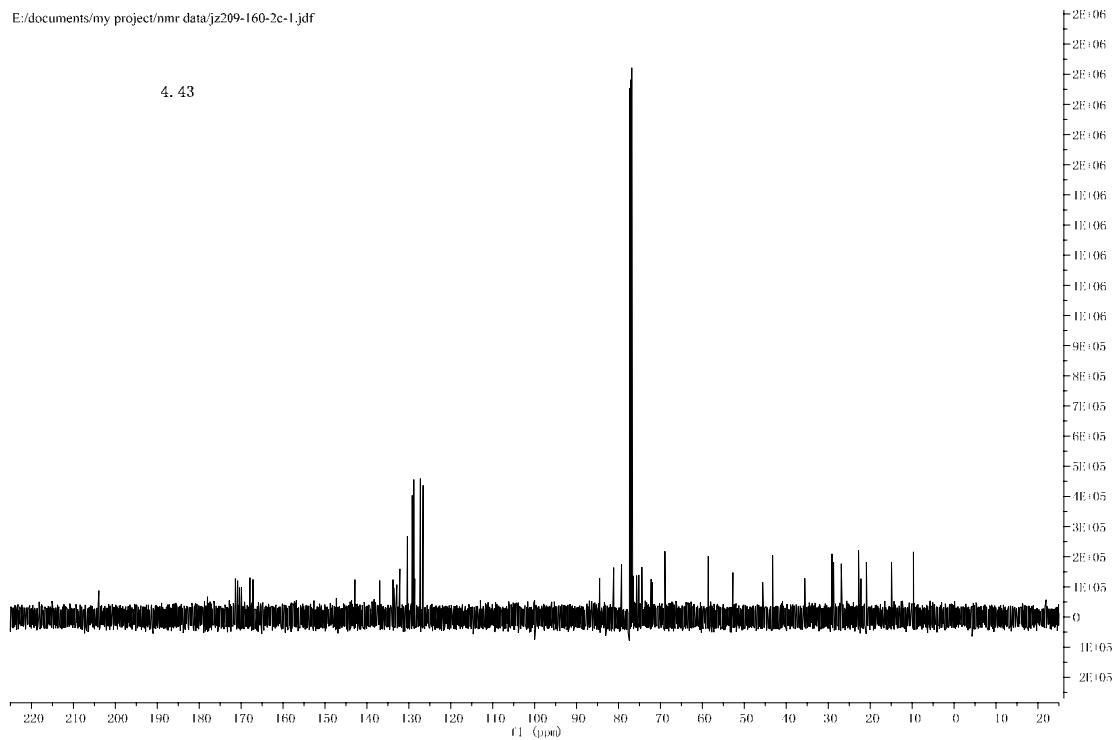
E:/documents/my project/nmr data/jz209-160-2h-1.jdf

4.43

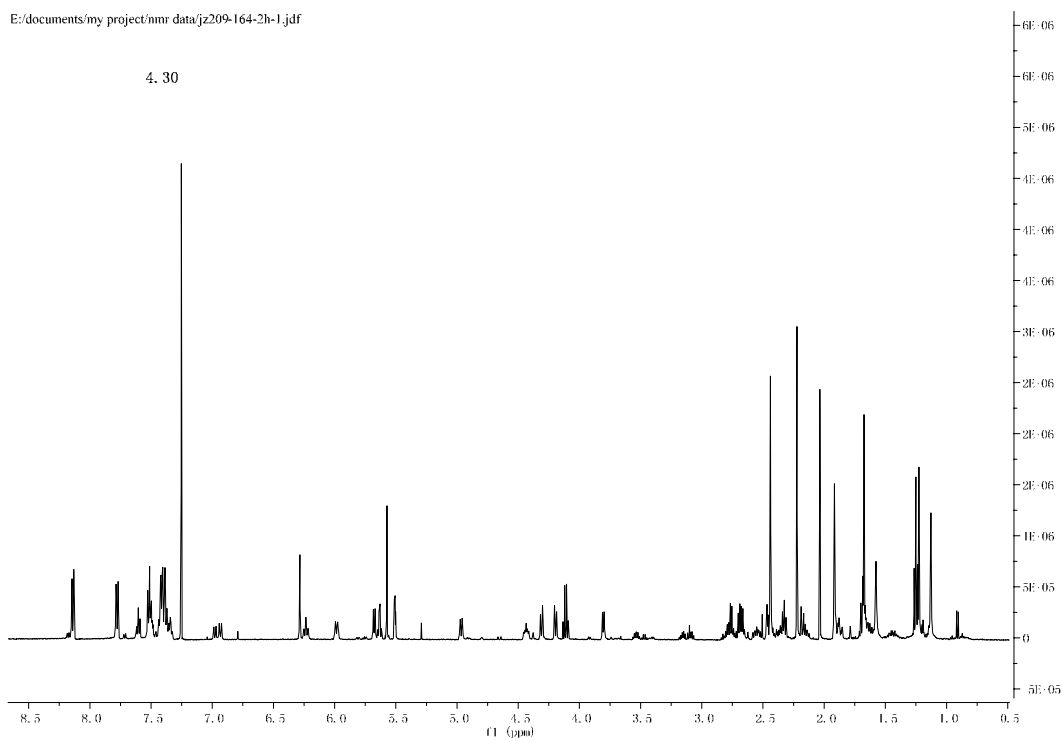


E:/documents/my project/nmr data/jz209-160-2c-1.jdf

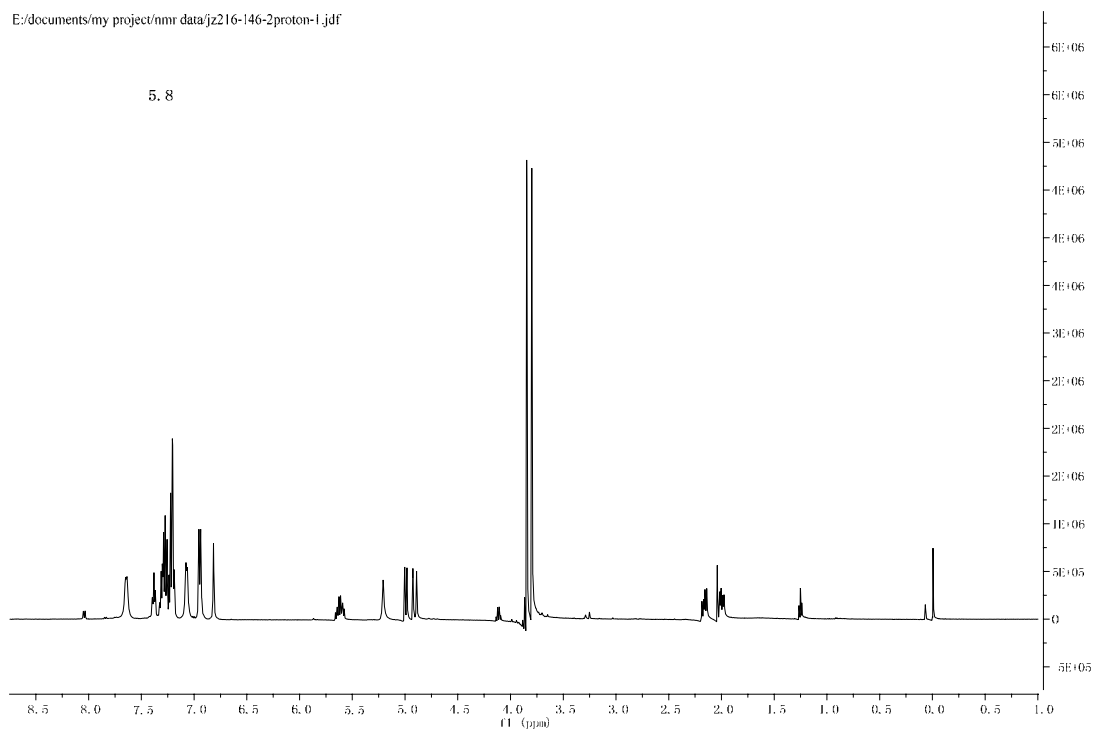
4.43



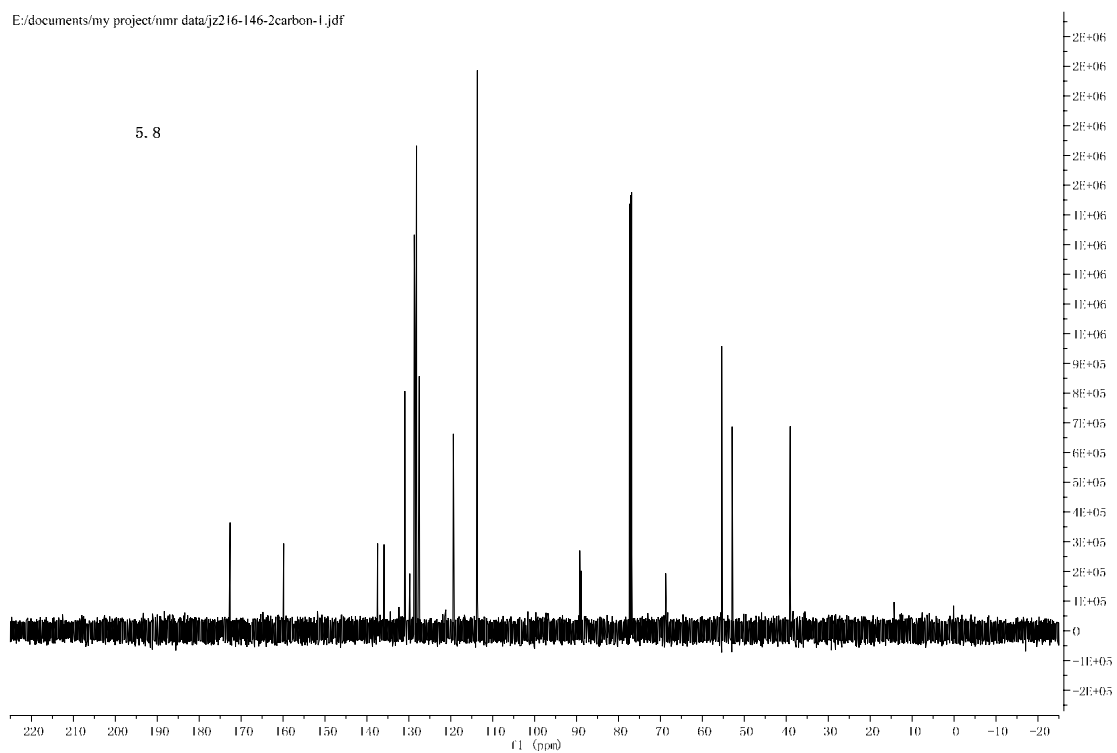
E:/documents/my project/nmr data/jz209-164-2h-1.jdf



E:/documents/my project/nmr data/jz216-146-2proton-1.jdf

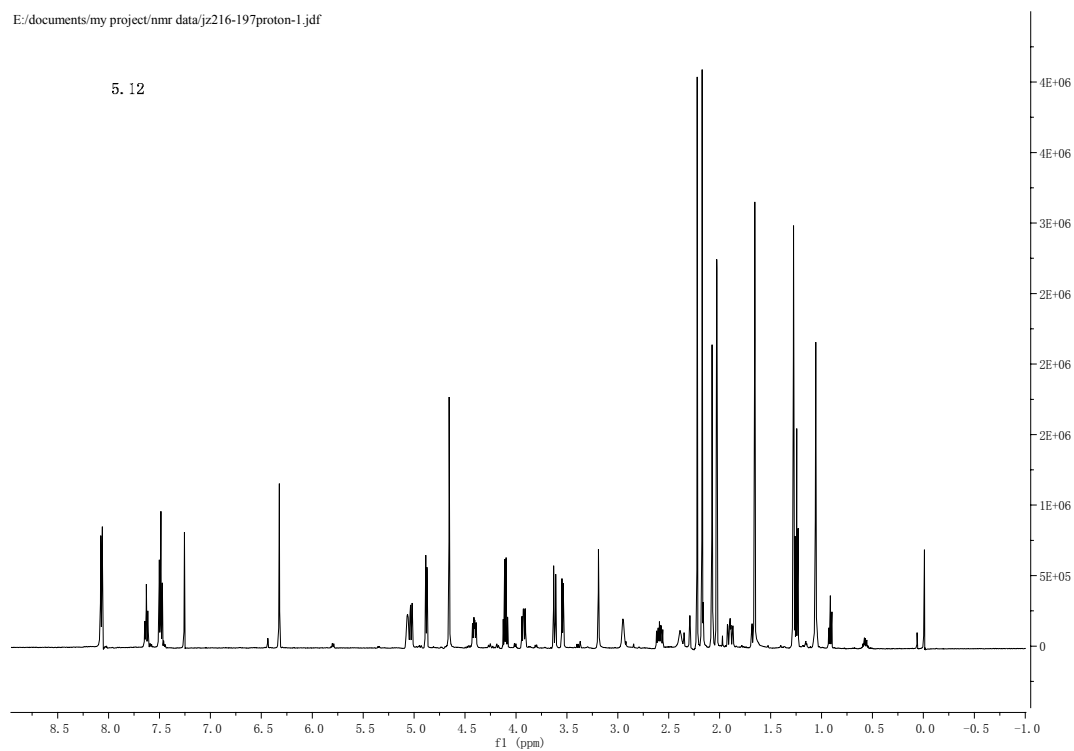


E:/documents/my project/nmr data/jz216-146-2carbon-1.jdf



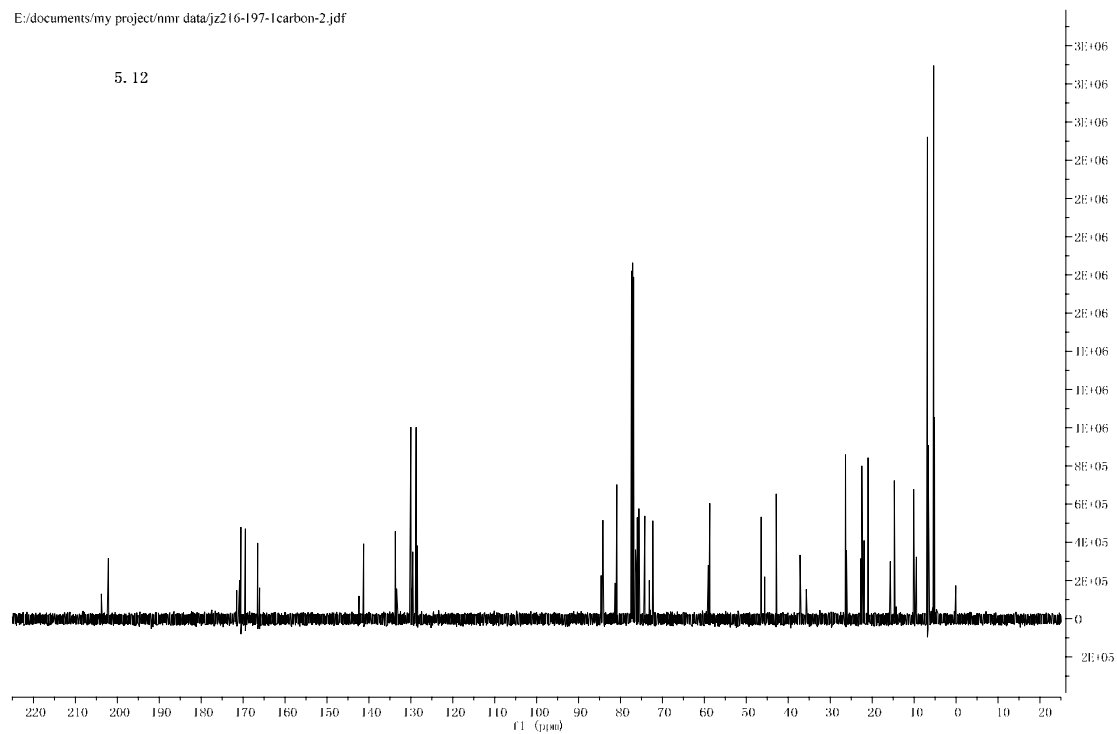
E:/documents/my project/nmr data/jz216-197proton-1.jdf

5. 12



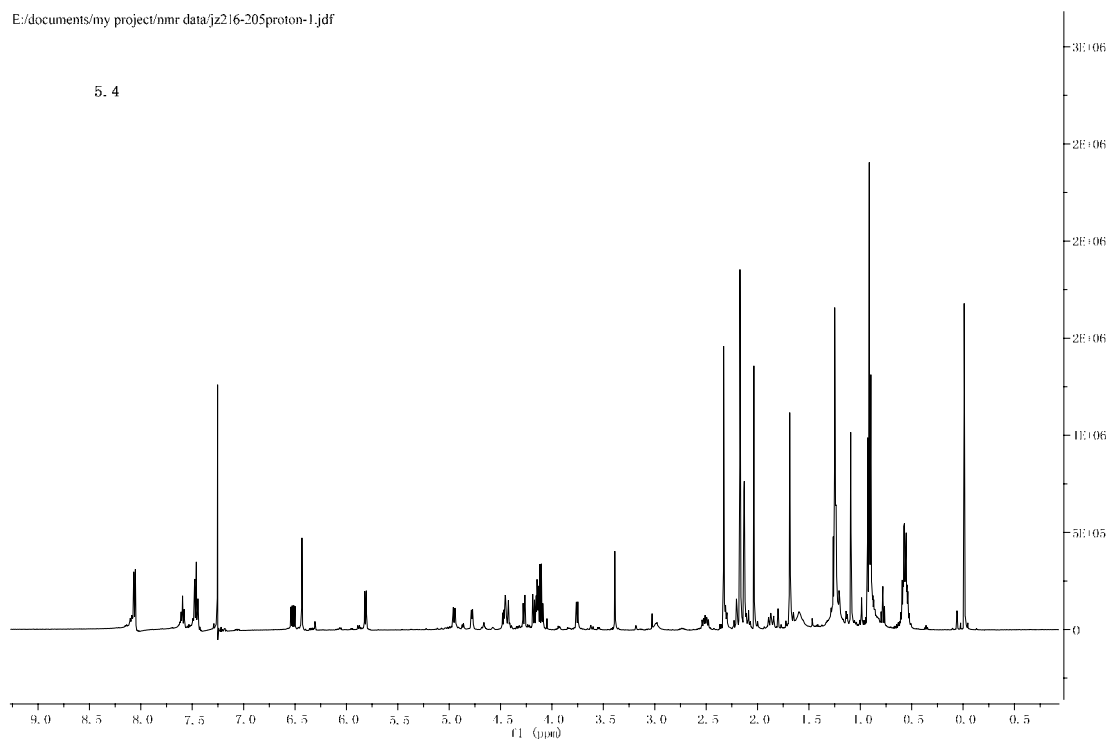
E:/documents/my project/nmr data/jz216-197-1carbon-2.jdf

5. 12



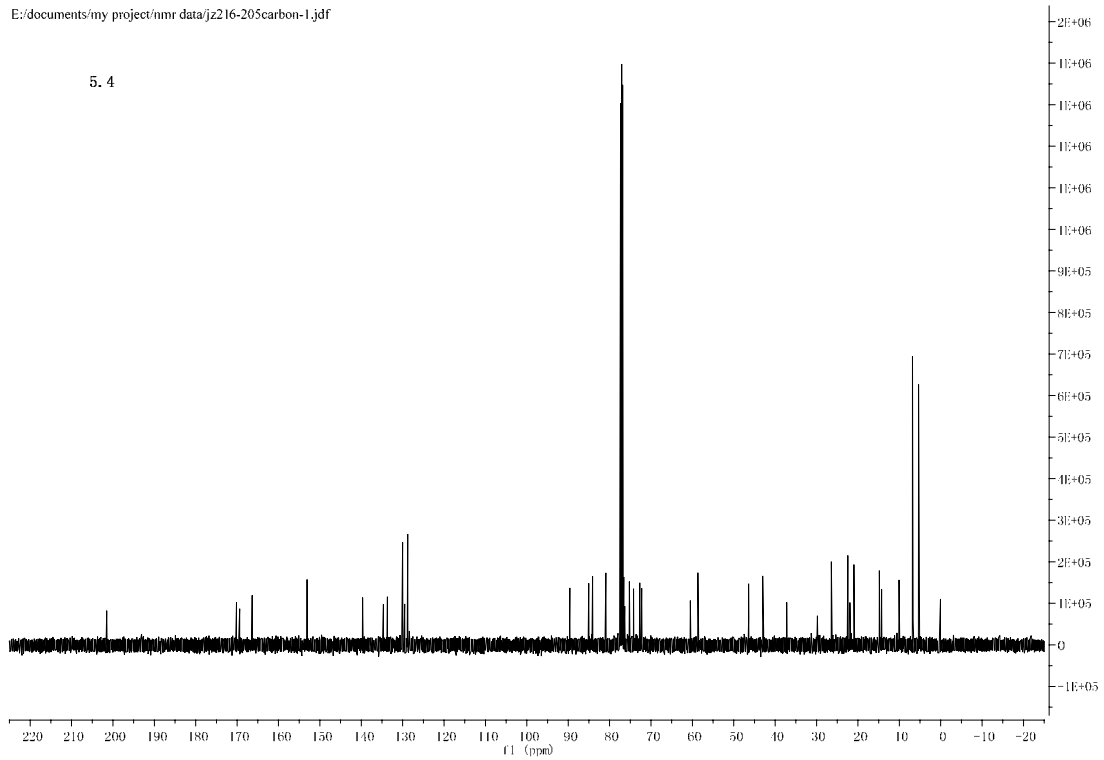
E:/documents/my project/nmr data/jz216-205proton-1.jdf

5.4



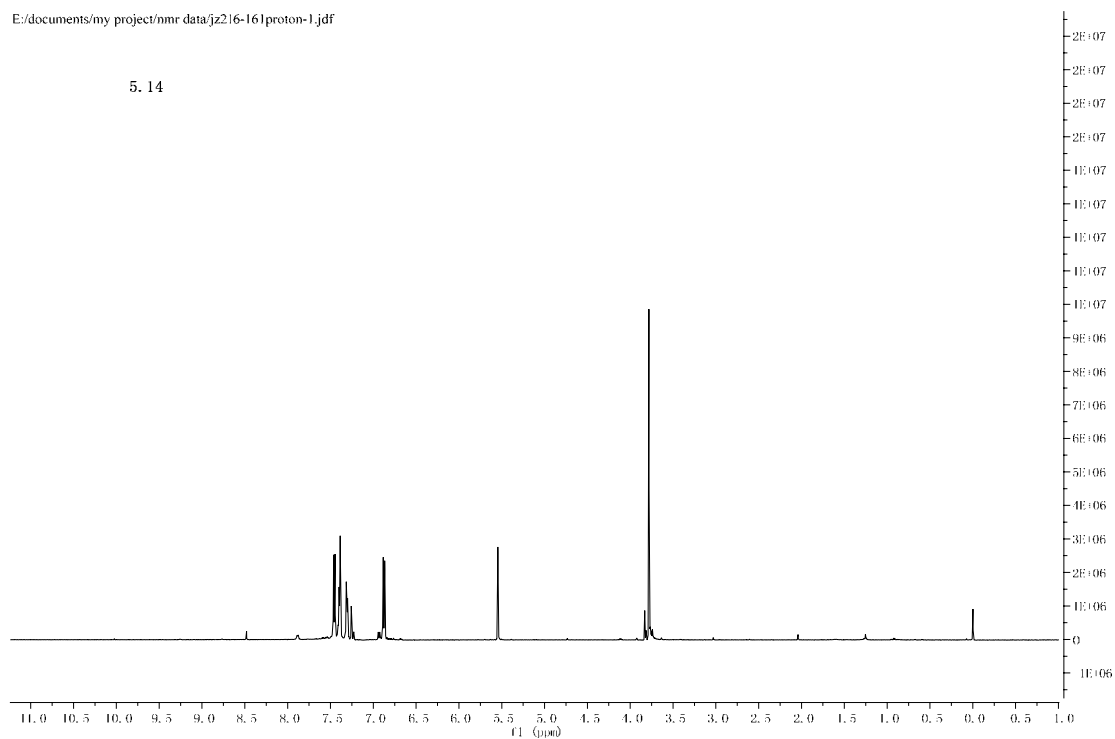
E:/documents/my project/nmr data/jz216-205carbon-1.jdf

5.4



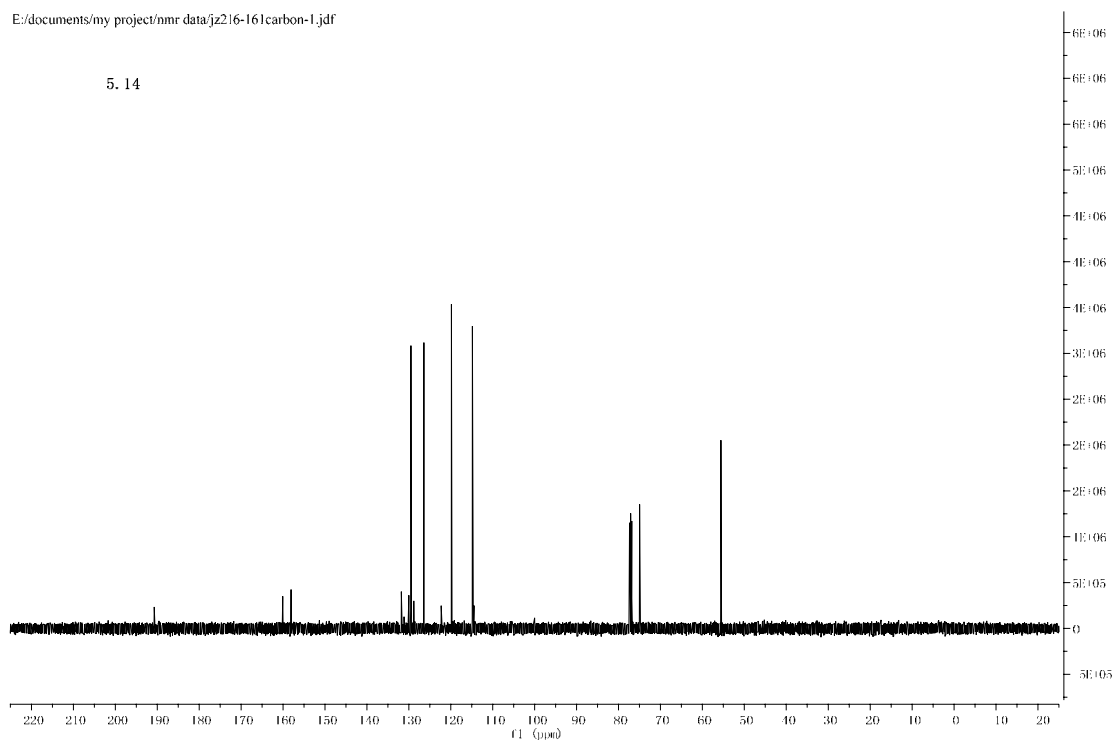
E:/documents/my project/nmr data/jz216-161proton-1.jdf

5.14



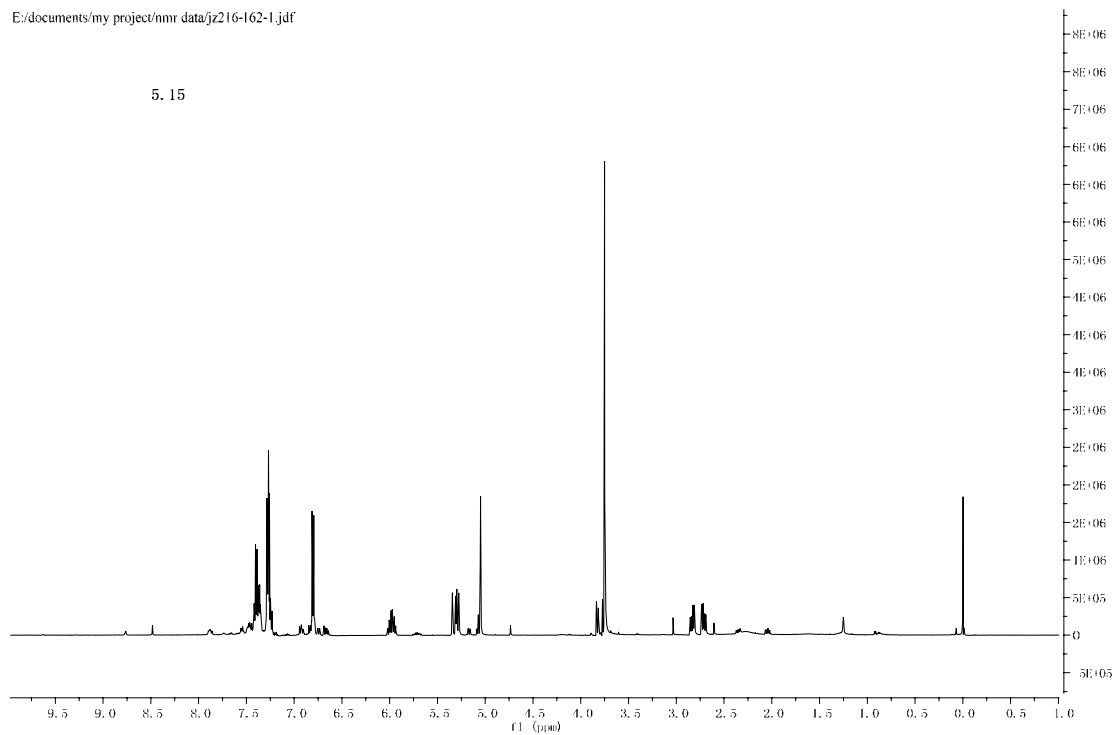
E:/documents/my project/nmr data/jz216-161carbon-1.jdf

5.14



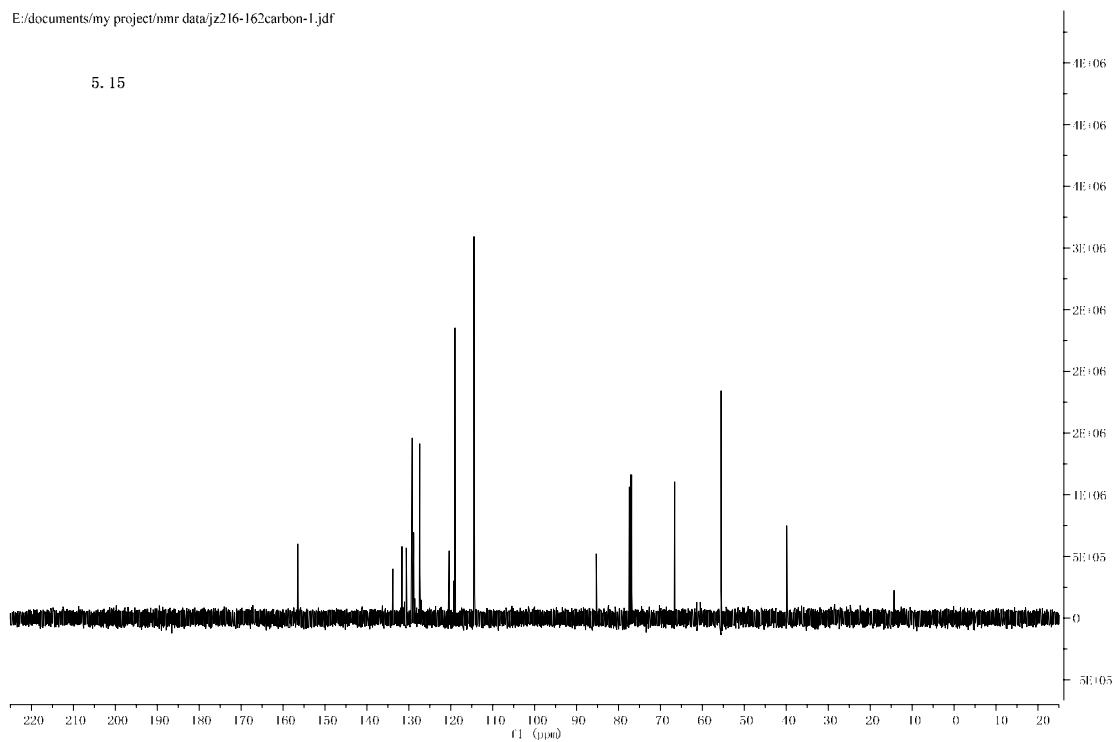
E:/documents/my project/nmr data/jz216-162-1.jdf

5.15



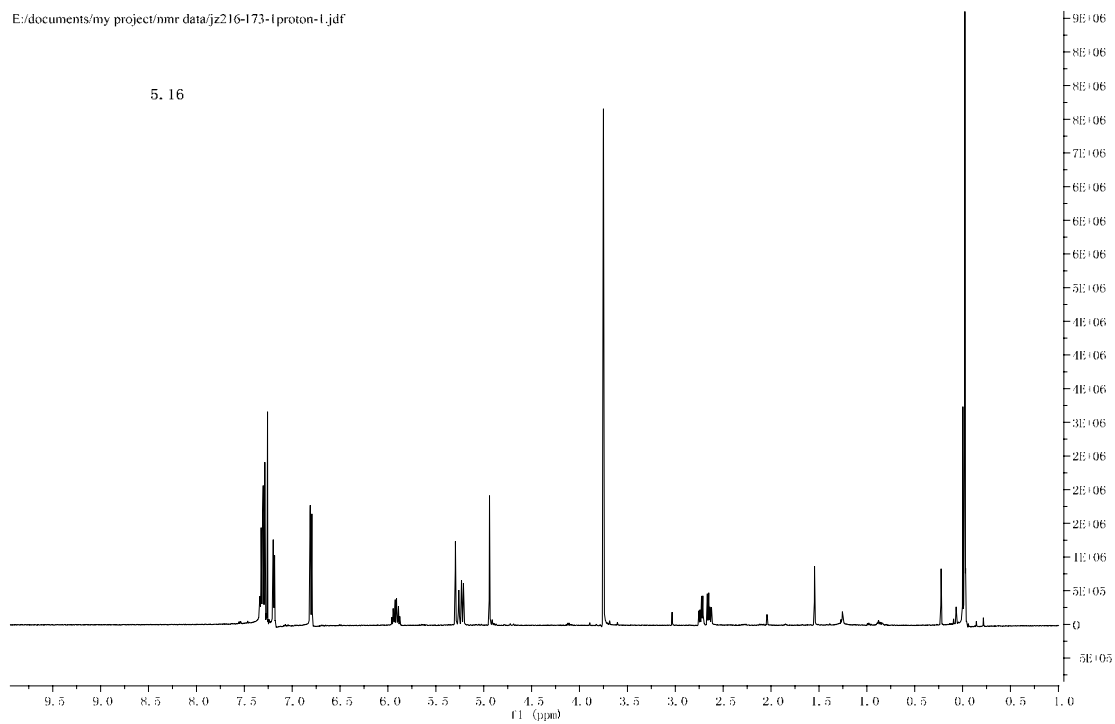
E:/documents/my project/nmr data/jz216-162carbon-1.jdf

5.15



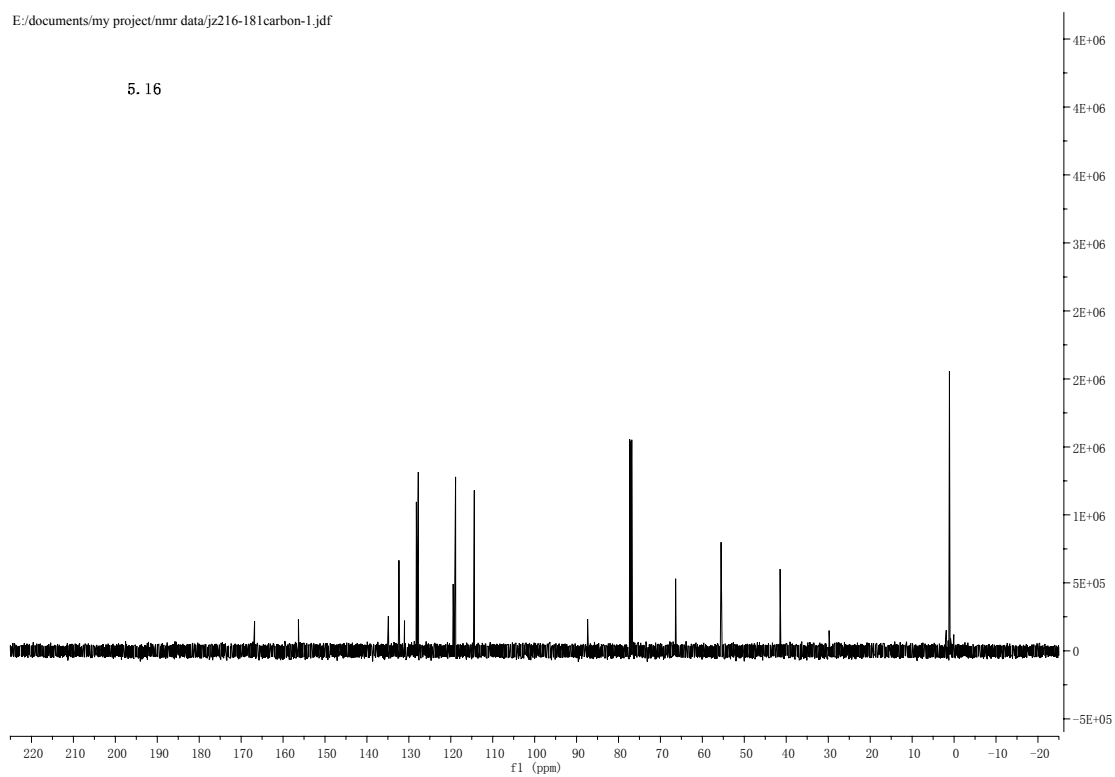
E:/documents/my project/nmr data/jz216-173-1-proton-1.jdf

5.16



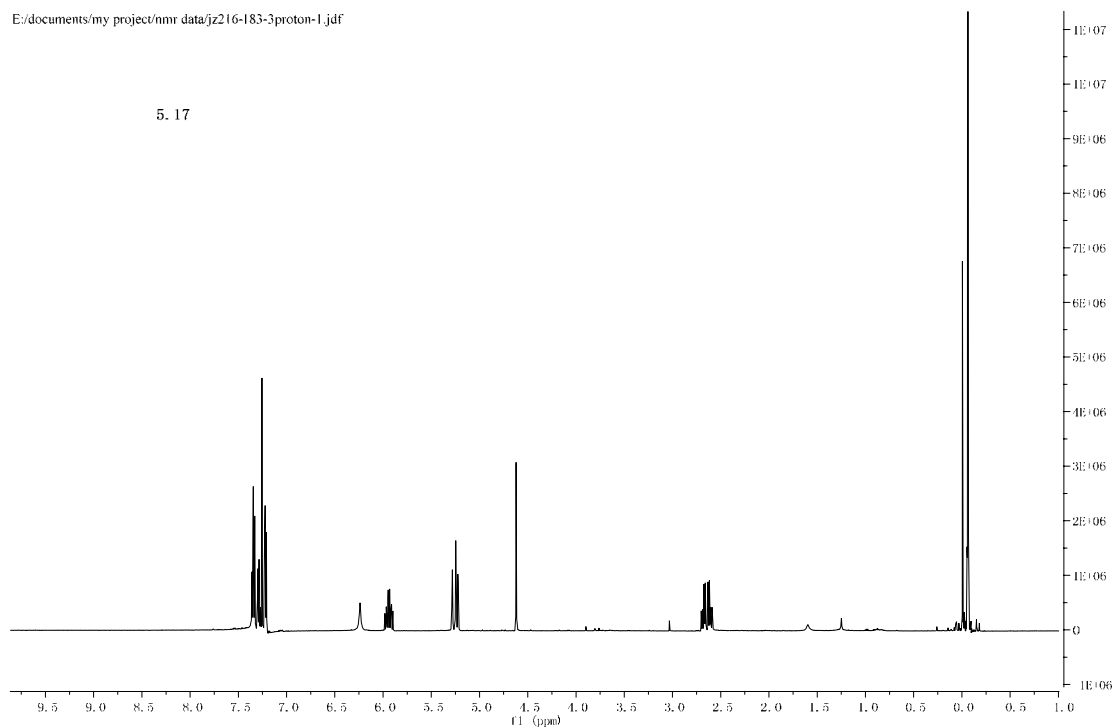
E:/documents/my project/nmr data/jz216-181carbon-1.jdf

5.16



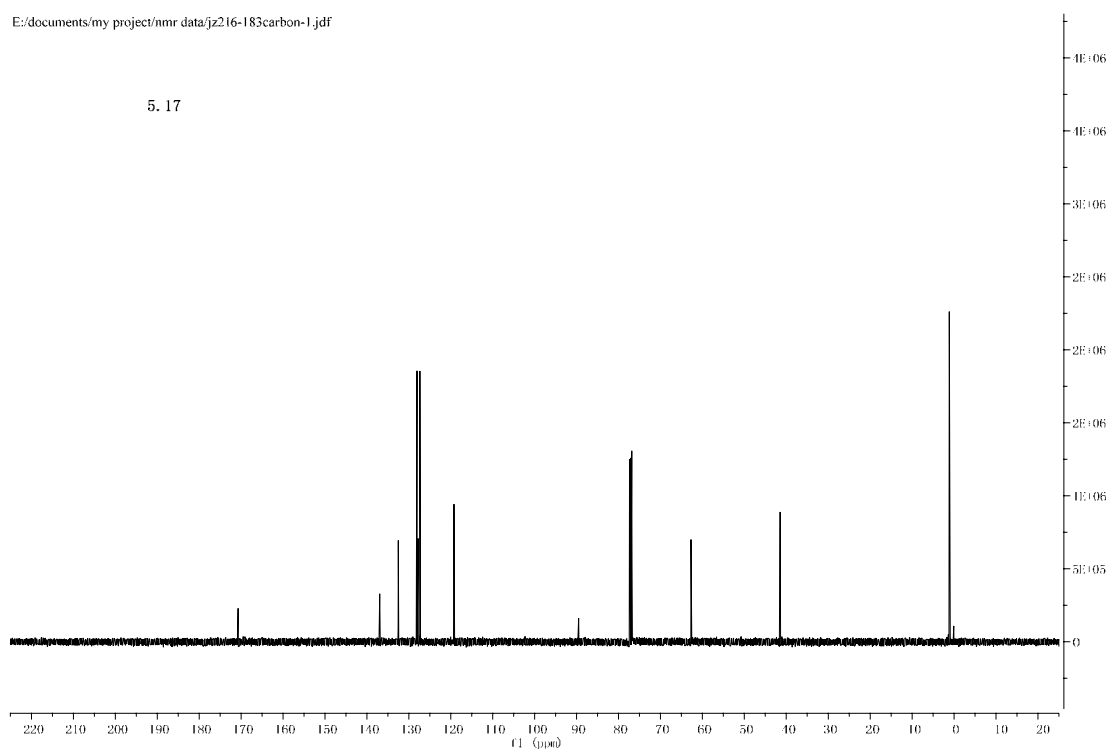
E:/documents/my project/nmr data/jz216-183-proton-1.jdf

5.17

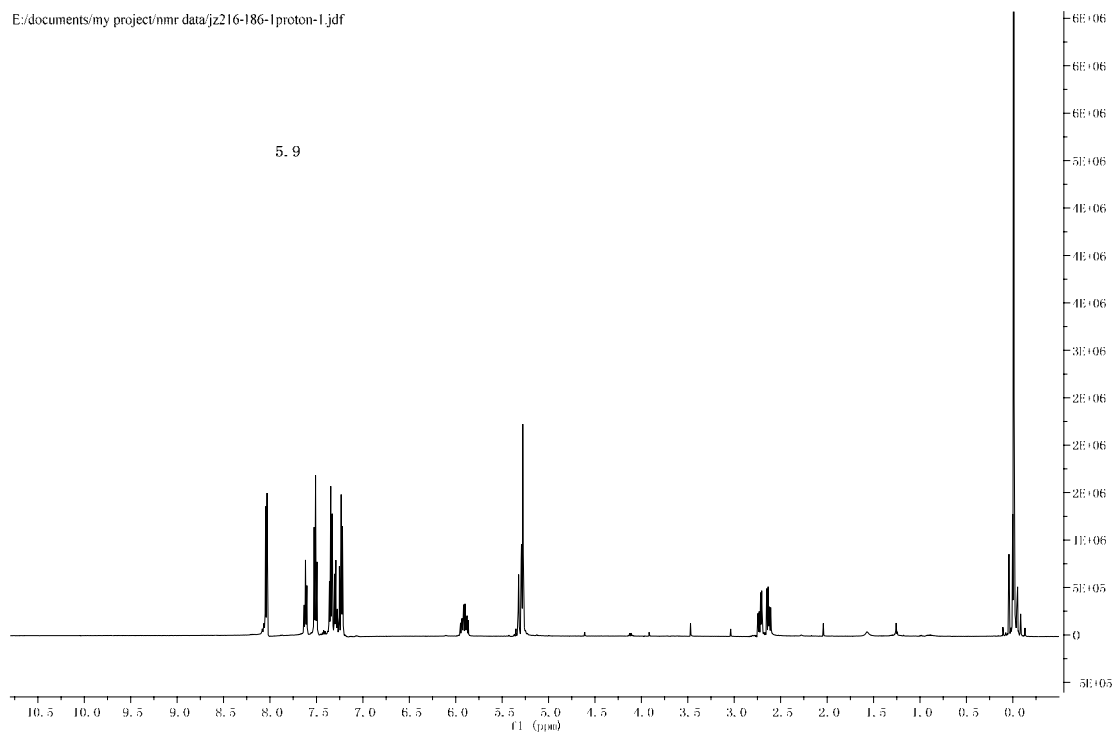


E:/documents/my project/nmr data/jz216-183carbon-1.jdf

5.17



E:/documents/my project/nmr data/jz216-186-1 proton-1.jdf



E:/documents/my project/nmr data/jz216-186-1 carbon-1.jdf

